SEPARATION OF PARTICLES FROM AIR BY DIFFUSIOPHORESIS

Axel MEISEN

THE SEPARATION OF MICRON-SIZE PARTICLES FROM AIR BY DIFFUSIOPHORESIS

DEPARTMENT OF CHEMICAL ENGINEERING

Ph.D.

The separation of micron-size particles from air by diffusiophoresis in a parallel plate collector was studied theoretically and experimentally. Particle-bearing air flowed under laminar conditions between two plates saturated with water and maintained at different temperatures. Water vapour diffused towards the cooler plate on which the particles deposited due to diffusiophoresis.

The collector performance was predicted by assuming that the particles adopt the fluid velocity and this was calculated numerically from the transport equations. These results (subsequently refined) were the basis for the design of the experimental apparatus.

Good agreement between experimental data and theoretical predictions was obtained and diffusiophoresis was found to depend strongly on the water vapour concentration and concentration gradient. To achieve complete particle removal approximately 1.5 lbs of water vapour per pound of air were required.

The effect of the momentum equation on diffusion through a stagnant gas was shown to be negligible under most conditions.

THE SEPARATION OF MICRON-SIZE PARTICLES FROM AIR BY DIFFUSIOPHORESIS

by

A. Meisen

A thesis submitted to the Faculty of Graduate Studies and Research in partial fulfilment of the requirements for the degree of Doctor of Philosophy.

Department of Chemical Engineering
McGill University,
Montreal

June 26, 1970

ABSTRACT

The removal of micron-size cigarette smoke particles from air by diffusiophoresis in a simple, parallel plate particle collector was studied theoretically and experimentally.

When a vapour diffuses through a stagnant gas which contains small particles, the particles are found to move in the same direction as the vapour and this phenomenon is termed "Diffusiophoresis". The primary cause of diffusiophoresis is that diffusion through a stagnant gas gives rise to a "bulk" flow in the fluid (Stefan flow). In the present study this effect was utilized by passing particle-bearing air under laminar conditions between two parallel plates (80" long, 12" wide) which were saturated with water and maintained at different temperatures. Water vapour thus diffused through the air towards the lower and cooler plate and the particles were deposited on this plate by diffusiophoresis.

The performance of the particle collector was predicted theoretically by assuming that the particles move with the local fluid velocity and the design of the experimental apparatus was based on these predictions. It was subsequently found that the experimental data agreed quantitatively with the theoretical results based on the afore-mentioned assumption.

The velocity field of the fluid was calculated by solving the fluid transport equations numerically with a minimum number of simplifying assumptions. From this work it was apparent that the diffusiophoretic velocity is a strong function

of the vapour concentration and concentration gradient in the particle collector.

It could be shown that between one and two pounds of water vapour are required to clean one pound of air and the operating costs of a particle collector employing diffusiophoresis are therefore high. -

It was also shown that diffusion through a stagnant gas is primarily determined by the continuity equations and that the momentum equations may be neglected if the mass fraction gradients of the diffusing species do not exceed 100 cm^{-1}.

ACKNOWLEDGEMENTS

The author wishes to express sincere appreciation to his supervisors, Professor E.J. Farkas, Dr. N.E. Cooke, and Dr. A.J. Bobkowicz, for their advice and assistance in this work. Professor E.J. Farkas' support and encouragement in all phases of this work is gratefully acknowledged. Dr. N.E. Cooke suggested the research project and recognized the diffusiophoretic effect independent of previously published work. Dr. A.J. Bobkowicz's advice in connection with the numerical work was most helpful.

Miss L. Cheung assisted the author with some of the computational and experimental work during the summer months of 1968 and 1969. Her capable help is much appreciated.

Thanks are also due to the technical staff of the Chemical Engineering Department of McGill University for helping the author with the design and construction of the experimental equipment.

Miss A. Finlayson and Miss S. Boucher participated in the typing of the manuscript and preparation of the drawings.

The author wishes to acknowledge the encouragement and patience of his wife Jeanne.

The work reported in this dissertation was supported by the National Research Council of Canada in the form of a Research Assistantship and Scholarship. The Council also provided funds for laboratory equipment and computer time.

GENERAL INDEX

INDEX OF FIGURES

INDEX OF TABLES

I. INTRODUCTION

Many chemical and metallurgical operations produce gaseous effluents which contain a large number of micron-size particles. These particles are a major source of air pollution and their loss frequently results in a decrease of process efficiency.

Particles larger than about 10 microns in diameter can be removed from gases economically and efficiently by cyclones or scrubbers. The collection efficiency of these methods, however, decreases sharply for smaller particles, and only electrostatic precipitators and filters are widely used industrially for the separation of particles less than 10 microns in diameter.

Unfortunately, neither technique is very economical. Filters have a relatively low capital cost, but their operating costs are high because they tend to 'plug', and thus require frequent replacement or cleaning. Furthermore, the pore size of filters which are capable of removing micron-size particles is small, and hence the pressure drop across the filters is high which results in high pumping costs.

Electrostatic precipitators are relatively inexpensive to operate, but their capital cost is great due to the high voltages required. Such precipitators also fail to remove particles which have a high electrical resistance unless special precautions are taken. For example, zinc oxide which is electrically non-conductive has to be pretreated with sulphur trioxide to convert it into the conductive zinc sulphate.

Since the two main industrial separation techniques have great cost disadvantages and can be adversely affected by the chemical nature of the particles, there is a need to investigate new techniques in the hope of discovering one which is free from the above-mentioned difficulties.

Diffusiophoresis is one such new technique, and it was the objective of the present study to investigate the removal of micron-size particles from air by this method. Diffusiophoresis is the name given to the phenomenon that, when a vapour diffuses through a particle-bearing gas, the particles move in the same direction as the vapour. The nature of diffusiophoresis is discussed in greater detail in Sections II and III.

The major advantage of particle-separation by diffusiophoresis is that the removal efficiency is independent of the chemical composition and only slightly dependent on particle size. The technique is therefore equally applicable to micron-size and submicron-size particles. The economics of diffusiophoresis were unknown, however, and it was a further objective of the present work to obtain some basic cost information.

Cigarette smoke particles suspended in air were used in this work because they could be readily obtained, and their size distribution is narrow and well documented in the literature. The mean particle size of cigarette smoke is approximately one micron.

The particle collector which removed the cigarette smoke

from the air consisted essentially of two large, horizontal, parallel plates. The particle-bearing air flowed between and parallel to these plates under laminar conditions. Water vapour was made to diffuse from one plate to the other by saturating them with water and maintaining them at different temperatures. The particles thus deposited on the cooler plate.

The simple parallel-plate configuration was selected for the collector in order to facilitate observation of the particle movement and make a good mathematical representation possible. Water vapour was chosen because it would be most likely employed for an industrial operation since it does not cause a secondary pollution problem and because of its low cost.

Since the magnitude of the diffusiophoretic effect was not well known at the beginning of this study, it was decided to estimate the collector performance theoretically and base the design of the experimental apparatus on these predictions.

The mathematical model which was developed for this purpose was based on the assumption that the particles move with the local fluid velocity. The velocity field in the particle collector was calculated by solving the fluid transport equations numerically with a minimum number of simplifying assumptions.

The particle settling length, i.e. the distance which particles move downstream in the collector before they reach the cooler plate, could be determined from the mathematical

model and it was found to be a strong function of the vapour concentration gradient and average vapour concentration in the particle collector. It was therefore decided to operate the collector at elevated temperatures (60 to 90 ^{o}C) and with plate spacings of a few centimeters.

It was subsequently discovered that the experimental results also agreed quantitatively with the theoretical predictions based on the above assumptions and the mathematical model did not require refinement in response to experimental findings. A more sophisticated mathematical model was however also developed in the later phases of this work in order to determine the influence which the thermophoretic and gravity effects have on the particle movements.

A. Originality

The following factors are considered to be the main original contributions of this work:

1. Construction and analysis of a large-scale particle collector separating micron-size particles from air by diffusiophoresis.

2. A numerical solution of the continuity, momentum, and energy equations for developed flow between large, parallel plates which are maintained at different temperatures and between which diffusion occurs.

3. Proof that the isothermal mass transfer by diffusion through a stagnant gas is governed primarily by the

continuity equations and that the effect of the momentum equation is negligible under most conditions.

II. LITERATURE REVIEW

As stated in Section I this study was concerned with the behaviour of particles in a gas mixture which flowed under laminar and fully developed conditions between large parallel plates. The plates were saturated with water and maintained at different temperatures so that concentration, velocity and temperature gradients existed in the gas mixture. These gradients can in principle be evaluated from the transport equations for the gas mixture. The concentration and temperature gradients give rise to particle motion and these phenomena are referred to as diffusiophoresis and thermophoresis respectively.

The literature on diffusiophoresis, thermophoresis, fluid transport equations and their solutions is therefore of interest in connection with this study and it is reviewed below.

A. Diffusiophoresis

Aitken was the first to report diffusiophoresis in his 1883 paper "On the Formation of Small Clear Spaces in Dusty Air"[1]. He observed that when a moist surface was suspended in dry, dusty air a small dust-free space occurred next to the surface. He attributed this phenomenon correctly to the evaporation of water from the surface but made no attempt to develop a mathematical expression relating the size of the dust-free space to the rate of evaporation or particle size. He also suspected that the evaporation was instrumental in

preventing the deposition of fine dust particles in the lungs of animals and men.

Aitken's work was not continued until Deriagin† and Dukhin published three papers in Russian in 1956 and 1957[2,3,4]. In these papers the authors recognized that the behaviour of aerosols in gas mixtures depends on the Knudsen number, Kn, which is the ratio of the mean free path, λ, of the gas molecules to the particle diameter, D_p, i.e.:

$$Kn = \lambda/D_p \qquad (II-1)$$

Hence there are three distinct regions: $Kn \ll 1$, $Kn \simeq 1$, $Kn \gg 1$, which Brock[5] termed slip-flow, transition, and free-molecule regimes and which correspond to large, intermediate, and small aerosol particles, respectively.

Deriagin and Dukhin[2,3,4] attempted to use Kinetic Theory in order to develop an expression for the force which diffusing gas mixtures exert on large aerosol particles. A knowledge of the velocity distribution of the gas molecules in the vicinity of the particle surface was however required in order to predict the net impulse delivered to the particle by the colliding gas molecules. Since the presence of a large particle affects the velocity distribution of the gas molecules in a manner which can only be determined by solving the Boltzmann integro-differential equations, Deriagin and Dukhin did not pursue this rigorous approach in their early papers[2,3,4]. Instead they postulated that a large aerosol particle moves with the Stefan flow velocity, i.e. the mass average velocity.

† The English spelling of the author's name varies and the one used here corresponds to that given in each paper cited.

Stefan[6] had predicted in 1881 that diffusion in a gas mixture can give rise to a mass average velocity. (See also Section III-C-1)

In 1957 Deriagin and Bakanov[7] and in 1959 Waldmann[8] independently developed equations for the force and velocity of small aerosol particles (Kn >> 1) in diffusing gas mixtures. The authors took a rigorous Kinetic Theory approach by calculating the momentum imparted to the aerosol particles on colliding with the gas molecules. In order to carry out this calculation it was necessary to know the velocity distribution and reflection of the gas molecules by the particles.

The authors[7,8] assumed that the small particles did not affect the velocity distribution of the gas molecules. This assumption implies that collisions between molecules by far exceed collisions between particles and molecules even in the vicinity of the particles. This is of course only correct when the particles are small and relatively far apart. Since the velocity distribution of gas molecules in diffusing gas mixtures is not strictly Maxwellian, the authors adopted Chapman and Cowling's approach[9] and expressed the distribution function in terms of the sum of Sonine polynomials. The first term of this sum is the Maxwell distribution and subsequent terms denote the deviation from Maxwellian behaviour. Deriagin, Bakanov, and Waldmann considered it sufficiently accurate to neglect all terms after the second. Carrying further terms would have achieved only slight improvement and resulted in much more complicated expressions.

Waldmann[8] assumed that fractions a_r and $(1 - a_r)$ of the molecules colliding with the aerosol particles are reflected diffusely and specularly, respectively. The fraction a_r is also called the "accommodation coefficient". Reflections are called "diffuse" when the speed and direction of the gas molecules leaving the particle surface are independent of the approach velocity and hence have a Maxwellian velocity distribution. It is easy to imagine that highly irregular particle surfaces lead to diffuse reflections. When the collisions between the particles and gas molecules are elastic the reflections are termed "specular".

Waldmann[8] obtained the following expression for the force, $\underline{F}_{dp}$, which a diffusing gas mixture consisting of N components exerts on a small aerosol particle moving with velocity $\underline{v}_p$:

$$\underline{F}_{dp} = -\frac{2}{3} D_p^2 \sqrt{2\pi k_B T}\, n \sum_{i=1}^{N} \left(1 + \frac{\pi}{8} a_{ri}\right) x_i \sqrt{m_i}\, (\underline{v}_p - \underline{v}_i) \qquad \text{(II-2)}$$

where k_B, T, n, x_i, m_i, and $\underline{v}_i$ are the Boltzmann constant, absolute temperature, molar density, mole fraction, molecular mass, and the mass velocity of component i, respectively. It has been shown by Waldmann[10,11] that Equation (II-2) can be simplified considerably when only a stationary particle and binary gas mixture are considered in which component B is at rest and component A diffuses:

$$\underline{F}_{dp} = -\frac{2}{3} D_p^2 \sqrt{2\pi k_B T}\, n \left(1 + \frac{\pi}{8} a_{rA}\right) \sqrt{m_A}\, \frac{D}{x_B}\, \underline{\nabla} x_A \qquad \text{(II-3)}$$

where D is the binary gas diffusivity.

At steady state a particle experiences no net force and its velocity was calculated [8] from Equation (II-2) by putting $\underline{F}_{dp}$ equal to zero. When the particle is located in a binary gas mixture in which component A diffuses and component B is at rest, the velocity is given by:

$$\underline{v}_p = - \left[\frac{(1 + \frac{\pi}{8} a_{rA}) \sqrt{m_A}}{(1 + \frac{\pi}{8} a_{rA}) x_A \sqrt{m_A} + (1 + \frac{\pi}{8} a_{rB}) x_B \sqrt{m_B}} \right] \frac{D}{x_B} \underline{\nabla} x_A \qquad \text{(II-4)}$$

or in terms of mass fractions, w_i, and molecular weights, M_i:

$$\underline{v}_p = - \left[\frac{(1 + \frac{\pi}{8} a_{rA}) \sqrt{M_A} M_B}{(1 + \frac{\pi}{8} a_{rA}) M_B \sqrt{M_A} x_A + (1 + \frac{\pi}{8} a_{rB}) M_A \sqrt{M_B} x_B} \right] * \frac{D}{w_B} \underline{\nabla} w_A \qquad \text{(II-5)}$$

The expressions developed by Deriagin and Bakanov [7] are very similar to Equations (II-3) and (II-4), except that the accommodation coefficients were all assumed to be zero, i.e. all gas molecules collide with the aerosol particles elastically.

Since the Stefan flow velocity in a gas mixture in which component A diffuses and component B is at rest is given by:

$$\underline{v}_y = - \frac{D}{w_B} \underline{\nabla} w_A \qquad \text{(II-6)}$$

Equation (II-5) implies that a very small particle moves with a velocity somewhat different from the Stefan velocity.

It is simple to show that $\underline{v}_y \geq \underline{v}_{dp}$.

Waldmann, Deriagin, and Bakanov did not report any experimental results on diffusiophoresis until 1960, and Facy's and Freise's short papers published in 1957 and 1958[12,13,14] provided the first experimental evidence for diffusiophoresis in modern times. Both authors were unaware of Aitken's earlier work[1].

Facy[12] suspended a liquid drop in air containing tobacco or magnesium oxide smoke. In the first set of experiments, the liquid was water and the air was dry so that the drop evaporated. Facy observed that the smoke particles moved away from the drop thus forming a clear space in its vicinity. The second set of experiments was conducted with a drop of sulphuric acid suspended in moist air so that water vapour diffused towards the drop. The smoke particles were found to accumulate near and deposit on the drop surface.

In an attempt to develop an equation for the behaviour of smoke particles in diffusing gases, Facy[13] recognized the importance of the Knudsen number and, following Einstein's technique[15], obtained the following expressions for small aerosol particles in binary mixtures in which only component A diffuses:

$$\underline{F}_{dp} = K_F \sigma \underline{\nabla} x_A \qquad \text{(II-7)}$$

and

$$\underline{v}_p = K'_F D \underline{\nabla} x_A \qquad \text{(II-8)}$$

where K_F and K'_F are constants. Equation (II-7) was derived by

considering the net momentum flux through a small area of size σ placed perpendicularly to the direction of diffusion. This flux was also regarded to be the force on a small aerosol particle of projected area σ, since the particle was assumed to be so small that it did not affect the velocity distribution of the gas molecules. Since Einstein's technique [15] leads to only an approximate result for the momentum flux, Facy introduced the constant K_F which had to be determined experimentally. Facy proceeded to calculate the steady velocity of a small aerosol particle by assuming that it experienced a drag force given by Epstein [16] for particles smaller than the mean free path of the gas molecules, i.e.:

$$\text{Drag force} \propto D_p \, \underline{v}_p \qquad \text{(II-9)}$$

Equation (II-8) follows then from Equation (II-7) and Equation (II-9).

Facy did not attempt to determine the constants K_F and K_F' experimentally, but it is clear that his expressions for small aerosol particles are similar to Waldmann's Equations (II-3) and (II-5).

Facy [13] also considered large aerosol particles for which the Knudsen number is very small and once again following Einstein's approach [15] he found that the force exerted on such a particle in a diffusing binary gas mixture in which one component is at rest is given by:

$$\underline{F}_{dp} = K_F^* \, D_p \, \underline{\nabla} \, x_A \qquad \text{(II-10)}$$

where K_F^* is a constant. Facy calculated the steady state velocity by equating $\underline{F}_{dp}$ to the Stokes drag force and obtained:

$$\underline{v}_p = K_F^{**} D \underline{\nabla} x_A \qquad \text{(II-11)}$$

where K_F^{**} is another constant.

Facy also attempted to find an expression for the velocity of particles in situations where the Knudsen number is approximately unity by equating $\underline{F}_{dp}$ to the drag force given by Cunningham, so that:

$$\underline{v}_p = (K_F'' + K_F''' \, Kn) \, D \underline{\nabla} x_A \qquad \text{(II-12)}$$

where K_F'' and K_F''' are further constants.

Facy did not perform accurate experiments in order to test the various expressions and determine the constants which he proposed.

Freise [14] studied the diffusiophoresis of small natural rubber particles in liquids. A butyl iodide drop was suspended in water and butyl alcohol diffused either from the butyl iodide into water or vice versa by saturating either liquid with butyl alcohol. Freise observed that the rubber particles moved in the direction in which the butyl alcohol diffused and suggested that the particle velocity is identical to the Stefan flow velocity. The latter assumption was not found to be quite correct since the observed particle velocity was somewhat higher than the Stefan flow velocity. He attributed this discrepancy primarily to turbulence in his system.

Schmitt and Waldmann published the first accurate experimental results on diffusiophoresis in 1960 and 1961[17,18]. They studied the behaviour of small, intermediate, and large silicone oil droplets in a variety of gas mixtures and also developed expressions for the force and steady state velocity of large particles.

The latter were obtained by a continuum mechanics approach. The Navier Stokes equations for creeping flow around spheres were solved subject to the boundary conditions that Stefan flow prevailed far away from the particle and that the tangential velocity at the particle surface was given by Kramers and Kistemaker's slip velocity[20]. These two authors had shown in 1943 that the fluid velocity parallel to a solid surface does not vanish at the boundary when diffusion occurs parallel to the surface. The velocity at the boundary was called the "diffusion-slip" or "diffusion-creep" velocity. The equations which were reported by Schmitt and Waldmann[17,18] for large particles are:

$$\underline{F}_{dp} = - 3\pi \mu D_p \left[1 + \left(\frac{M_A - M_B}{M^* + \sqrt{M_A M_B}} \right) x_B \right] \frac{D}{x_B} \underline{\nabla} x_A \qquad \text{(II-13)}$$

$$\underline{v}_p = \left[1 + \left(\frac{M_A - M_B}{M^* + \sqrt{M_A M_B}} \right) x_B \right] \frac{D}{x_B} \underline{\nabla} x_A \qquad \text{(II-14)}$$

where $$M^* = x_A M_A + x_B M_B \qquad \text{(II-15)}$$

and μ is the gas viscosity.

It can be easily shown that Equation (II-14) is equivalent to Equation (II-5) if the accommodation coefficients are assumed to be zero. Waldmann and Schmitt[17,18] pointed out that it is fortuitous that the expressions for the steady state velocities for small and large aerosol particles are exactly identical.

The experiments which Waldmann and Schmitt performed were carried out in a modified Millikan Oil Drop apparatus[19]. The apparatus consisted essentially of two wire screens which could be electrically charged and therefore used to hold the silicon oil droplets in a fixed position. The screens were mounted in a glass tube at right angles to the tube axis. The ends of the tube were connected to large flasks which contained the pure components of the binary gas mixtures which were studied. Diffusion of the gases occurred from one flask to the other through the wire screens and hence past the silicone droplets. The behaviour of the latter could be observed with a microscope.

Waldmann and Schmitt[17,18] found good agreement between experimental results and Equations (II-3) and (II-5) for small aerosol particles. However, it was reported that Equation (II-13) and (II-14) which had been developed for large particles did not agree with the experimental results. After studying various gases the authors suggested the following empirical relationship for the force and steady state velocity of large aerosol particles:

$$\underline{F}_{dp} = - 3\pi \mu D_p \left[1 + \left(A_w \frac{M_A - M_B}{M_A + M_B} + B_w \frac{\sigma_A - \sigma_B}{\sigma_A + \sigma_B}\right) x_B\right] \frac{D}{x_B} \underline{\nabla} x_A \qquad \text{(II-16)}$$

and

$$\underline{v}_p = \left[1 + \left(A_w \frac{M_A - M_B}{M_A + M_B} + B_w \frac{\sigma_A - \sigma_B}{\sigma_A + \sigma_B}\right) x_B\right] \frac{D}{x_B} \underline{\nabla} x_A \qquad \text{(II-17)}$$

where A_w and B_w are two empirical constants whose values depend on the gas mixture, and σ_i denotes the diameter of molecule i.

In Schmitt's paper of 1961[18] a simple particle collector used to separate cigarette smoke from air was briefly mentioned. The apparatus consisted of two parallel, horizontal surfaces (10 cms long, 3 cms wide) which were approximately 0.1 cms apart and between which smoky air was passed. The upper surface consisted of porous asbestos through which steam was injected and the lower surface was a water-cooled copper plate. Due to the temperature and hence partial pressure difference of water vapour at the surfaces, diffusion occurred from the top to the bottom plate. Without giving further details Schmitt reported that the particle collector completely removed the cigarette smoke from the air.

Bakanov and Deriagin published another theoretical paper on the diffusiophoresis of small aerosol particles in 1960[21]. The assumptions and principles of their work were very similar to those employed earlier[7] with the exception that temperature gradients in the diffusing gas mixture were also considered. It was found that the steady state particle velocity could be obtained by adding the diffusiophoretic and thermophoretic forces. The latter will be discussed in Section II-B.

A further theoretical paper on the behaviour of small particles in gas mixtures was published by Mason and Chapman in 1962[22]. These authors did not follow Waldmann's[8] assumption that molecules are reflected by the particle surface either specularly or diffusely with a Maxwellian velocity distribution. Instead they assumed that a fraction, a_d, of the gas molecules which collide with the aerosol particles are reflected with unchanged speed relative to the particles but with a random scattering angle. The remaining particles are assumed to be reflected specularly.

Mason and Chapman developed the expression for the steady state particle velocity by regarding the aerosol particle as a large molecule and calculating the impulse given to the particle by colliding gas molecules. They found that for a binary mixture in which component A diffuses and component B is at rest:

$$\underline{v}_p = - \left[\frac{(1 + \frac{4}{9} a_{dA}) \sqrt{m_A}}{(1 + \frac{4}{9} a_{dA}) \sqrt{m_A}\, x_A + (1 + \frac{4}{9} a_{dB}) \sqrt{m_B}\, x_B} \right] * \frac{D}{x_B} \underline{\nabla} x_A \qquad \text{(II-18)}$$

which is the same as Equation (II-4) except that $\pi a_{ri}/8$ is replaced by $4a_{di}/9$. Since Mason and Chapman did not report any experimental results and since neither a_{ri} nor a_{di} could be calculated accurately, it was not possible to test their assumptions.

Goldsmith, Delafield, and Cox[23,24] were the first to show experimentally that diffusiophoresis could be employed to separate very small particles (Kn>>1) continuously from

a gas stream. The apparatus used consisted of two parallel plates (30 cms long, 10 cms wide) which were kept a few millimeters apart by means of spacers. One surface was lined with absorbent paper and saturated with water. Water vapour diffused from this plate through the particle - bearing air stream to the opposite plate which was lined with paper saturated with sulphuric acid.

The particles used in this study were obtained by evaporating an electrically heated nichrome wire in an air stream and adding radioactive thorium. The thorium was adsorbed on the particles and their location could therefore be detected with a Pollak counter[25].

Air containing these radioactive particles was passed between the parallel plates already described. The authors[23, 24] reported that the particles were completely removed from the air since no radiation could be detected in the exhaust gas. The apparatus was dismantled after each run and the absorbent papers were analysed with a Pollak counter or by exposing them to a photographic plate.

It was found that only the paper saturated with sulphuric acid was radioactive thus indicating that the particles were deposited on the surface towards which the water vapour diffused. Furthermore, it was found that in each experiment there was a certain distance from the leading edge of the plate beyond which no radioactivity could be detected.

The analysis of the experimental results was somewhat

difficult because the water vapour, which diffused towards the plate saturated with sulphuric acid, decreased the acid strength continuously. Furthermore, the radioactivity of the "acid plate" did not terminate at a definite distance from the entrance of the particle collector.

By assuming that the concentration profile of water vapour was linear between the plates and that the velocity profile was parabolic, Goldsmith et al. could express the experimental particle velocities due to diffusiophoresis by the following equation:

$$\underline{v}_p = - 1.9 * 10^{-4} \Delta P_{H_2O} / GAP \qquad (II-19)$$

where ΔP_{H_2O} is the vapour pressure difference between the plates and GAP is the plate spacing. The units for $\underline{v}_p$, P_{H_2O} and GAP are cms/sec, millibars and cms, respectively. Equation (II-19) is in good agreement with Waldsmann's expression when the accommodation coefficients and x_A are neglected in the bracket of Equation (II-4). The latter was very small in the work of Goldsmith et al. because most of their experiments were conducted at room temperature. At elevated temperatures and high vapour fluxes Equation (II-19) can be expected to be inaccurate because the assumptions on which it is based are no longer valid.

In 1963 Brock attempted to develop rigorous expressions for the diffusiophoretic force and steady state velocity for large aerosol particles[5]. He stated that the diffusio-

phoresis of large particles was due to an average mass velocity in diffusing mixtures (i.e. the Stefan flow) and the diffusion-creep at the particle surface. However, instead of relying on Kramers and Kistemaker's[20] expression for the diffusion-creep, Brock derived it by employing the Chapman and Cowling second-order approximation for the velocity distribution function of diffusing gases and by stipulating that the momentum flux towards the surface is constant.

Brock thus obtained the following expression for the diffusiophoretic force on a large stationary aerosol particle which is suspended in a binary gas mixture in which component A diffuses and component B is at rest:

$$\underline{F}_{dp} = 3\pi \mu D_p \left[\frac{(\frac{n}{\rho})(M_B - M_A)(1 + 2c_m Kn) - D_p c_{dm} Kn}{1 + 3 c_m Kn} \right] \underline{\nabla} x_A \qquad \text{(II-20)}$$

The constants c_m and c_{dm} are complicated functions of the accommodation coefficients of the gas molecules.

Equation (II-20) is very general and it can be shown that it reduces to the same form as Waldmann's Equation (II-16) when $M_A \simeq M_B$. The applicability of Equation (II-20) is however restricted because the accommodation coefficients are generally unknown.

Derjaguin, Yalamov, and Storozhilova adopted a new approach in 1966 for calculating the steady state velocity of large aerosol particles in binary gas mixtures[26]. By

employing principles of irreversible thermodynamics, the authors were able to show that the diffusion-creep velocity is negligible which is contrary to previous findings[5,20]. Derjaguin et al. then used the normal boundary conditions for creeping flow around spheres and arrived at the following expression for the steady state velocity of a large aerosol particle in a binary mixture in which component B is at rest:

$$\underline{v}_p = \frac{-D}{M_A / M_B + w_A (1 - M_A / M_B)} \underline{\nabla} w_A \qquad \text{(II-21)}$$

This equation indicates that the particles do not move with the Stefan velocity as given by Equation (II-6). The agreement of Equation (II-21) with experimental results of Derjaguin et al.[26] and Waldmann[10] was however poor. The reason for this is that the authors[26] used an incorrect expression for the mass average velocity in the derivation of Equation (II-21).

Derjaguin et al. also reported some diffusiophoresis experiments with large aerosol particles. Their apparatus, which was described in detail in Reference (27), consisted essentially of two small, parallel plates spaced 0.7 cms apart. The lower one was saturated with water and the upper plate contained phosphorous pentoxide. Air was passed continuously between the plates and water vapour diffused from the lower to the upper surface. A small stream of vaseline aerosol particles was injected isokinetically into the centre of the air stream and the deflection of the particle stream was observed with a microscope.

By measuring the deflection, assuming a parabolic velocity

profile of the air stream, and logarithmic concentration profile, the particle velocity could be calculated. It was possible to operate the apparatus at reduced pressures and hence measure the particle velocity for various Knudsen numbers.

As pointed out earlier the agreement between Equation (II-21) and the experimental results was not very good. Apart from the deficiencies of Equation (II-21) the experimental errors were probably significant due to the skill required in measuring the deflection of the particle stream with a microscope. The authors did not provide an estimate of the experimental accuracy.

In 1967 Brock[28] attempted to calculate the force on a stationary aerosol particle in the transition regime, i.e. where the Knudsen number is approximately unity. Brock adopted a first order perturbation technique to calculate the velocity distribution function of the gas molecules in the vicinity of the aerosol particles. From this distribution function it was then possible to obtain the following expression for the force on a stationary aerosol particle in a gas mixture in which component B is at rest and A diffusing:

$$\underline{F}_{dp} = -\frac{2}{3} D_p^2 \, n \, (2\pi \, M_A \, R_c \, T)^{\frac{1}{2}} \, (1 + \frac{\pi}{8}) \left[1 - \frac{0.071}{Kn} \left(\frac{2 \, M_B}{M_A + M_B}\right)\right] * \frac{D}{x_B} \, \underline{\nabla} \, x_A \qquad \text{(II-22)}$$

Brock compared Equation (II-22) with the experimental results obtained by Schmitt and Waldmann[17,18] and found

the agreement to be within 10%.

In addition to the papers discussed above three review articles on diffusiophoresis have been published[29,30,31].

B. Thermophoresis

The literature review of the thermophoretic effect which is presented in this section is not as extensive as the review carried out on diffusiophoresis. The reasons for this are that good review articles have already been published[29,30,31] and that the thermophoretic effect did not play a decisive rôle in this study.

Tyndall[33], Lord Rayleigh[34,35], and Aitken[1] were the first to report the thermophoretic effect. They described experiments in which hot surfaces were suspended in cold gases laden with very fine dust particles and noted that small dust-free spaces developed adjacent to the hot surfaces. Through careful experimentation Aitken[1] was able to show that the dust-free spaces were solely due to temperature gradients in the gas.

A mathematical theory was however not developed until 1924 when Einstein [15] presented his explanation of the thermophoretic effect (also called "radiometer effect") based on Kinetic Theory. He recognized that the nature of thermophoresis depended on the size of the smoke particle, D_p, relative to the mean free path of the gas molecules, λ. When the Knudsen number ($= \lambda/D_p$) is large, the velocity distribution is not significantly affected

by the particles and the particle behaviour is simple to predict. The velocity distribution is however changed when the particles are large in comparison with the mean free path and the particle behaviour cannot be found unless this change is known. Hence thermophoresis and diffusiophoresis are similarly dependent on the Knudsen number.

Einstein[15] determined the force which small particles experience when they are in a gas in which a temperature gradient exists, by calculating the net momentum transfer through a small surface σ. The surface was at right angles to the direction of the heat flux. The velocity distribution of the gas molecules was assumed to be given by:

$$\frac{1}{2} m u^2 = \frac{3}{2} k_B T \qquad \text{(II-23)}$$

where u and m are the velocity and mass of the gas molecules, respectively. Thus Einstein obtained the following expression for the thermophoretic force, $\underline{F}_{tp}$, on a small particle:

$$\underline{F}_{tp} = - \frac{\pi}{8} D_p^2 \frac{P\lambda}{T} \underline{\nabla} T \qquad \text{(II-24)}$$

Equation (II-24) indicates that the particles experience a force in the direction of declining temperature. This is in agreement with Aitken's finding[1] that "Particles are 'attracted' by cold surfaces and 'repelled' by hot surfaces".

Einstein calculated the steady state velocity, $\underline{v}_p$, of a small particle under the influence of the thermophoretic force by assuming the particle experiences a drag given by $- \frac{\pi}{3} D_p^2 n u m \underline{v}_p$, equating the drag to $\underline{F}_{tp}$ and rearranging

slightly:

$$\underline{v}_p = -\frac{1}{8} u \frac{\lambda}{T} \underline{\nabla} T \qquad \text{(II-25)}$$

Similar equations were derived by Cawood[36].

Equations (II-24) and (II-25) were found to be in good agreement with experiments conducted by Hettner[37], Edith Einstein[38] and Watson[39].

A. Einstein[15] also considered the thermophoretic force on a large particle (i.e. the case where Kn << 1). He assumed that a pressure,

$$-\frac{1}{2} \frac{P\lambda}{T} \underline{\nabla} T$$

is exerted on an annular ring which surrounds the projected area of the particle and is λ units wide. Hence the thermophoretic force for a large particle is:

$$\underline{F}_{tp} = -\frac{\pi}{2} D_p^2 \frac{P\lambda^2}{T} \underline{\nabla} T \qquad \text{(II-26)}$$

This equation was in good agreement with experiments carried out on particles of low thermal conductivity by Rosenblatt and La Mer[40].

Epstein[41] pointed out in 1927 that Einstein's Equation (II-26) was only correct for particles which have a very low thermal conductivity in comparison with the gas, because Einstein had assumed that the particles did not affect the temperature distribution of the gas. Epstein calculated the thermophoretic force on a large sphere in a gas which had a linear temperature distribution far away from the sphere. The tem-

perature distribution in the sphere was taken into consideration and Epstein[41] assumed that the tangential gas velocity at the particle surface was the Maxwell thermal-creep velocity. He thus found:

$$\underline{F}_{tp} = -\frac{9\pi}{2} D_p \frac{k}{2k + k_p} \frac{\mu^2}{\rho T} \underline{\nabla} T \qquad \text{(II-27)}$$

where k and k_p are the thermal conductivities of the gas and particle, respectively. By letting $\mu = 0.499\ \rho u \lambda$ and $\rho u^2 = (\frac{8}{\pi})\ P$ (see Reference 42), Equation (II-27) reduces to:

$$\underline{F}_{tp} = -8.95\ D_p \frac{k}{2k + k_p} \frac{P\lambda^2}{T} \underline{\nabla} T \qquad \text{(II-28)}$$

This equation is similar to Einstein's Equation (II-26) when $k_p << k$. The coefficients in Equations(II-26) and (II-27) are however somewhat different.

The steady state velocity of a large particle in a temperature gradient was found[41] by equating $\underline{F}_{tp}$ to the Stokes drag, $3\pi\ \mu\ D_p\ \underline{v}_p$, i.e.:

$$\underline{V}_p \simeq \frac{3}{\pi\mu} \frac{k}{2k + K_p} \frac{P\lambda^2}{T} \underline{\nabla} T \qquad \text{(II-29)}$$

The experimental results of Rosenblatt and LaMer[40] obtained with tricresyl particles also agreed well with Equations (II-28) and (II-29).

Waldmann[8], Deryagin and Bakanov[43] reconsidered the thermophoresis of small particles by using the Chapman-Enskog[9] method. The objective was to obtain a more precise estimate of

the velocity distribution function in a gas with a temperature gradient than Einstein[15] had used. The net momentum imparted to the particles by colliding gas molecules was calculated exactly and the thermophoretic force and particle velocity were therefore shown to be given by:

$$\underline{F}_{tp} = -\frac{8}{15} D_p^2 k_{trans} \frac{\pi m}{8 k_B T} \underline{\nabla} T \qquad \text{(II-30)}$$

and

$$\underline{v}_p = -\frac{1}{5(1 + \pi a/8)} \frac{k_{trans}}{P} \underline{\nabla} T \qquad \text{(II-31)}$$

where k_{trans} and a are the translational part of the thermal conductivity and accommodation coefficient, respectively. Schmitt[44] showed that these expressions agreed well with his experimental results.

In 1961 Schadt and Cadle[45] reported experiments with large, well-conducting sodium chloride aerosol particles. Contrary to Equation (II-29) which indicates that $\underline{v}_p$ tends to zero as k_p becomes large, the authors found sodium chloride aerosols moved with a finite velocity in a temperature gradient.

Brock[46] extended Epstein's work on large particles in 1962 by not only considering the thermal-creep velocity but also the temperature jump and friction slip at the particle surfact. He thus obtained the following expression for the thermophoretic force:

$$\underline{F}_{tp} = -\frac{9}{2} \frac{\pi \mu^2 D_p}{\rho T} \frac{2(k + C_t k_p Kn)}{(1 + 3C_m Kn)(2k + k_p + 2C_t k_p Kn)} \underline{\nabla} T \qquad \text{(II-32)}$$

where

$$C_t = \frac{15}{8} \frac{2 - \alpha_t}{\alpha_t} \tag{II-33}$$

$$C_m = \frac{2 - \alpha_m}{\alpha_m} \tag{II-34}$$

and α_t and α_m are the thermal and momentum accommodation coefficients, respectively.

Equation (II-32) agrees well with Schadt and Cadle's[45] experimental data and it is seen that $\underline{F}_{tp}$ does not tend to zero for large k_p. The coefficients C_t and C_m can however not be predicted accurately and the equation is therefore of somewhat limited use.

In later papers[47,48] Brock further improved Equation (II-32) and also considered the thermophoretic force in the transition regime where the Knudsen number is approximately unity[49,50].

Several papers by Russian authors[51,27] have also been published in the recent past. These authors showed by a derivation based on irreversible thermodynamics that expressions similar to Brock's Equation (II-32) could be obtained.

C. Transport Equations

The continuity, momentum, and energy equations, which are referred to as fluid "transport" equations, were used to calculate the concentration, velocity, and temperature profiles in the particle collector. The transport equations are special formulations of the conservation of mass, momentum, and energy principles and can be derived either by a continuum mechanical or molecular approach. Numerous derivations can be found in the literature but the most general and comprehensive were presented by Bird, Stewart, Lightfoot, Curtiss, Hirschfelder, Chapman, and Cowling[52,53,9].

However, since the derivations performed by the aforementioned authors are complicated and involve some implicit assumptions, the transport equations were re-derived in this study and are presented in Section III. Only Newtonian fluids were considered.

The general transport equations are non-linear, coupled, partial differential equations and very difficult to solve analytically except for simple cases. Extensive solutions are available for situations where only one of the transport equations needs to be considered and where the physical properties of the fluid can be regarded as constant. In connection with this study the following cases are of interest:

a) Isothermal Diffusion between Parallel Plates:

Jost[54], Crank[55], Sherwood and Pigford[56], and Bird *et al.*[52] presented solutions for diffusion of a vapour from one plate through a stationary gas to an opposite, parallel

plate under isothermal conditions and for constant diffusivity. Jost disregarded the Stefan velocity and thus showed that the concentration profile of the vapour is linear whereas Crank, Sherwood, Pigford and Bird et al. included the Stefan flow in their calculations and found a logarithmic concentration profile. None of the latter authors calculated the Stefan flow velocity explicitly.

Crank[55] also obtained some solutions where the diffusivity was a simple function of fluid composition and suggested numerical procedures for more complex relations between diffusivity and composition.

b) Developed Fluid Flow between Horizontal, Parallel Plates:

It is simple to show[52] that the developed velocity profile between parallel plates is parabolic provided the fluid viscosity is constant and no diffusion occurs between the plates. Bird et al.[52] also considered the problem of developed flow between parallel plates when the plates are kept at different temperatures and the viscosity is a function of temperature. In the absence of natural convection (i.e. the upper plate is maintained at a higher temperature than the lower plate) the momentum equation does not affect the energy equation. Hence it is possible to obtain the temperature profile from the energy equation and use this in the subsequent solution of the momentum equation. Analytical solutions are possible when the fluid properties are very simple functions of temperature and numerical methods have to be used for more

general cases.

Diffusion of vapour between the plates not only affects the fluid density and viscosity but also introduces an additional term into the momentum equation (see Equation (III-72)) but this has not been considered in the literature for a parallel plate geometry.

c) Heat Transfer between Parallel Plates:

Carslaw and Jaeger[57], Jakob[58], and Bird et al.[52] considered the case of heat conduction through a gas between parallel plates in the absence of convection and diffusion. They showed that the temperature profile was linear for constant fluid properties. Cases with variable properties were also considered and simple analytical or numerical solutions were presented.

The diffusion of vapour between the plates results in an additional heat flux (see for example the books by Eckert[59], Jakob[58], Spalding[60], and Bird et al.[52]) and gives rise to a further term in the energy equation. Solutions to such extended energy equations have not yet been reported for parallel plate geometries.

Apart from the above highly simplified solutions for mass, momentum, and heat transfer between parallel plates no other literature on the transport equations was of direct assistance in this study. However, the very extensive work on simultaneous heat, mass and momentum transfer in laminar boundary layers

was relevant (see for example References 60,61,62).

Since no analytical solutions could be found or obtained for the coupled transport equations governing the concentration, velocity, and momentum profiles in the particle collector, numerical solutions were sought. The equations for a parallel-plate particle collector operating under developed conditions are ordinary, non-linear, coupled differential equations with variable coefficients. Many different methods for solving such equations have been reported in the literature (eg. References 63 to 68), but the single- and multi-step techniques have been found most successful and simple to use. In this study the Kutta-Merson single-step method[68] was used since it was convenient and gave accurate results.

III. THEORY

A derivation of the general fluid transport equations is presented in Section III-A. In Section III-C it is shown how these equations can be simplified for a parallel plate particle collector operating under developed conditions and an explanation of the Stefan flow is also given.

The simplified or "reduced" transport equations for the particle collector are second order, non-linear, coupled, ordinary differential equations with boundary conditions (i.e. composition, velocity, and temperature) defined at the two plates. The Kutta-Merson integration technique cannot treat such split-boundary value problems unless they are redefined as initial value problems. In the present study this was accomplished by estimating the gradients of the concentration, velocity, and temperature profiles at the upper plate from approximate solutions of the transport equations. Such approximate solutions are obtained in Section III-D.

This is followed by a detailed discussion of the particle equations, the Kutta-Merson integration technique, and the Newton-Raphson method. The latter was employed to determine the correct gradients of the concentration, velocity, and temperature profiles from the approximate gradients.

A. General Transport Equations

The transport equations, i.e. continuity, momentum and energy equations, are special formulations of the law of conservation of mass, momentum and energy, respectively, when applied to a moving fluid. The transport equations will be derived by applying the conservation laws to a control volume which is fixed in space but completely pervious to the flow of mass, momentum and energy. The conservation laws may be stated as:

Rate of accumulation of a quantity in the control volume	=	Net input of the quantity into the control volume	+	Source strength	(III-1)

By 'quantity' is meant either mass, momentum or energy.

The shape of the control volume is arbitrary. Its total volume and surface area are denoted by V_o and S_o, respectively. It is convenient to define a vector $d\underline{S}$ whose magnitude is dS, i.e. an element of surface, and whose direction is normal to the surface and pointing outwards.

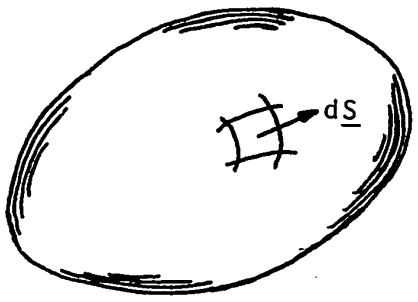

Control Volume

1. Continuity Equations

The law of mass-conservation may be applied to the fluid as a whole or just to a particular chemical constituent, k, of the fluid thus yielding the so called total continuity equation and the continuity equation for the k-th component, respectively.

1a. Total Continuity Equation

The total mass contained in the control volume is:

$$\int_{V_o} \rho \, dV$$

where dV and $\int_{V_o}$ denote an element of volume and a volume integral, respectively. Hence the rate of accumulation of mass in the control volume is given by:

$$\frac{\partial}{\partial t} \int_{V_o} \rho \, dV$$

The rate at which mass is flowing into the volume is given by the surface integral:

$$- \int_{S_o} \rho \, \underline{v} \cdot d\underline{S}$$

The minus sign results from defining the direction of $d\underline{S}$ to be pointing out of the control volume. The integral

$$\int_{S_o} \rho \, \underline{v} \cdot d\underline{S}$$

thus denotes the rate at which mass is leaving the control volume.

There is no source of mass in the control volume. Hence Equation (III-1) for the conservation of mass becomes:

$$\frac{\partial}{\partial t} \int_{V_o} \rho \, dV = - \int_{S_o} \rho \, \underline{v} \cdot d\underline{S} \qquad \text{(III-2)}$$

The surface integral can be transformed into a volume integral by Green's formula so that Equation (III-2) becomes:

$$\int_{V_o} \left[\frac{\partial \rho}{\partial t} + \underline{\nabla} \cdot \rho \underline{v}\right] \, dV = 0 \qquad \text{(III-3)}$$

Since Equation (III-3) must be valid for a control volume of any size, it follows that:

$$\frac{\partial \rho}{\partial t} + \underline{\nabla} \cdot \rho \underline{v} = 0 \qquad \text{(III-4)}$$

This is the total continuity equation. It may be written in terms of the subtantive derivative:

$$\frac{D\rho}{Dt} + \rho \, \underline{\nabla} \cdot \underline{v} = 0 \qquad \text{(III-5)}$$

where the substantive derivative is defined as:

$$\frac{D}{Dt} = \frac{\partial}{\partial t} + \underline{v} \cdot \underline{\nabla} \qquad \text{(III-6)}$$

1b. Continuity Equation for k-th Component

The mass of component k in the control volume is:

$$\int_{V_o} \rho \, w_k \, dV$$

so that the rate of accumulation is:

$$\frac{\partial}{\partial t} \int_{V_o} \rho \, w_k dV$$

The net input of k into the control volume occurs by diffusion and bulk flow, i.e.

$$-\int_{S_o} (\underline{j}_k + \rho \, w_k \, \underline{v}) \cdot d\underline{S} \qquad \text{(III-7)}$$

where $\underline{j}_k$ denotes the diffusive flux of k.

Since component k is neither created nor destroyed in the control volume, there is no source term and Equation

(III-1) when applied to the mass of species k becomes:

$$\int_{V_o} \frac{\partial}{\partial t} (\rho\, w_k)\, dV + \int_{S_o} (\underline{j}_k + \rho\, w_k\, \underline{v}) \cdot d\underline{S} = 0 \qquad \text{(III-8)}$$

Green's theorem is used to transform the surface integral into a volume integral. Equation (III-8) thus becomes:

$$\int_{V_o} \left[\frac{\partial}{\partial t} (\rho\, w_k) + \underline{\nabla} \cdot (\underline{j}_k + \rho\, w_k\, \underline{v}) \right] dV = 0 \qquad \text{(III-9)}$$

Since this equation is valid regardless of the size of the control volume, it follows that:

$$\frac{\partial}{\partial t} \rho\, w_k + \underline{\nabla} \cdot (\underline{j}_k + \rho\, w_k\, \underline{v}) = 0 \qquad \text{(III-10)}$$

Equation (III-10) may be simplified by multiplying Equation (III-4) by w_k, i.e.:

$$w_k \frac{\partial \rho}{\partial t} + w_k\, \underline{\nabla} \cdot \rho\, \underline{v} = 0 \qquad \text{(III-11)}$$

and subtracting Equation (III-11) from Equation (III-10):

$$\rho \frac{\partial w_k}{\partial t} + \underline{\nabla} \cdot \underline{j}_k + \rho\, \underline{v} \cdot \underline{\nabla} w_k = 0 \qquad \text{(III-12)}$$

or in terms of the substantive derivative:

$$\rho \frac{Dw_k}{Dt} = - \underline{\nabla} \cdot \underline{j}_k \qquad \text{(III-13)}$$

In the absence of thermal and pressure diffusion, the diffusive flux of component k is given by Fick's law, i.e.:

$$\underline{j}_k = - \rho\, D\, \underline{\nabla} w_k \qquad \text{(III-14)}$$

so that Equation (III-13) becomes:

$$\rho \frac{Dw_k}{Dt} = \underline{\nabla} \cdot \rho\, D\, \underline{\nabla} w_k \qquad \text{(III-15)}$$

This is the continuity equation for component k.

2. Momentum Equation

The momentum equation is obtained by equating the rate of accumulation of momentum in the control volume, V_o, to the sum of the net momentum flux into V_o and the forces acting on the control volume. There are two kinds of forces: body forces and surface forces. The only body force considered here is that due to gravity, $\underline{g}$, and the surface forces are divided into pressure, P, and shear forces, $\underline{\tau}$.

Hence:

$$\frac{\partial}{\partial t}\int_{V_o} \rho\, \underline{v}\, dV = -\int_{S_o} \rho\, (\underline{v}\,\underline{v}) \cdot d\underline{S} - \int_{S_o} (P + \underline{\tau})\, d\underline{S} + \int_{V_o} \rho\, \underline{g}\, dV \qquad \text{(III-16)}$$

where $-\int_{S_o} \rho\, (\underline{v}\,\underline{v}) \cdot d\underline{S}$ denotes the net flux of momentum into the control volume by bulk flow.

If the vector $\underline{v}$ is defined as:

$$\underline{v} = v_1\underline{e}_1 + v_2\underline{e}_2 + v_3\underline{e}_3 \qquad \text{(III-17)}$$

where $\underline{e}_1$, $\underline{e}_2$ and $\underline{e}_3$ are unit vectors, the dyadic product $(\underline{v}\,\underline{v})$ is given by:

$$(\underline{v}\,\underline{v}) = \begin{pmatrix} v_1v_1 & v_1v_2 & v_1v_2 \\ v_2v_1 & v_2v_2 & v_2v_3 \\ v_3v_1 & v_3v_2 & v_3\,v_3 \end{pmatrix} \qquad \text{(III-18)}$$

Transforming the surface integrals in Equation (III-16) to volume integrals by Green's theorem and using the same argument for the arbitrary size of the control volume gives:

$$\frac{\partial \underline{v}\rho}{\partial t} = -\underline{\nabla} \cdot (\rho\, \underline{v}\,\underline{v}) - \underline{\nabla} P - \underline{\nabla} \cdot \underline{\tau} + \rho\, \underline{g} \qquad \text{(III-19)}$$

The dyadic product may be split:

$$\rho\frac{\partial \underline{v}}{\partial t} + \underline{v}\frac{\partial \rho}{\partial t} = - \underline{v}\,\underline{\nabla} \cdot \rho\,\underline{v} - \rho\,\underline{v} \cdot \underline{\nabla}\,\underline{v} - \underline{\nabla} P - \underline{\nabla} \cdot \underline{\tau} + \rho\,\underline{g} \qquad \text{(III-20)}$$

Multiplying Equation (III-4) by $\underline{v}$ gives:

$$\underline{v}\frac{\partial \rho}{\partial t} = - \underline{v}\,\underline{\nabla} \cdot \rho\,\underline{v} \qquad \text{(III-21)}$$

which is subtracted from Equation (III-20):

$$\rho\frac{D\underline{v}}{Dt} = - \underline{\nabla} P - \underline{\nabla} \cdot \underline{\tau} + \rho\,\underline{g} \qquad \text{(III-22)}$$

The stress tensor $\underline{\tau}$ is given by:

$$\underline{\tau} = - \mu\,(\underline{\nabla} \cdot \underline{v} + (\underline{\nabla} \cdot \underline{v})^{+}) + (\tfrac{2}{3}\mu - \kappa)(\underline{\nabla} \cdot \underline{v})\,\underline{\delta}$$

where $\underline{\delta}$ is the unit tensor, $(\underline{\nabla} \cdot \underline{v})^{+}$ is the transpose of $\underline{\nabla} \cdot \underline{v}$, μ is the "shear viscosity" (or just "viscosity") and κ is the "bulk viscosity". The latter is very small for gases and is neglected. The stress tensor is therefore:

$$\underline{\tau} = - \mu\,\{\,\underline{\nabla} \cdot \underline{v} + (\underline{\nabla} \cdot \underline{v})^{+} - \tfrac{2}{3}(\underline{\nabla} \cdot \underline{v})\,\underline{\delta}\,\} \qquad \text{(III-23)}$$

Hence Equation (III-22) becomes:

$$\rho\frac{D\underline{v}}{Dt} = - \underline{\nabla} P + \underline{\nabla} \cdot \mu\,\{\,\underline{\nabla} \cdot \underline{v} + (\underline{\nabla} \cdot \underline{v})^{+} - \tfrac{2}{3}(\underline{\nabla} \cdot \underline{v})\,\underline{\delta}\,\} + \rho\,\underline{g} \qquad \text{(III-24)}$$

3. Mechanical Energy Equation

The mechanical energy equation is required for simplifying the energy equation which will be derived in the following section. The mechanical energy equation is obtained by forming the dot product of Equation(III-22) with $\underline{v}$:

$$\rho \frac{D}{Dt}\left(\frac{1}{2} v^2\right) = - \underline{v} \cdot \underline{\nabla} P - \underline{v} \cdot \left[\underline{\nabla} \cdot \underline{\tau}\right] + \rho \underline{v} \cdot \underline{g} \qquad \text{(III-25)}$$

The following identities are given without proof:

$$- \underline{v} \cdot \underline{\nabla} P = P \underline{\nabla} \cdot \underline{v} - \underline{\nabla} \cdot P \underline{v} \qquad \text{(III-26)}$$

$$- \underline{v} \cdot \left[\underline{\nabla} \cdot \underline{\tau}\right] = \underline{\tau} : \underline{\nabla} \underline{v} - \underline{\nabla} \cdot \left[\underline{\tau} \cdot \underline{v}\right] \qquad \text{(III-27)}$$

$\underline{\tau} : \underline{\nabla} \underline{v}$ is the viscous dissipation denoted by $- \phi$.

Equation (III-25) can therefore be simplified:

$$\rho \frac{D}{Dt}\left(\frac{1}{2} v^2\right) = P \underline{\nabla} \cdot \underline{v} - \underline{\nabla} \cdot P \underline{v} - \phi - \underline{\nabla} \cdot \left[\underline{\tau} \cdot \underline{v}\right] + \rho \underline{v} \cdot \underline{g} \qquad \text{(III-28)}$$

4. Energy Equation

The total energy of a mass of fluid can be expressed by the sum of its internal and kinetic energy. The rate at which energy therefore accumulates in the control volume is:

$$\frac{\partial}{\partial t} \int_{V_o} \rho \left(\hat{E} + \frac{1}{2} v^2\right) dV$$

where $\hat{E}$ is the internal energy per unit mass of fluid.

The total energy of the control volume changes due to:

a) energy transport by bulk flow, i.e.:

$$-\int_{S_o} \rho \underline{v} \left(\hat{E} + \frac{1}{2} v^2\right) \cdot d\underline{S}$$

b) energy transport by thermal and enthalpy diffusion:

$$-\int_{S_o} (\underline{q} + \underline{H}_d) \cdot d\underline{S}$$

c) work done against gravity:

$$\int_{V_o} \rho \, \underline{v} \cdot \underline{g} \; dV$$

d) work done against surface force:

$$-\int_{S_o} (\underline{\tau} \cdot \underline{v} + P \, \underline{v}) \cdot d\underline{S}$$

Hence, applying Equation (III-1) for the conservation of total energy, and using Green's theorem:

$$\begin{aligned} \frac{\partial}{\partial t} \rho \left(\hat{E} + \frac{1}{2} v^2\right) = & - \underline{\nabla} \cdot \rho \, \underline{v} \left(\hat{E} + \frac{1}{2} v^2\right) - \underline{\nabla} \cdot \underline{q} \\ & - \underline{\nabla} \cdot \underline{H}_d + \rho \, \underline{v} \cdot \underline{g} \\ & - \underline{\nabla} \cdot P \, \underline{v} - \underline{\nabla} \cdot \left[\underline{\tau} \cdot \underline{v}\right] \end{aligned} \qquad \text{(III-29)}$$

Introducing the substantive derivative reduces Equation (III-29) to:

$$\begin{aligned} \rho \frac{D}{Dt} \left(\hat{E} + \frac{1}{2} v^2\right) + \left(\hat{E} + \frac{1}{2} v^2\right) \frac{\partial \rho}{\partial t} = & \\ - \left(\hat{E} + \frac{1}{2} v^2\right) \underline{\nabla} \cdot \rho \, \underline{v} - \underline{\nabla} \cdot \underline{q} - \underline{\nabla} \cdot \underline{H}_d & \\ + \rho \, \underline{v} \cdot \underline{g} - \underline{\nabla} \cdot P \, \underline{v} - \underline{\nabla} \cdot \left[\underline{\tau} \cdot \underline{v}\right] & \end{aligned} \qquad \text{(III-30)}$$

Multiplying the total continuity Equation (III-4) by $\left(\hat{E} + \frac{1}{2} v^2\right)$

and subtracting the result from Equation (III-30) gives:

$$\rho \frac{D}{Dt}\left(\hat{E} + \frac{1}{2} v^2\right) = - \underline{\nabla} \cdot \underline{q} - \underline{\nabla} \cdot \underline{H}_d + \rho \underline{v} \cdot \underline{g} - \underline{\nabla} \cdot P \underline{v} - \underline{\nabla} \cdot \left[\underline{\tau} \cdot \underline{v}\right] \qquad \text{(III-31)}$$

The mechanical energy Equation (III-28) may now be used to remove the kinetic energy term from Equation (III-31):

$$\rho \frac{D}{Dt} \hat{E} = - \underline{\nabla} \cdot \underline{q} - \underline{\nabla} \cdot \underline{H}_d - P \underline{\nabla} \cdot \underline{v} + \phi \qquad \text{(III-32)}$$

Equation (III-32) is the desired energy equation. A more useful form is obtained by expressing the internal energy in terms of temperature and the specific heat.

The total internal energy, E, of a mass of fluid is related to the total enthalpy, H, by the thermodynamic relation:

$$H = E + P V \qquad \text{(III-33)}$$

or

$$dH = dE + d(P V) \qquad \text{(III-34)}$$

In general, the enthalpy of a system is a function of its temperature, pressure and the masses of the various chemical components present, i.e.:

$$H = H(T, P, m_1, m_2, \ldots m_N) \qquad \text{(III-35)}$$

where m_k is the mass of chemical species k in the system. Forming the total differential of Equation (III-35):

$$dH = \left(\frac{\partial H}{\partial T}\right)_{P,m} dT + \sum_{k=1}^{N} \left(\frac{\partial H}{\partial m_k}\right)_{\substack{T,P \\ m_i \\ i \neq k}} dm_k + \left(\frac{\partial H}{\partial P}\right)_{T,m} dP \qquad \text{(III-36)}$$

where the subscript m refers to constant total mass and composition.

Dividing Equation (III-36) by the total mass of the system, m, gives:

$$d\hat{H} = \left(\frac{\partial \hat{H}}{\partial T}\right)_{P,m} dT + \sum_{k=1}^{N} \left(\frac{\partial H}{\partial m_k}\right)_{\substack{T,P \\ m_i \\ i \neq k}} dw_k + \left(\frac{\partial \hat{H}}{\partial P}\right)_{T,m} dP \qquad \text{(III-37)}$$

where $\hat{H}$ is the enthalpy per unit mass and w_k is the mass fraction of species k. By definition, the specific heat at constant pressure and partial mass enthalpy are:

$$C_P = \left(\frac{\partial \hat{H}}{\partial T}\right)_{P,m} \qquad \text{(III-38)}$$

$$\overline{H}_k = \left(\frac{\partial H}{\partial m_k}\right)_{\substack{T,P \\ m_i \\ i \neq k}} \qquad \text{(III-39)}$$

Dividing Equation (III-34) by the total mass of the system and substituting Equation (III-37) yields:

$$d\hat{E} = C_P\, dT + \sum_{k=1}^{N} \overline{H}_k\, dw_k + \left[\left(\frac{\partial \hat{H}}{\partial P}\right)_{T,m} - \hat{V}\right] dP - P d\hat{V} \qquad \text{(III-40)}$$

where $\hat{V}$ is the volume per unit mass, i.e.:

$$\hat{V} = 1/\rho \qquad \text{(III-41)}$$

When the substantive derivative of Equation (III-40) is formed, i.e.:

$$\frac{D\hat{E}}{Dt} = C_P \frac{DT}{Dt} + \sum_{k=1}^{N} \overline{H}_k \frac{Dw_k}{Dt} + \left[\left(\frac{\partial \hat{H}}{\partial P}\right)_{T,m} - \hat{V}\right] \frac{DP}{Dt} - P \frac{D\hat{V}}{Dt} \qquad \text{(III-42)}$$

the result may be used to express the energy equation (III-32) in terms of the temperature T, i.e.:

$$\rho C_p \frac{DT}{Dt} = -\rho \sum_{k=1}^{N} \overline{H}_k \frac{Dw_k}{Dt} - \rho \left[\left(\frac{\partial \hat{H}}{\partial P} \right)_{T,m} - \hat{V} \right] \frac{DP}{Dt}$$

$$+ \rho P \frac{D\hat{V}}{Dt} - \underline{\nabla} \cdot \underline{q} - \underline{\nabla} \cdot \underline{H}_d - P \underline{\nabla} \cdot \underline{v} + \phi \qquad \text{(III-43)}$$

But from Equation (III-41):

$$\rho \hat{V} = 1$$

and the following identity is valid:

$$\rho \frac{D\hat{V}}{Dt} = \rho \frac{D\ 1/\rho}{Dt} = -\frac{1}{\rho} \frac{D\rho}{Dt} \qquad \text{(III-44)}$$

From Equation (III-5):

$$P \rho \frac{D\hat{V}}{Dt} = P \underline{\nabla} \cdot \underline{v} \qquad \text{(III-45)}$$

Equation (III-43) therefore reduces to:

$$\rho C_p \frac{DT}{Dt} = -\rho \sum_{k=1}^{N} \overline{H}_k \frac{Dw_k}{Dt} - \rho \left(\frac{\partial \hat{H}}{\partial P} \right)_{T,m} \frac{DP}{Dt}$$

$$+ \frac{DP}{Dt} - \underline{\nabla} \cdot \underline{q} - \underline{\nabla} \cdot \underline{H}_d + \phi \qquad \text{(III-46)}$$

The energy fluxes $\underline{q}$ and $\underline{H}_d$ will be discussed next.

a) Energy Transfer by Conduction

Energy can be transferred through a fluid by conduction, i.e. molecules exchange energy on colliding, but their mean relative positions remain unchanged. The heat flux by conduction is given by Fourier's Law:

$$\underline{q} = -k \underline{\nabla} T \qquad \text{(III-47)}$$

b) Energy Transfer by Enthalpy Diffusion

When molecules diffuse under a concentration gradient from a region of high to low temperature, they carry enthalpy with them and hence there is an enthalpy flux. This flux is given by:

$$\underline{H}_d = \sum_{k=1}^{N} \overline{H}_k \, \underline{j}_k \qquad \text{(III-48)}$$

Hence:

$$\underline{\nabla} \cdot \underline{H}_d = \underline{\nabla} \cdot \left(\sum_{k=1}^{N} \overline{H}_k \, \underline{j}_k \right)$$

$$= \sum_{k=1}^{N} \underline{\nabla} \cdot \left(\overline{H}_k \, \underline{j}_k \right)$$

$$= \sum_{k=1}^{N} \underline{j}_k \cdot \underline{\nabla} \, \overline{H}_k + \sum_{k=1}^{N} \overline{H}_k \, \underline{\nabla} \cdot \underline{j}_k \qquad \text{(III-49)}$$

Substituting Equation (III-47) and (III-49) into the energy equation (III-46) gives:

$$\rho \, C_p \, \frac{DT}{Dt} = - \rho \left(\frac{\partial \hat{H}}{\partial P} \right)_{T,m} \frac{DP}{Dt} + \frac{DP}{Dt} + \underline{\nabla} \cdot k \, \underline{\nabla} \, T$$

$$- \sum_{k=1}^{N} \underline{j}_k \cdot \underline{\nabla} \, \overline{H}_k + \phi \qquad \text{(III-50)}$$

This equation can be simplified further by expressing $\left(\frac{\partial \hat{H}}{\partial P} \right)_{T,m}$ in terms of $\hat{V}$ and T. From thermodynamics:

$$\left(\frac{\partial \hat{H}}{\partial P} \right)_{T,m} = T \left(\frac{\partial \hat{S}}{\partial P} \right)_{T,m} + \hat{V} \qquad \text{(III-51)}$$

and:

$$\left(\frac{\partial \hat{S}}{\partial P}\right)_{T,m} = - \left(\frac{\partial \hat{V}}{\partial T}\right)_{P,m} \qquad \text{(III-52)}$$

which is a Maxwell relation. Thus:

$$\left(\frac{\partial \hat{H}}{\partial P}\right)_{T,m} = - T \left(\frac{\partial \hat{V}}{\partial T}\right)_{P,m} + \hat{V} \qquad \text{(III-53)}$$

Substituting Equation (III-53) into Equation (III-50) and rearranging gives the energy equation in the most useful form for the present purpose:

$$\rho C_p \frac{DT}{Dt} = \underline{\nabla} \cdot k \underline{\nabla} T + \left(\frac{\partial \ell n \hat{V}}{\partial \ell n T}\right)_{P,m} \frac{DP}{Dt} - \sum_{k=1}^{N} \underline{j}_k \underline{\nabla} \overline{H}_k + \phi$$

(III-54)

B. Summary of General Transport Equations

$$\frac{D\rho}{Dt} = -\rho \underline{\nabla} \cdot \underline{v} \qquad \text{(III-5)}$$

$$\rho \frac{Dw_k}{Dt} = \underline{\nabla} \cdot \rho D \underline{\nabla} w_k \qquad \text{(III-15)}$$

$$\rho \frac{D\underline{v}}{Dt} = -\underline{\nabla} P + \underline{\nabla} \cdot \mu \{ \underline{\nabla} \cdot \underline{v} + (\underline{\nabla} \cdot \underline{v})^+ - \frac{2}{3} (\underline{\nabla} \cdot \underline{v}) \underline{\delta} \} + \rho \underline{g} \qquad \text{(III-24)}$$

$$\rho C_P \frac{DT}{Dt} = \underline{\nabla} \cdot k \underline{\nabla} T + \left(\frac{\partial \ell n \hat{V}}{\partial \ell n T} \right)_{P,m} \frac{DP}{Dt} - \sum_{k=1}^{N} \underline{j}_k \underline{\nabla} \overline{H}_k + \phi \qquad \text{(III-54)}$$

C. Reduced Transport Equations

The transport equations (III-5), (III-15), (III-24) and (III-54) constitute a set of coupled, non-linear partial differential equations with variable coefficients. Since there are no analytical techniques to solve such equations in general and even numerical methods are difficult to apply, a simple particle-collector geometry and mode of operation were chosen. These are:

1. The particle-collector consists of two infinite, parallel and horizontal plates. The plates extend to infinity in the x- and z-direction; see Fig.1

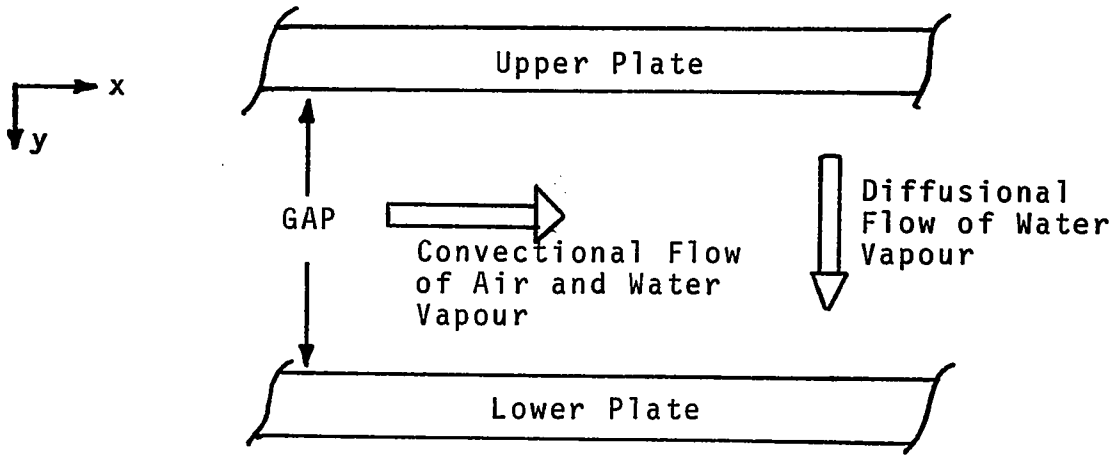

FIG. 1 MASS FLUXES IN PARTICLES COLLECTOR

2. Air flows between and parallel to the plates under a pressure gradient. The flow is laminar.

3. The upper and lower plates are saturated with water and do not permit air to pass. The temperature of the upper plate is higher than that of the lower one, so that water vapour diffuses downwards as shown by the arrow in Fig. 1 .
4. The particle-collector is operated under developed conditions, i.e. all dependent variables are functions of y only.

In addition to the above conditions, it was decided to make the following assumptions in order to simplify the general transport equations further:

5. The fluid in the particle-collector is regarded as a binary mixture of water vapour and air (denoted by A and B, respectively). Although air is itself a mixture of various gases, its constituents behave sufficiently similarly - at least in comparison with condensing water vapour - in order to be treated as a single component.
6. The air-water vapour mixture is ideal.
7. The rheological behaviour of the fluid in the particle-collector is Newtonian. Its bulk viscosity is negligible.
8. Viscous dissipation is negligible.

Conditions 1 to 8 reduce the general transport equations to a set of ordinary differential equations with variable coefficients. Before presenting these simplifications, a simple physical argument is given for the existence of a bulk flow velocity perpendicular to the plates, i.e. why $v_y \neq 0$.

1. Bulk Flow Perpendicular to Plates

A control surface, MN, is considered which is parallel to the plates and completely pervious to the flow of material; see Fig. 2 .

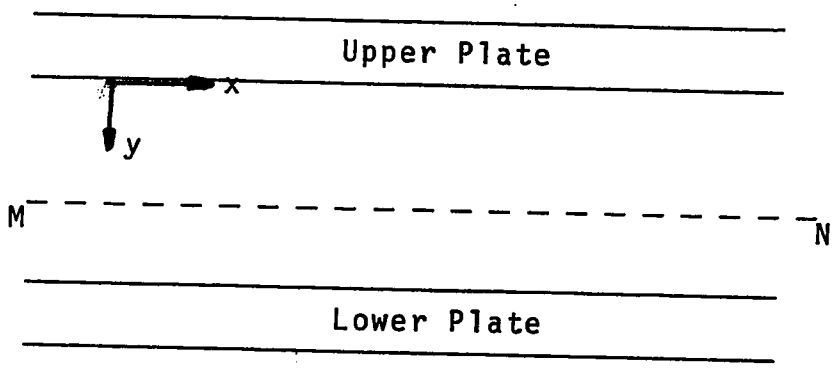

FIG. 2 CONTROL SURFACE IN PARTICLE COLLECTOR

Since the conditions in the particle-collector are developed, and no air passes through the plates, there can be no net flow of air across plane MN. Hence the air is "stagnant" as far as its motion in the y-direction is concerned.

On the other hand, a net flow of water vapour occurs across the control surface MN. The water vapour concentration profile remains unchanged because the rate at which water evaporates from the upper plate equals the rate at which water vapour condenses on the lower plate.

The general nature of the water vapour and air concentration profiles is considered next. Since water vapour diffuses towards and condenses on the lower plate, the water vapour concentration decreases with increasing y; see Fig. 3 .

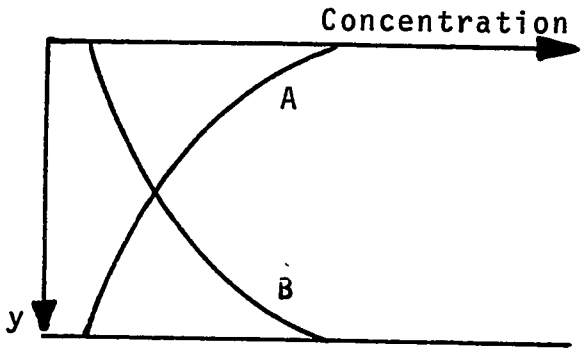

FIG. 3 APPROXIMATE CONCENTRATION PROFILES IN PARTICLE COLLECTOR

The total pressure at any x is constant (see also Appendix I) and hence the air concentration must increase with increasing y.

Since molecules diffuse in the direction of lower concentration, the nature of the water vapour and air profiles implies that water vapour and air diffuse in the direction of increasing and decreasing y, respectively.

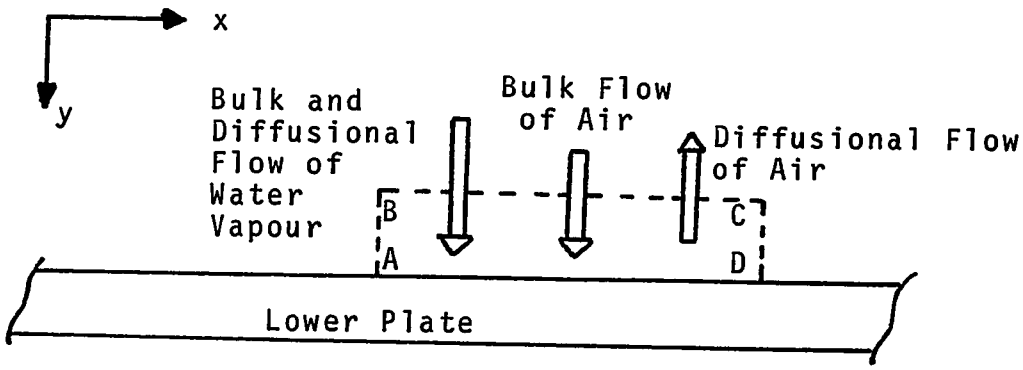

FIG. 4 CONTROL VOLUME IN PARTICLE COLLECTOR

On consideration of the control volume ABCD at the lower plate (Fig. 4) it is evident that, during a small time interval,

water vapour is removed from the control volume by condensation at the lower plate, and that a nearly equal amount diffuses into the control volume across BC.

However, air will tend to diffuse away from the lower plate since its concentration decreases with decreasing y. Thus at the end of the small time interval, fewer molecules are in the control element than at the beginning. Fewer molecules in the volume means a reduction in pressure which causes a bulk flow of fluid-mixture into ABCD.

Since the diffusion of air molecules out of and their return by bulk flow into the element ABCD occur simultaneously (rather than consecutively as described above), no noticeable reduction in pressure occurs. Furthermore, since there is no net motion of air in the y-direction (as pointed out earlier), the diffusional and bulk flow of air must be equal and opposite.

In summary it may be said that there is a bulk flow in the y-direction and directed towards the lower plate, i.e. $v_y > 0$. This flow is caused by the diffusion of water vapour through the air and it is sometimes referred to as "Stefan Flow". It is this flow which gives rise to diffusiophoresis.

Having shown that $v_y \neq 0$, the general transport equations may be simplified with the aid of conditions 1 to 8.

2. Total Continuity Equation

$$\frac{d}{dy} \rho v_y = 0 \qquad \text{(III-55)}$$

or:

$$\rho v_y = C1 \qquad \text{(III-56)}$$

where C1 is an integration constant.

3. Continuity Equation for Water Vapour

$$\frac{d}{dy} \rho_A v_y = \frac{d}{dy} \rho D \frac{dw_A}{dy} \qquad \text{(III-57)}$$

which may be integrated to:

$$\rho_A v_y = \rho D \frac{dw_A}{dy} + C2 \qquad \text{(III-58)}$$

where C2 is another integration constant.

4. Continuity Equation for Air

$$\frac{d}{dy} \rho_B v_y = \frac{d}{dy} \rho D \frac{dw_B}{dy} \qquad \text{(III-59)}$$

or, upon integration:

$$\rho_B v_y = \rho D \frac{dw_B}{dy} + C3 \qquad \text{(III-60)}$$

where C3 is a further integration constant. Since $\rho_B v_y$ and $\rho D\, dw_B/dy$ denote the transport of air by bulk flow and molecular diffusion, respectively, and since there is no net motion of air in the y-direction, the two modes in which B is transported must be equal and in opposite directions, i.e.:

$$\rho_B v_y = \rho D \frac{dw_B}{dy} \qquad \text{(III-61)}$$

Hence: $C3 = 0$ (III-62)

Adding Equation (III-61) and Equation (III-58), and recalling that:

$$w_A + w_B = 1 \qquad \text{(III-63)}$$

so that $dw_A/dy = - dw_B/dy$, one obtains:

$$(\rho_A + \rho_B) v_y = C2 \qquad \text{(III-64)}$$

But since:

$$\rho_A + \rho_B = \rho \qquad \text{(III-65)}$$

therefore:

$$\rho v_y = C2 \qquad \text{(III-66)}$$

and hence, by comparing Equation (III-66) and (III-56):

$$C1 = C2 \qquad \text{(III-67)}$$

Substituting Equation (III-66) into Equation (III-58) gives:

$$(\rho_A - \rho)\, v_y = \rho D \frac{dw_A}{dy} \qquad \text{(III-68)}$$

or:

$$v_y = \frac{D}{(w_A - 1)} \frac{dw_A}{dy} \qquad \text{(III-69)}$$

The right hand side of this expression is not zero so that $v_y \neq 0$ as was already proved by the arguments presented in Section III-C-1.

Equation (III-69) may be rewritten with the aid of Equation (III-67), i.e.:

$$\frac{dw_A}{dy} = \frac{C1\ (w_A - 1)}{\rho D} \qquad \text{(III-70)}$$

and:

$$v_y = C1/\rho \qquad \text{(III-71)}$$

Since C1 is a constant, it may be evaluated at any point in the fluid. The upper plate is the most convenient point because all variables other than dw_A/dy are known. The latter has to be estimated.

5. Momentum Equation

The general momentum equation (III-24) is a vector equation which has three components representing the conser-

vation of x, y and z-momentum. In the present particle-collector, the x and y-momentum equations are non-vanishing, but only the former is of importance. The significance of the latter is discussed in Appendix I. The z-momentum equation vanishes because there is no momentum transfer in this direction.

The x-momentum equation reduces under the present conditions to:

$$\rho v_y \frac{dv_x}{dy} = - \frac{dP}{dx} + \frac{d}{dy} \mu \frac{dv_x}{dy} \qquad \text{(III-72)}$$

where it is assumed that P is only a function of x (see also Appendix I). dP/dx is assumed to be constant and denoted by DELPX. Equation (III-72) hence becomes:

$$C1 \frac{dv_x}{dy} = - DELPX + \frac{d}{dy} \mu \frac{dv_x}{dy} \qquad \text{(III-73)}$$

where use was made of Equation (III-56). Equation (III-73) can be integrated once and rearranged to give:

$$\frac{dv_x}{dy} = \frac{1}{\mu} \left[C1 \cdot v_x + DELPX \cdot y - C4 \right] \qquad \text{(III-74)}$$

where C4 is an integration constant.

6. Energy Equation

For an ideal gas mixture:

$$\left(\frac{\partial \ell n V}{\partial \ell n T} \right)_{P,m} = 1 \qquad \text{(III-75)}$$

and:

$$\bar{H}_k = H_k \qquad \text{(III-76)}$$

so that the general energy equation reduces to:

$$\rho v_y C_P \frac{dT}{dy} = \frac{d}{dy} k \frac{dT}{dy} + v_x \frac{dP}{dx} - \sum_{k=1}^{N} j_{y,k} \frac{dH_k}{dy} \qquad \text{(III-77)}$$

where $j_{y,k}$ denotes the diffusional mass flux of species k in the y-direction.

Further, for an ideal gas the enthalpy is defined as:

$$H_k = \int_1 C_{Pk} \, dT \qquad \text{(III-78)}$$

where '1' and C_{Pk} denote a convenient reference state and the specific heat at constant pressure of species k, respectively.

The derivative with respect to y of Equation (III-78) can be written as:

$$\frac{dH_k}{dy} = \frac{d}{dy} \int_1 C_{Pk} \, dT = C_{Pk} \frac{dT}{dy} \qquad \text{(III-79)}$$

Equation (III-77) thus becomes for a two component mixture:

$$C1 \cdot C_P \frac{dT}{dy} = \frac{d}{dy} k \frac{dT}{dy} + v_x \, DELPX + \rho D \frac{dw_A}{dy} (C_{PA} - C_{PB}) \frac{dT}{dy} \qquad \text{(III-80)}$$

where $j_{y,k}$ were replaced by Fick's law, Equation (III-14), and use was also made of Equation (III-56) and (III-63).

The derivative dw_A/dy can be replaced by Equation (III-70), and Equation (III-80) therefore becomes upon rearrangement:

$$\frac{d}{dy} k \frac{dT}{dy} = \left(C1 \cdot C_{PA}\right) \frac{dT}{dy} - v_x \, DELPX \qquad \text{(III-81)}$$

In order to solve this second order equation numerically, it is convenient to rewrite it in terms of two first order equations, i.e.:

$$\frac{d}{dy} TKTDOT = \left(C1 \cdot C_{PA}\right) \frac{TKTDOT}{k} - v_x \, DELPX \qquad \text{(III-82)}$$

$$\frac{dT}{dy} = \frac{TKTDOT}{k} \qquad \text{(III-83)}$$

7. Boundary Conditions

The reduced transport equations (III-70), (III-74), (III-82), and (III-83) have to be solved simultaneously subject to the following boundary conditions:

At $y = 0$

$$w_A = w_{AU} \qquad \text{(III-85)}$$

$$v_x = 0 \qquad \text{(III-86)}$$

$$T = TU \qquad \text{(III-87)}$$

and at $y = GAP$[†]

$$w_A = w_{AL} \qquad \text{(III-88)}$$

$$v_x = 0 \qquad \text{(III-89)}$$

$$T = TL \qquad \text{(III-90)}$$

Since both plates contain liquid water, the gas mixture in the particle-collector is saturated with water vapour at $y = 0$ and $y = GAP$. w_{AU} and w_{AL} are therefore not independent but given by the vapour pressure relationship for water and TU and TL, respectively.

[†] The plate spacing is denoted by GAP.

In order to solve the transport equations by a numerical integration technique starting at y = 0, it is necessary to know the values of TKTDOT at y = 0 and the integration constants C1 and C4. These constants may be determined in various ways. In this work they are related to the concentration and temperature gradients at the upper plate, i.e.:

$$C1 = \left[\frac{\rho D}{w_A - 1}\frac{dw_A}{dy}\right]_u \qquad \text{(III-91)}$$

$$C4 = \left[-\mu\frac{dv_x}{dy}\right]_u \qquad \text{(III-92)}$$

and

$$\left[TKTDOT\right]_u = \left[k\frac{dT}{dy}\right]_u \qquad \text{(III-93)}$$

where the subscript 'u' indicates the expression in brackets is to be evaluated at the upper plate. Equations (III-91), (III-92), and (III-93) are obtained by substituting the boundary conditions at y = 0 into Equations (III-70), (III-74), and (III-82).

Since ρ, D, w_A, μ, and k are known at y = 0, only the gradients $\left[dw_A/dy\right]_u$, $\left[dv_x/dy\right]_u$, and $\left[dT/dy\right]_u$ remain to be evaluated. This can be achieved by integrating the transport equations separately and assuming constant coefficients. The resulting gradients are only approximate and their use in the simultaneous numerical integration of Equations (III-70), (III-74), (III-82), and (III-83) may not satisfy the boundary conditions at y = GAP exactly. The approximate gradients serve, however, as good starting values of a numerical search for the correct gradients at the upper plate.

D. Approximate Solutions of the Transport Equations and Gradients at the Upper Plate

1. Continuity Equation

The diffusivity, D, in Equation (III-70) is assumed to be constant. The density, ρ, of a binary ideal gas mixture is given by:

$$\rho = \frac{P\ M_A}{R_c\ T}\ \frac{1}{M_R - w_A\ M_{RS}} \qquad \text{(III-94)}$$

where M_A, M_B = molecular weight of water-vapour and air, respectively

R_c = universal gas constant

$$M_R = M_A/M_B \qquad \text{(III-95)}$$

$$M_{RS} = M_R - 1 \qquad \text{(III-96)}$$

Substituting Equation (III-94) into Equation (III-70) and integrating gives:

$$\int_o^y \frac{dw_A}{(w_A - 1)(M_R - w_A\ M_{RS})} = CR\ .\ y + I_1 \qquad \text{(III-97)}$$

where:

$$CR = C1\left(\frac{R_c\ T}{P\ M_A\ D}\right) \qquad \text{(III-98)}$$

and: I_1 is an integration constant

Equation (III-97) can be expressed in terms of partial fractions, i.e.:

$$\int_o^y \frac{dw_A}{(w_A - 1)} + M_{RS}\int_o^y \frac{dw_A}{(M_R - w_A\ M_{RS})} = CR\ .\ y + I_1 \qquad \text{(III-99)}$$

and therefore:

$$\ell n \left(\frac{w_A - 1}{M_R - w_A M_{RS}} \right) = CR \cdot y + I_1 \qquad \text{(III-100)}$$

The boundary conditions:

$$y = 0 \qquad w_A = w_{AU}$$

$$y = GAP \qquad w_A = w_{AL}$$

can be used to eliminate the constants in Equation (III-100), giving:

$$\frac{w_A - 1}{M_R - w_A M_{RS}} = \left(\frac{M_R - w_{AU} M_{RS}}{w_{AU} - 1} \right)^{\left(\frac{y}{GAP} - 1\right)} \left(\frac{w_{AL} - 1}{M_R - w_{AL} M_{RS}} \right)^{\left(\frac{y}{GAP}\right)} \qquad \text{(III-101)}$$

Putting:

$$EC = \frac{M_R - w_{AU} M_{RS}}{w_{AU} - 1} \qquad \text{(III-102)}$$

$$F = \frac{w_{AL} - 1}{M_R - w_{AL} M_{RS}} \qquad \text{(III-103)}$$

Equation (III-101) may be written as:

$$\frac{w_A - 1}{M_R - w_A M_{RS}} = (EC.F)^{\frac{y}{GAP}} / EC \qquad \text{(III-104)}$$

Differentiating Equation (III-104) with respect to y gives:

$$\frac{dw_A}{dy} = (M_R - w_A M_{RS})^2 (EC.F)^{\frac{y}{GAP}} \left(\frac{\ell n(EC.F)}{GAP.EC} \right) \qquad \text{(III-105)}$$

At the upper plate, y=0 and therefore:

$$\left(\frac{dw_A}{dy} \right)_u = (M_R - w_A M_{RS})^2 \left(\frac{\ell n(EC.F)}{GAP.EC} \right) \qquad \text{(III-106)}$$

Hence, C1 can be determined from Equations (III-91) and (III-106).

2. Momentum Equation

Equation (III-74) can be integrated by assuming that μ is constant. Defining the constants:

$$\alpha = C1/\mu \qquad \text{(III-107)}$$

$$\beta = DELPX/\mu \qquad \text{(III-108)}$$

$$\gamma = C4/\mu \qquad \text{(III-109)}$$

allows Equation (III-74) to be written as:

$$(D' - \alpha)\, v_{\ddot{x}} = \beta y + \gamma \qquad \text{(III-110)}$$

where D' denotes the differential operator, d/dy. Equation (III-110) is a linear non-homogeneous differential equation whose complementary solution and particular integral are:

$$v_{xc} = A_0 \exp(\alpha y) \qquad \text{(III-111)}$$

and:

$$v_{xp} = A_1 y + A_2 \qquad \text{(III-112)}$$

respectively. A_0, A_1, and A_2 are constants which can be shown to be:

$$A_1 = -\beta/\alpha \qquad \text{(III-113)}$$

$$A_2 = -(\beta + \alpha\gamma)/\alpha^2 \qquad \text{(III-114)}$$

The general solution of Equation (III-110) is therefore:

$$v_x = A_0 \exp(\alpha y) - (\beta/\alpha)\, y - (\beta + \alpha\gamma)/\alpha^2 \qquad \text{(III-115)}$$

Using the boundary conditions:

$$y = 0 \qquad v_x = 0$$

$$y = GAP \qquad v_x = 0$$

gives:

$$A_0 = (\beta + \alpha\gamma)/\alpha^2 \qquad \text{(III-116)}$$

and:

$$\frac{\beta + \alpha}{\alpha^2} = \left(\frac{\beta}{\alpha}\right)\left(\frac{GAP}{\exp(\alpha\, GAP) - 1}\right) \qquad \text{(III-117)}$$

Hence Equation (III-115) becomes:

$$v_x = \left(\frac{GAP.\beta}{\alpha}\right)\left[\frac{\exp(\alpha y) - 1}{\exp(\alpha\, GAP) - 1} - \frac{y}{GAP}\right] \qquad \text{(III-118)}$$

or:

$$v_x = \frac{GAP.DELPX}{C1}\left[\frac{\exp\left(\frac{C1.y}{\mu}\right) - 1}{\exp\left(\frac{C1.GAP}{\mu}\right) - 1} - \frac{y}{GAP}\right] \qquad \text{(III-119)}$$

Differentiating with respect to y:

$$\frac{dv_x}{dy} = \frac{GAP.DELPX}{C1}\left[\frac{\frac{C1}{\mu}\exp\left(\frac{C1.y}{\mu}\right)}{\exp\left(\frac{C1.GAP}{\mu}\right)} - \frac{1}{GAP}\right] \qquad \text{(III-120)}$$

and:

$$\left(\frac{dv_x}{dy}\right)_u = \frac{DELPX}{C1}\left[\frac{GAP.C1}{\mu\left(\exp\left(\frac{C1.GAP}{\mu}\right) - 1\right)} - 1\right] \qquad \text{(III-121)}$$

C4 can therefore be found from Equations (III-121) and (III-92).

3. Energy Equation

The energy equation (III-81) is in a convenient form for obtaining an approximate solution. It is assumed that k, C_{PA}, C_{PB} and w_A are constant and evaluated at the upper plate. The last term in Equation (III-81), i.e. v_x DELPX, may be neglected in the approximate solution because it is very small in comparison with the other terms. Equation (III-81) may therefore be written as:

$$\frac{d^2T}{dy^2} = K1\,\frac{dT}{dy} \qquad \text{(III-122)}$$

where: $K1 = \left[C1.C_{PA} / k\right]_u$ (III-123)

Equation (III-122) is a homogeneous linear differential equation, the solution of which is:

$$T = G + HC\exp(K1.y) \quad \text{(III-124)}$$

where the integration constants G and HC are evaluated from the boundary conditions:

$y = 0$ $T = TU$

$y = GAP$ $T = TL$

and found to be:

$$G = \frac{TU \exp(K1.GAP) - TL}{\exp(K1.GAP - 1)} \quad \text{(III-125)}$$

$$HC = \frac{TU - TL}{1 - \exp(K1.GAP)} \quad \text{(III-126)}$$

Hence the approximate value for the differential coefficient dT/dy at the upper plate is:

$$\left[\frac{dT}{dy}\right]_u = HC.K1 = \frac{K1\,(TU - TL)}{1 - \exp(K1.GAP)} \quad \text{(III-127)}$$

Hence $\left[TKTDOT\right]_u$ can be obtained approximately from Equations (III-93) and (III-127).

E. Physical Properties of Gas Mixture

In order to obtain accurate numerical solutions to the transport equations, the various transport coefficients were regarded as functions of temperature and composition. Literature data were used for the transport coefficients of the pure components and they were then combined to give the values for air-water vapour mixtures.

1. Diffusivity

The binary diffusion coefficient for water vapour in air was evaluated from the formula given in the International Critical Tables[69]:

$$D = 0.220 \left(\frac{T}{273}\right)^{1.75} \left(\frac{1}{P}\right) \qquad \text{(III-128)}$$

where: D = diffusivity, cm^2/sec

T = absolute temperature, ^oK

P = pressure, atm

2. Viscosity

F. G. Keyes[70] suggested the following semi-empirical formula for the viscosity for air and water vapour:

$$\mu_{A,B} = \frac{a_o T}{1 + (a/T)*10^{-a_1/T}} * 10^{-5} \qquad \text{(III-129)}$$

where: $\mu_{A,B}$ = viscosity of A or B, gram/(cm sec)

T = absolute temperature, ^oK

and:

	Water Vapour, A	Air, B
a_o =	1.501	1.488
a =	446.8	122.1
a_1 =	0	5.0

Equation (III-129) is accurate to within about 3%. The pressure dependence of μ was neglected for present operating conditions.

3. Thermal Conductivity of Pure Components

F. G. Keyes suggested an equation similar to Equation (III-129) for the thermal conductivity(70):

$$k_{A,B} = \frac{c_o T}{1 + (c/T)\ 10^{-c_1/T}} * 10^{-5} \qquad \text{(III-130)}$$

where: $k_{A,B}$ = thermal conductivity of A or B, cals/(sec cm ^oK)

T = absolute temperature, ^oK

and:

	Water Vapour, A	Air, B
c_o =	1.546	0.632
c =	1737.3	245.0
c_1 =	12.0	12.0

Equation (III-130) is also accurate to within 3% and the pressure effect is neglected.

4. Viscosity and Thermal Conductivity of a Water Vapour-Air Mixture

The viscosity and thermal conductivity of a water vapour-air mixture can be obtained from values for the pure components by Wilke's formula(52):

$$\mu = \sum_{k=1}^{N} \frac{x_k \mu_k}{\sum_{j=1}^{N} x_j \Psi_{kj}} \qquad \text{(III-131)}$$

$$k = \sum_{k=1}^{N} \frac{x_k k_k}{\sum_{j=1}^{N} x_j \Psi_{kj}} \qquad \text{(III-132)}$$

where:

$$\Psi_{kj} = \frac{1}{\sqrt{8}}\left(1 + \frac{M_k}{M_j}\right)^{-1/2}\left[1 + \frac{\mu_k}{\mu_j}\left(\frac{M_j}{M_k}\right)^{1/4}\right]^2 \qquad \text{(III-133)}$$

x_k = mole fraction of component k

M_k = molecular weight of component k

5. Specific Heats of Pure Components

The three term power series suggested by Hougen, Watson and Ragatz [71] was used for the specific heat of component k:

$$C_{Pk} = \frac{1}{M_k}(a_c + b_c T + c_c T^2) \qquad \text{(III-134)}$$

The constants a_c, b_c and c_c have the following values:

	a_c	$10^3 b_c$	$10^6 c_c$
N_2	6.457	1.389	-0.069
O_2	6.117	3.167	-1.005
H_2O, vapour	7.136	2.640	0.0459

The pressure effect was neglected.

6. Specific Heat of Water Vapour-Air Mixture

As stated in assumption 5 of Section III-C, the air was regarded as one component consisting of 21% O_2 and 79% N_2. Neglecting heat of mixing and combining the specific heats of nitrogen and oxygen in proportion of mole percent gives:

$$C_{PB} = 0.2202 + 6.077 \times 10^{-5} T - 9.158 \times 10^{-9} T^2 \qquad \text{(III-135)}$$

and also:

$$C_{PA} = 0.3964 + 1.467 \times 10^{-4} T + 2.55 \times 10^{-9} T^2 \qquad \text{(III-136)}$$

where the units are cals/(gram ^oK). The specific heat of a

water vapour - air mixture is therefore:

$$C_p = w_A \cdot C_{PA} + (1 - w_A)\, C_{PB} \qquad \text{(III-137)}$$

7. Saturated Vapour Pressure of Water

In order to determine the composition of the water vapour - air mixture at the plates, i.e. fin w_{AU} and w_{AL}, it was necessary to know the vapour pressure of water as a function of temperature. The International Critical Tables[69] give such data in tabular form. A power series was generated for this data so that interpolation was unnecessary and computer storage space could be conserved. The series was obtained by means of the CURFIT program developed by McGill University's Computing Centre. The expression used is:

$$PSAT = \exp (11.628596 - 3698.693 * TR - 238258.79 * TR^2) \qquad \text{(III-138)}$$

where:

PSAT = Saturated vapour pressure of water in atmospheres absolute

TR = 1/T, the reciprocal absolute temperature in $^oK^{-1}$

A three term power series was adequate to reproduce the steam table data to four significant figures.

8. Condensation between the Plates

When the partial pressure of water exceeds the local saturated vapour pressure, PSAT, condensation may occur and

a mist may form between the plates. The smoke particles act as condensation nuclei and only a low degree of supersaturation can therefore be maintained.

F. Particle Equations

As pointed out in Section II-A, the particle behaviour in a diffusing binary gas mixture is dependent on the Knudsen number which is the ratio of the mean free path of the gas molecules to the particle diameter. The mean free path of gas molecules is given by[53]:

$$\lambda \simeq \frac{k_B T}{\sqrt{2} P \pi \sigma^2} \qquad \text{(III-139)}$$

and the values of λ are presented for nitrogen, oxygen, and water vapour at a pressure of 1 atmosphere and temperatures of 300 and 373 ^{o}K below:

	300^{o}K	373^{o}K
λ_{N_2}, cms	$6.54*10^{-6}$	$8.14*10^{-6}$
λ_{O_2}, cms	$6.92*10^{-6}$	$8.59*10^{-6}$
λ_{H_2O}, cms	$5.47*10^{-6}$	$6.80*10^{-6}$

The diameter of cigarette smoke particles was found by Keith and Derrick[72] to be approximately $0.8*10^{-4}$ cms. The Knudsen number is therefore of the order of 0.1 which corresponds to the slip-flow regime[5]. Hence only the equations for large aerosol particles which were discussed in Section II are of interest here.

Particles in a diffusing binary mixture and in a temperature gradient experience four different forces: the diffusiophoretic force, $\underline{F}_{dp}$, the thermophoretic force, $\underline{F}_{tp}$,

the force due to gravity, $\underline{F}_g$, and the drag force, $\underline{F}_d$. According to Newton the sum of these forces is equal to the product of the mass and acceleration of the particles. Hence:

$$\rho \frac{\pi}{6} D_p^3 \frac{d\underline{v}_p}{dt} = \underline{F}_{dp} + \underline{F}_{tp} + \underline{F}_g - \underline{F}_d \qquad \text{(III-140)}$$

Since the particles are very small ($D_p \simeq 10^{-4}$ cms), the term on the left hand side of Equation (III-140) may be neglected. This is equivalent to saying that the particles always move with the velocity corresponding to the local forces or that the inertia of the particles is negligible, i.e.:

$$0 \simeq \underline{F}_{dp} + \underline{F}_{tp} + \underline{F}_g - \underline{F}_d \qquad \text{(III-141)}$$

This equation is the basis for the subsequent two models.

1. Model I

The simplest model consists of assuming that the particles move with the local fluid velocity, $\underline{v}$, and hence follow the fluid stream lines. The particle velocities in the x- and y-directions are therefore:

$$v_{yp} = v_y \qquad \text{(III-142)}$$

and

$$v_{xp} = v_x \qquad \text{(III-143)}$$

where v_y and v_x are obtained by solving the fluid transport equations.

This simple model implies that only the Stefan flow gives rise to the diffusiophoretic force in the y-direction (i.e. $F_{dpy} = 3 \pi \mu D_p v_y$) and that this is exactly equal to the Stokes drag in the same direction (i.e. $F_{dy} = -3 \pi \mu D_p v_{yp}$). All other forces are negligible.

The particle trajectory may be obtained by calculating the distance, SL, travelled by a particle in the x-direction during a certain time, i.e.:

$$SL = \int_o v_{xp} \, dt = \int_o v_x \, dt \qquad \text{(III-144)}$$

Since by definition:

$$v_y = dy / dt \qquad \text{(III-145)}$$

Equation (III-144) can be written as:

$$SL = \int_o (v_x / v_y) \, dy \qquad \text{(III-146)}$$

and a plot of x_p versus y constitutes the trajectory of a particle starting at the upper plate. It may be noted that the trajectories for this model coincide with the fluid stream lines.

The settling length of a particle starting at the upper plate, i.e. the distance which a particle travels in the x-direction before it reaches the lower plate,is therefore:

$$SL = \int_o^{GAP} (v_x / v_y) \, dy \qquad \text{(III-147)}$$

Similarly the settling time, i.e. the time taken by a particle to move from the upper plate to the lower plate, is:

$$ST = \int_o^{GAP} \frac{dy}{v_{yp}} = \int_o^{GAP} \frac{dy}{v_y} \qquad \text{(III-148)}$$

2. Model II

Model I may be extended by including the expressions for the diffusiophoretic and thermophoretic forces considered in Section II and by considering the gravitational effects as well.

Several equations for the diffusiophoretic force were discussed in Section II but only Waldmann's Equations(II-13) and (II-16) can be used without a prior experimental determination of the accommodation coefficients or other constants. Waldmann's equation may be written for the y-direction as:

$$F_{dpy} = - 3\pi \mu D_p (1 + x_B \sigma_{AB}) \frac{D}{x_B} \frac{dx_A}{dy} \qquad \text{(III-149)}$$

or

$$F_{dpy} = - 3\pi \mu D_p (1 + x_B \sigma_{AB}) \frac{D}{(x_A/M_A + x_B/M_B)^2 M_A M_B x_B} \frac{dw_A}{dy} \qquad \text{(III-150)}$$

where the slip-factor σ_{AB} was given by Waldmann as:

$$\sigma_{AB} = \frac{M_A - M_B}{x_A M_A + x_B M_B + \sqrt{M_A M_B}} \qquad \text{(III-151)}$$

or

$$\sigma_{AB} = A_w \left(\frac{M_A - M_B}{M_A + M_B}\right) + B_w \left(\frac{\sigma_A - \sigma_B}{\sigma_A + \sigma_B}\right) \qquad \text{(III-152)}$$

The latter equation is semi-empirical and represented Schmitt and Waldmann's experimental data[10,18] better than Equation (III-151). A_w and B_w were found to be 0.95 and -1.05, respectively and σ_{AB} for water vapour diffusing through air is therefore - 0.26.

Epstein's Equation (II-27) may be used for estimating the thermophoretic force. Although Brock's expressions are more accurate they cannot be used since the accommodation coefficients are unknown. Thermal conductivities of cigarette-smoke particles have not been reported in the literature and a value of $k_p = 10^{-3}$ cal./(sec cm ^oK), which corresponds to that of sand, was therefore chosen. Hence the ratio of the fluid to particle thermal conductivity is approximately 0.06 and the Epstein equation is valid, i.e. the thermophoretic force acting in the y-direction is:

$$F_{tpy} = -\frac{9}{4}\frac{\pi \mu^2 D_p}{\rho T}\left(\frac{2k}{2k + k_p}\right)\frac{dT}{dy} \qquad \text{(III-153)}$$

In case k_p was under-estimated significantly, Equation (III-153) would no longer be valid and one of Brock's expressions should be used. The thermophoretic force obtained from the latter would however be close to the value of F_{tpy} calculated from Equation (III-153) by using $k_p = 10^{-3}$ cal/(sec cm ^oK) since the force is not a very strong function of k_p. Furthermore, it will be shown that the thermophoretic force is very small in the particle collector of this study.

The force on a particle in the y-direction due to

gravity is:

$$F_{gy} = \frac{\pi}{6} D_P^3 (\rho_p - \rho) g \qquad \text{(III-154)}$$

Stokes' law may be used to calculate the drag on the particles in the y-direction:

$$F_{dy} = - 3 \pi \mu D_P v_{yp} \qquad \text{(III-155)}$$

Hence Equation (III-141) becomes for the y-direction:

$$0 = - 3 \pi \mu D_P (1 + x_B \sigma_{AB}) \frac{D}{x_B} \frac{dx_A}{dy} - \frac{9}{4} \frac{\pi \mu^2 D_P}{\rho T} \left(\frac{2 k}{2k + k_P} \right) \frac{dT}{dy} + \frac{\pi}{6} D_P^3 (\rho_P - \rho) g - 3 \pi \mu D_P v_{yp} \qquad \text{(III-156)}$$

or

$$v_{yp} = - (1 + x_B \sigma_{AB}) \frac{D}{x_B} \frac{dx_A}{dy} - \frac{3}{4} \frac{\mu}{\rho T} \left(\frac{2 k}{2k + k_P} \right) \frac{dT}{dy} + \frac{D_P^2}{18 \mu} (\rho_P - \rho) g \qquad \text{(III-157)}$$

which may also be written as:

$$v_{yp} = v_{ydp} + v_{ytp} + v_{yg} \qquad \text{(III-158)}$$

where v_{ydp}, v_{ytp}, and v_{yg} are the velocities due to the diffusiophoretic, thermophoretic, and gravity effects, respectively.

The particle velocity in the x-direction is assumed to coincide with the local fluid velocity, i.e.:

$$v_{xp} = v_x \qquad \text{(III-159)}$$

The particle trajectory and settling time are given by the following equations:

$$SLP = \int_o (v_{xp} / v_y)\, dy \qquad \text{(III-160)}$$

and

$$STP = \int_o (1. / v_{yp})\, dy \qquad \text{(III-161)}$$

G. Operating-Cost Factors

The water-vapour and pumping-power requirements of a particle collector utilizing the diffusiophoretic effect are important factors in estimating the operating costs of such a collector and may be obtained from the transport and particle equations.

The mass flow rate of dry air through the particle collector is given by:

$$M_{Air} = W \int_{o}^{GAP} (\rho - \rho_{H_2O})\, v_x\, dy \qquad \text{(III-162)}$$

where W is the width of the apparatus.

When the settling length of a particle is denoted by SL (given by Equation (III-148)), the minimum water vapour requirement for removing the particles is:

$$M_{H_2O} = W * C1 * SL \qquad \text{(III-163)}$$

since C1 denotes the flux of water vapour.

The amount of water vapour required to clean unit mass of air is called the operating ratio, ORATIO, and it is given by:

$$ORATIO = M_{H_2O} / M_{Air} \qquad \text{(III-164)}$$

The work which is required to pump unit mass of air through the particle collector which is SL cms long is:

$$WORK = - DELPX * SL * Q / M_{Air} \qquad \text{(III-165)}$$

where Q is the volumetric gas flow rate in the particle collector, i.e.:

$$Q = W \int_0^{GAP} v_x \, dy \qquad \text{(III-166)}$$

The above calculations are based on SL rather than SLP since Model I represented the experimental results of this study better than Model II.

H. Numerical Work

The numerical work consisted of two parts:

1. The integration of the transport and particle equations by the Kutta-Merson technique
2. Determination of the gradients dw_A/dy, dv_x/dy and dT/dy at the upper plate by the Newton-Raphson technique.

These two parts will now be discussed in turn.

1. Numerical Integration

The equations which have to be integrated numerically are summarized below:

Transport Equations:

$$\frac{dw_A}{dy} = \frac{C1\ (w_A - 1)}{\rho\ D} \qquad \text{(III-70)}$$

$$\frac{dv_x}{dy} = (C1 * v_x + DELPX * y - C4) / \mu \qquad \text{(III-74)}$$

$$\frac{d\ TKTDOT}{dy} = C1 * C_{PA} * TKTDOT / k - v_x\ DELPX \qquad \text{(III-82)}$$

$$\frac{dT}{dy} = TKTDOT / k \qquad \text{(III-83)}$$

Particle Equations - Model I:

$$\frac{dSL}{dy} = v_x / v_y \qquad \text{(III-167)}$$

$$\frac{dST}{dy} = 1. / v_y \qquad \text{(III-168)}$$

Particle Equations - Model II:

$$\frac{d\ SLP}{dy} = v_x \ / \ v_{yp} \qquad \text{(III-169)}$$

$$\frac{d\ STP}{dy} = 1. \ / \ v_{yp} \qquad \text{(III-170)}$$

Operating - Cost Relation Equations:

$$\frac{d\ M_{Air}}{dy} = W\ (\rho - \rho_A)\ v_x \qquad \text{(III-171)}$$

$$\frac{dQ}{dy} = W * v_x \qquad \text{(III-172)}$$

where Equations (III-167 to -172) were obtained by differentiating Equations (III-146,-148,-160,-161,-162,-166), respectively.

The above equations may be written in matrix form:

$$\frac{d}{dy}\begin{bmatrix} w_A \\ v_x \\ TKTDOT \\ T \\ SL \\ ST \\ SLP \\ STP \\ M_{Air} \\ Q \end{bmatrix} = \begin{bmatrix} C1 * (w_A - 1) \ / \ \rho D \\ (C1 * v_x + DELPX * y - C4) \ / \ \mu \\ C1 * C_{PA} * TKTDOT \ / \ k - v_x * DELPX \\ TKTDOT \ / \ k \\ v_x \ / \ v_y \\ 1. \ / \ v_y \\ v_x \ / \ v_{yp} \\ 1. \ / \ v_{yp} \\ W\ (\rho - \rho_A)\ v_x \\ W * v_x \end{bmatrix} \qquad \text{(III-173)}$$

or

$$\frac{dZ}{dy} = F(y,Z) \qquad \text{(III-174)}$$

where Z and F (y,Z) correspond to the column vectors on the left hand- and the right hand-side of Equation (III-173), respectively. The latter vector is written as F (y,Z) to emphasize that it is a function of the independent variable y and the dependent variable Z.

Equation (III-174) is a first order, non-linear, ordinary differential equation and the Kutta - Merson numerical integration technique[68] was used to solve it. This method is a single - step integration technique since the dependent variable at mesh - point (n+1) is calculated from the results obtained at mesh - point n only. When the dependent variable at n is denoted by Z_n (i.e. $Z_n = Z(y_n)$) then the Kutta - Merson technique is as follows:

$$Z_{n+1} = Z_n + \frac{1}{2}(K1 + 4\,K4 + K5), \quad n = 0,1,2,... \qquad \text{(III-175)}$$

where

$$K1 = \frac{1}{3} h\, F(y_n, Z_n) \qquad \text{(III-176)}$$

$$K2 = \frac{1}{3} h\, F(y_n + h/3, Z_n + K1) \qquad \text{(III-177)}$$

$$K3 = \frac{1}{3} h\, F(y_n + h/3, Z_n + K1/2 + K2/2) \qquad \text{(III-178)}$$

$$K4 = \frac{1}{3} h\, F(y_n + h/2, Z_n + 3/8\,K1 + 9/8\,K3) \qquad \text{(III-179)}$$

$$K5 = \frac{1}{3} h\, F(y_n + h, Z_n + \frac{3}{2} K1 - \frac{9}{2} K3 + 6\,K4) \qquad \text{(III-180)}$$

h is the integration step-size

y_o corresponds to y = 0.

The integration - error, ε, is of the order of h^5 and the following criterion was suggested by Merson[68] for its estimation:

$$5\,\varepsilon = K1 - 9/2\,K3 + 4\,K4 - 1/2\,K5 \qquad \text{(III-181)}$$

Since this error is a function of the step-size, h, Merson recommended that the step-size should be either halved or doubled in order to meet the desired accuracy by adopting the procedure given below:

(i) If the right-hand side of Equation (III-181) is greater than five times the pre-assigned accuracy, h is halved and the integration from y_n to y_{n+1} is repeated.

(ii) If the right-hand side of Equation (III-181) is less than 5/32 of the desired accuracy, h is doubled.

(iii) If neither (i) nor (ii) are true, h remains the same.

2. Newton - Raphson Technique

The Newton - Raphson technique was employed in order to determine the gradients of the mass fraction, velocity, and temperature at the upper plate (i.e. $(dw_A/dy)_u$, $(dv_x/dy)_u$, $(dT/dy)_u$) so that the boundary conditions at the lower plate were satisfied. The gradients could not be found analytically and a trial and error procedure was required.

When the gradients are denoted by:

$$X(1) = (dw_A / dy)_u$$
$$X(2) = (dv_x / dy)_u \qquad \text{(III-182)}$$
$$X(3) = (dT / dy)_u$$

and the calculated values of w_A, v_x, and T based on these gradients are denoted by Z(1), Z(2), and Z(3), respectively then:

$$Z(1) = f_1' (X(1))$$
$$Z(2) = f_2' (X(1), X(2)) \qquad \text{(III-183)}$$
$$Z(3) = f_3' (X(1), X(3))$$

where the functions f_1', f_2', and f_3' correspond to the numerically integrated transport equations. The errors at the lower plate can be defined as:

$$E(1) = Z(1) - w_{AL}$$
$$E(2) = Z(2) \qquad \text{(III-184)}$$
$$E(3) = Z(3) - TL$$

and Equations (III-183) and (III-184) may be combined to give the vector equation:

$$E = f(X) \qquad \text{(III-185)}$$

In the Newton - Raphson technique Equation (III-185) is expanded in a Taylor series and all non-linear terms are neglected, i.e.:

$$E(X + \delta X) = E(X) + \left.\frac{df}{dX}\right|_X \delta X \qquad \text{(III-186)}$$

where

$$\frac{df}{dX} = \begin{bmatrix} \frac{\partial f_1}{\partial X(1)} & 0 & 0 \\ \frac{\partial f_2}{\partial X(1)} & \frac{\partial f_2}{\partial X(2)} & 0 \\ \frac{\partial f_3}{\partial X(1)} & 0 & \frac{\partial f_3}{\partial X(3)} \end{bmatrix} \qquad \text{(III-187)}$$

$$\delta X = X_{i+1} - X_i \qquad \text{(III-188)}$$

The subscripts i and i+1 denote the ith and (i+1)th estimates of X, respectively. Since it is desired to reduce the error at the lower plate to zero, i.e.:

$$E(X + \delta X) = E(X_{i+1}) = 0 \qquad \text{(III-189)}$$

Equation (III-186) becomes:

$$0 = E(X_i) + \left.\frac{df}{dX}\right|_{X_i} (X_{i+1} - X_i) \qquad \text{(III-190)}$$

or

$$X_{i+1} = X_i - E(X_i) \left[\left.\frac{df}{dX}\right|_{X_i}\right]^{-1} \qquad \text{(III-191)}$$

When X_i, $E(X_i)$, and $df/dX\big|_{X_i}$ are known, an improved set of gradients (i.e. X_{i+1}) can be found which reduces the errors at the lower plate.

Since the function f is not known explicitly, the elements in Equation (III-186) are evaluated numerically by changing the values of the gradients at the upper plate slightly and noting the corresponding changes in the errors.

IV. EXPERIMENTAL APPARATUS AND PROCEDURE

As stated earlier, the experimental particle-collector consisted of two horizontal, large, parallel plates. Both plates were saturated with water and, since the temperature of the upper plate was higher than that of the lower plate, water vapour diffused towards the latter. Air which contained the smoke particles flowed between the plates. A general view of the apparatus is presented in Fig. 5 and 6. A detailed account of the experimental equipment follows.

A. Sizing of Apparatus

The overall dimensions of the experimental apparatus were determined by the plate spacings and the particle settling lengths. From the mathematical model it was known that 1 to 5 cms spacings were of greatest interest. Settling lengths up to 120 cms were expected, although these lengths are also strong functions of gas flow rate and plate temperatures.

The particle settling lengths determined the minimum length the plates must have in order to effect complete particle removal. However, since this study was primarily concerned with the behaviour of the particles in the region where the concentration, velocity, and temperature profiles are developed, allowance had to be made for the developing regions, also called "entrance lengths", near the leading edge of the plates. The total plate length was given by:

Entrance length + Settling length

The entrance lengths for the velocity, temperature, and concentration profiles are denoted by E_v, E_t, and E_c, respectively.

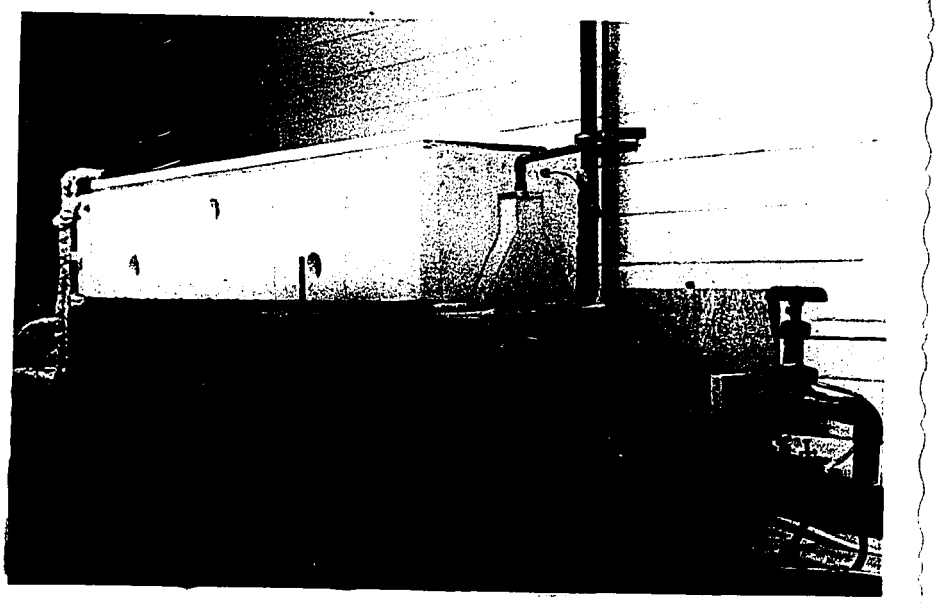

FIG. 5 GENERAL VIEW OF PARTICLE COLLECTOR

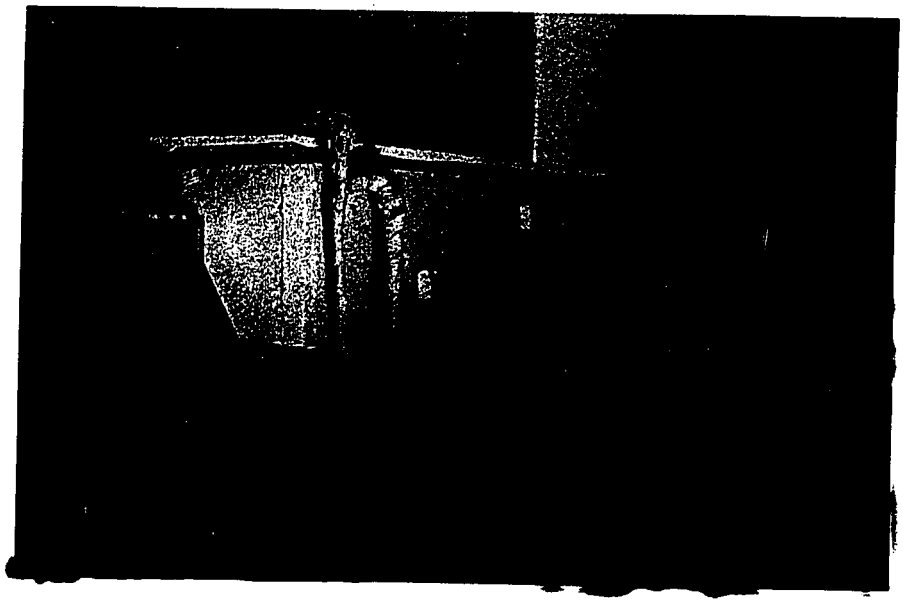

FIG. 6 GENERAL VIEW OF PARTICLE COLLECTOR

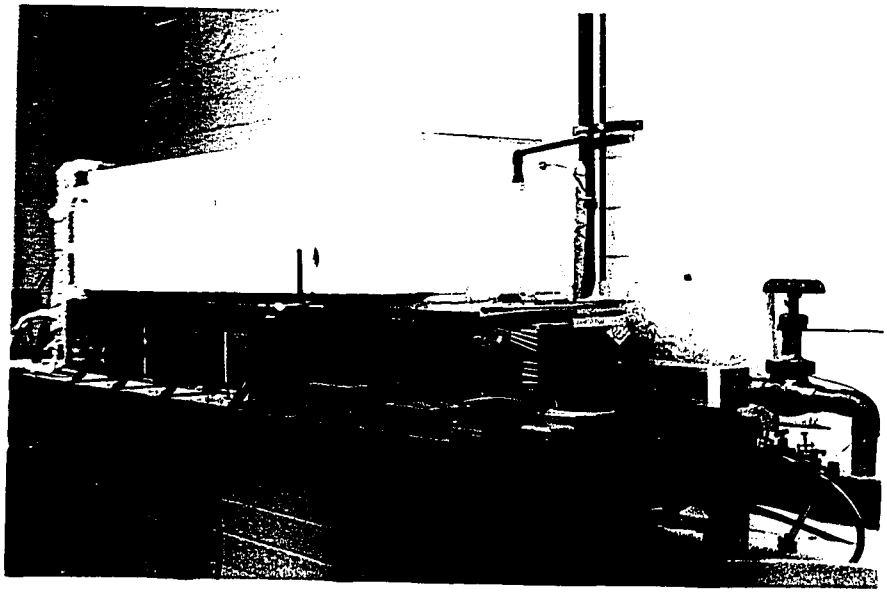

FIG. 5 GENERAL VIEW OF PARTICLE COLLECTOR

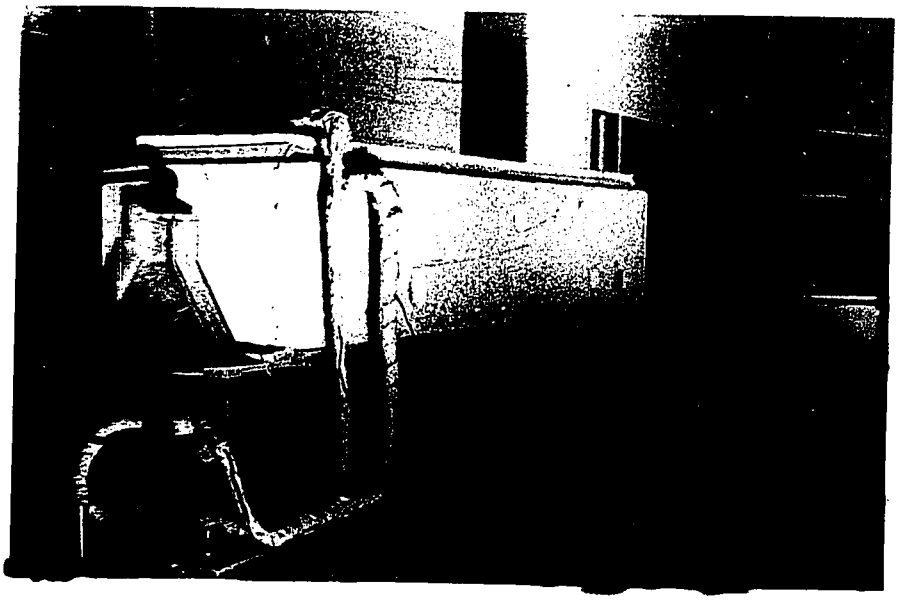

FIG. 6 GENERAL VIEW OF PARTICLE COLLECTOR

It will shortly be shown that $E_v > E_t > E_c$.

Instead of developing all three profiles simultaneously, it was decided to subdivide the plates into three parts:

1) A region where no diffusion of water vapour occurred and only the temperature and velocity profiles were developing.

2) A subsequent region where diffusion of steam was started and the velocity and temperature profiles underwent minor further changes.

3) The fully developed region.

This arrangement made it possible to observe the particles in the region where primarily the concentration profile was developing and where the turbulence present at the leading edges was absent.

Various formulae have been proposed for estimating the entrance lengths. The velocity entrance length is given by:

$$E_v = \alpha^1 \text{ Re GAP} \qquad \text{(IV-1)}$$

where α^1 is a constant whose value is given by Schiller and Schlichting as 0.025 and 0.04, respectively[61]. The Reynolds number is based on the plate spacing and the mean velocity parallel to the plates. Hence for GAP = 5 cms. and Re = 200, E_v = 40 cms.

Schlichting[61] suggests that the temperature and concentration entrance lengths are approximately given by 0.83 E_v and 0.68 E_v, respectively. Hence for the above E_v of 40 cms., E_t = 33.2 and E_c = 27.2 cms. Thus the total entrance length is: $E_v + E_c \simeq$ 80 cms and the total plate length is:

$$80 + 120 = 200 \text{ cms or } 80"$$

The plate width, W, was chosen to be 12" since this is more than 6 times the maximum plate spacing and thereby eliminated the effect of the side-walls in the centre of the collector.

B. Plate Materials

The upper and lower plates were saturated with water and served as a source and sink of water vapour, respectively. The plates had to be porous in order to permit the continuous addition and removal of water. Apart from this feature, the "ideal" plate should have the following properties:

i) The material must be wetted by water so that all pores are completely filled and no air passes through the plates.

ii) The average pore size should be less than 5 microns in order to prevent excessive dripping.

iii) High thermal conductivity and resistance to thermal shock.

iv) Mechanical rigidity, i.e. no appreciable sagging should occur when the plates are supported around their circumference.

v) Availability in large sizes, preferably 12" x 80". Smaller sections could, however, be joined.

vi) Reasonable cost and availability.

A large number of materials was investigated and the results are summarized in Appendix II. None of the materials fulfilled conditions i) to vi) and a compromise had to be made.

It was decided to use thin sheets of blotting paper (approximately 1 mm. thick). These satisfied all conditions moderately well except iv). Wet blotting paper has little strength and therefore required a support.

C. Plate Supports

The supports for the blotting paper had to have the following properties:

a) Sufficient strength to keep the papers flat

b) High open area to permit passage of water vapour

c) Resistance to corrosion by boiling water.

A stainless steel screen of small mesh-size satisfied these properties. However, in order to obtain a flat screen measuring approximately 12" x 80", the screen had to be put under considerable tension. This required special facilities and a heavy support frame.

Instead of the screen, it was therefore decided to support the blotting papers on thin, stretched stainless steel wires spaced 3/8" apart. The wires used were 0.015" in diameter and they could be stretched individually by means of a screw adjustment mechanism.

A sketch of this mechanism is given in Figure 7 . The wires passed below a 3/4" DIA. aluminum rod and were wound around 10-32 brass screws. The screws were mounted on a 2-1/2" x 2-1/2" aluminum angle and held in place by brass bolts and lock-washers. The wires were fastened to the screws by soldering with an acid flux. Tightening of the wires could be accomplished by loosening the nuts, turning the screws and fastening the nuts again.

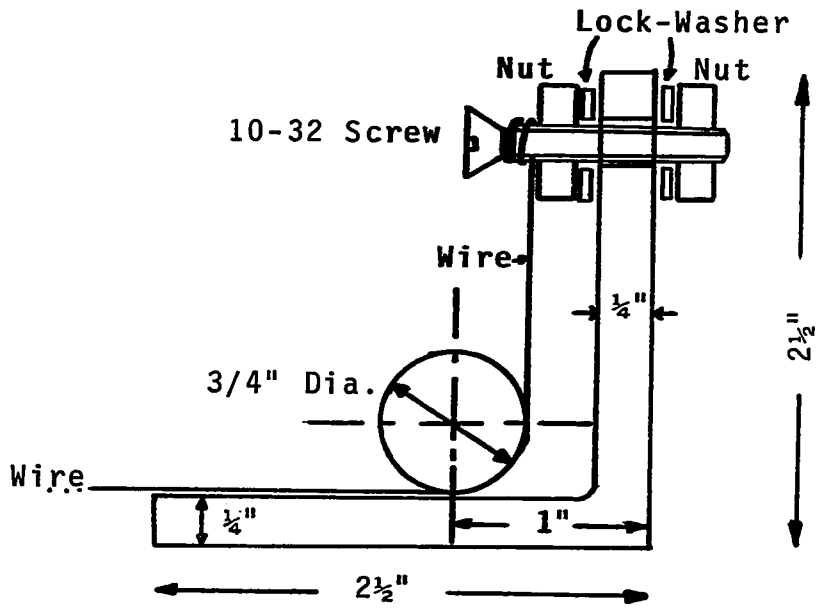

FIG. 7 ADJUSTMENT MECHANISM OF PLATE - SUPPORT WIRES

To prevent the frame from distorting, the wires were put under equal tension. This condition was reached when, upon plucking, the wires emitted the same sound.

The aluminum angles with the wire adjustment mechanisms were connected by two 3/4" x 3/4" aluminum bars as shown in Figure 8. In the case of the upper plate, two 1-1/2" x 2-1/2" aluminum angles were screw-mounted on the bars in order to prevent them from bending. A similar arrangement was not necessary for the lower plate because the wires were under less tension and the upper plate rested on the bars, thus keeping them straight.

D. Plate Spacers

The distance between the plates was adjusted by varying the support size for the lower plate and the spacers between the plates, cf. Figure 9.

A diagram of the plate spacers is presented in Figure 10. The spacers were cut from 3/4" square aluminum bars and the length of GAP determined the distance between the sheets of blotting paper. The spacers rested on the square bars of the lower plate, and, since the latter was $\frac{3}{4}$ inches wider than the upper plate (Figure 10), a step was cut into the plate spacers. The 1-1/2" x 2-1/2" angle mounted on the upper plate rested on the top of this step.

The size of the lower plate supports was selected so that the upper plate was always in the same position, ie. dimension H1 in Figure 9 remained unchanged. In this way a good seal could be made between the upper plate and the vapour reservoir (see next section) but it did require cutting new botton plate

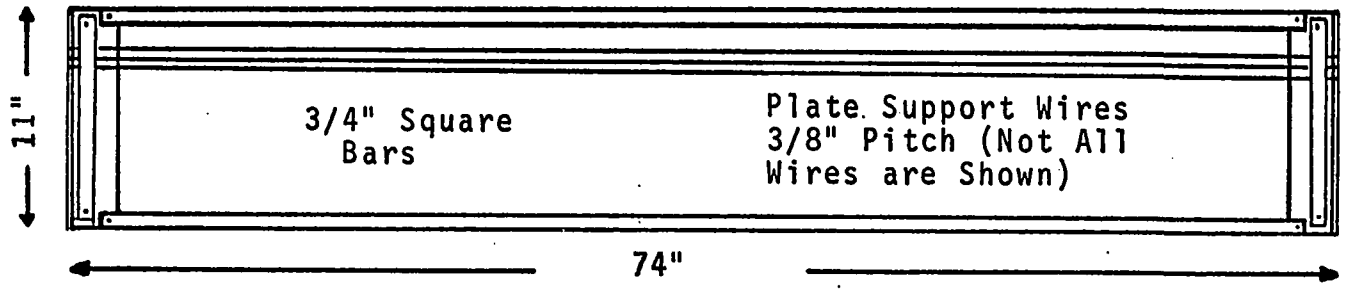

Note: 2½"x1½" angles mounted on 3/4" square bars are omitted

FIG. 8 PLAN - VIEW OF UPPER PLATE

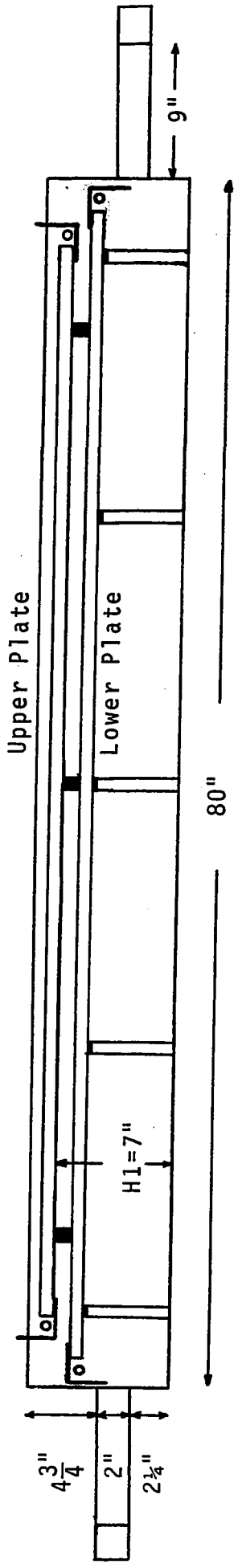

FIG. 9 SIDE VIEW OF PARTICLE COLLECTOR
(Vapour Box Omitted)

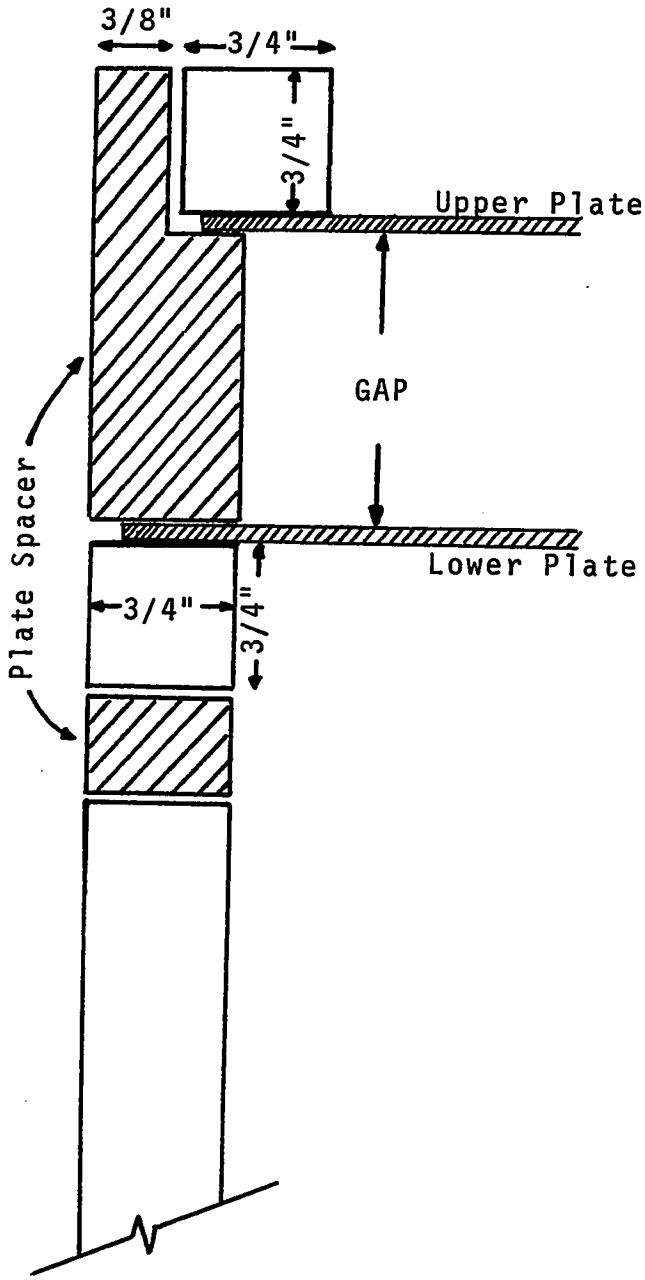

FIG. 10 PLATE SPACER ASSEMBLY

supports for each plate spacing.

E. Heating of the Upper Plate

The main purpose of the upper plate was to act as a source water vapour. This was accomplished by keeping it saturated with water and at a temperature higher than that of the lower plate. The partial pressure of water vapour at the upper plate was therefore higher than that at the lower plate and the desired diffusion of water vapour occurred.

The evaporation of water from the upper plate required the transfer of heat to it in order to maintain the plate at a constant temperature. Various ways of heating the plate (i.e. electrical heating, heating by conduction) were investigated. Since the latent heat of vaporization of water is high and hence the heat load was great, the most convenient method was to pass steam over the plate. When the temperature of the plate fell, steam condensed thus heating the plate and keeping it moist at all times.

The heat liberated on condensation of the steam passed through the plate by conduction, and hence there was a temperature difference between the side of the plate where the steam condensed and the side where the water evaporated. The magnitude of this difference depended on the thickness and thermal conductivity of the moist blotting paper and the rate of evaporation. At TU $\leq 90^{o}C$ and GAP $\geq$ 1 cm, the difference was estimated to be less than $6^{o}C$. The thickness and thermal conductivity of the blotting paper were assumed to be 0.1 cm

and $1.6 * 10^{-3}$ cals (sec cm $^{o}K)^{-1}$, respectively. For carrying out and analysing the experiments it was not necessary to know the temperature difference.

Since the highest attainable temperature in the vapour box was 100 ^{o}C, a temperature difference of 6 ^{o}C indicates that the maximum temperature of the lower side of the upper plate was 94 ^{o}C. For the present study higher temperatures were neither necessary nor practical and steam heating of the upper plate was therefore appropriate.

Steam was passed over the upper plate by ejecting it through two spray nozzles (1/4 J SS - 73160SS made by Spraying Systems Co.). The steam was confined in a so-called vapour box which is shown in Fig. 5 , and the temperature of the upper plate could be regulated by adjusting the steam flow rate.

F. Vapour Box

The rectangular vapour box had a removable lid with two 3" DIA holes. The purpose of the latter was to ensure that the pressure inside the vapour box was very close to atmospheric by permitting steam to escape through them. The front panel of the vapour box had three sight-glasses for observation of the nozzles.

In order to prevent excessive condensation on the walls during start-up and to reduce the heat loss from the vapour box, the box had double walls between which hot air was passed. Each wall and the lid were heated separately (see also Section IV-G).

The walls consisted of 0.04" thick aluminum sheets which were bolted to aluminum frames made from 1" x 1/2" bars.

Air-tight seals between the sheets and the frame were obtained by applying RTV Silastic Cement (Dow Corning #731).

One inch thick panels of styrofoam insulation were glued to the outside of the vapour box with Silastic Cement in order to reduce the heat loss to the surroundings.

G. Heating of the Vapour Box Walls

Hot air, which heated the walls of the vapour box as stated in the last section, was obtained by passing air from the laboratory supply through a copper coil placed above the flame of a Bunsen burner (see Fig. 6). The temperature of the hot air was regulated by adjusting the flame or flow rate.

The temperatures of the air entering and leaving the walls were measured with Iron-Constantan thermocouples and indicated by a potentiometer (Type 421-801 made by Assembly Products, Chagrin Falls, Ohio, USA).

Neither the air flow rate nor the temperature had to be controlled very accurately. However, the flow rate should not be so high that the pressure inside the walls buckled the aluminum sheets.

H. Cooling of the Lower Plate

Water vapour condensed on the lower plate. This conden-

sation caused a release of heat and formation of a liquid film. In order to keep the temperature of the lower plate constant and prevent build-up of condensate, the plate was placed in a plastic box through which cooling water could be circulated (see Fig. 9 and 11). The level of the water was adjusted to coincide with the blotting paper of the lower plate. The condensate was free to pass through the blotting paper.

Steam could be injected into the cooling water tank and thus preheat the water to the desired temperature. The noise resulting from implosions which occurred when steam came into contact with cool water was reduced by fitting a 3/8" bronze sparger nozzle to the outlet of the steam-line.

The sides of the transparent plastic box were sufficiently high to accommodate the upper and lower plates and permit observation of the smoky air passing between them. However, the view tended to be impaired by drop-wise condensation on the plastic walls and this had to be eliminated.

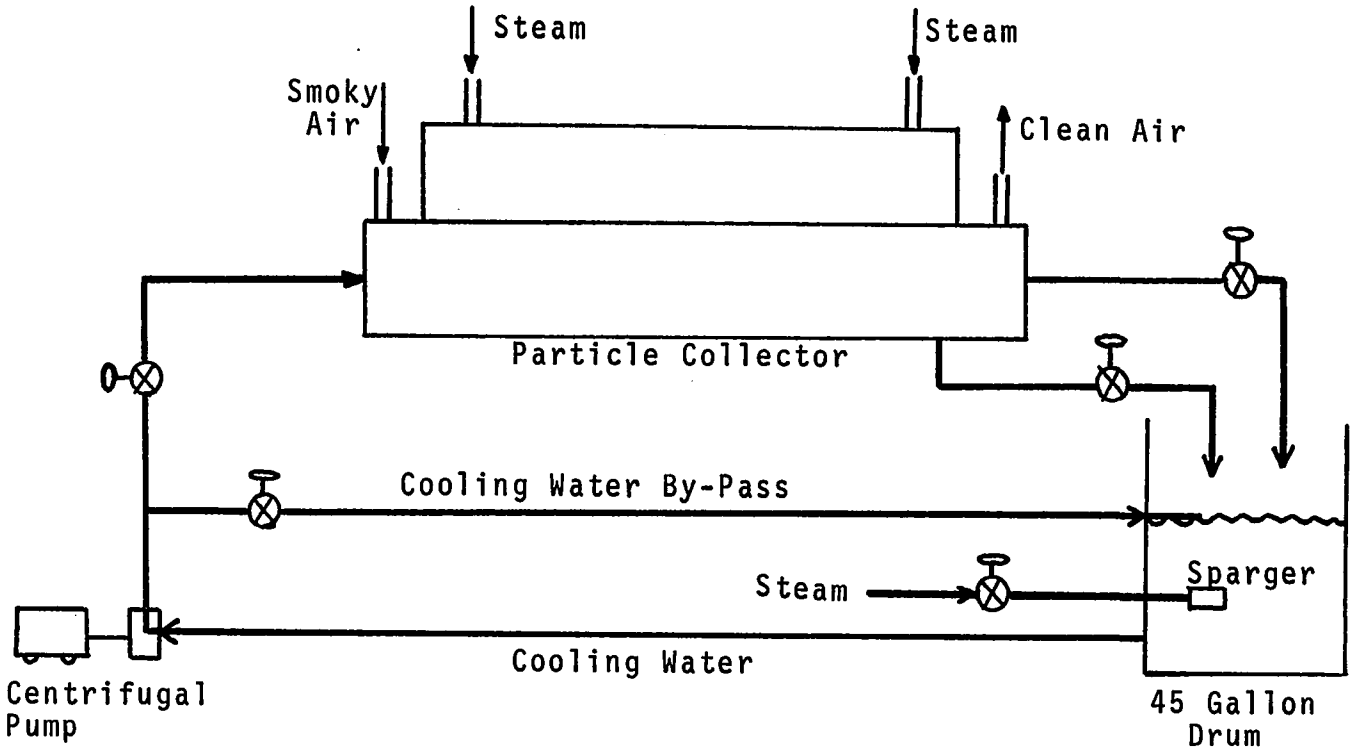

FIG. 11 SCHEMATIC FLOW DIAGRAM

I. Condensation Prevention on Side Walls

Condensation on the front wall of the plastic box was prevented by electrically heated nichrome wires which compensated the heat loss through the wall. These wires were 0.015" in diameter and spaced 3/16" apart so that they did not interfere significantly with the smoke observation.

The temperature of the wires was not accurately controlled but just set sufficiently high to prevent condensation. There was hence a possibility for the wires to exceed the melting point of the plastic. Small strips of Teflon tape were mounted on the plastic at 2 feet intervals in order to prevent the wires from touching the plastic and thus melting it.

There was no space for anchoring the heating wires inside the plastic box and they were therefore led through holes in its end walls. Ten inch sections of insulated copper wire were soldered to the nichrome wires so that these sections were in contact with the end walls and no melting occurred.

Since the nichrome wires expanded on heating, they were kept stretched by attaching them to springs which in turn were connected to an electrical distributor board (see Figure 12).

The nichrome heating wires were connected in parallel so that electrical contact between the springs was tolerable. The electrical power dissipated in the wires was obtained from the 110 volt mains and regulated by a Variac rheostat.

The rear wall of the plastic box was heated by a 2" wide heating tape. This reduced the heat loss through that wall and also prevented condensation.

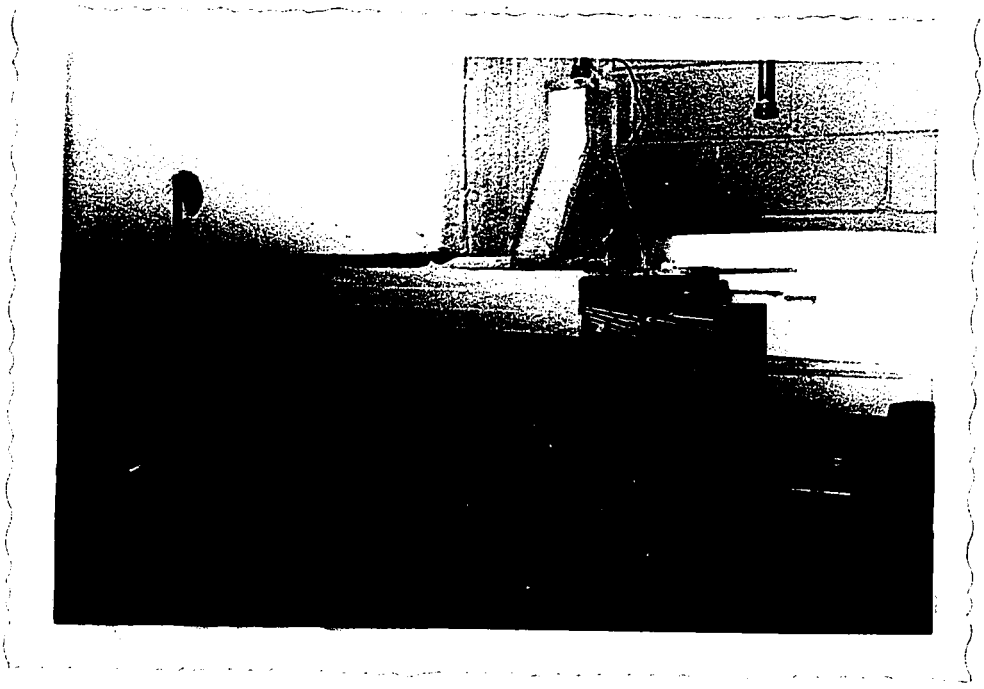

Fig. 12 SPRING-MOUNTED HEATING WIRES AND OTHER ELECTRICAL EQUIPMENT

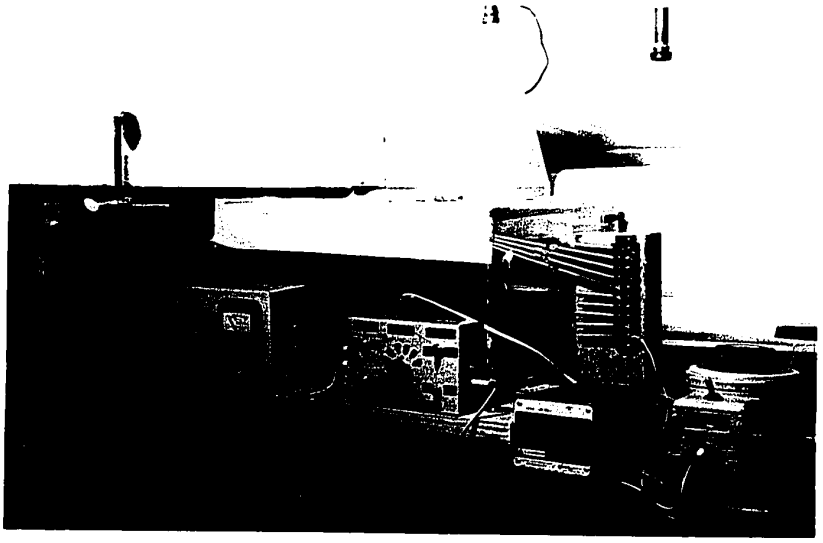

Fig. 12 SPRING-MOUNTED HEATING WIRES AND OTHER ELECTRICAL EQUIPMENT

J. Smoke Generator

Since the present particle-collector employing diffusiophoresis is primarily applicable for the removal of micron-size particles, a technique for generating such particles had to be found. A La Mer or other standard particle generator was not available in the Department, and other methods had to be investigated.

Stannic chloride, titanium chloride and ammonium chloride smokes were tried, but all were found to agglomerate very rapidly, resulting in excessively large particles and plugging of the tubes. Cigarette smoke, however, proved to be ideal for the present work. It could be easily formed, the particles were of micron-size, and agglomeration was not severe because it was observed that the smoke had a negligible settling velocity under the influence of gravity alone. Furthermore, properties of cigarette smoke are well documented in the literature.

Cigarette smoke was formed by passing air coming from a compressed air cylinder through a cigarette under a positive pressure (see Figure 13). The cigarette was lit and inserted into a fluted copper tube which fitted into a rubber stopper and led to a 'splash flask' in order to remove drops of tar from the smoke. The smoke then passed through a U-tube filled with glass wool which retained any coarse particles.

The air flow through the cigarette was regulated by a micrometer valve and the smoke could be diluted by mixing it with air passing through the small globe valve (see Figure 13).

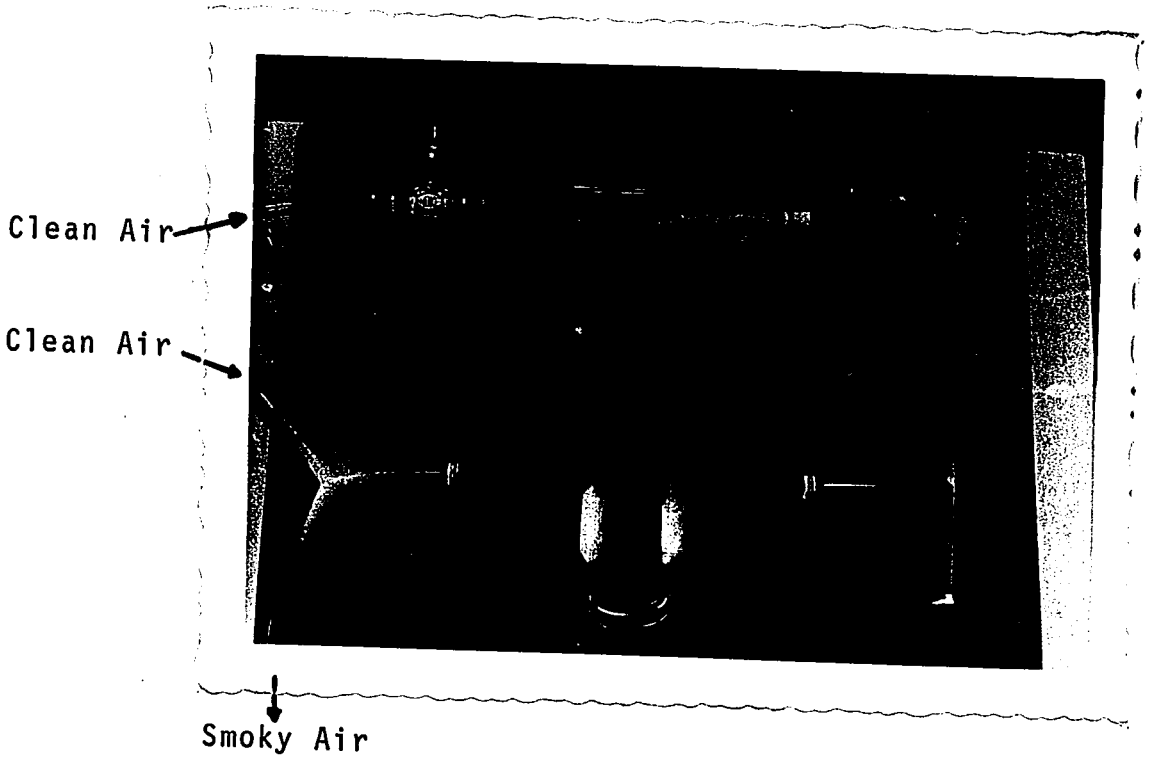

Fig. 13 CIGARETTE - SMOKE GENERATOR

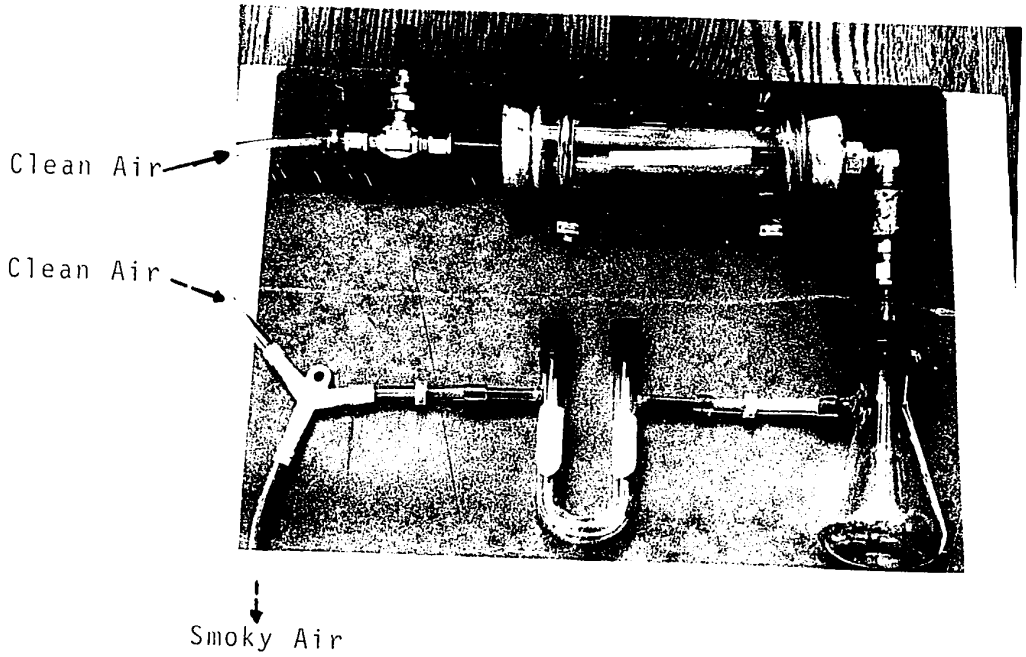

Fig. 13 CIGARETTE - SMOKE GENERATOR

Compressed air from a cylinder was used because it gave a very steady air flow rate and because only a small flow was required. The total flow of dry air was measured by a rotameter (Brooks 5-15-1, aluminum float).

K. Velocity Measurements

The linear velocities and the total volumetric flow rate between the plates were measured with a special anemometer and rotameter, respectively.

1. Anemometer

Since the linear velocities between the plates were less than 30 cms/sec, it was not possible to measure them with standard Pitôt tubes or hot-wire anemometers. A special DISA Low Velocity Anemometer (Type 55D80) was employed instead. This instrument was capable of measuring velocities between 0 and 30 cms/sec within about 5% accuracy. Fig. 14 shows the anemometer and associated electronic equipment. Technical details on the anemometer are given in Reference (73). A further advantage of the instrument was that it had to be calibrated only once, and could then be used for other gases at different temperatures without recalibration.

The Low Velocity Anemometer differed from ordinary anemometers because the hot wire was vibrated parallel to the direction of flow. The wire axis was perpendicular to the flow direction. When a constant current is passed through such a vibrating anemometer wire the voltage, e, across the wire terminals is given by:

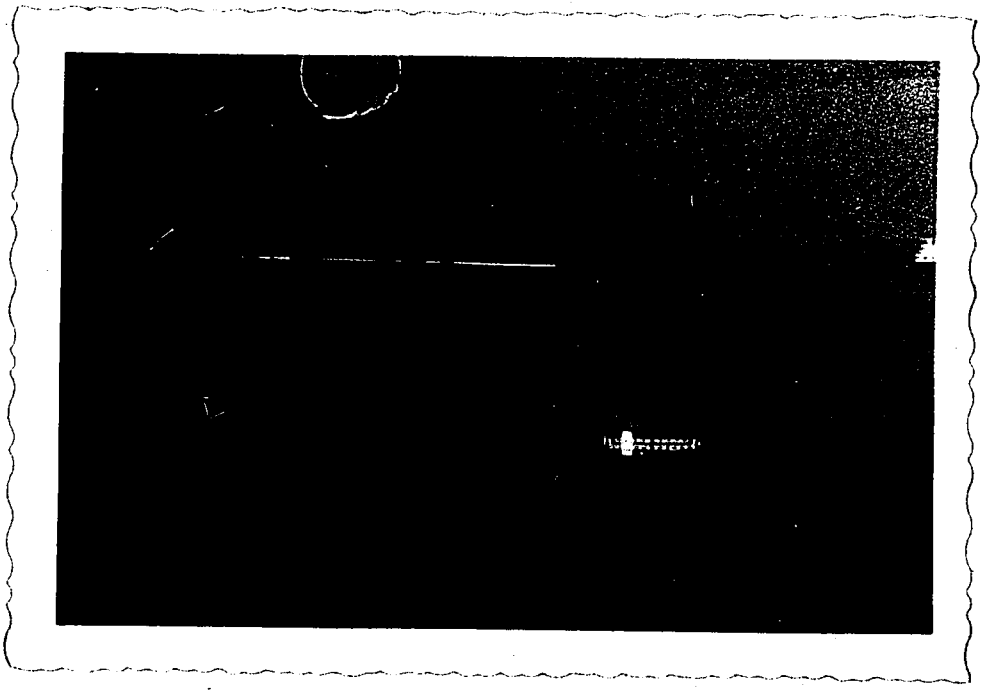

Fig. 14 LOW VELOCITY ANEMOMETER AND ASSOCIATED ELECTRONIC EQUIPMENT

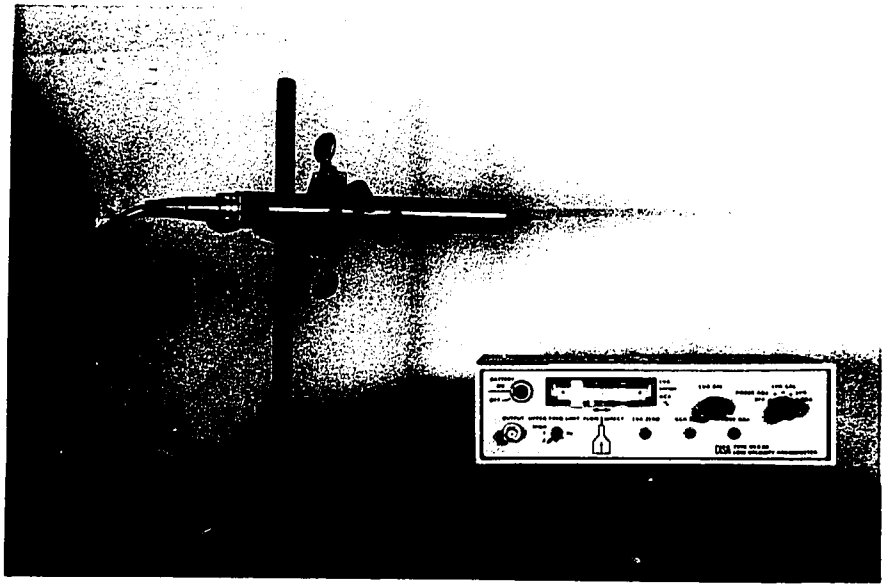

Fig. 14 LOW VELOCITY ANEMOMETER AND ASSOCIATED ELECTRONIC EQUIPMENT

$$e = a' + b' (v_x + v_a \sin \omega t)^2 \qquad \text{(IV-2)}$$

where a' and b' are constants, v_x is the gas velocity to be measured and v_a is the amplitude of the wire vibration velocity. The constants a' and b' are functions of the electrical parameters of the anemometer and the fluid properties and can be regarded as the product of two further constants. For example b' may be expressed by:

$$b' = b_f * b_e \qquad \text{(IV-3)}$$

where b_f and b_e are only dependent on the fluid properties and electrical parameters respectively.

When Equation (IV-2) is written as:

$$e = a' + b'(v_x^2 + \tfrac{1}{2}v v_a^2) + b'(2v_x v_a \sin\omega t - \tfrac{1}{2} v_a \cos 2\omega t) \qquad \text{(IV-4)}$$

and the DC component is eliminated one obtains:

$$e_{ac} = 2 b' v_x v_a \sin \omega t - \tfrac{1}{2} v_a^2 b' \cos 2\omega t \qquad \text{(IV-5)}$$

The last term on the right hand side of the above equation is known as the "second harmonic" of the "signal" e_{ac}.

The signal is a periodic function and its mean value can be obtained from the following equation:

$$E_a = \frac{1}{\pi}\int_{\alpha}^{\pi+\alpha} e_{ac}\, d(\omega t) + \frac{-1}{\pi}\int_{\pi+\alpha}^{2\pi+\alpha} e_{ac}\, d(\omega t) \qquad \text{(IV-6)}$$

i.e. the sign of the signal is reversed every half period. α is a small angle and indicates that the sign reversal does not occur when $e_{ac} = 0$ but shortly afterwards.

Substituting Equation (IV-5) into (IV-6) and carrying out the integration gives:

$$E_a = \left(\frac{8}{\pi} v_a (\cos \alpha) b'\right) v_x \qquad \text{(IV-7)}$$

or for a particular fluid and anemometer setting

$$E_a = K_a v_x \qquad \text{(IV-8)}$$

where $$K_a = \frac{8}{\pi} v_a (\cos \alpha) b' \qquad \text{(IV-9)}$$

Hence the DC voltage E_a is proportional to the fluid velocity, v_x.

K_a could be found by calibrating the instrument with air at room temperature. When the anemometer is to be used for measuring velocities in an air-water vapour mixture at elevated temperatures, the fluid properties and hence b_f are different which in turn would lead to a new K_a and thus render the initial calibration useless. However, it is possible to compensate for a change in b_f by varying the electrical parameter b_e so that b' is always the same. This compensation was simple to perform. Since the amplitude of the second harmonic is a function of b' only (for a given v_a) and is readily measured, it was only necessary to adjust the parameter b_e until the amplitude of the second harmonic for the gas mixture equalled that of the calibration fluid. Hence once the amplitudes of the second harmonics were matched, the same b' and therefore the same K_a were assured, and only one calibration with one fluid was required.

The amplitude of the vibration velocity, v_a, of the wire and the amplitude of the second harmonic were adjusted by aligning the meter pointer with the red mark in the PROB.ADJ. and LVA.CAL. position, respectively.

A variable power supply set to deliver about 9 volts was used to power the anemometer. The output from the anemometer could be read from the instrument-meter and a Hewlett Packard strip-chart recorder.

a) Velocity Calibration of the Anemometer

Special equipment was built to carry out the velocity calibration of the low velocity anemometer and it is shown in Fig. 15 and 16.

Air from either the laboratory supply or a compressed air cylinder was passed through a porous brass filter and throttled in a pressure reducer before entering a 12' long, 1" I.D., plexi-glass pipe. The volumetric flow rate of the air was determined by passing the air leaving the pipe through a precision wet gas meter.

The anemometer was located 9 feet downstream from the pipe entrance. The entrance length for laminar flow and a maximum axial velocity of 30 cms/sec was estimated to be 21 inches. Hence the anemometer was located where the velocity profile was fully developed.

The anemometer was inserted into the pipe through an air-tight port in the pipe-wall. The anemometer holder was mounted on a traverse so that the anemometer wire could be moved back and forth along the pipe radius. The traverse was spring loaded and its position adjustable by a micrometer screw.

The calibration was carried out with the anemometer wire located at the pipe centre and perpendicular to the direction

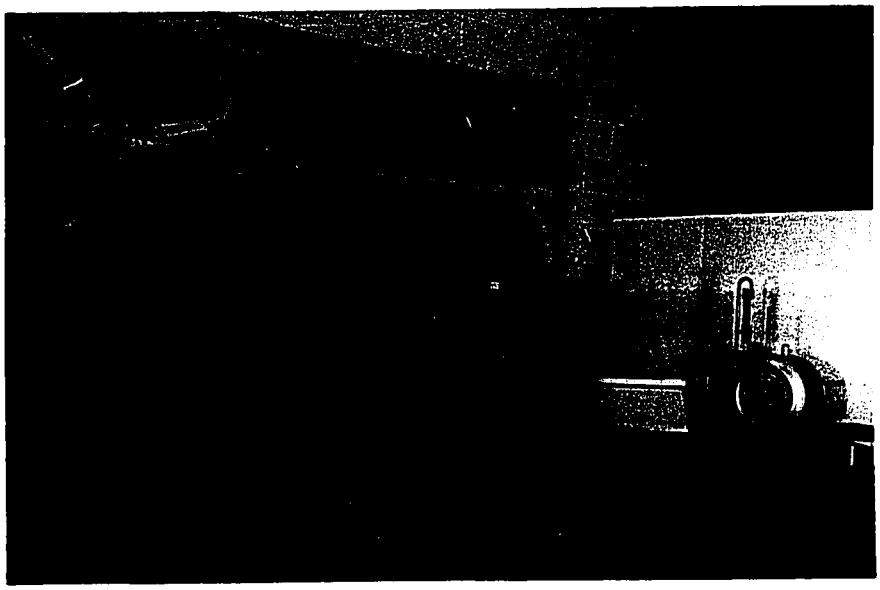

Fig. 15 LOW VELOCITY ANEMOMETER CALIBRATION EQUIPMENT (General View)

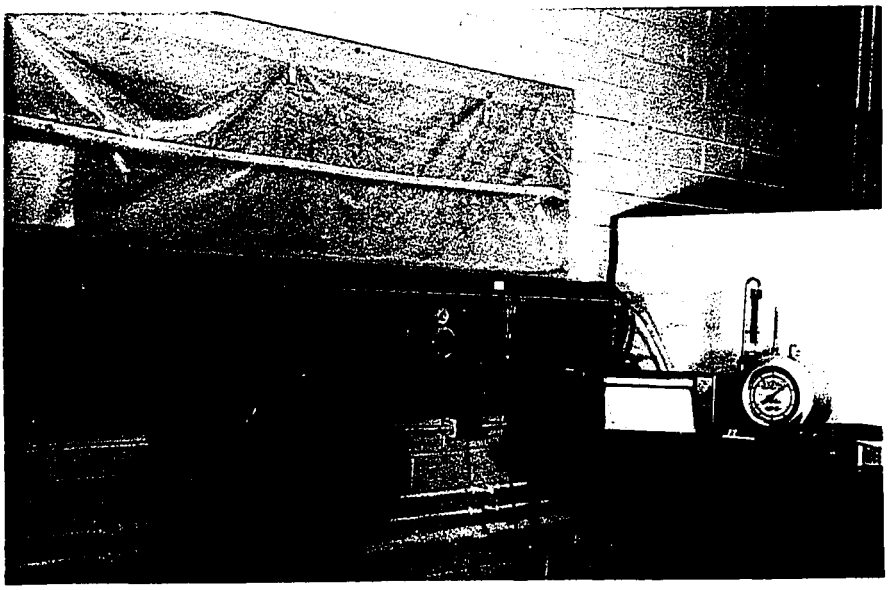

Fig. 15 LOW VELOCITY ANEMOMETER CALIBRATION EQUIPMENT (General View)

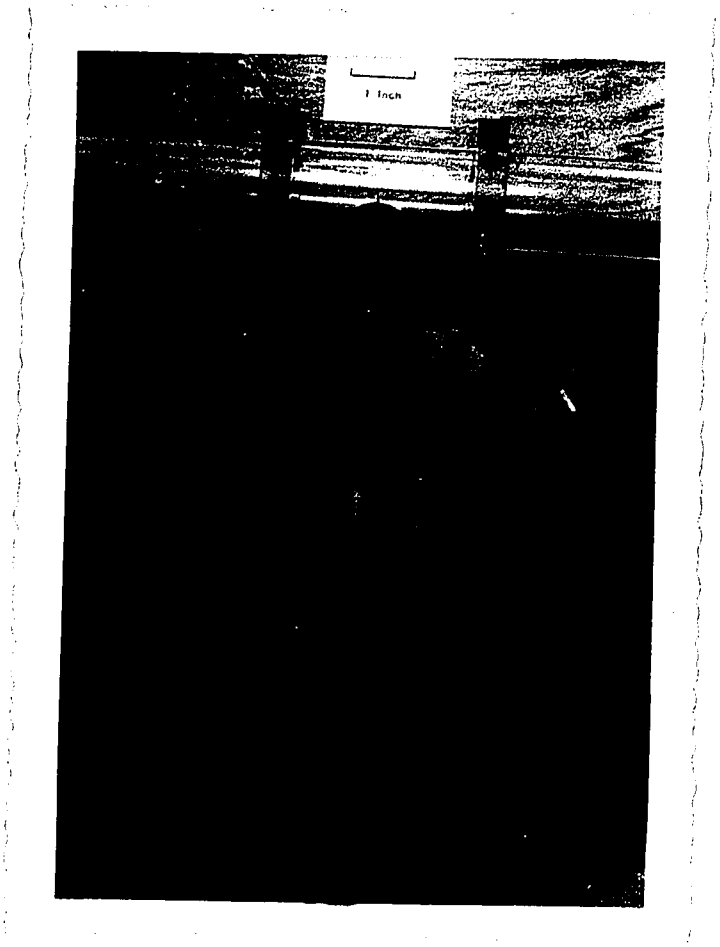

Fig. 16 LOW VELOCITY ANEMOMETER CALIBRATION EQUIPMENT (Close-up of Traversing Mechanism)

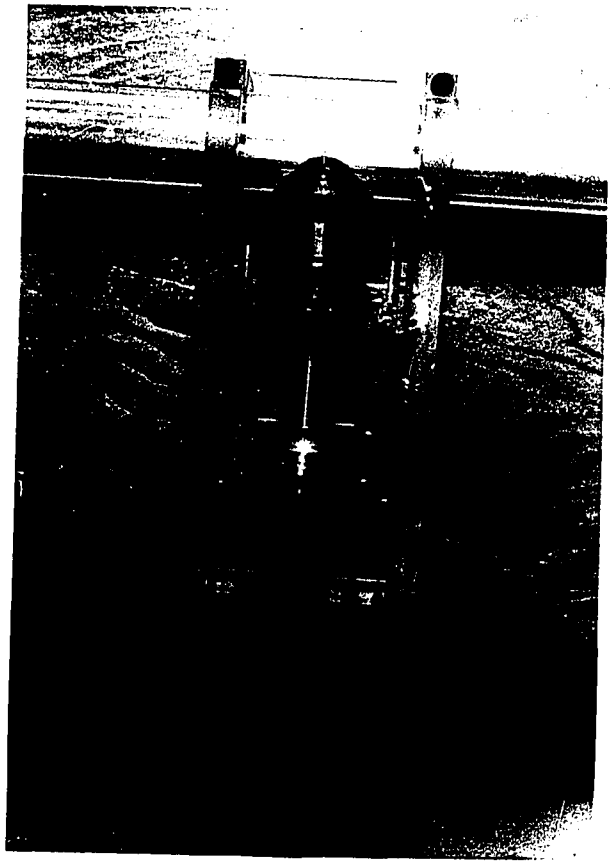

Fig. 16 LOW VELOCITY ANEMOMETER CALIBRATION EQUIPMENT (Close-up of Traversing Mechanism)

of flow. These two adjustments were made separately.

(i) Centre Adjustment

Since the centre velocity is a maximum and twice the average linear velocity for Poiseuille flow, the centering could be performed as follows: After air had been passed through the pipe for some time and steady state was achieved, the anemometer wire was moved back and forth with the traverse and finally positioned at the point where the maximum velocity was measured.

(ii) Perpendicular Adjustment

The anemometer wire could be positioned with respect to the flow because the maximum heat loss and hence velocity reading occurred when the wire was perpendicular to the flow direction. Hence rotating the probe holder around its own axis and selecting the position which gave the maximum velocity reading placed the wire in the desired position.

The precision wet gas meter which was used to determine the volumetric air flow rate in the pipe had been tested and found accurate prior to the anemometer calibration. Since the air from either the laboratory supply or the compressed air cylinder was essentially dry, the wet gas meter readings were corrected for the vapour pressure of water.

The calibration curve is based on data given in Table 1 and is shown in Fig. 17. The relationship between gas velocity and recorder deflection was very nearly linear thus confirming Equation (IV-8).

Table 1

Anemometer-Calibration Data

Room temperature: 28°C

Anemometer Reading on Recorder	Volume of Air Measured, V (cu. ft.)	Duration of Measurement, t (secs)	Velocity at Anemometer, v_x (cms/sec)†
0.50	0.03	388.6	0.83
0.98	0.05	247.7	2.17
1.00	0.05	243.8	2.20
1.50	0.06	184.5	3.50
1.99	0.10	238.2	4.52
2.50	0.10	191.7	5.61
3.00	0.10	164.2	6.55
3.50	0.10	141.2	7.62
4.02	0.10	125.3	8.59
4.50	0.10	112.3	9.58
5.00	0.10	102.5	10.50
5.47	0.10	93.4	11.52
6.00	0.10	86.4	12.40
6.50	0.10	79.3	13.56
7.00	0.10	74.8	14.38
7.50	0.10	68.8	15.64
7.99	0.10	65.2	16.50
8.50	0.10	60.8	17.70
8.99	0.10	57.9	18.50
9.50	0.20	107.8	19.96
9.95	0.20	103.8	20.73

†The following relationship was used to calculate the linear velocity at the anemometer wire:

$$v_x = \frac{8}{D_t^2 \pi} (1 - PSAT/P) (V/t)$$

where the tube diameter, D_t, and the saturated vapour pressure of water, PSAT, at room temperature are 2.54 cms and 28.349mm Hg, respectively. Hence:

$$v_x = \frac{8}{2.54^2 \pi} (1 - 28.349/760) \, 30.48^3 \, (V/t) \text{ cms/sec}$$

$$= 10759.941 \, (V/t) \text{ cms/sec}$$

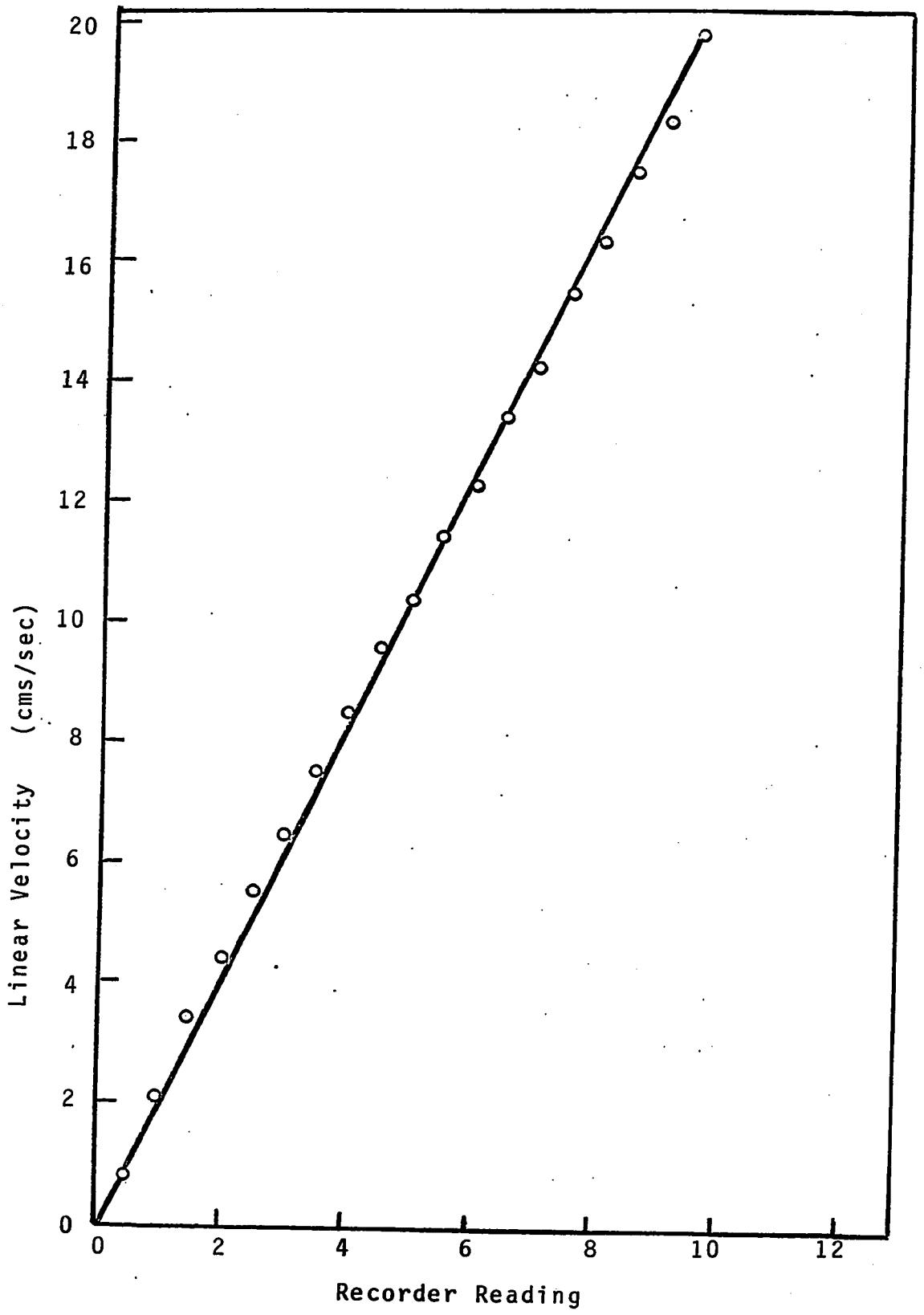

FIG. 17 CALIBRATION CURVE FOR LOW VELOCITY HOT WIRE ANEMOMETER

2. Rotameter

The volumetric air flow rate from the compressed air cylinder to the parallel plate particle collector was measured with a rotameter (Brooks 5-15-1, Aluminum float). The rotameter was calibrated with a precision wet gas meter and the calibration curve based on data in Table 2 is shown in Fig. 18.

L. Temperature Measurements

1. Thermistor and Thermistor Circuit

The temperature profile in the air-water vapour mixture between the plates of the particle collector was measured with a thermistor mounted in the tip of a hypodermic needle. It was decided to use a thermistor rather than a thermocouple because of its superior reproducibility and convenient mounting.

The particular thermistor used was obtained from Victory Engineering Corp., Springfield, New Jersey, and had the code number NM-22-60-32-B. This code implies that a thermistor bead of 0.01" diameter was embedded in the tip of a 6" long hypodermic needle. The needle diameter was 0.028" and it was therefore possible to measure "point" temperatures.

Thermistors are semi-conductors whose resistance, R, changes exponentially with the absolute temperature, T, according to the equation:

$$R = A_{th} \exp (B_{th}/T) \qquad \text{(IV-10)}$$

where A_{th} and B_{th} are constants, which were 0.082 ohms and 3033.026 ^{o}K, respectively, for the thermistor used in this study. The values of these constants indicate the strong

Table 2

Rotameter Calibration

Room Temperature: 29 ^{o}C

Volume of Air Measured, V (cu. ft)	Duration of Measurement, t (secs)	Volumetric Flow Rate, (cc/sec)	Float Height
0.07	345.2	5.74	0.5
0.20	62.8	90.18	10.0
0.20	42.5	123.10	13.0
0.20	49.0	115.58	12.4
0.20	54.1	104.68	11.2
0.20	65.7	86.20	9.3
0.20	75.4	75.11	8.0
0.20	85.6	66.16	7.0
0.20	99.5	56.92	6.0
0.20	118.4	47.83	5.0
0.10	73.7	38.42	4.0
0.10	96.5	29.34	3.0
0.10	144.8	19.56	2.0
0.05	141.8	9.98	1.0
0.20	59.3	95.50	10.5
0.20	48.7	116.29	12.3
0.20	60.0	94.40	10.1

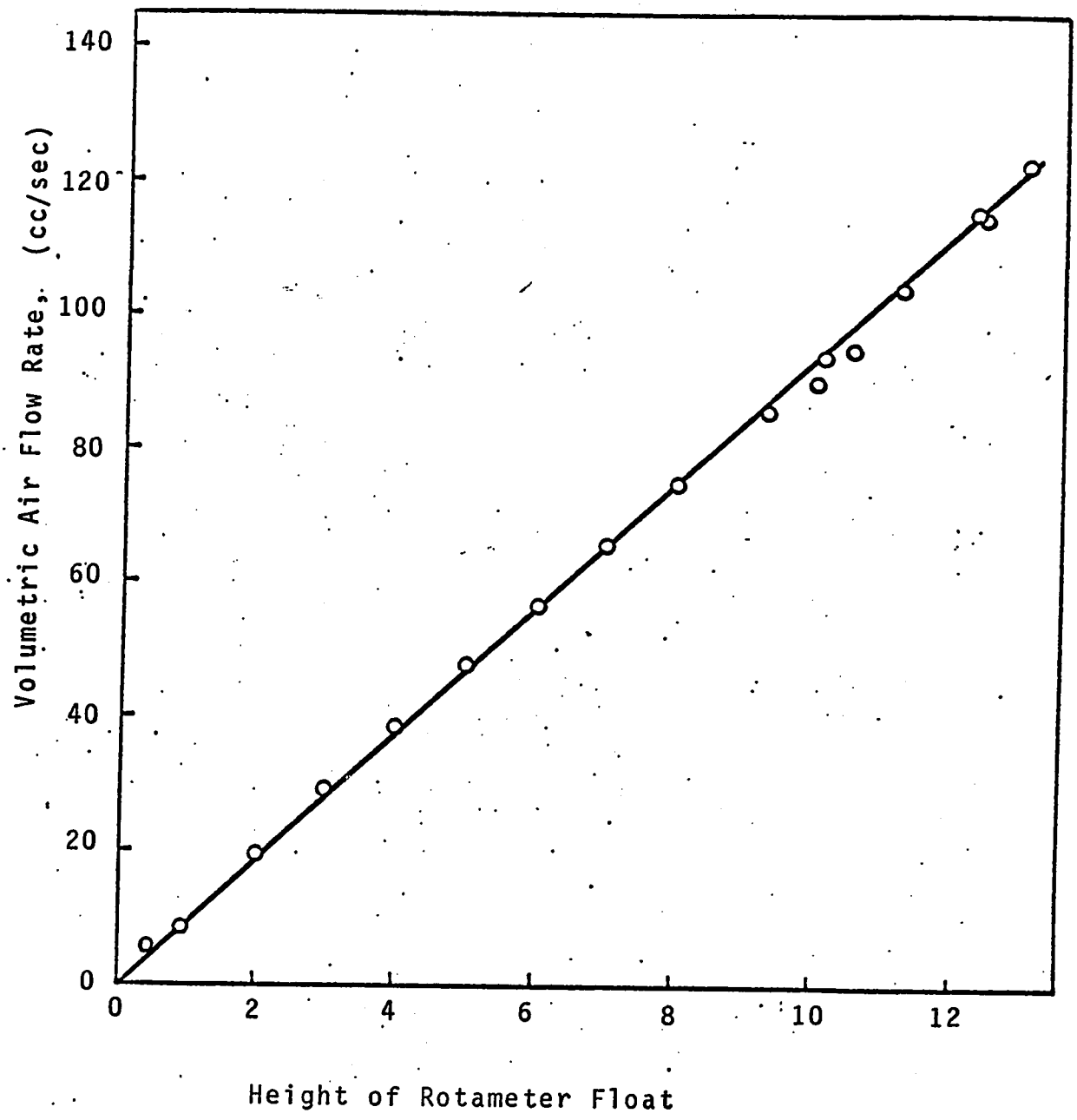

FIG. 18 CALIBRATION CURVE FOR ROTAMETER

dependence of R on T and hence the extreme sensitivity of the thermistor.

The resistance of a thermistor can be found most conveniently be incorporating it in a Wheatstone bridge circuit. There are two different ways of operating such a bridge:

(i) The bridge is balanced at every temperature by adjusting the variable resistor in parallel with the thermistor. When the resistance of the variable resistor and the other resistors in the bridge are accurately known the thermistor-resistance can be calculated.

(ii) The Wheatstone bridge is only balanced at one temperature. When the temperature is different, a potential difference across the bridge terminals results. The magnitude of this voltage is related to the thermistor resistance.

It was decided to adopt the second method because it was simpler to measure and record a voltage than a resistance. However, care had to be taken that the electrical power dissipated in the thermistor did not cause it to heat up when the Wheatstone bridge was not balanced.

The potential difference across the bridge terminals was displayed on a 1 mV Hewlett Packard strip chart recorder and a 1 volt power supply was used to energize the bridge circuit.

Temperatures in the particle-collector were expected to be between about 20 and 100^{o}C. Since this temperature range is rather large and the relationship between temperature and thermistor-resistance is highly non-linear, the accuracy of the measurements could be improved by splitting the temperature range into two sections: approximately 20 to 60^{o}C and 60^{o} to 100^{o}C.

These sections are subsequently referred to as the "low" and "high" scale.

Fig.19 and 20 show the circuit diagram and the casing of the circuit with the thermistor, respectively. The circuit diagram was somewhat more complex than a standard Wheatstone bridge because it consisted really of two bridges (one for the "low" and "high" scale each) and had special provisions for adjusting the circuit.

In order to obtain maximum accuracy the recorder-pen deflection should be full and zero at approximately 20°C (60°C) and 60°C (100°C), respectively for the "low" ("high") scale. One method of achieving this for the low scale was by inserting the thermistor into a 60°C bath and adjusting potentiometer R3 until zero recorder-pen deflection resulted. Full scale deflection could similarly be obtained by varying potentiometer RV when the thermistor was placed in a 20°C bath. An analogous procedure could be used for the "high" scale. The disadvantage of this method was that temperature baths of 20, 60, and 100°C had to be available whenever the circuit needed to be set.

This difficulty was overcome by replacing the thermistor with fixed resistors when the circuit had to be adjusted. Precision resistors of 2422.75, 698.3, and 269.22 ohms were available and these corresponded to thermistor resistances at approximately 20, 60 and 100°C, respectively.

The circuit could be set to give zero and full deflection of the recorder-pen at approximately 60 and 20°C, respectively, by adopting the following procedure:

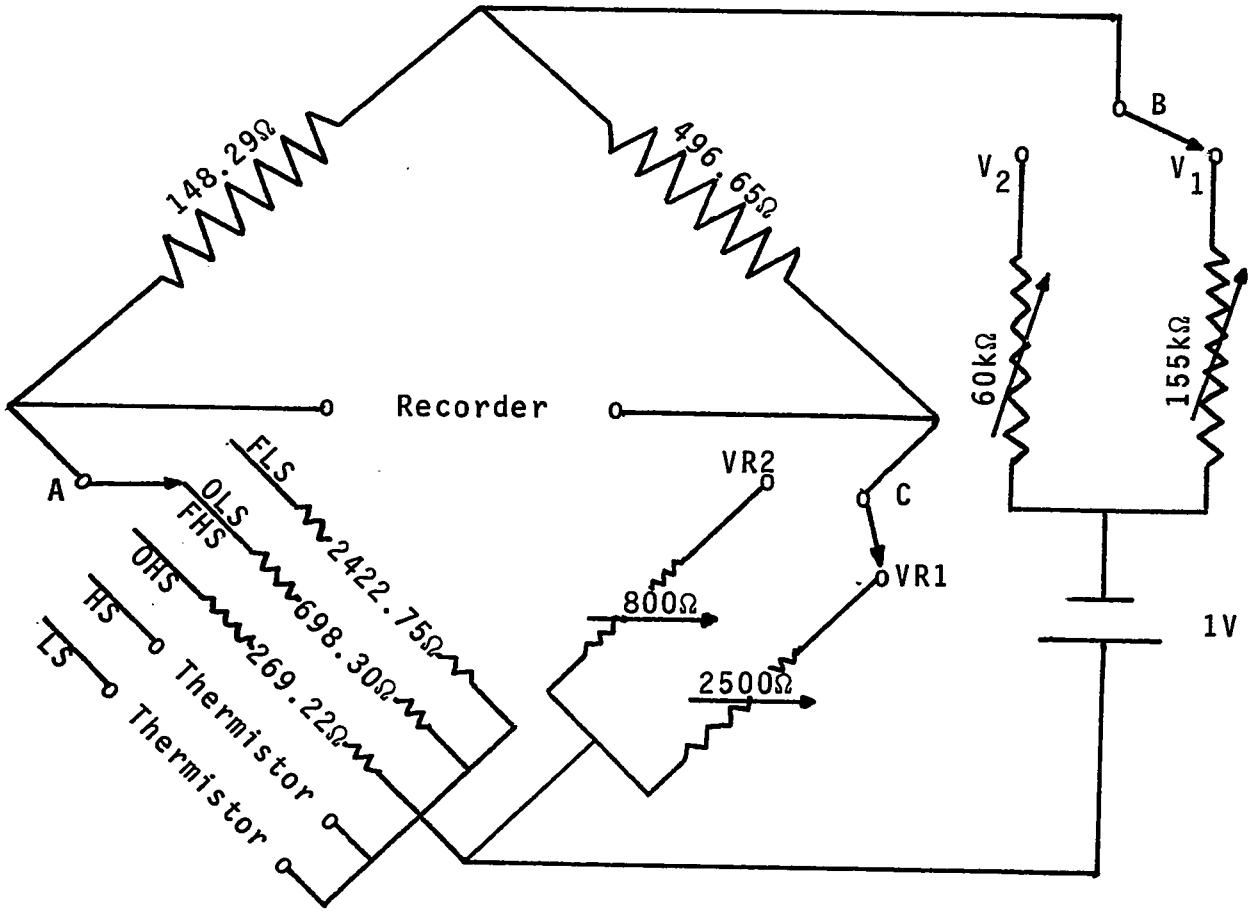

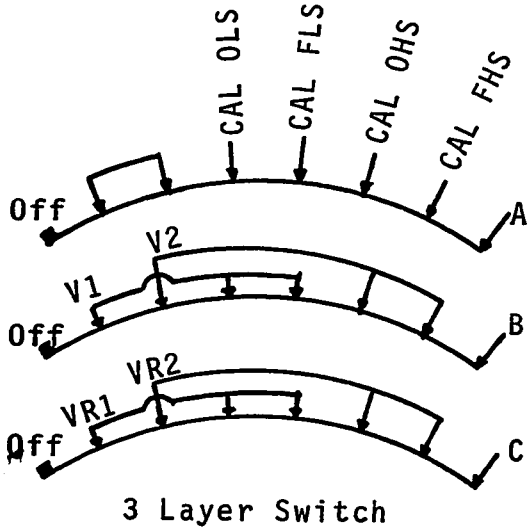

3 Layer Switch

LEGEND

CAL = Calibration
OLS = Zero Deflection on Low Scale
FLS = Full Deflection on Low Scale
OHS = Zero Deflection on High Scale
FHS = Full Deflection on High Scale
LS = Low Scale
HS = High Scale

FIG. 19 THERMISTOR CIRCUIT

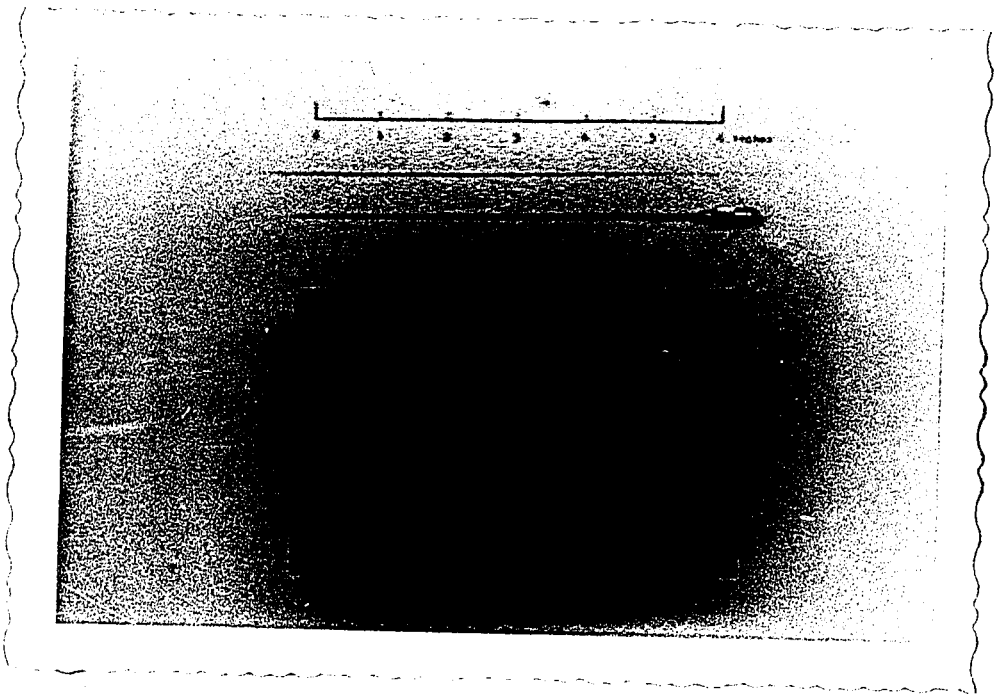

Fig. 20 THERMISTOR AND THERMISTOR-CIRCUIT BOX

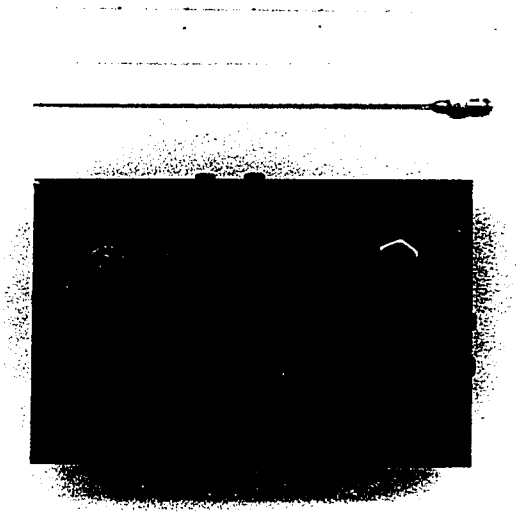

Fig. 20 THERMISTOR AND THERMISTOR-CIRCUIT BOX

(i) The three-layer switch was placed into position 3 thus substituting the thermistor by the 698.3 ohm resistor. Potentiometer R 3 was then adjusted to yield a zero deflection of the recorder-pen.

(ii) The switch was set into position 4 thus replacing the thermistor with the 2422.75 ohm resistor. Potentiometer RV was then varied until a full-deflection of the recorder pen was obtained.

The circuit was then ready for temperature measurements with the thermistor in the 20 to 60°C range. The procedure for the high temperature scale was analogous to the one described above except that the switch was placed into positions 5 and 6.

2. Thermistor Calibration

The thermistor constants A_{th} and B_{th} were not accurately specified by the manufacturer and had to be determined experimentally. This was equivalent to performing a temperature-calibration of the thermistor and its associated circuit.

The thermistor-resistance, R, was found at a number of temperatures, T, and a plot of ℓn R versus 1/T was prepared (T was expressed in degrees Kelvin). The intercept and slope of the resulting straight line corresponded to $\ell n\ A_{th}$ and B_{th} respectively.

The measurements were made by placing the thermistor into an electrically heated oven whose temperature was rising very slowly. The oven temperature was measured with a Beckmann precision mercury-in-glass thermometer. The thermometer was immersed in the oven only as far as the 20°C mark and the

observed temperature TO had to be corrected since part of the thermometer-stem was at atmospheric temperature. The corrected temperature TC was given by:

$$TC = TO + 1.6 * 10^{-4} (TO - 20)(TO - T_{room}) \quad \text{(IV-11)}$$

where T_{room} is the room temperature.

The thermistor resistance, R, could be found from the deflection of the recorder-pen. The calculation is explained by means of the simplified circuit diagram below.

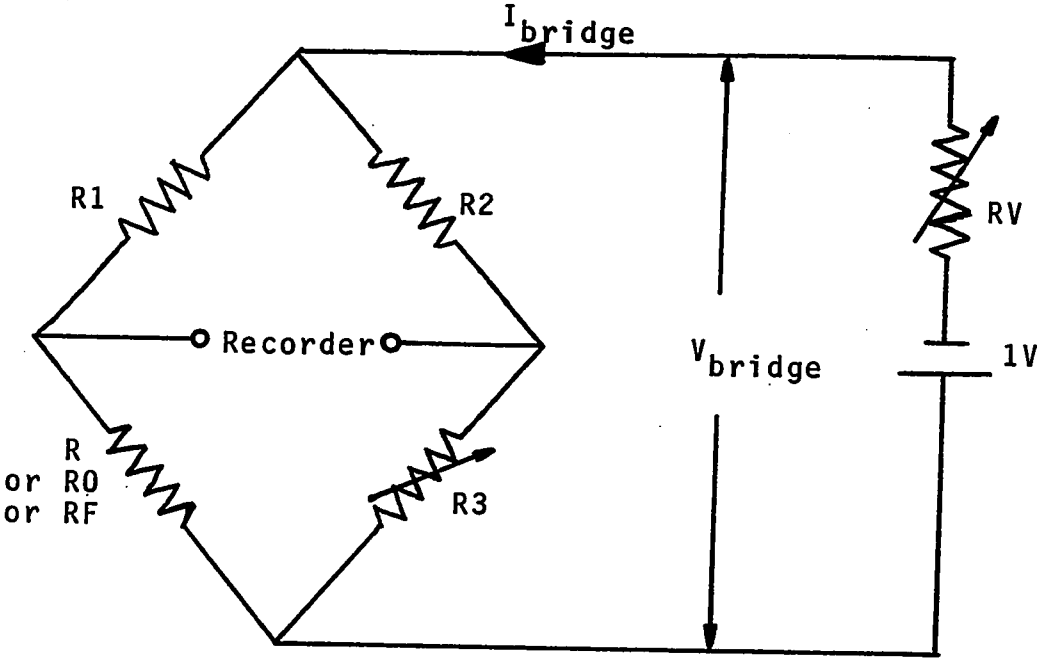

R, RO and RF denote the thermistor resistance, the resistances giving a zero and full recorder-pen deflection, respectively.

As explained earlier, resistance RO was first switched into the bridge circuit and R3 was adjusted until the bridge was balanced, i.e.:

$$R3 = (RO/R1) * R2 \quad \text{(IV-12)}$$

Similarly, RF was then switched into the circuit and RV was adjusted until a potential difference of 1 mV developed across the recorder terminals thus resulting in full scale deflection of the pen, i.e.:

$$0.001 = V_{bridge}\left[\frac{RF}{R1 + RF} - \frac{R3}{R2 + R3}\right] \qquad \text{(IV-13)}$$

The effective voltage across the bridge inputs could be found as follows:

The total bridge resistance, R_{bridge}, was:

$$R_{bridge} = \frac{R1 + RF + R2 + R3}{(R1 + RF)(R2 + R3)} \qquad \text{(IV-14)}$$

and the current flowing into the bridge was:

$$I_{bridge} = \frac{1.0}{(R_{bridge} + RV)} \qquad \text{(IV-15)}$$

Hence:

$$V_{bridge} = \frac{1.0}{R_{bridge} + RV}\ R_{bridge} \qquad \text{(IV-16)}$$

and hence Equation (IV-13) becomes:

$$0.001 = \frac{(R1 + RF)(R2 + R3)}{(R1 + RF + R2 + R3)}\left[\frac{1}{RV + \frac{(R1 + RF)(R2 + R3)}{R1 + RF + R2 + R3}}\right] * \left[\frac{RF}{R1 + RF} - \frac{R3}{R2 + R3}\right] \qquad \text{(IV-17)}$$

or:

$$0.001 = \frac{(R1 + RF)(R2 + R3)}{RV\,(R1 + RF + R2 + R3) + (R1 + RF)(R2 + R3)} * \left[\frac{RF}{R1 + RF} - \frac{R3}{R2 + R3}\right] \qquad \text{(IV-18)}$$

Putting:

$$\begin{aligned} TC1 &= R3/(R2 + R3) \\ TC2 &= R2 + R3 \\ TC3 &= (R1 + RF)(R2 + R3) \\ TC4 &= RF/(RF + R1) - TC1 \\ TC5 &= R1 + RF + R2 + R3 \end{aligned} \qquad \text{(IV-19)}$$

simplifies Equation (IV-18) to:

$$0.001 = \frac{TC3 * TC4}{RV * TC5 + TC3} \qquad \text{(IV-20)}$$

and hence:

$$RV = \frac{TC3 * TC4 - 0.001 * TC3}{0.001 * TC5} \qquad \text{(IV-21)}$$

When the thermistor was switched into the bridge and a pen-deflection of D* units was observed on the recorder, the thermistor resistance R could be found from Equation (IV-18) after replacing RF by R and the 1 mV potential difference across the recorder terminals by 0.0001 D* . It is noted that at full scale-deflection D* = 10. Hence:

$$0.0001\ D^* = \frac{(R1 + R)(R2 + R3)}{RV\ (R1 + R + R2 + R3) + (R1 + R)(R2 + R3)} * \left[\frac{R}{R + R1} - \frac{R3}{R2 + R3}\right] \qquad \text{(IV-22)}$$

Putting:

$$\begin{aligned} TC6 &= R1 + R2 + R3 \\ TC7 &= TC6 * RV + R1 * TC2 \\ TC8 &= RV + TC2 \\ TC9 &= TC2 * (1 - TC7)/TC8 \\ TC10 &= TC2 * R1 * TC1/TC8 \\ TC11 &= TC7/TC8 \end{aligned} \qquad \text{(IV-23)}$$

it can be shown that:

$$R = \frac{0.0001 * TC11 * D^* + TC10}{TC9 - 0.0001\ D^*} \qquad \text{(IV-24)}$$

When the recorder-pen deflection was D* at a temperature T, the thermistor resistance R corresponding to this temperature could therefore be found.

Table 3 gives the experimental measurements of recorder-pen deflections and temperatures. Fig. 21 is a plot of ℓn R versus 1/T. A least square fit procedure was used to draw the best straight line through the experimental points and the equation of this line was found to be:

$$\ell n\ R = -2.5 + 3033.026/T \qquad \text{(IV-25)}$$

3. Self-Heating of Thermistor

When the Wheatstone bridge circuit was not balanced, a small current flowed through the thermistor and could lead to heating and thus errors in the temperature measurements. This possible error was investigated as follows and was found to be insignificant.

The current in the thermistor was a maximum when the recorder-pen deflected fully, i.e. a potential difference of 1 mV was developed across the recorder terminals. Under these conditions V_{bridge} is given by:

$$0.001 = V_{bridge}\left(\frac{RF}{R1 + RF} - \frac{R3}{R2 + R3}\right) \qquad \text{(IV-26)}$$

where R3 is given by Equation (IV-12). The corresponding

Table 3

Thermistor-Calibration Data

1. Low Temperature Scale:

TO, °C	T_{room}, °C	TC, °C	1./TC, $^{o}K^{-1}$	D*	R, ohms	ℓn R
26.10	27.15	26.10	0.003342	8.58	2099.5	7.6494
27.00	27.30	27.00	0.003332	8.25	2025.9	7.6138
28.00	27.30	28.00	0.003320	7.95	1960.8	7.5811
29.00	27.40	29.00	0.003309	7.64	1895.4	7.5472
30.00	27.40	30.00	0.003299	7.34	1833.7	7.5141
31.00	27.50	31.01	0.003288	7.03	1771.6	7.4795
32.00	27.55	32.01	0.003277	6.69	1705.3	7.4415
33.00	27.60	33.01	0.003266	6.38	1646.4	7.4064
34.00	27.60	34.01	0.003255	6.11	1596.4	7.3755
35.00	27.60	35.02	0.003245	5.82	1543.8	7.3420
36.00	27.70	36.02	0.003234	5.55	1496.0	7.3105
37.00	27.65	37.03	0.003224	5.27	1447.4	7.2775
38.00	27.60	38.03	0.003213	5.01	1403.3	7.2466
39.00	27.60	39.03	0.003203	4.75	1360.1	7.2153
40.00	27.60	40.04	0.003193	4.48	1316.9	7.1824
41.00	27.60	41.05	0.003183	4.23	1276.1	7.1516
42.00	27.60	42.05	0.003172	3.97	1235.3	7.1191
43.00	27.75	43.06	0.003162	3.72	1196.9	7.0875
44.00	27.70	44.06	0.003152	3.50	1163.6	7.0593
45.00	27.70	45.07	0.003142	3.26	1127.9	7.0281
46.00	27.70	46.08	0.003132	3.03	1094.3	6.9979
47.00	27.75	47.08	0.003123	2.81	1062.7	6.9685
48.00	27.75	48.09	0.003113	2.59	1031.5	6.9388
49.00	27.80	49.10	0.003103	2.38	1002.2	6.9100
50.00	27.85	50.11	0.003093	2.15	970.7	6.8780
51.00	27.85	51.11	0.003084	1.94	942.3	6.8483
52.00	27.90	52.12	0.003074	1.75	916.9	6.8210
53.00	27.90	53.13	0.003065	1.55	890.6	6.7919
54.00	28.00	54.14	0.003055	1.36	866.0	6.7638
55.00	28.00	55.15	0.003046	1.18	842.9	6.7368
56.00	28.00	56.16	0.003037	0.99	818.8	6.7079
57.00	28.00	57.17	0.003027	0.80	795.1	6.6785
58.00	28.00	58.18	0.003018	0.63	774.1	6.6517
59.00	28.00	59.19	0.003009	0.44	750.9	6.6213
60.00	28.00	60.20	0.003000	0.29	732.3	6.5969
61.00	28.00	61.22	0.002991	0.11	711.3	6.5671
61.80	28.00	62.03	0.002983	0.0	698.3	6.5486

Table 3 contd

2. High Temperature Scale:

TO, °C	T_{room}, °C	TC, °C	1./TC, $^{o}K^{-1}$	D*	R, ohms	ℓn R
61.40	25.10	61.64	0.002987	9.85	690.4	6.5372
62.00	25.10	62.25	0.002981	9.70	682.5	6.5257
63.10	25.10	63.36	0.002972	9.43	668.4	6.5049
64.00	25.20	64.27	0.002964	9.14	653.5	6.4823
65.00	25.30	65.29	0.002955	8.82	637.3	6.4572
66.00	25.20	66.30	0.002946	8.49	620.8	6.4310
67.20	25.30	67.52	0.002935	8.10	601.7	6.3997
68.00	25.30	68.33	0.002928	7.84	589.1	6.3786
69.00	25.30	69.34	0.002920	7.52	573.8	6.3523
70.00	25.40	70.36	0.002911	7.20	558.8	6.3258
71.00	25.40	71.37	0.002902	6.90	544.9	6.3005
72.00	25.40	72.39	0.002894	6.59	530.7	6.2742
73.00	25.40	73.40	0.002885	6.29	517.1	6.2483
74.00	25.40	74.42	0.002877	5.99	503.8	6.2221
75.00	25.40	75.44	0.002869	5.70	491.0	6.1965
76.00	25.00	76.46	0.002860	5.44	479.7	6.1732
77.00	25.40	77.47	0.002852	5.16	467.7	6.1478
78.00	25.40	78.49	0.002844	4.85	454.5	6.1192
79.10	25.40	79.61	0.002835	4.61	444.5	6.0968
80.00	25.50	80.52	0.002827	4.37	434.5	6.0742
81.00	25.50	81.54	0.002819	4.10	423.4	6.0483
82.00	25.50	82.56	0.002811	3.83	412.4	6.0221
83.00	25.50	83.58	0.002803	3.60	403.2	5.9994
84.00	25.50	84.60	0.002795	3.37	394.0	5.9765
85.00	25.50	85.62	0.002787	3.13	384.6	5.9522
86.00	25.50	86.64	0.002779	2.91	376.0	5.9296
87.00	25.50	87.66	0.002771	2.69	367.5	5.9067
88.00	25.50	88.68	0.002764	2.46	358.7	5.8824
89.00	25.50	89.70	0.002756	2.25	350.7	5.8599
90.00	25.60	90.72	0.002748	2.05	343.1	5.8381
91.00	25.60	91.74	0.002740	1.84	335.3	5.8150
92.00	25.70	92.76	0.002733	1.63	327.5	5.7915
93.10	25.60	93.89	0.002724	1.40	319.0	5.7653
94.00	25.90	94.81	0.002718	1.23	312.9	5.7457
95.00	26.10	95.83	0.002710	1.06	306.7	5.7259
96.00	26.30	96.85	0.002703	0.88	300.2	5.7045
97.00	26.40	97.87	0.002695	0.69	293.4	5.6817
98.00	26.50	98.89	0.002688	0.52	287.4	5.6609
99.00	26.50	99.92	0.002680	0.36	281.8	5.6411
100.00	26.60	100.94	0.002673	0.19	275.8	5.6198
101.00	26.70	101.96	0.002666	0.04	270.6	5.6007

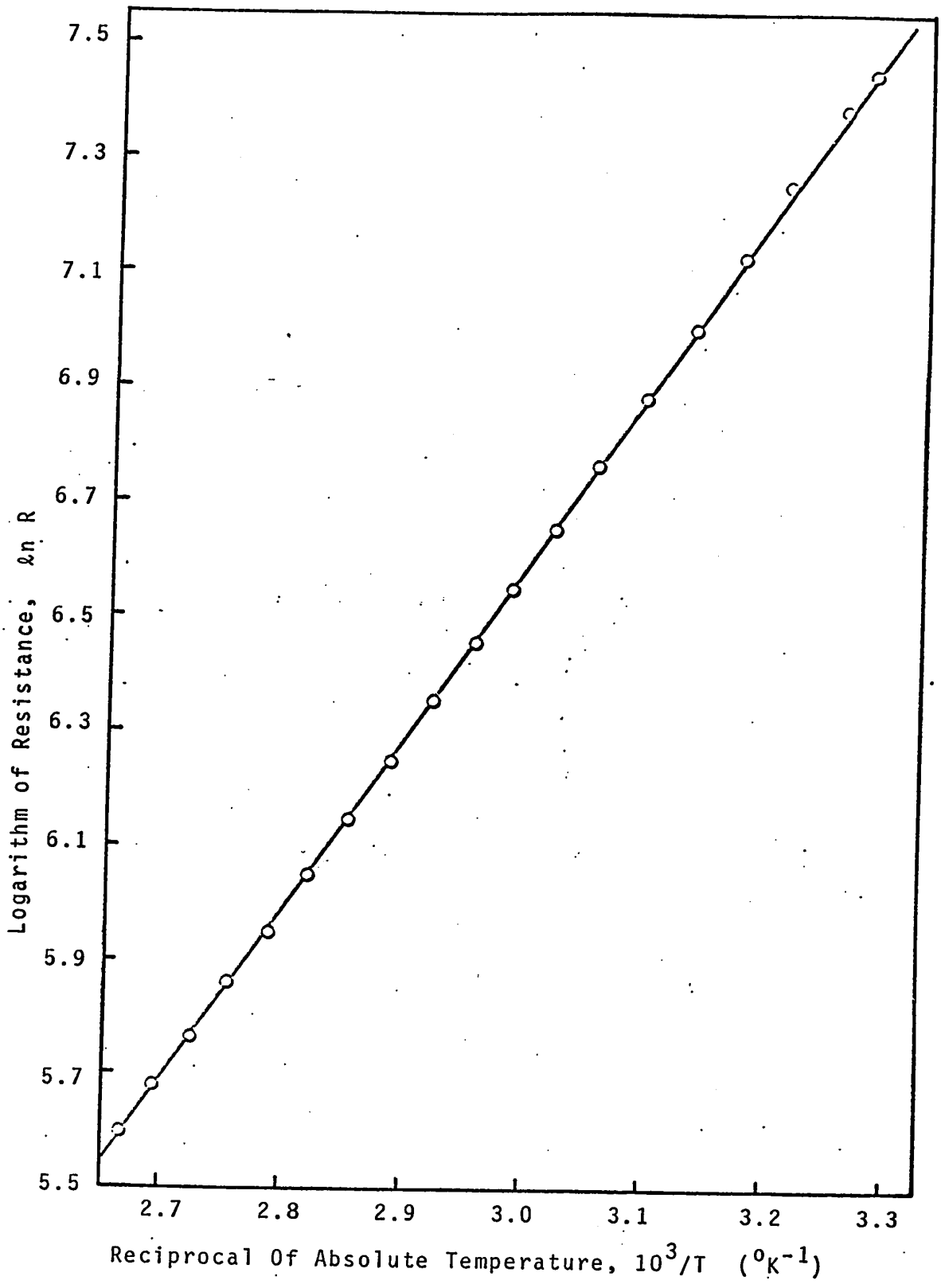

FIG. 21 THERMISTOR RESISTANCE VS TEMPERATURE

current through the thermistor is:

$$I_{thermistor} = V_{bridge} / (RF + R1) \qquad \text{(IV-27)}$$

and hence the power dissipated in the thermistor is:

$$P_{thermistor} = I^2_{thermistor} * RF \qquad \text{(IV-28)}$$

Substituting the values for the various resistances into the above equations gives $P_{thermistor} = 1.7 * 10^{-8}$ and $=2.9 * 10^{-8}$ watts for the low and high temperature scales, respectively.

The dissipation constant of the thermistor used in this study was approximately $9 * 10^{-5}$ watts / ^{o}C, i.e. when $9 * 10^{-5}$ watts of electrical energy are dissipated in the thermistor while keeping it in stagnant air, the temperature of the thermistor is 1 ^{o}C above that of the surroundings.

The temperature errors due to electrical heating of the thermistor are therefore estimated to be less than $1.7 * 10^{-8} / 9 * 10^{-5} = 0.00019$ and $2.9 * 10^{-8} / 9 * 10^{-5} = 0.0003$ ^{o}C for the low and high temperature scales, respectively. These errors are clearly negligible.

M: Probe Holders

In order to obtain the velocity and temperature profiles of the fluid between the plates the probes, i.e. the thermistor and anemometer, had to be mounted in such a way that their position was adjustable. Three simple and identical probe holders were therefore constructed and they are shown in Fig 22.

The main part of the holders consisted of a plastic plate with a 2 cms diameter hole into which the anemometer could be inserted. A 1" wide and 3½" long vertical slot was cut into the side wall of the particle collector and the alignment was such that the anemometer protruded through the plastic plate into the particle collector. The plastic plate was held against the side-wall by two angle-pieces and free to slide up and down. Stop-cock grease was used to reduce the friction and to prevent leakage of fluid from the particle-collector.

Since the thermistor needle was only 0.028" in diameter (compared with 2 cms for the anemometer stem), the above arrangement was adapted to the thermistor by inserting a 2cms plug into the anemometer port. This plug had in turn a 0.03" hole in its centre through which the thermistor could be inserted into the particle-collector.

The three probe holders were located approximately 3, 3½, and 4 feet from the entrance of the particle-collector and could therefore be used to determine whether developed conditions prevailed.

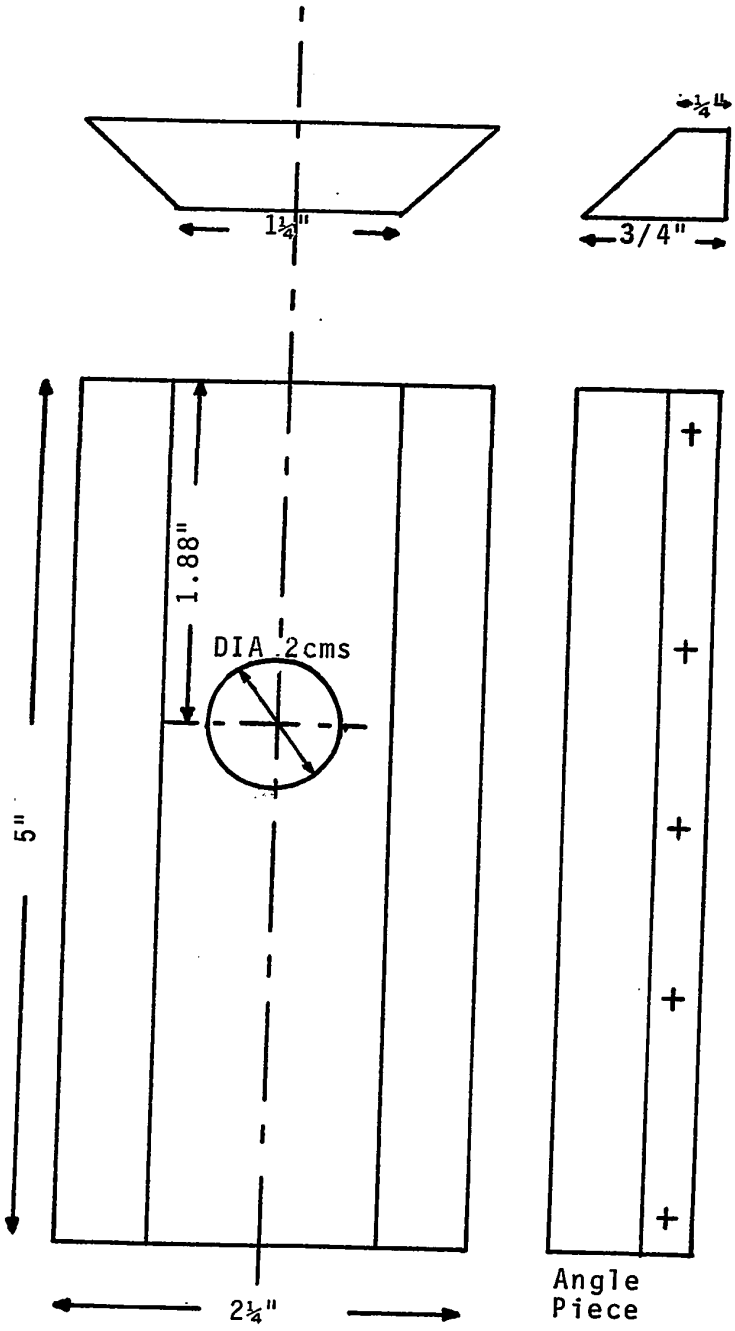

FIG. 22 PROBE HOLDER

N. Probe Position Measurements

Since the thermistor and anemometer were used to determine the temperature and velocity profiles respectively, the location of these probes had to be known in relation to the plates of the particle-collector. The probe position was determined by means of a cathetometer which was situated so that the tip of the thermistor and anemometer probes could be observed through the cathetometer-telescope. A microscope lamp was used to illuminate the probes.

The cathetometer was aligned relative to the particle-collector by focussing the telescope on the edges of the "upper" and "lower" plates of the collector.

0. Experimental Procedure

1. Start-Up

a) The tank in the cooling water circuit is filled with tap-water and the water is circulated by starting the centrifugal pump.

b) The flow-rate of the cooling water is adjusted by means of the bypass and the valve at the outlet of the particle collector so that the lower plate is just wetted. The adjustment is repeated whenever necessary.

c) Steam is injected into the cooling water in order to raise it to the desired lower plate temperature.

d) Hot air is introduced into the walls of the vapour-box by preheating air from the laboratory supply with a Bunsen burner.

e) Steam is injected into the vapour-box and its flow rate is adjusted until the desired upper plate temperature is attained.

f) The electrical current to the nichrome wires is slowly increased until condensation of water-vapour on the front-side of the particle collector is prevented.

g) The heating tape at the back-side of the particle collector is switched on.

2. Settling Length of Particles

a) The air-flow through the particle-collector is started.

b) A cigarette is lit and inserted into the smoke-generator.

c) After smoky air has entered the particle-collector for some time and a definite settling length is observed, the latter is measured.

d) The flow-rate of smoky-air into the particle-collector is measured.

e) The temperatures at the upper and lower plates are measured with the thermistor.

3. Settling Time of Particles

a) Smoky air is passed through the particle-collector at a high flow rate so that the entire space between the upper and lower plates is filled with smoke.

b) The temperatures of the upper and lower plates are measured with the thermistor.

c) The air is shut off and the time taken for the smoke to settle is measured. This is the particle settling time.

d) The temperatures of the plates are measured again to make sure that they remain unchanged

4. Temperature Measurements

a) The thermistor circuit is adjusted according to the

procedure described in Section IV-L.

b) The cathetometer-telescope is focused on the upper plate in order to establish the position of the particle collector in relation to the cathetometer.

c) The position of the thermistor tip is measured with the cathetometer. The microscope lamp is used to illuminate the thermistor.

d) In order to obtain temperature profiles, the thermistor position is adjusted by means of the probe-holder which can be moved vertically. The thermistor positions and the corresponding temperatures are recorded.

e) Since approximately five minutes are required to obtain a temperature profile, the plate temperatures are taken before and after the profile measurements in order to check that they remain constant.

5. Velocity Profiles

a) After the electronic equipment has warmed up, the anemometer is introduced into the particle collector.

b) The anemometer wire is placed perpendicularly to the direction of the flow by observing it through the cathetometer telescope.

c) The upper plate and lower plate temperatures are measured.

d) The gas-flow through the particle collector is stopped and the anemometer circuit is adjusted in the PROB.ADJ and LVA.CAL positions (see Section IV-K).

e) The gas-flow is started and the anemometer reading is recorded. The anemometer position is determined by means of the cathetometer.

f) The anemometer position is changed and steps (c) to (e) are repeated.

6. Test for Developed Operating Conditions

a) The thermistor is placed at an arbitrary position between the plates and the gas-flow rate through the particle-collector is varied. When the thermistor reading remains constant, conditions are developed.

b) Temperature and velocity profiles are measured at the three probe support-positions. When the profiles coincide, the particle collector operates under developed conditions.

7. Warning

The maximum operating temperature of the apparatus is $95^{o}C$. Higher temperatures result in thermal stress-cracking of the plastic components.

V. RESULTS AND DISCUSSION

This section is divided into three main parts: General Considerations, Theoretical Results, Experimental Results. Since many theoretical results were obtained before the experimental work was completed, their discussion precedes the treatment of the experimental findings.

A. General Considerations

The two most significant results of the present study are the following:

(i) The simple parallel plate collector separated micron-size particles from air effectively.

(ii) The collector performance could be predicted theoretically before experimental data were available.

Models I and II indicated that the particles would be deposited on the lower plate of the collector and that the primary mechanism responsible for deposition would be diffusiophoresis. These general predictions were readily confirmed experimentally.

Figure 23 shows a close-up view of the particle separation. Smoky air (bright area) enters the particle collector continuously at the left and flows towards the right. Water vapour diffuses from the upper to the lower plate and causes the particles to move towards the latter. The particles thus deposit on the lower plate and smoke-free air leaves the particle collector on the right.

The particle movement towards the lower plate could

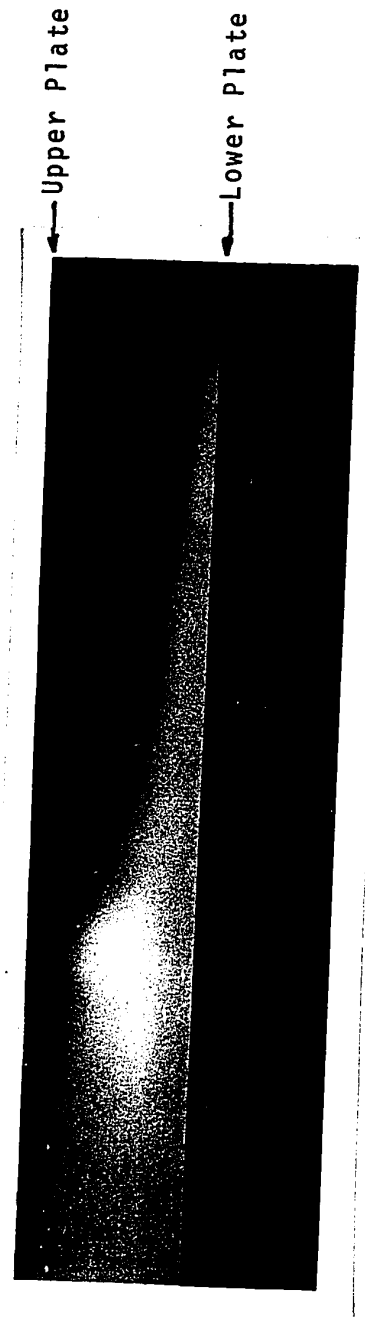

FIG. 23 SMOKE PARTICLES SETTLING IN COLLECTOR

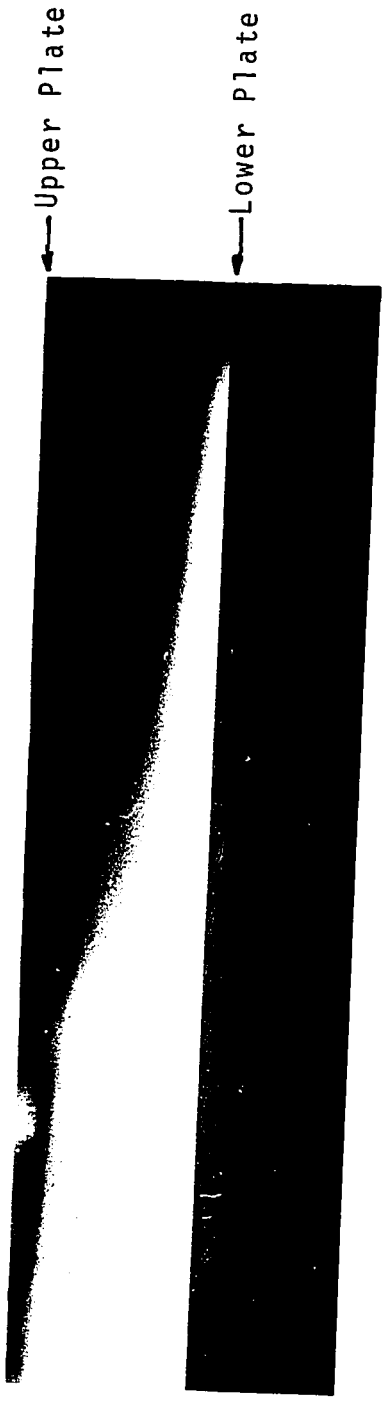

FIG. 23 SMOKE PARTICLES SETTLING IN COLLECTOR

also be observed by introducing smoky air into the collector and then stopping the air supply. The smoke cloud initially filled most of the space between the plates but after the flow was stopped, the upper surface of the cloud was seen to descend. The clear space between the upper plate and the smoke cloud increased as time progressed until the entire cloud had deposited on the lower plate.

In addition to the above observations a build up of a brownish scum could be noted on the lower plate after extended operation of the particle collector. The upper plate remained however clean. This again proved that the particles moved towards the lower plate.

The effect primarily responsible for the particle movement normal to the plates was diffusiophoresis and neither thermophoresis nor gravity played an important rôle. The gravity effect was negligible because no significant particle movement towards the lower plate could be observed when the collector was operated isothermally and without diffusion of water vapour between the plates. Similarly, thermophoresis was unimportant because the smoke particles were not removed when the plates of the collector were kept at temperatures differing by less than $25^{o}C$ and when no diffusion of water vapour occurred. The thermophoretic effect would have become significant for higher plate temperature differences, but the experiments were conducted at $(TU - TL) \leq 25\ ^{o}C$.

1. Operating Conditions

The experiments were performed at elevated temperatures ranging from approximately 65 to 90 ^{o}C in order to obtain high differences of water vapour pressure and hence diffusiophoretic forces. The upper temperature limit of 90 ^{o}C was due to the materials of construction of the particle collector. It was possible to operate the apparatus with lower plate temperatures less than 65 ^{o}C but under such conditions substantial condensation occurred between the plates when smoke particles were present. Condensation could be detected by illuminating the smoke with polychromatic light and observing the refraction of the light into its spectrum colours (i.e. observing a "rainbow").

The plate spacings which were investigated experimentally in this study were 1.5, 2.0, 2.5, and 3.0 cms. Spacings less than 1.5 cms were impractical because the plates were not perfectly flat and this would have resulted in significant errors. The maximum plate spacing used was 3.0 cms because larger ones led to excessive condensation and very large particle settling lengths and times. The latter is due to the fact that the diffusiophoretic force is approximately proportional to the vapour pressure gradient.

The theoretical results were calculated for the same conditions under which experimental data were obtained in order to permit comparison between the theoretical and experimental results.

B. Theoretical Results

As pointed out in Section III-F-1 the basic assumption underlying Model I is that the particles move with the local fluid velocity. Hence this model requires only a solution of the transport equations since these equations define the fluid velocity.

The effects on the particle velocity due to thermophoresis and gravity are also taken into consideration in Model II (see also Section III-F-2). Furthermore, Schmitt and Waldmann's expression[10,18] is used for the diffusiophoretic force.

1. Particle Trajectory (Model I)

Figure 24[†] (based on data given in Table 4) shows a typical particle trajectory which was calculated by solving the transport equations for a particle starting at the upper plate. This trajectory also corresponds to a fluid stream line. From Fig. 24 it is apparent that the particle is rapidly carried in the x-direction in the central region between the plates where v_x is large. Near the plates the velocity parallel to the plates is small and the particle moves rapidly perpendicularly to the plates.

The distance which the particle moves downstream before reaching the lower plate is the settling length and it will be considered next.

[†]All figures and tables subsequently cited in this Section are given on pages 152a to 198.

2. Theoretical Particle Settling Lengths (Model I)

The particle settling lengths are of interest in connection with the minimum size which a particle collector must have in order to achieve separation. The Model I results for plate spacings of 1.5, 2.0, 2.5, and 3.0 cms are listed and plotted in Tables 5, 7, 9, 11 and Figures 25, 26, 27, 28, respectively. (The latter figures also contain experimental data based on Tables 6, 8, 10, and 12 but these will not be discussed until later). The results were calculated for lower plate temperatures of 83.2, 76.8, and 68.5 ^{o}C and at various upper plate temperatures.

As may be seen from Tables 5, 7, 9, and 11 the settling lengths were not all calculated at the same mass flow rate of air through the particle collector since DELPX rather than M_{Air} was specified in the computer program. However, Fig. 29 and Table 13 show that the settling lengths are proportional to the mass flow rate of dry air and the pressure gradient in the particle collector. The reason for this is that C1 is small and hence C1 * (dv_x/dy) is insignificant in comparison with the other terms in Equation (III-73). Hence it is possible to convert the settling lengths to the same basis, i.e. a mass flow rate of dry air of 0.0216 gm/sec which corresponds to a rotameter reading of 2.0. The Model I settling lengths converted to the same basis are given in the seventh column of Tables 5 to 12 and these converted lengths are shown in Figures 25 to 28.

From Figures 25 to 28 it is apparent that the settling lengths of the particles are strong, increasing functions of the temperature difference between the upper and lower plates, (TU - TL), for a given plate spacing. Since (TU - TL) determines the vapour pressure gradient in the particle collector this observation implies that the diffusiophoretic velocity is strongly dependent on this gradient. This result follows because the Model I particle velocity was calculated from Equation (III-69) or (III-71).

Similarly it may be seen from Figures 25 to 28 that the settling lengths are a function of the lower plate temperature for a given TU and plate spacing. Hence diffusiophoresis is dependent on the average collector temperature or equivalently on the average mass fraction of water vapour. This result again follows from Equation (III-69) since the term $(w_A - 1)$ enters into the expression.

By comparing Figures 25 to 28 it is found that the particle settling lengths increase with increasing plate spacing for given plate temperatures. This again implies that the diffusiophoretic velocity is related to the concentration gradient and since this gradient decreases with increasing plate spacing (for given plate temperatures), the settling lengths are also increasing functions of plate spacing.

In Figures 25 to 28 the experimental data are also shown and it is evident that they agree well with the Model I results. The experimental data are somewhat scattered but they follow the

same trends as the theoretical results. The scatter is due to experimental short-comings which will be considered in Section V-C.

3. Theoretical Particle Settling Times (Model I)

Figures 30, 31, 32, and 33 show the Model I theoretical settling times for the four different plate spacings as functions of the upper and lower plate temperatures.

The settling times are seen to increase sharply for decreasing (TU - TL), decreasing average collector temperature, and increasing plate spacing. This behaviour is due to the fact that the settling time is inversely related to the settling velocity and the latter is given by Equation (III-69).

The experimental data are also shown in Figures 30 to 33 and they are found to agree well with the Model I results thus confirming the assumption that the particles move with the local fluid velocity. The scatter of the experimental data is similar to that found in measuring the particle settling lengths and will be considered in Section V-B.

4. Model II Results

In the "normal" Model II the particle diameter, D_p, particle density, ρ_p, and particle thermal conductivity, k_p, are 0.8 microns, 1 gm/cm^3, and 0.006 cal/(sec cm ^oK), respectively. Furthermore, Schmitt and Waldmann's semi-empirical expression for the diffusion slip factor is assumed (i.e. $\sigma_{AB} = - 0.26$).

Table 15 shows v_{yp} and v_y, i.e. the particle velocity

calculated by Model II and I, as a function of distance from the upper plate (GAP = 2.0 cms, TU = 90 ^{o}C, and TL = 76.8 ^{o}C). It is seen that the Model I particle velocity is approximately 3% less than that of Model II and similar results may be obtained for other plate temperatures and plate spacings. The difference in the results obtained from Model I and II is therefore very small.

The individual contributions to the Model II particle velocity are also given in Table 15 (see Equation (III-158)). The thermophoretic velocity, v_{ytp}, is seen to be about two orders of magnitude smaller than the diffusiophoretic velocity. The velocity due to gravity is approximately only one order of magnitude less than the diffusiophoretic velocity and it is even more significant when (TU - TL) is smaller that 13.2 ^{o}C.

The result of making various changes in Model II is shown in Table 16. When the particle density or particle diameter is increased the particle velocity is found to increase accordingly. This behaviour is due to the change in the gravity effect since it is an increasing function of the particle density and diameter.

When Kramers and Kistemaker's expression for the diffusion slip velocity is used to calculate the diffusiophoretic velocity (i.e. σ_{AB} is given by Equation (III-151)), the particle velocity is slightly larger than that calculated with the "normal" version of Model II.

When the thermal conductivity of the particles is lowered,

the particle velocity increases due to an increase in the thermophoretic force. Column 8 of Table 16 shows the particle velocity when the thermal conductivity is zero.

In summary it may be said that the changes in particle density, thermal conductivity, and particle diameter do not affect the particle velocity to a great extent provided $D_p < 2$ microns and the temperatures lie within the range considered in this study. When $D_p > 2$ microns the effect on the particle velocity due to gravity becomes significant and when $D_p >> 2$ microns diffusiophoresis and thermophoresis become insignificant in comparison with the gravity effect.

5. Operating Ratio

Table 17 gives a list of operating ratios of the particle collector used in this study. The operating ratio, ORATIO, is the mass of water vapour required to clean unit mass of air as calculated by Model I. It is seen that the ratio lies between approximately 1 and 2 which implies that the cost of water vapour is a major factor in the operation of a particle collector employing the diffusiophoretic effect.

From Table 17 it is also noted that ORATIO is only dependent on the plate temperatures and independent of the plate spacings. The reason for this is obvious when ORATIO is written in dimensionless form.

6. Work

The energy, WORK, required to pass one gram of air through

a particle collector SL centimeters long (i.e. the minimum length a collector must have in order to remove all particles) is shown in Table 17.

It is noted that WORK increases with decreasing (TU - TL) and increasing GAP which is due to the fact that SL is a strong function of the temperature difference of the plates and plate spacing. The magnitude of WORK is however very small and pumping costs are unlikely to be a major contribution to the operating cost of a particle collector employing diffusiophoresis.

7. Theoretical Results of Transport Equations

Theoretical temperature profiles are presented in Figures 34 to 37. These figures also show the experimental temperature measurements (based on data given in Tables 18 to 21) and the agreement between the experimental and theoretical results is seen to be good thus confirming the theoretical calculations.

Figure 38 shows a theoretical velocity profile and also some experimental data (see also Tables 22 and 23). The profile is very nearly parabolic and the agreement between the calculated and experimental results indicates that the transport equations were solved correctly.

Owing to severe experimental difficulties, it was not possible to measure the concentration profiles of water vapour in the particle collector, but a theoretical profile is presented in Fig. 39. The profile is seen to be almost linear for the plate temperatures chosen, but the non-linearity increases with increasing differences of water vapour pressure at the plates.

A total mass density profile, i.e. a plot of ρ versus y, is shown in Fig. 40 and this relationship is also seen to be slightly non-linear and the density increases as the lower (cooler) plate is approached.

Figure 41 shows the velocity, v_y, normal to the plates as a function of distance from the upper plate and for a particular plate spacing and set of plate temperatures. The velocity v_y is decreasing for increasing y and the relationship is slightly non-linear. The non-linearity becomes more pronounced as the concentration difference between the plates increases.

Figures 42 to 45 are plots of water vapour diffusivity, viscosity, thermal conductivity, and specific heat versus the distance from the upper plate for GAP = 2.5 cms, TU = 78.5 ^{o}C, and TL = 67.5 ^{o}C. It may be seen that the physical properties of the fluid vary non-linearly. The variations are small but any accurate model describing the behaviour of the particle collector ought to take them into consideration.

Figures 39 to 45 were drawn from the calculated results given in Table 24.

8. Performance of Computer Program

The computer program used for solving the transport and particle equations may be found in Appendix III. The program was written in FORTRAN G and run on McGill University's IBM 360 computers.

In order to calculate one case, i.e. solve the transport,

particle, and operating-cost equations for a particular set of plate temperatures, plate spacing, and pressure gradient in the particle collector, approximately five seconds of computer time were required (this includes the time required for the trial and error procedure). The calculated results are consistent to four significant figures when the error of integration, ε, is less than 10^{-4}.

As pointed out in Section III, the concentration, velocity, and temperature gradients at the upper plate had to be obtained by a trial and error procedure. It was found that approximately five trials were necessary in order to select the proper gradients so that the calculated results agree with the stipulated conditions at the lower plate within an accuracy of 0.001 percent.

C. Experimental Results

Measurements of the experimental settling times and lengths were of great interest in connection with this study. As can be seen from Fig. 23 the division between the smoky and clean regions was not very sharp. This was due to slight fluctuations in plate temperatures, gas flow rate, and occasional release of water drops from the upper plate. The particle diffusivity also affected the sharpness of the smoky region, but since the particles were of the order of a micron in diameter, their diffusivity was very small and the effect was therefore insignificant.

The somewhat gradual transition between the smoky and clean regions made it difficult to measure the particle settling length and settling time very accurately. A further significant contribution to the experimental error was that the upper and lower plates were not perfectly parallel. Since the plates were quite large (12"x80") and consisted of blotting paper as described in Section IV-B this was unavoidable.

1. Experimental Particle Settling Lengths

The experimental results for plate spacings of 1.5, 2.0, 2.5, and 3.0 cms are listed and plotted in Tables 6, 8, 10, 12, and Figures 25, 26, 27, 28, respectively. Measurements were made at lower plate temperatures of approximately 83.2, 76.8, and 68.5 ^{o}C and at various upper plate temperatures. The settling lengths were not all measured at the same mass flow

rate of air. From Fig. 29† it is seen that the settling length is proportional to the mass flow rate of air and hence it was possible to convert the measured settling lengths to the same basis, i.e. a mass flow rate of 0.0216 grams of air / sec which corresponded to a rotameter reading of 2.0 (see also Section V-A-2). These converted settling lengths are plotted in Figures 25, 26, 27, and 28.

From these figures it is seen that the experimental settling lengths agree well with the theoretical results predicted by Model I. Although the experimental data are somewhat scattered due to the experimental short-comings already mentioned, they follow the same trends as the Model I results, i.e. the settling lengths are decreasing functions of (TU - TL) and the average water vapour concentration in the collector and increasing functions of plate spacing.

2. Experimental Particle Settling Times

Figures 30, 31, 32, and 33 show the experimental particle settling times for the four different plate spacings as functions of the upper and lower plate temperatures.

The settling times are seen to increase sharply for decreasing (TU - TL), average collector temperature, and increasing plate spacings. Hence the settling time is inversely related to the diffusiophoretic velocity.

---

† Fig. 29 is based on Table 13 and Table 14.

The results from Model I are also shown in Figures 30 to 33 and they are found to agree well with the experimental data. The scatter of the latter is similar to that found in measuring particle settling lengths.

3. Experimental Temperature Profiles

Experimental temperature profiles for each plate spacing are presented in Fig. 34, 35, 36, and 37. The theoretical temperature profiles obtained by solving the transport equations are also shown in Fig. 34 to 37 and the agreement between the experimental and theoretical results is seen to be good, thus confirming the theoretical work.

It may be noted that the temperature profiles are non-linear which indicates that neither the physical properties of the gas mixture are constant nor the heat flux resulting from enthalpy diffusion is negligible.

4. Experimental Velocity Profile

A velocity profile obtained from experimental data is plotted in Fig. 38. The theoretical velocity profile obtained by solving the transport equations is also shown in Fig. 38 and the agreement between these results is fairly good. Both the experimental and theoretical results show that the velocity profile is not exactly parabolic but is a slightly distorted parabola. This behaviour results from the facts that the physical properties of the fluid are not constant and momentum transport results also from diffusion of water vapour.

The velocity measurements could only be made in the central region of the space between the plates and when GAP = 3.0 cms. This was due to the large diameter of the anemometer stem (2. cms). Furthermore it was difficult to use the anemometer for extended periods of time because water drops occasionally fell from the upper plate and broke the fine anemometer wire.

5. Tests for Developed Conditions

Experimental temperature profiles taken at two probe ports approximately one foot apart are shown in Fig.46[†]. It is seen that the profiles at the two locations are in good agreement thus indicating developed flow.

Furthermore it was observed that the temperature at any point between the surfaces did not vary with air flow rate through the particle collector (in the range of flow rates used). This also proved that the conditions were developed.

[†]Figure 46 is based on data given in Tables 25 and 26.

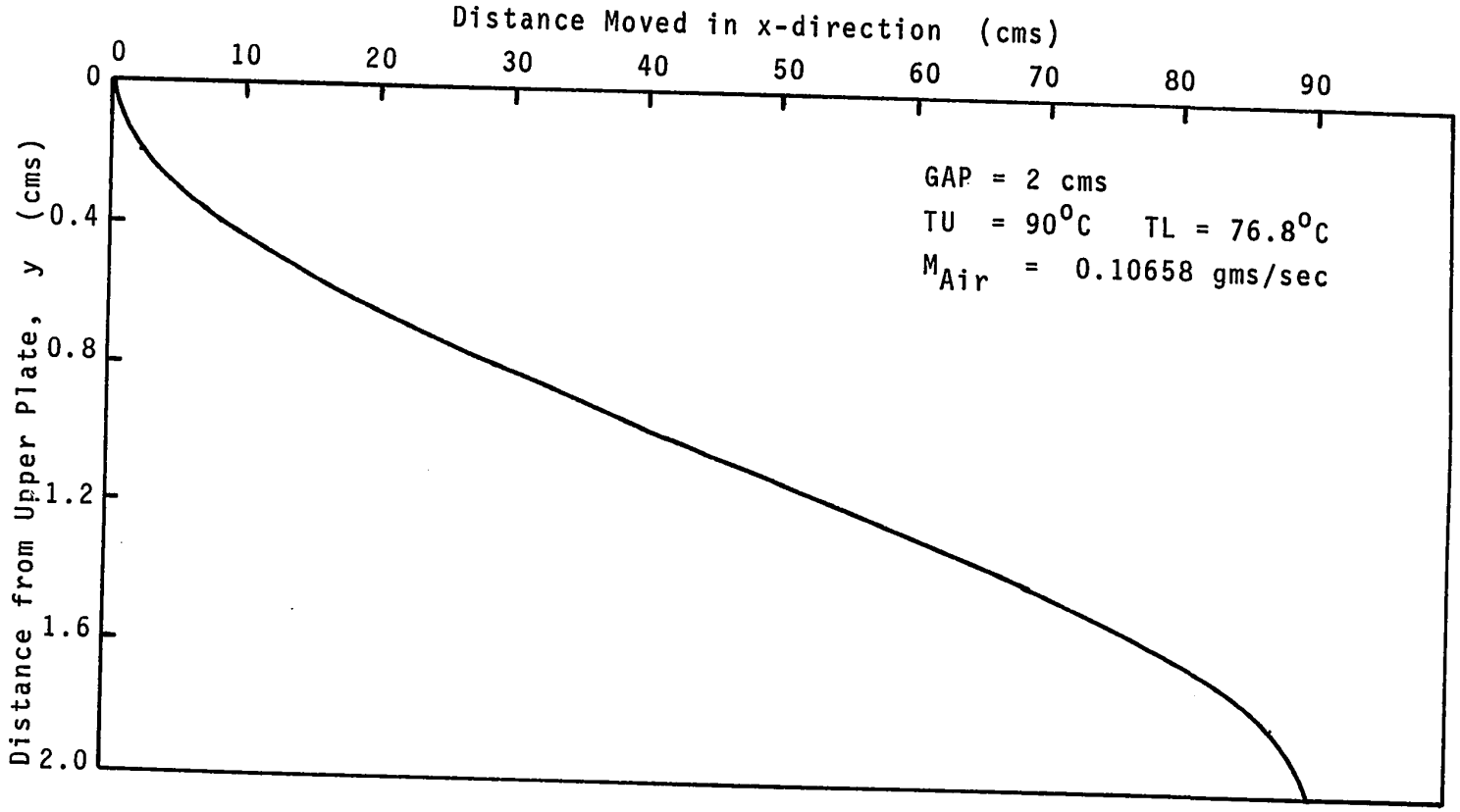

FIG. 24 PARTICLE TRAJECTORY (Model I)

4

Table 4

Particle Trajectory (Model I)

GAP = 2 cms

TU = 90 ^{o}C TL = 76.8 ^{o}C

M_{Air} = 0.10658 gms/sec

Distance from Upper Plate, (cms)	Distance moved in x-direction, (cms)
0.0	0.00
0.2	2.14
0.4	8.15
0.6	17.30
0.8	28.83
1.0	41.84
1.2	55.36
1.4	68.27
1.6	79.32
1.8	87.13
2.0	90.12

Table 5

Theoretical Settling Lengths and Times for GAP = 1.5 cms (Model I)

Temperature of Upper Plate, TU (^{o}C)	Temperature of Lower Plate, TL (^{o}C)	Settling Length, SL (cms)	Mass Flow Rate of Dry Air, M_{Air}(gm/sec)	Corrected Settling Length, † SL_c (cms)	Settling Time, ST (secs)
90	83.2	43.75	0.040537	23.30	18.56
88	83.2	69.66	0.043335	34.70	29.81
87	83.2	92.76	0.044588	44.91	39.88
86	83.2	132.32	0.045760	62.42	57.14
85	83.2	215.77	0.046859	99.40	93.59
84	83.2	507.80	0.047894	228.86	221.21
90	76.8	28.51	0.044964	13.69	12.44
88	76.8	37.85	0.048037	17.01	16.63
86	76.8	51.16	0.050701	21.78	22.65
84	76.8	71.83	0.053046	29.23	32.05
82	76.8	108.43	0.055134	42.45	48.73
81	76.8	139.83	0.056097	53.81	63.07
80	76.8	190.88	0.057012	72.27	86.39
79	76.8	288.41	0.057883	107.55	130.95
78	76.8	548.61	0.058714	201.69	249.86
90	68.5	22.42	0.049109	9.86	10.03
88	68.5	27.92	0.052444	11.50	12.56
86	68.5	34.64	0.055338	13.50	15.69
84	68.5	43.09	0.057886	16.07	19.65
82	68.5	54.09	0.060156	19.41	24.83
80	68.5	68.98	0.062199	23.94	31.86
78	68.5	90.26	0.064052	30.42	41.94

† converted for an air flow rate of 0.0216 gm/sec

Table 6

Experimental Data on Settling Lengths and Times for GAP = 1.5 cms

Temperature of Upper Plate, TU		Temperature of Lower Plate, TL		Settling Length, SL	Rotameter Reading,	Corrected Settling Length, † SL_c	Settling Time, ST
D* (High Scale)	^oC	D* (High Scale)	^oC	(cms)		(cms)	(secs)
2.21	89.8	3.80	83.3	86.6	6	28.9	21.9
3.07	86.1	3.79	83.1	52.5	2	52.5	50.6
2.88	86.9	3.80	83.3	39.8	2	39.8	44.3
3.51	84.2	3.78	83.1	65.1	1	130.2	-
4.65	79.6	5.41	76.8	69.1	2	69.1	91.7
4.20	81.4	5.41	76.8	43.5	2	43.5	56.2
3.39	84.8	5.42	76.8	31.6	2	31.6	30.1
2.70	87.7	5.38	76.9	28.3	4	14.2	16.3
2.27	89.8	5.41	76.8	22.4	4	11.2	14.9
2.82	87.2	7.84	68.6	27.0	6	9.0	14.5
4.59	79.9	7.80	68.6	20.5	2	20.5	34.4
4.12	81.7	7.92	68.4	49.6	4	24.8	23.9
3.54	84.1	7.87	68.5	35.8	6	11.9	17.5
3.16	85.7	7.89	68.4	33.4	6	11.1	17.8
2.29	89.6	7.86	68.5	35.7	6	11.9	11.1

† converted for an air flow rate of 0.0216 gm/sec

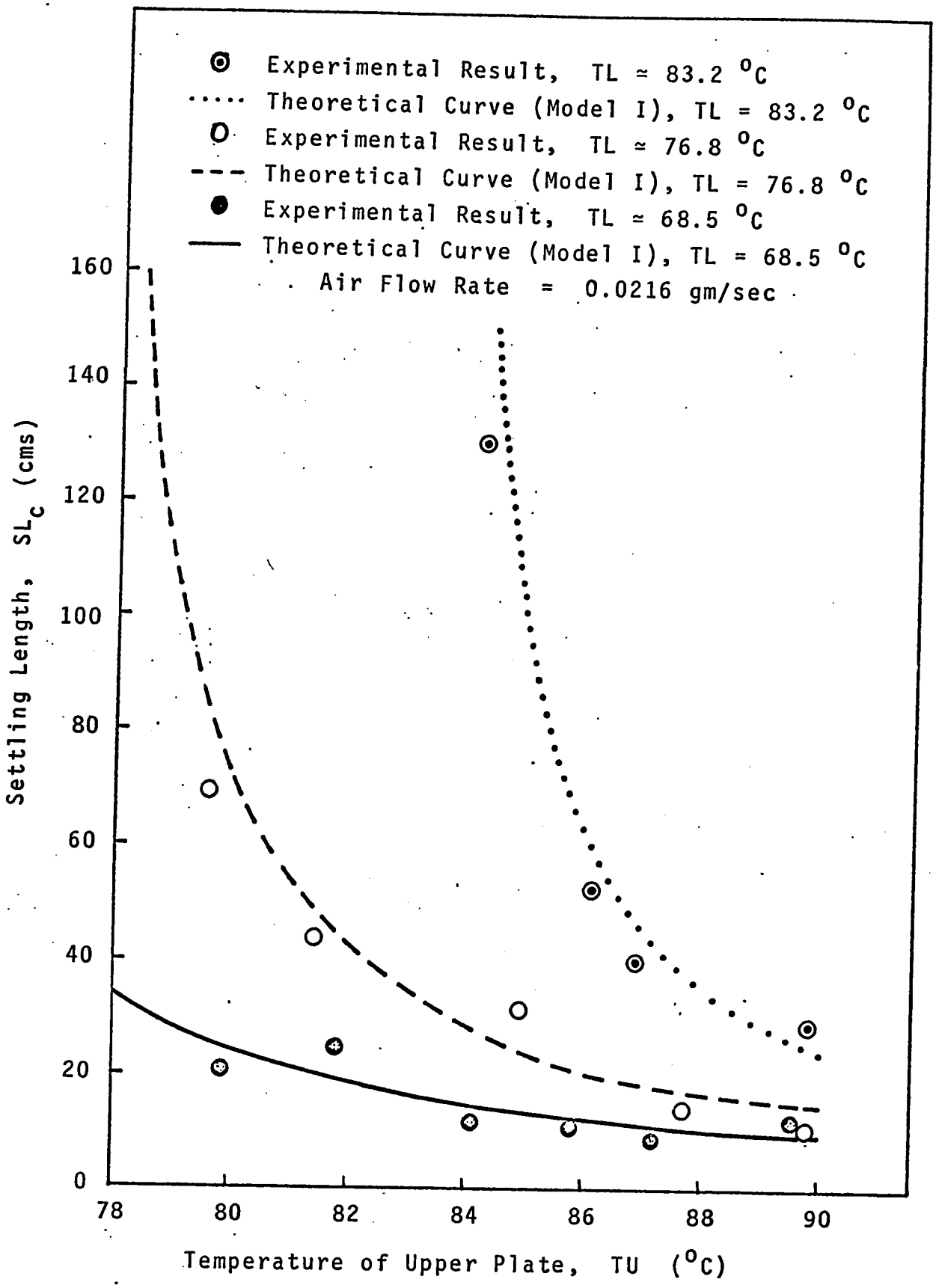

FIG.25 SETTLING LENGTH VS UPPER PLATE TEMPERATURE (GAP = 1.5 cms)

Table 7

Theoretical Settling Lengths and Times for GAP = 2 cms (Model I)

Temperature of Upper Plate, TU (^{o}C)	Temperature of Lower Plate, TL (^{o}C)	Settling Length, SL (cms)	Mass Flow Rate of Dry Air, M_{Air}(gm/sec)	Corrected Settling Length, † SL_c (cms)	Settling Time, ST (secs)
90	68.5	70.86	0.11641	13.14	17.84
88	68.5	88.23	0.12431	15.32	22.34
86	68.5	109.47	0.13117	18.02	27.89
84	68.5	136.20	0.13721	21.43	34.94
82	68.5	170.95	0.14259	25.88	44.14
80	68.5	218.02	0.14743	31.92	56.65
78	68.5	285.28	0.15183	40.56	74.55
90	76.8	90.12	0.10658	18.25	22.12
88	76.8	119.61	0.11387	22.77	29.57
86	76.8	161.68	0.12018	29.04	40.27
84	76.8	227.02	0.12574	38.97	56.98
82	76.8	342.68	0.13069	56.60	86.64
81	76.8	441.92	0.13297	71.74	112.12
80	76.8	603.28	0.13514	96.36	153.57
79	76.8	911.53	0.13720	143.41	232.80
78	76.8	1733.90	0.13917	268.94	444.20
90	83.2	138.28	0.09609	31.06	33.00
88	83.2	220.16	0.10272	46.27	53.00
87	83.2	293.17	0.10569	59.88	70.90
86	83.2	418.18	0.10847	83.22	101.58
85	83.2	681.95	0.11107	132.54	166.38
84	83.2	1604.90	0.11353	305.15	393.26

† converted for an air flow rate of 0.0216 gm/sec

Table 8

Experimental Data on Settling Lengths and Times for GAP = 2 cms

Temperature of Upper Plate, TU		Temperature of Lower Plate, TL		Settling Length, SL	Rotameter Reading,	Corrected Settling Length, † SL_c	Settling Time, ST
D* (High Scale)	^oC	D* (High Scale)	^oC	(cms)		(cms)	(secs)
3.56	84.02	7.89	68.46	24.7	2	24.7	37.2
2.56	88.38	7.88	68.49	32.0	4	16.0	19.1
2.28	89.67	7.85	68.58	36.4	4	18.2	16.8
4.12	81.73	7.90	68.42	20.5	2	20.5	43.2
4.60	79.85	7.90	68.42	37.0	2	37.0	61.3
5.02	78.20	7.88	68.49	31.0	2	31.0	76.0
4.63	79.70	5.41	76.80	89.5	2	89.5	-
4.65	79.70	5.45	76.70	60.7	1	121.4	-
4.28	81.40	5.39	76.89	58.6	2	58.6	145.9
3.37	84.82	5.39	76.89	46.2	2	46.2	49.3
2.23	89.90	5.35	77.03	30.3	4	15.2	24.4
3.28	85.20	3.77	83.15	130.0	2	130.0	138.3
3.22	85.46	3.77	83.15	90.2	2	90.2	120.1
3.18	85.98	3.80	83.03	84.5	2	84.5	107.5
2.86	87.03	3.79	83.07	49.6	2	49.6	67.1
2.60	88.19	3.71	83.40	47.8	2	47.8	47.6

† converted for an air flow rate of 0.0216 gm/sec

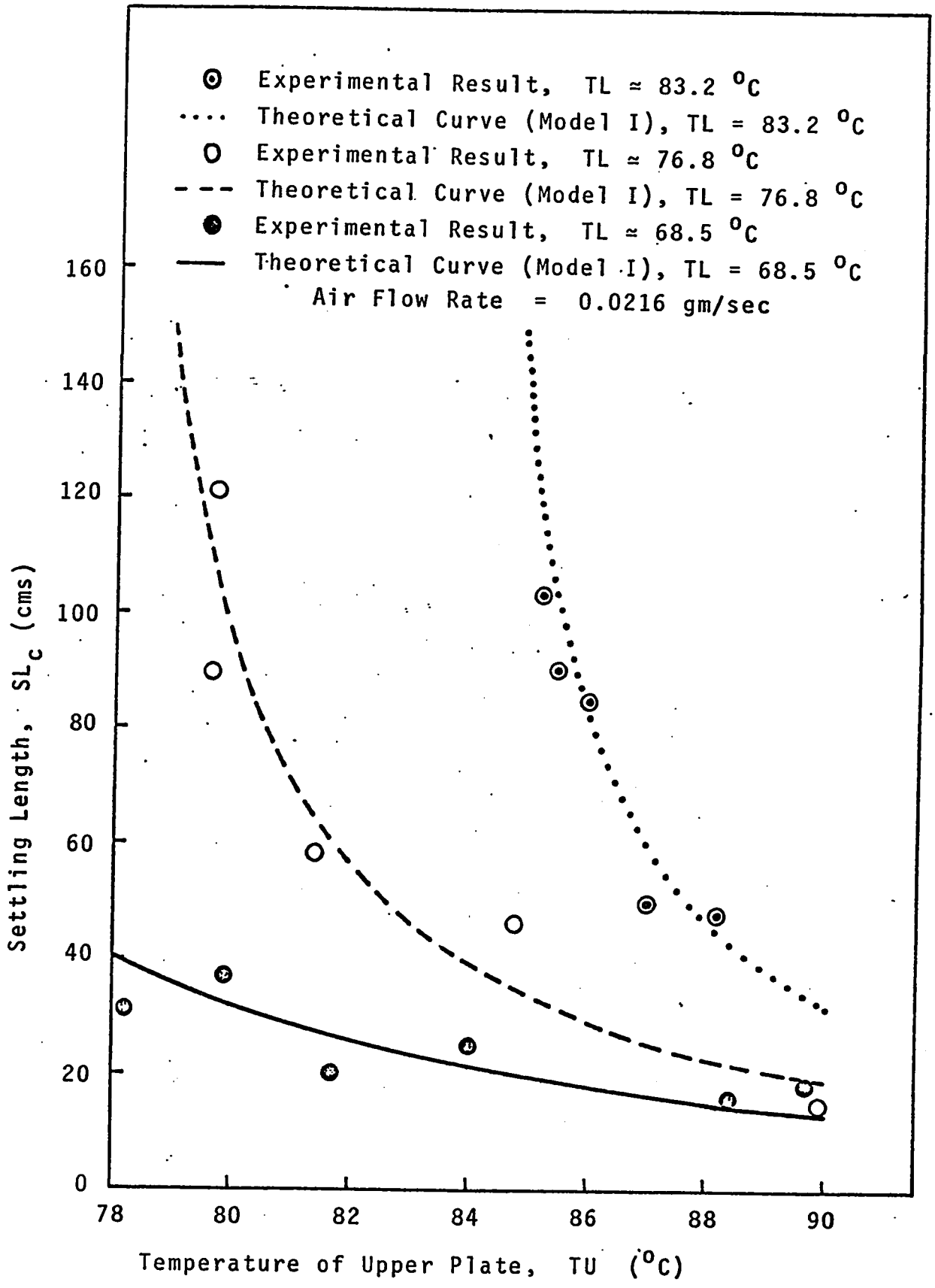

FIG.26 SETTLING LENGTH VS UPPER PLATE TEMPERATURE (GAP = 2cms)

Table 9

Theoretical Settling Lengths and Times for GAP = 2.5 cms (Model I)

Temperature of Upper Plate, TU (^{o}C)	Temperature of Lower Plate, TL (^{o}C)	Settling Length, SL (cms)	Mass Flow Rate of Dry Air, M_{Air}(gm/sec)	Corrected Settling Length, † SL_c (cms)	Settling Time, ST (secs)
90	83.2	337.60	0.18767	38.82	51.57
88	83.2	537.50	0.20062	57.82	82.82
87	83.2	715.75	0.20642	74.82	110.77
86	83.2	1021.00	0.21185	104.00	158.72
85	83.2	1664.90	0.21694	165.62	259.97
84	83.2	3918.20	0.22173	381.34	614.47
90	76.8	220.01	0.20817	22.81	34.57
88	76.8	292.03	0.22239	28.34	46.20
86	76.8	394.74	0.23473	36.29	62.93
84	76.8	554.25	0.24558	48.70	89.03
82	76.8	836.63	0.25525	70.73	135.37
81	76.8	1078.90	0.25971	89.65	175.18
80	76.8	1472.90	0.26394	120.42	239.96
79	76.8	2225.40	0.26798	179.21	363.75
78	76.8	4233.10	0.27182	336.06	694.07
90	68.5	173.00	0.22735	16.42	27.87
88	68.5	215.41	0.24280	19.15	34.90
86	68.5	267.26	0.25619	22.51	43.58
84	68.5	332.51	0.26799	26.77	54.59
82	68.5	417.36	0.27850	32.34	68.97
80	68.5	532.28	0.28796	39.89	88.51
78	68.5	696.48	0.29653	50.69	116.49

† converted for an air flow rate of 0.0216 gm/sec

Table 10

Experimental Data on Settling Lengths and Times for GAP = 2.5 cms

Temperature of Upper Plate, TU		Temperature of Lower Plate, TL		Settling Length, SL	Rotameter Reading,	Corrected Settling Length, † SL_c	Settling Time, ST
D* (High Scale)	^oC	D* (High Scale)	^oC	(cms)		(cms)	(secs)
2.27	89.7	7.83	68.6	40.0	6	13.3	26.7
3.15	85.8	7.84	68.6	35.7	4	17.8	41.2
3.52	84.1	7.94	68.4	33.1	2	33.1	55.1
4.13	81.7	7.88	68.5	29.2	2	29.2	76.8
4.58	79.9	7.87	68.5	38.3	2	38.3	91.2
5.05	78.2	7.90	68.4	47.3	2	47.3	115.4
2.23	89.9	5.49	76.7	43.9	4	22.0	33.8
2.77	87.4	5.40	76.8	39.1	2	39.1	52.7
3.33	84.9	5.42	76.8	51.2	2	51.2	76.0
4.21	81.4	5.40	76.8	75.3	2	75.3	148.8
4.69	79.5	5.43	76.7	64.3	1	128.6	-
2.89	86.9	3.79	83.1	65.8	2	65.8	119.0
3.08	86.0	3.75	83.2	96.5	2	96.5	154.2
2.22	89.9	3.77	83.2	43.2	2	43.2	50.2

† converted for an air flow rate of 0.0216 gm/sec

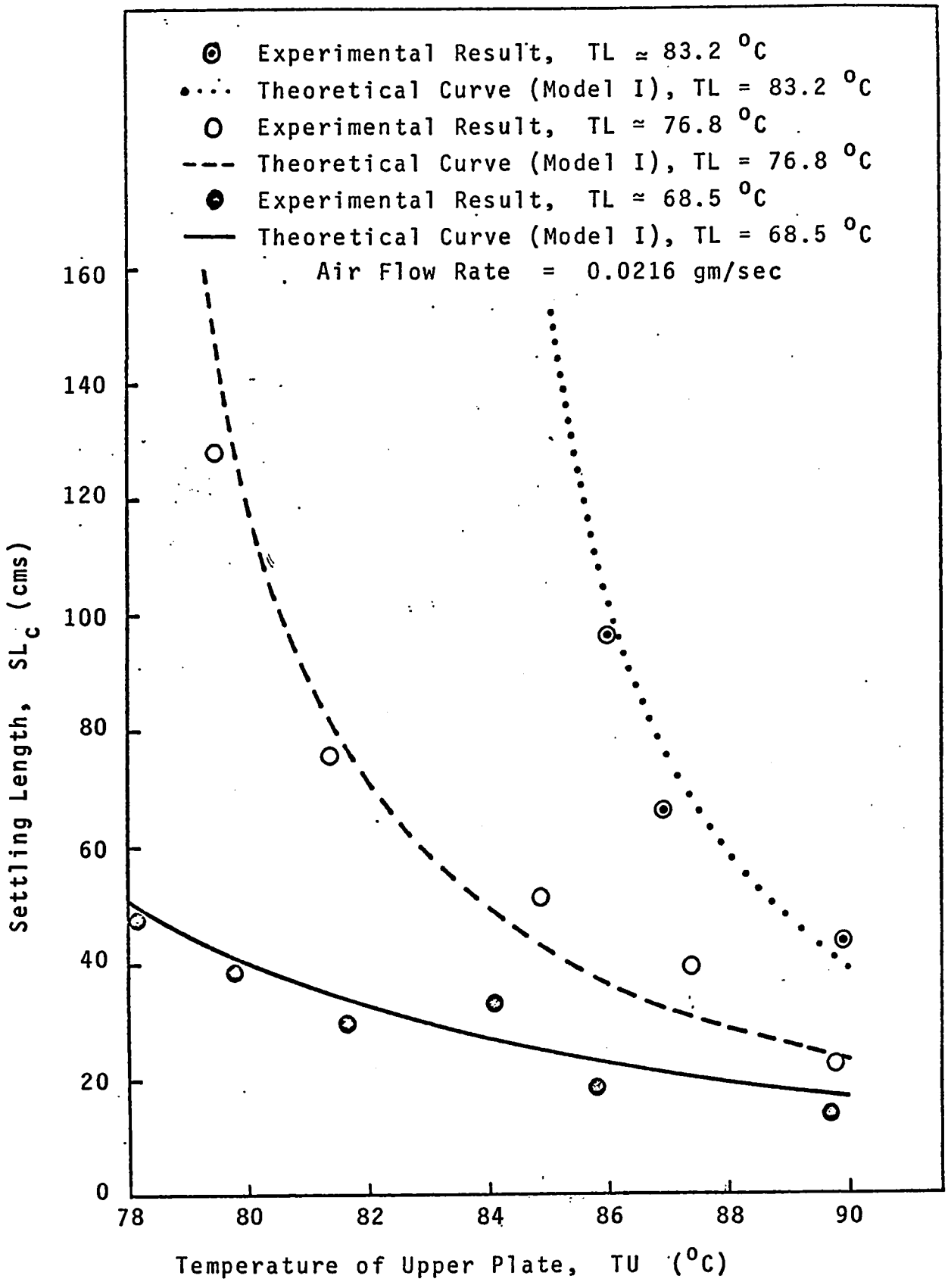

FIG.27 SETTLING LENGTH VS UPPER PLATE TEMPERATURE (GAP = 2.5 cms)

Table 11

Theoretical Settling Lengths and Times for GAP = 3 cms (Model I)

Temperature of Upper Plate, TU (^{o}C)	Temperature of Lower Plate, TL (^{o}C)	Settling Length, SL (cms)	Mass Flow Rate of Dry Air, M_{Air} (gm/sec)	Corrected Settling Length, † SL_c (cms)	Settling Time, ST (secs)
90	83.2	700.05	0.32429	46.63	74.26
88	83.2	1114.60	0.34667	69.40	119.25
87	83.2	1484.20	0.35670	89.82	159.51
86	83.2	2117.10	0.36608	124.83	228.55
85	83.2	3452.40	0.37487	198.80	374.36
84	83.2	8124.80	0.38315	457.73	884.84
90	76.8	456.22	0.35971	27.38	49.77
88	76.8	605.54	0.38430	34.01	66.53
86	76.8	818.53	0.40561	43.56	90.61
84	76.8	1149.30	0.42437	58.46	128.20
82	76.8	1734.80	0.44107	84.90	194.94
81	76.8	2237.20	0.44877	107.61	252.26
80	76.8	3054.10	0.45609	144.54	345.54
79	76.8	4614.60	0.46306	215.11	523.80
78	76.8	8777.80	0.46971	403.39	999.45
90	68.5	358.73	0.39287	19.71	40.13
88	68.5	446.68	0.41955	22.98	50.26
86	68.5	554.20	0.44270	27.02	62.76
84	68.5	689.49	0.46309	32.14	78.61
82	68.5	865.43	0.48125	38.82	99.32
80	68.5	1103.70	0.49759	47.88	127.45
78	68.5	1444.20	0.51241	60.84	167.74

† converted for an air flow rate of 0.0216 gm/sec

Table 12

Experimental Data on Settling Lengths and Times for GAP = 3 cms

Temperature of Upper Plate, TU		Temperature of Lower Plate, TL		Settling Length, SL	Rotameter Reading,	Corrected Settling Length, † SL_c	Settling Time, ST
D* (High Scale)	^oC	D* (High Scale)	^oC	(cms)		(cms)	(secs)
2.26	89.8	5.42	76.8	32.4	2	32.40	50.0
2.66	87.9	5.42	76.8	30.9	2	30.90	71.6
3.37	84.8	5.45	76.7	58.8	2	58.80	114.3
4.23	81.3	5.45	76.7	91.2	2	91.20	-
4.68	79.5	5.43	76.7	78.6	1	157.20	-
2.85	87.0	3.75	83.2	78.9	2	78.90	168.3
3.08	86.0	3.76	83.2	59.7	1	119.40	-
2.22	90.0	3.80	83.0	48.9	2	48.90	73.1
2.23	89.6	7.80	68.7	34.3	4	17.15	41.5
3.16	85.7	7.82	68.7	36.1	2	36.10	68.1
3.51	84.0	7.84	68.6	32.2	2	32.20	76.0
4.15	81.6	7.89	68.4	38.2	2	38.20	104.5
4.61	79.8	7.88	68.5	46.2	2	46.20	134.0
5.01	78.2	7.90	68.4	67.3	2	67.30	173.2

† converted for an air flow rate of 0.0216 gm/sec

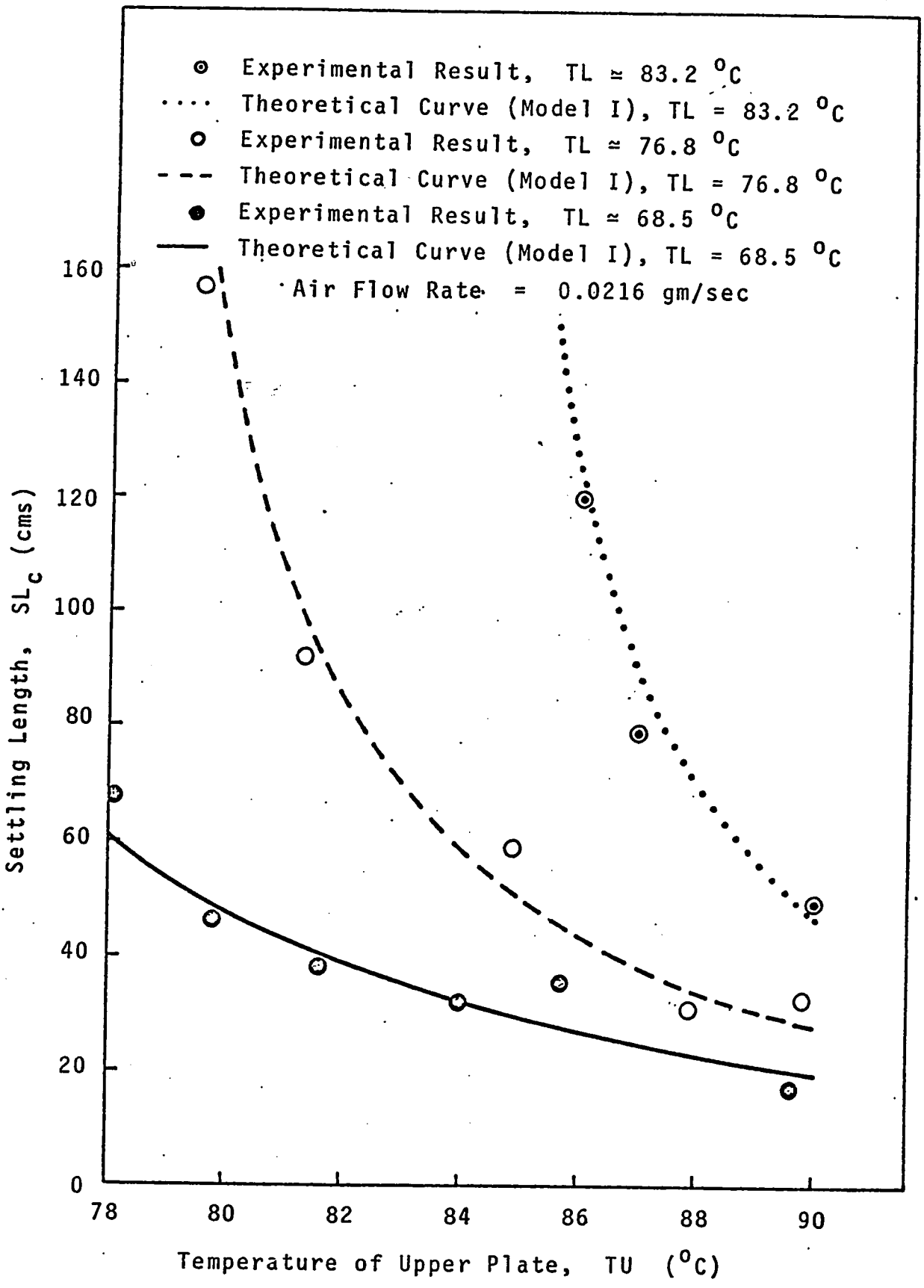

FIG. 28 SETTLING LENGTH VS UPPER PLATE TEMPERATURE (GAP = 3 cms)

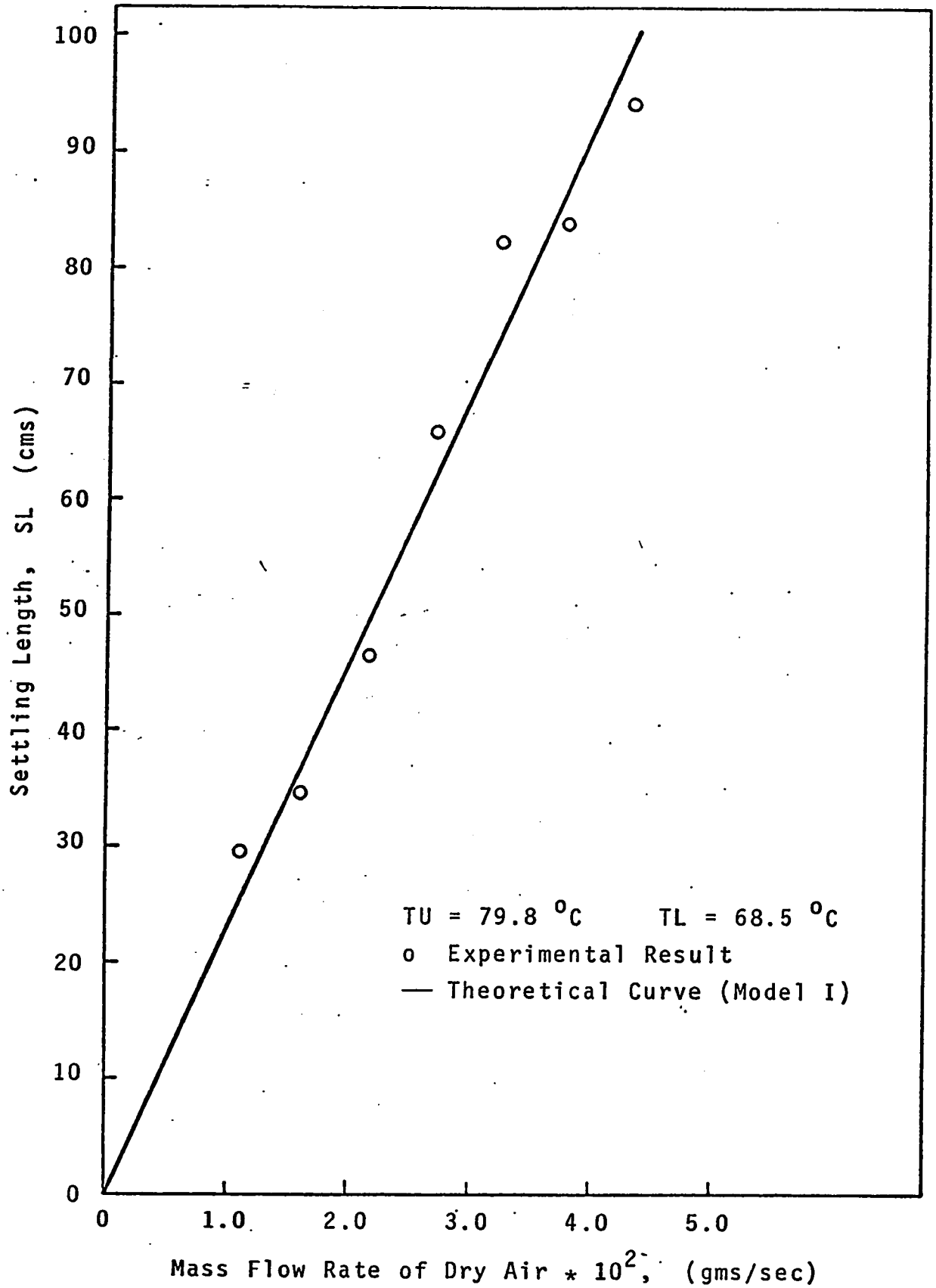

FIG. 29 MASS FLOW RATE OF DRY AIR VS SETTLING LENGTH (GAP = 3 cms)

Table 13

Mass Flow Rate of Dry Air vs. Settling Length (Model I)

TU = 79.8°C TL = 68.5°C

GAP = 3 cms

DELPX * 10^5 ($gm/sec^2\ cm^2$)	M_{Air} * 10^2 (gm/sec)	SL (cms)
4	0.985	22.35
6	1.478	33.52
8	1.970	44.70
10	2.463	55.87
12	2.956	67.05
14	3.448	78.22
16	3.941	89.40
18	4.433	100.57
20	4.926	111.74

Table 14

Mass Flow Rate of Dry Air vs. Settling Length

(Experimental Data)

TU = 79.8 ^{o}C TL = 68.5 ^{o}C

GAP = 3 cms

Position of Rotameter Float	Mass Flow Rate of Dry Air, $M_{Air} * 10^2$ (gm/	Settling Length, SL (cms)
2.0	2.1590	46.2
1.5	1.6193	34.5
1.0	1.0795	29.5
3.0	3.2385	82.2
3.5	3.7783	83.6
4.0	4.3180	93.8
2.5	2.6988	65.6

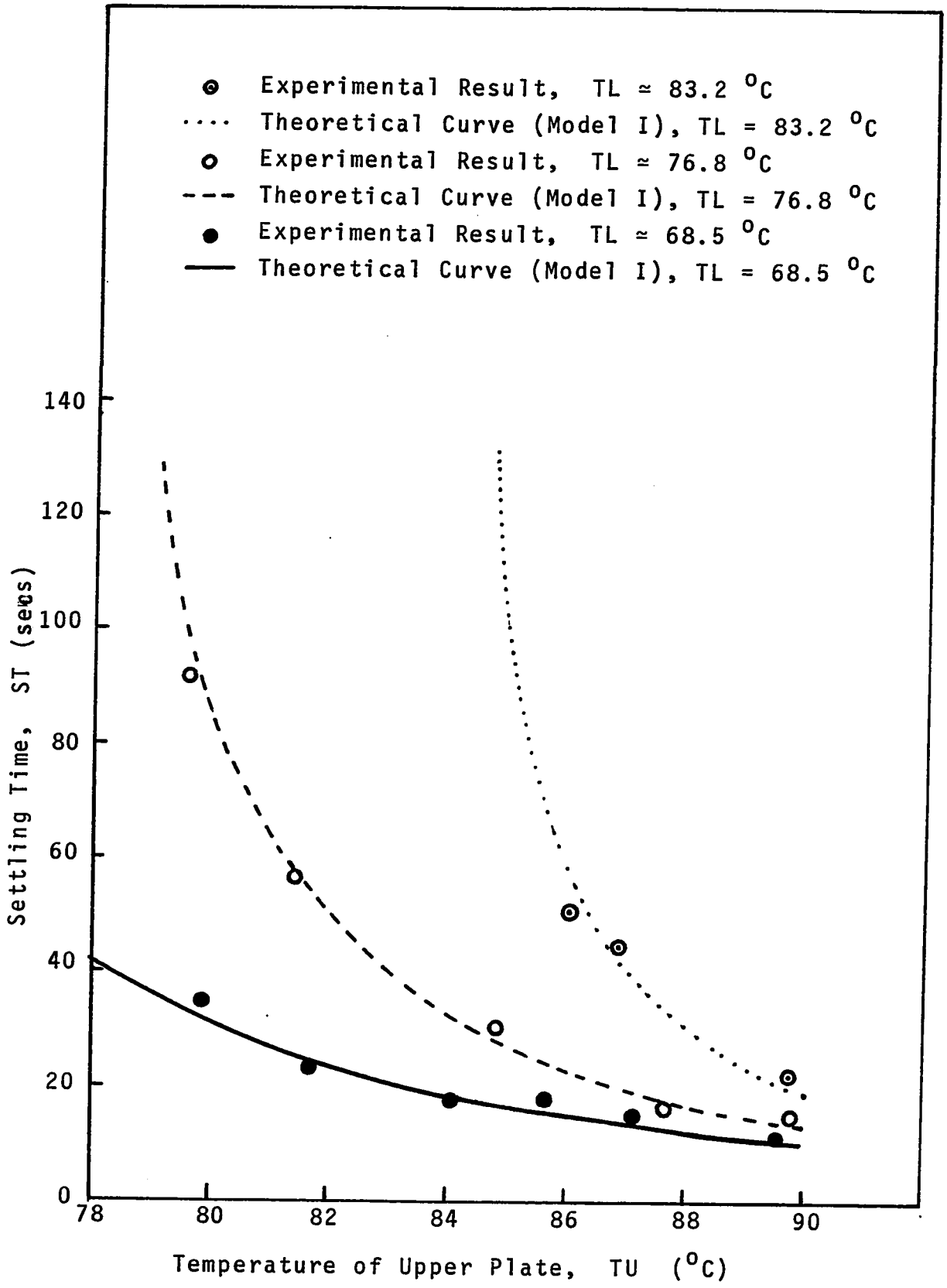

FIG. 30 SETTLING TIME VS UPPER PLATE TEMPERATURE (GAP = 1.5 cms)

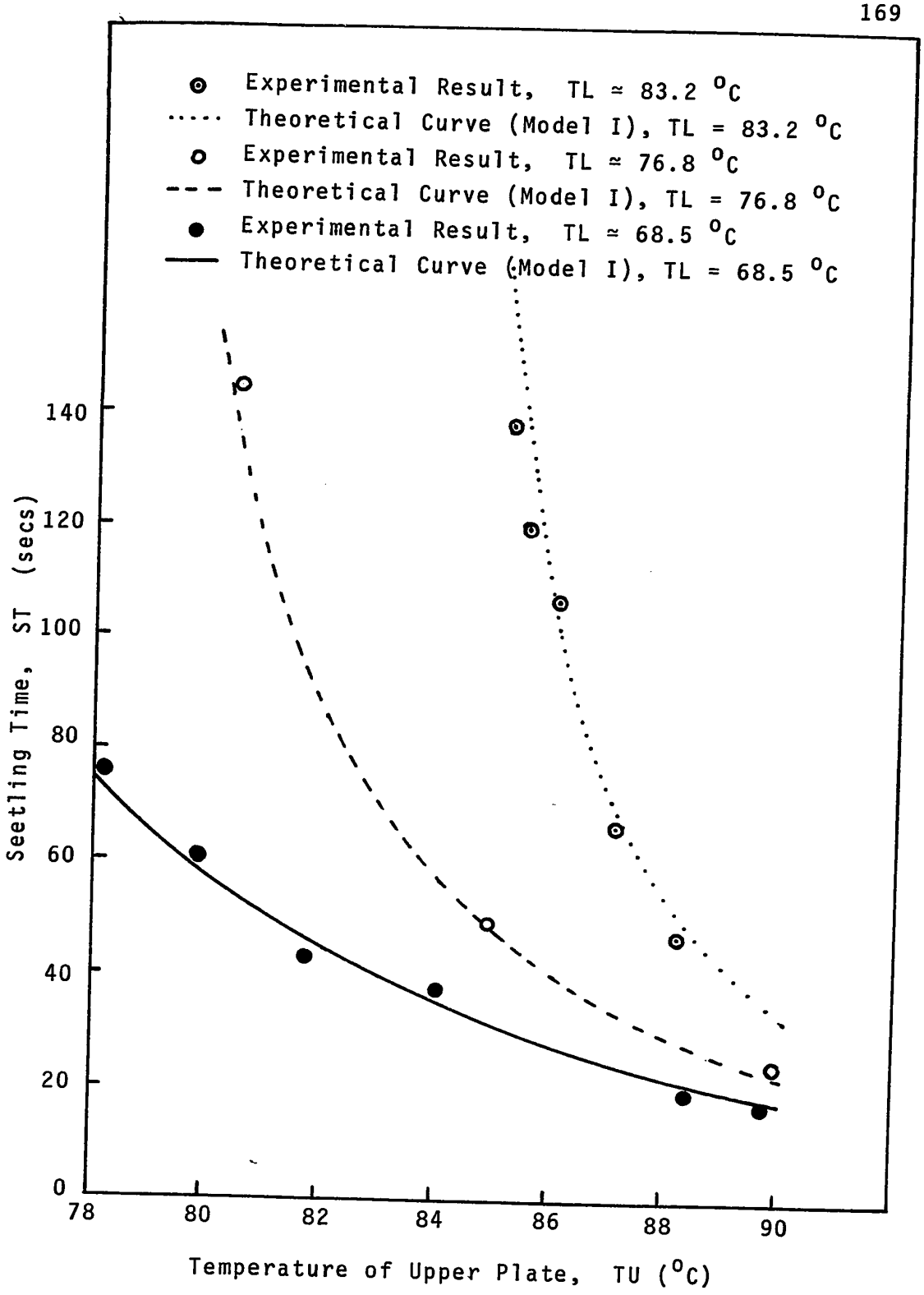

FIG. 31 SETTLING TIME VS UPPER PLATE TEMPERATURE (GAP = 2 cms)

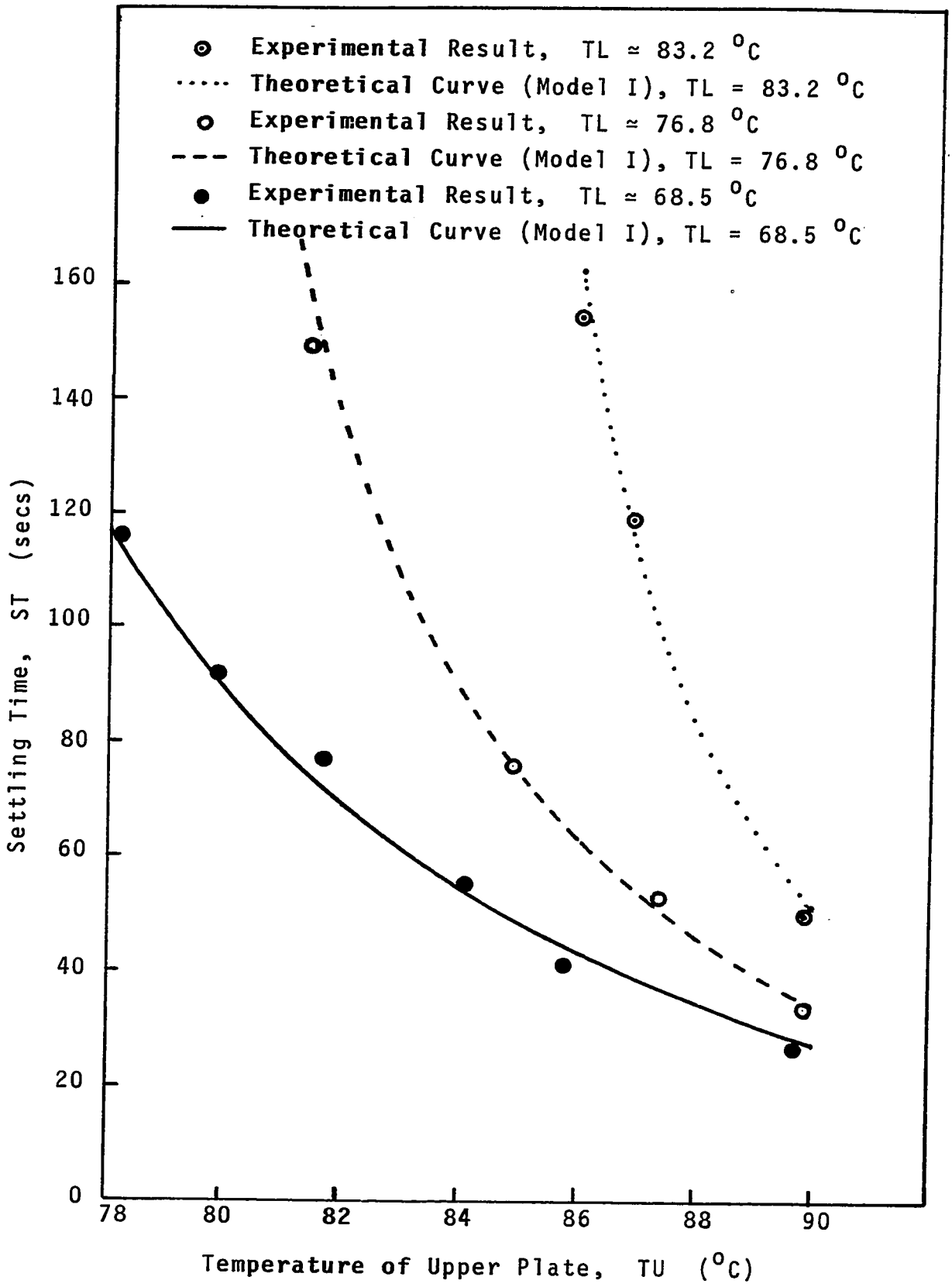

FIG. 32 SETTLING TIME VS UPPER PLATE TEMPERATURE (GAP = 2.5 cms)

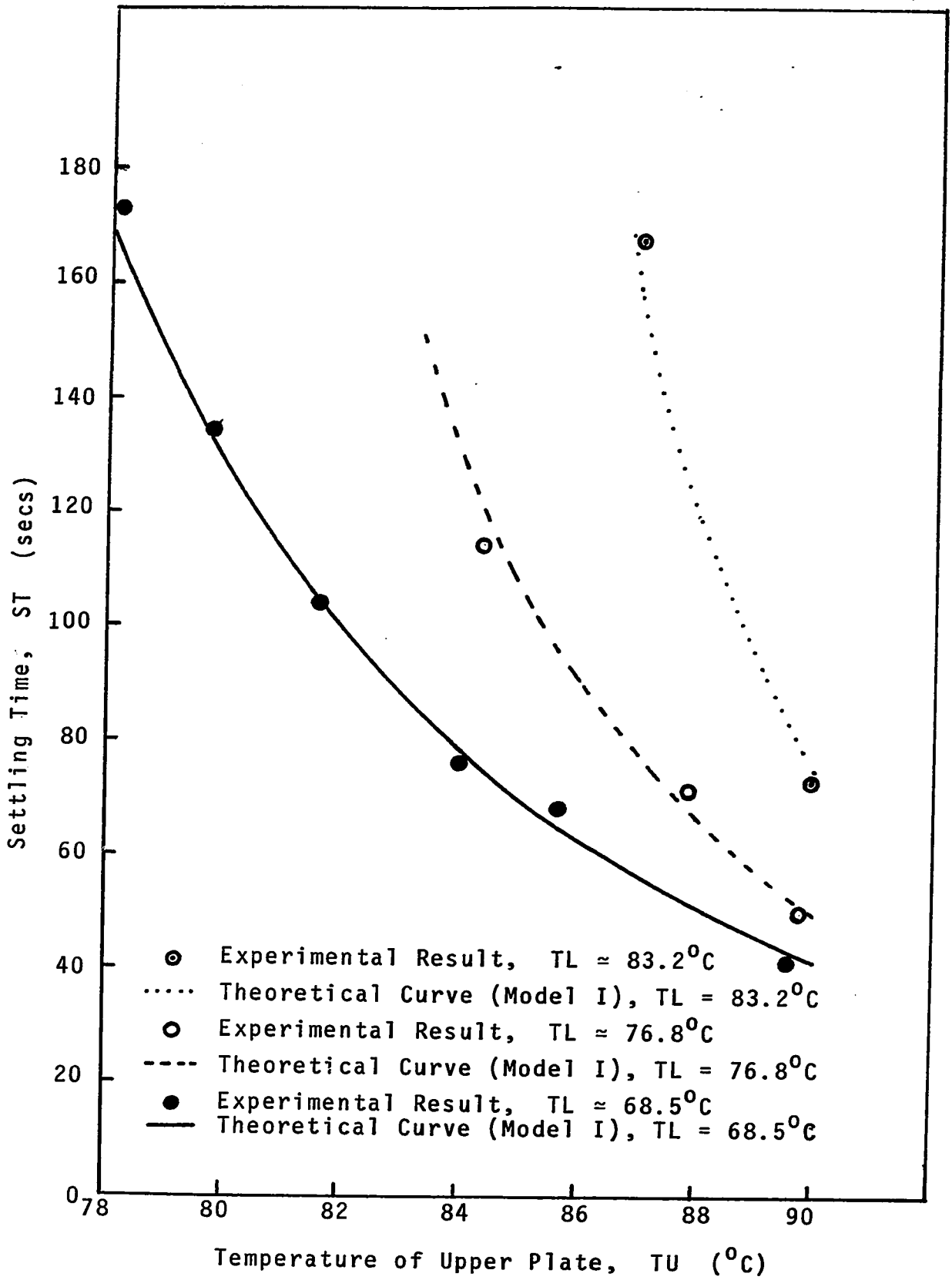

FIG. 33 SETTLING TIME VS UPPER PLATE TEMPERATURE (GAP = 3 cms)

GAP= 2.00 TU= 363.00 TL= 349.85 DELPX= -0.20266E-02
DP = 0.30000E-04 RP = 1.0000
H= 0.10000E-01 EMAX= 0.10000E-05 TOL= 0.10000E-03

Y = 0.0
VY = 0.97774E-01 SL = 0.0 ST = 0.0
VYP = 0.99486E-01 SLP = 0.0 STP = 0.0
VYDP= 0.97051E-01 VYTP= 0.13761E-03 VYG = 0.22475E-02

Y = 0.20000D 00
VY = 0.96538E-01 SL = 0.21439D 01 ST = 0.20585D 01
VYP = 0.98302E-01 SLP = 0.21948D 01 STP = 0.20214D 01
VYDP= 0.95957E-01 VYTP= 0.20785E-03 VYG = 0.22268E-02

Y = 0.40000D 00
VY = 0.95238E-01 SL = 0.81457D 01 ST = 0.41441D 01
VYP = 0.97265E-01 SLP = 0.79971D 01 STP = 0.40658D 01
VYDP= 0.94936E-01 VYTP= 0.23012E-03 VYG = 0.22054E-02

Y = 0.60000D 00
VY = 0.93872E-01 SL = 0.17303D 02 ST = 0.62592D 01
VYP = 0.96108E-01 SLP = 0.16942D 02 STP = 0.61343D 01
VYDP= 0.92671E-01 VYTP= 0.25459E-03 VYG = 0.21832E-02

Y = 0.80000D 00
VY = 0.92437E-01 SL = 0.28829D 02 ST = 0.84061D 01
VYP = 0.94924E-01 SLP = 0.28193D 02 STP = 0.82282D 01
VYDP= 0.92482E-01 VYTP= 0.28146E-03 VYG = 0.21603E-02

Y = 0.10000D 01
VY = 0.90932E-01 SL = 0.41843D 02 ST = 0.10587D 02
VYP = 0.93716E-01 SLP = 0.40834D 02 STP = 0.10349D 02
VYDP= 0.91268E-01 VYTP= 0.31091E-03 VYG = 0.21366E-02

Y = 0.12000D 01
VY = 0.89355E-01 SL = 0.55358D 02 ST = 0.12806D 02
VYP = 0.92488E-01 SLP = 0.53820D 02 STP = 0.12497D 02
VYDP= 0.90033E-01 VYTP= 0.34317E-03 VYG = 0.21121E-02

Y = 0.14000D 01
VY = 0.87773E-01 SL = 0.69266D 02 ST = 0.15065D 02
VYP = 0.91246E-01 SLP = 0.66361D 02 STP = 0.14574D 02
VYDP= 0.88731E-01 VYTP= 0.37844E-03 VYG = 0.20869E-02

Y = 0.16000D 01
VY = 0.85977E-01 SL = 0.79324D 02 ST = 0.17368D 02
VYP = 0.89996E-01 SLP = 0.76056D 02 STP = 0.16781D 02
VYDP= 0.87512E-01 VYTP= 0.41695E-03 VYG = 0.20609E-02

Y = 0.18000D 01
VY = 0.84173E-01 SL = 0.89132D 02 ST = 0.19719D 02
VYP = 0.88746E-01 SLP = 0.85394D 02 STP = 0.19110D 02
VYDP= 0.86253E-01 VYTP= 0.45894E-03 VYG = 0.20334E-02

Y = 0.20000D 01
VY = 0.82292E-01 SL = 0.99117D 02 ST = 0.22122D 02
VYP = 0.87536E-01 SLP = 0.94717D 02 STP = 0.21438D 02
VYDP= 0.84996E-01 VYTP= 0.50445E-03 VYG = 0.20045E-02

TABLE 16

PARTICLE VELOCITIES IN Y - DIRECTION FOR DIFFERENT VERSIONS OF MODEL II

Distance from Upper Plate, (cms)	Particle Velocity in y-direction (cms/sec)						
	Model I	Model II					
		Normal†	ρ_p = 3.3gm/cm³	D_p = 0.4 x10^{-4}cms	D_p = 1.6 x10^{-4}cms	σ_{AB}	k_p = 0 cal/(sec cm °K)
0.0	0.0978	0.0995	0.1047	0.0978	0.1062	0.0999	0.1010
0.2	0.0965	0.0984	0.1035	0.0967	0.1051	0.0988	0.1001
0.4	0.0952	0.0973	0.1023	0.0956	0.1039	0.0978	0.0991
0.6	0.0939	0.0961	0.1011	0.0945	0.1027	0.0967	0.0981
0.8	0.0924	0.0949	0.0999	0.0933	0.1014	0.0956	0.0972
1.0	0.0909	0.0937	0.0986	0.0921	0.1001	0.0945	0.0962
1.2	0.0894	0.0925	0.0974	0.0909	0.0988	0.0934	0.0952
1.4	0.0877	0.0912	0.0960	0.0896	0.0975	0.0923	0.0943
1.6	0.0860	0.0900	0.0947	0.0884	0.0962	0.0912	0.0933
1.8	0.0842	0.0887	0.0934	0.0872	0.0948	0.0902	0.0924
2.0	0.0823	0.0875	0.0921	0.0860	0.0935	0.0891	0.0915

† Normal Model II: ρ_p = 1 gm/cm³, D_p = 0.8x10^{-4} cms, σ_{AB} = - 0.26, k_p = 0.001 cal/(sec cm °K)

TABLE 17

OPERATING RATIO AND WORK

GAP cms	TU °C	TL °C	ORATIO	WORK ergs/gm†
1.5	90	83.2	1.9995	235.74
1.5	88	83.2	1.8868	348.04
1.5	87	83.2	1.8402	448.40
1.5	86	83.2	1.7985	620.44
1.5	85	83.2	1.7612	983.67
1.5	84	83.2	1.7274	2255.20
1.5	90	76.8	1.8099	134.71
1.5	88	76.8	1.7140	166.17
1.5	86	76.8	1.6387	211.18
1.5	84	76.8	1.5778	281.24
1.5	82	76.8	1.5276	405.45
1.5	80	76.8	1.4855	685.51
1.5	79	76.8	1.4669	1016.90
1.5	90	68.5	1.6686	94.66
1.5	88	68.5	1.5848	109.71
1.5	86	68.5	1.5187	128.14
1.5	84	68.5	1.4652	151.35
1.5	82	68.5	1.4210	181.58
1.5	80	68.5	1.3838	222.55
1.5	78	68.5	1.3522	281.11
1.5	76	68.5	1.3251	371.40
2.0	90	83.2	1.9995	745.05
2.0	88	83.2	1.8868	1100.00
2.0	86	83.2	1.7985	1960.90
2.0	84	83.2	1.7274	7127.50
2.0	90	76.8	1.8099	425.75
2.0	88	76.8	1.7140	525.19
2.0	86	76.8	1.6387	667.45
2.0	84	76.8	1.5778	888.87
2.0	82	76.8	1.5276	1281.40
2.0	80	76.8	1.4855	2166.50
2.0	78	76.8	1.4497	6007.80
2.0	90	68.5	1.6686	299.17
2.0	88	68.5	1.5848	346.75
2.0	86	68.5	1.5187	404.97
2.0	84	68.5	1.4652	478.34
2.0	82	68.5	1.4210	573.87
2.0	80	68.5	1.3838	703.36
2.0	78	68.5	1.3522	888.44

†To convert to H.P./SCFM multiply by 2.277×10^{-14}

TABLE 17 (Cont.)

GAP cms	TU °C	TL °C	ORATIO	WORK ergs/gm
2.5	90	83.2	1.9995	1819.00
2.5	88	83.2	1.8868	2685.50
2.5	86	83.2	1.7985	4787.30
2.5	84	83.2	1.7274	17401.00
2.5	90	76.8	1.8099	1039.40
2.5	88	76.8	1.7140	1282.20
2.5	86	76.8	1.6387	1629.50
2.5	84	76.8	1.5778	2170.10
2.5	82	76.8	1.5276	3128.50
2.5	80	76.8	1.4855	5289.40
2.5	78	76.8	1.4497	14668.00
2.5	90	68.5	1.6686	730.39
2.5	88	68.5	1.5848	846.56
2.5	86	68.5	1.5187	988.70
2.5	84	68.5	1.4652	1167.80
2.5	82	68.5	1.4210	1401.10
2.5	80	68.5	1.3838	1717.20
2.5	78	68.5	1.3522	2169.10
3.0	90	83.2	1.9995	3771.80
3.0	88	83.2	1.8868	5568.70
3.0	86	83.2	1.7985	9927.00
3.0	84	83.2	1.7274	36083.00
3.0	90	76.8	1.8099	2155.30
3.0	88	76.8	1.7140	2658.80
3.0	86	76.8	1.6387	3378.90
3.0	84	76.8	1.5778	4499.90
3.0	82	76.8	1.5276	6487.20
3.0	80	76.8	1.4855	10968.00
3.0	90	68.5	1.6686	1514.50
3.0	88	68.5	1.5848	1755.40
3.0	86	68.5	1.5187	2050.20
3.0	84	68.5	1.4652	2421.60
3.0	82	68.5	1.4210	2905.20
3.0	80	68.5	1.3838	3560.80
3.0	78	68.5	1.3522	4497.80
3.0	76	68.5	1.3251	5942.40

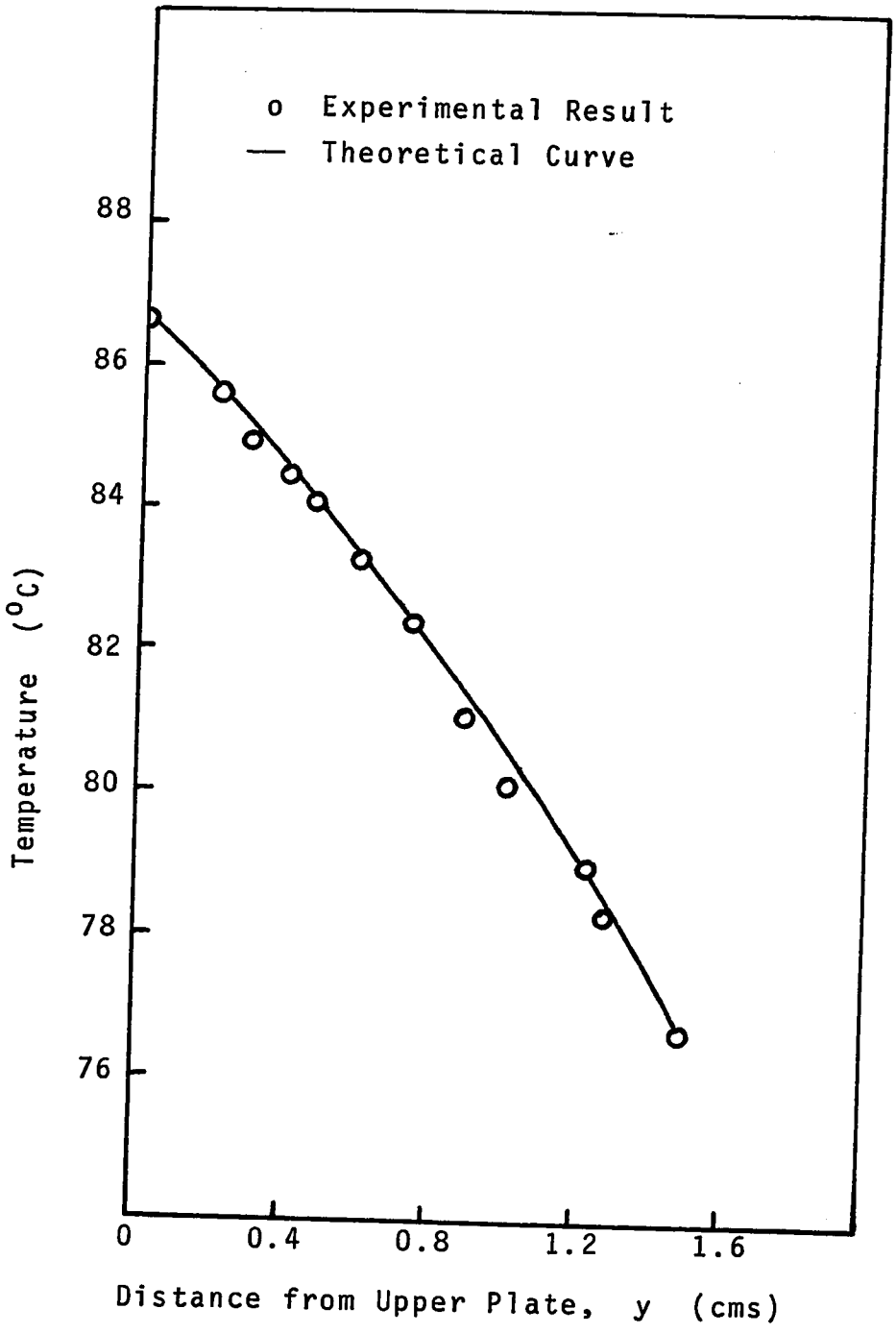

FIG. 34 TEMPERATURE PROFILE (GAP = 1.5 cms)

Table 18

Temperature Profile

Experimental Data for GAP = 1.5 cms

Cathetometer Reading for

- Upper Surface = 57.07 cms
- Lower Surface = 55.57 cms

Cathetometer Reading, (cms)	Distance from Upper Plate, y (cms)	Temperature D* (High Scale)	Temperature ^{o}C
57.07	0.00	2.96	86.60
56.87	0.20	3.19	85.60
56.78	0.29	3.35	84.91
56.67	0.40	3.46	84.44
56.60	0.47	3.55	84.06
56.47	0.60	3.74	83.27
56.33	0.74	3.96	82.38
56.18	0.89	4.30	81.02
56.01	1.06	4.53	80.12
55.84	1.23	4.85	78.89
55.78	1.29	5.02	78.25
55.57	1.50	5.47	76.60

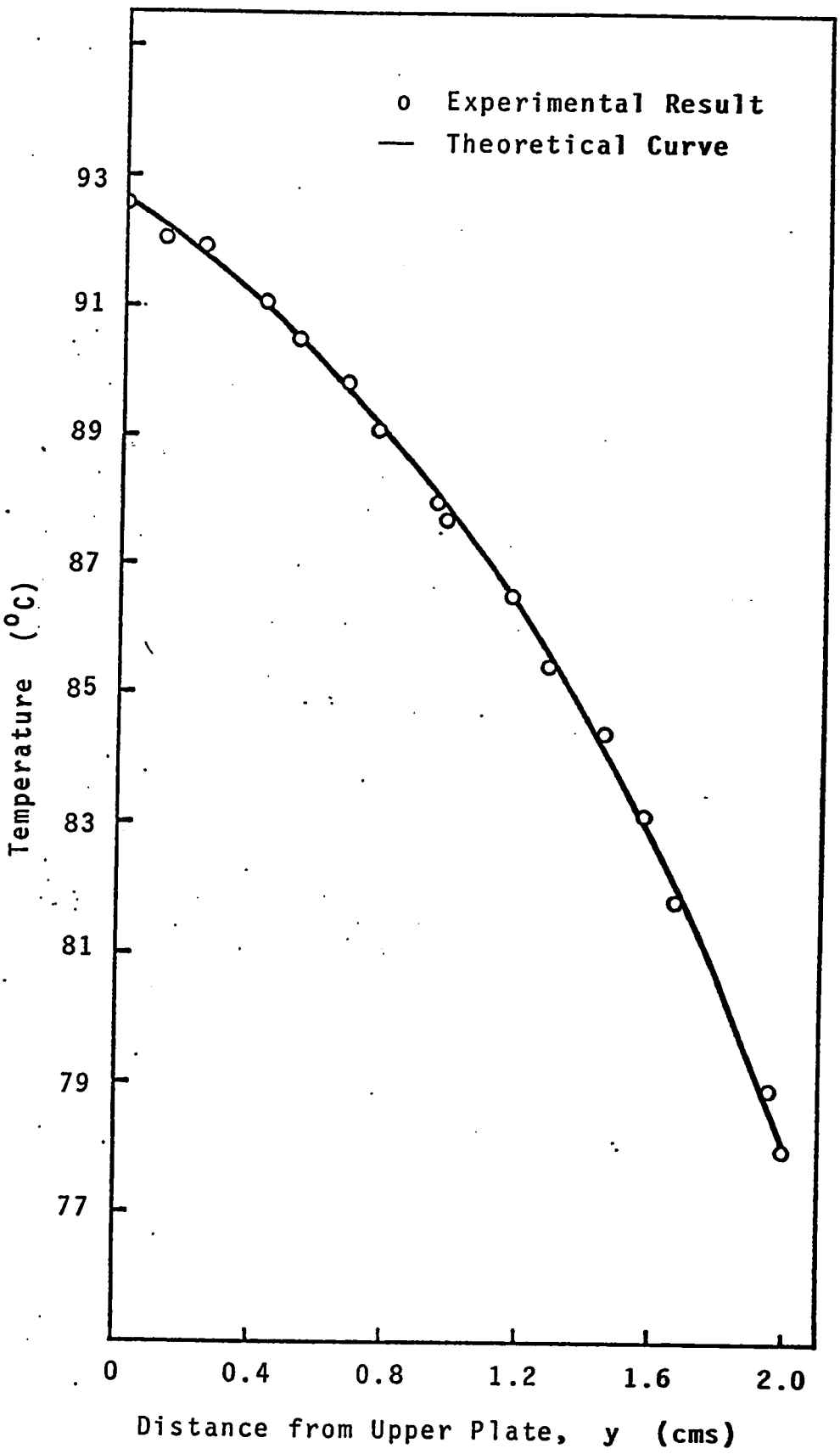

FIG.35 TEMPERATURE PROFILE (GAP = 2 cms)

Table 19

Temperature Profile

Experimental Data for GAP = 2 cms

Cathetometer Reading for:

- Upper Surface = 57.27 cms
- Lower Surface = 55.27 cms

Cathetometer Reading, (cms)	Distance from Upper Plate, y (cms)	Temperature D* (High Scale)	Temperature ^{o}C
57.27	0.00	1.67	92.60
57.15	0.12	1.78	92.06
57.03	0.24	1.81	91.92
56.85	0.42	1.99	91.04
56.75	0.52	2.11	90.47
56.60	0.67	2.25	89.81
56.50	0.77	2.41	89.07
56.33	0.94	2.66	87.93
56.29	0.98	2.71	87.70
56.10	1.17	2.98	86.50
55.99	1.28	3.22	85.46
55.82	1.45	3.47	84.40
55.70	1.57	3.78	83.11
55.60	1.67	4.10	81.81
55.31	1.96	4.83	78.95
55.27	2.00	5.08	78.00

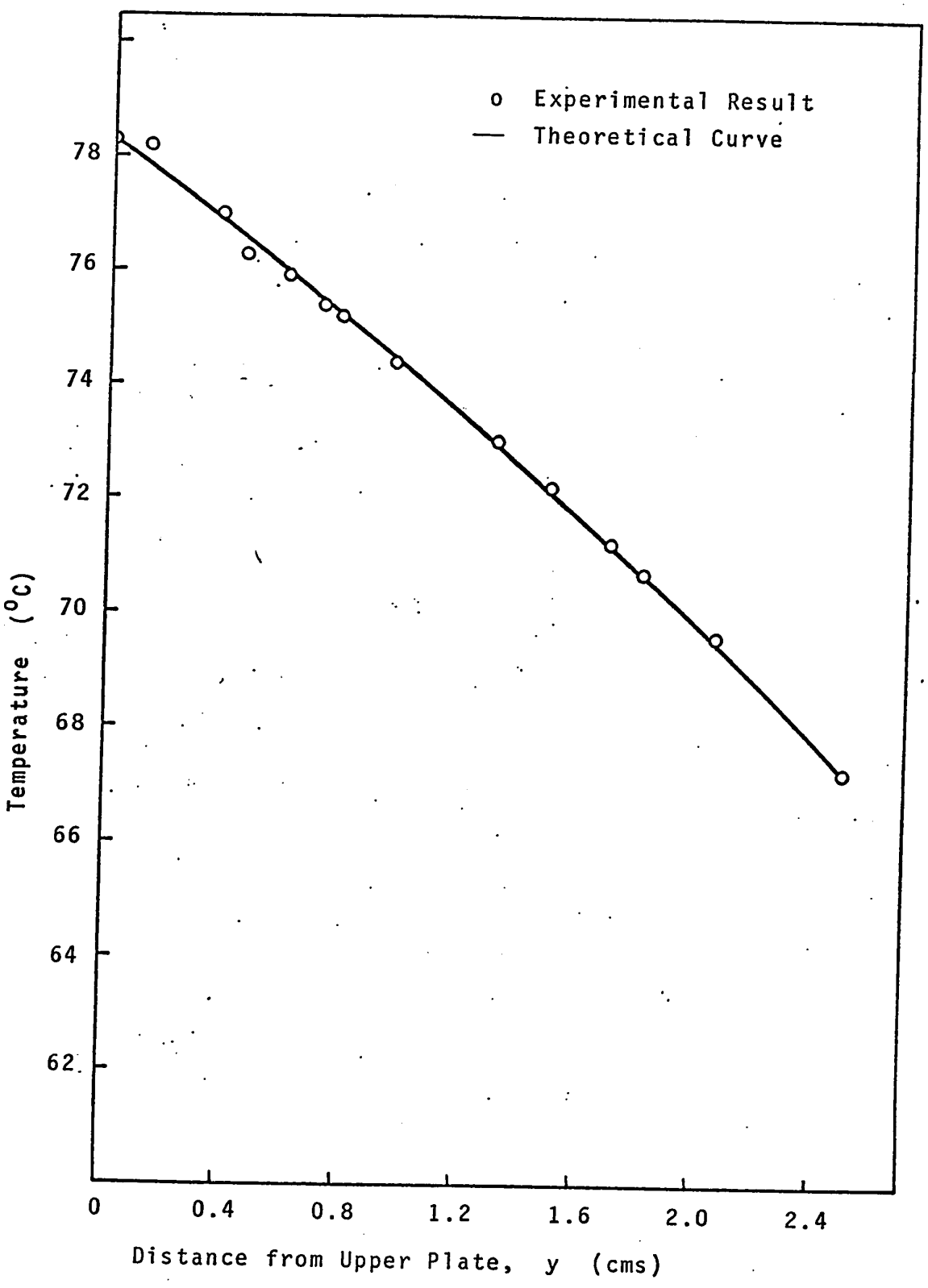

FIG. 36 TEMPERATURE PROFILE (GAP = 2.5 cms)

Table 20

Temperature Profile

Experimental Data for GAP = 2.5 cms

Cathetometer Reading for

- Upper Surface = 57.20 cms
- Lower Surface = 54.70 cms

Cathetometer Reading, (cms)	Distance from Upper Plate, y (cms)	Temperature D* (High Scale)	Temperature ^{o}C
57.20	0.00	4.99	78.3
56.83	0.37	5.32	77.1
56.75	0.45	5.55	76.3
56.60	0.60	5.67	75.9
56.42	0.78	5.85	75.2
56.24	0.96	6.08	74.4
55.89	1.31	6.50	73.0
55.71	1.49	6.72	72.2
55.50	1.70	7.03	71.2
55.39	1.81	7.20	70.7
55.14	2.06	7.52	69.6
54.40	2.50	8.28	67.2
56.48	0.78	5.81	75.4
57.08	0.12	5.03	78.2
57.20	0.00	4.99	78.3
54.70	2.50	8.28	67.2

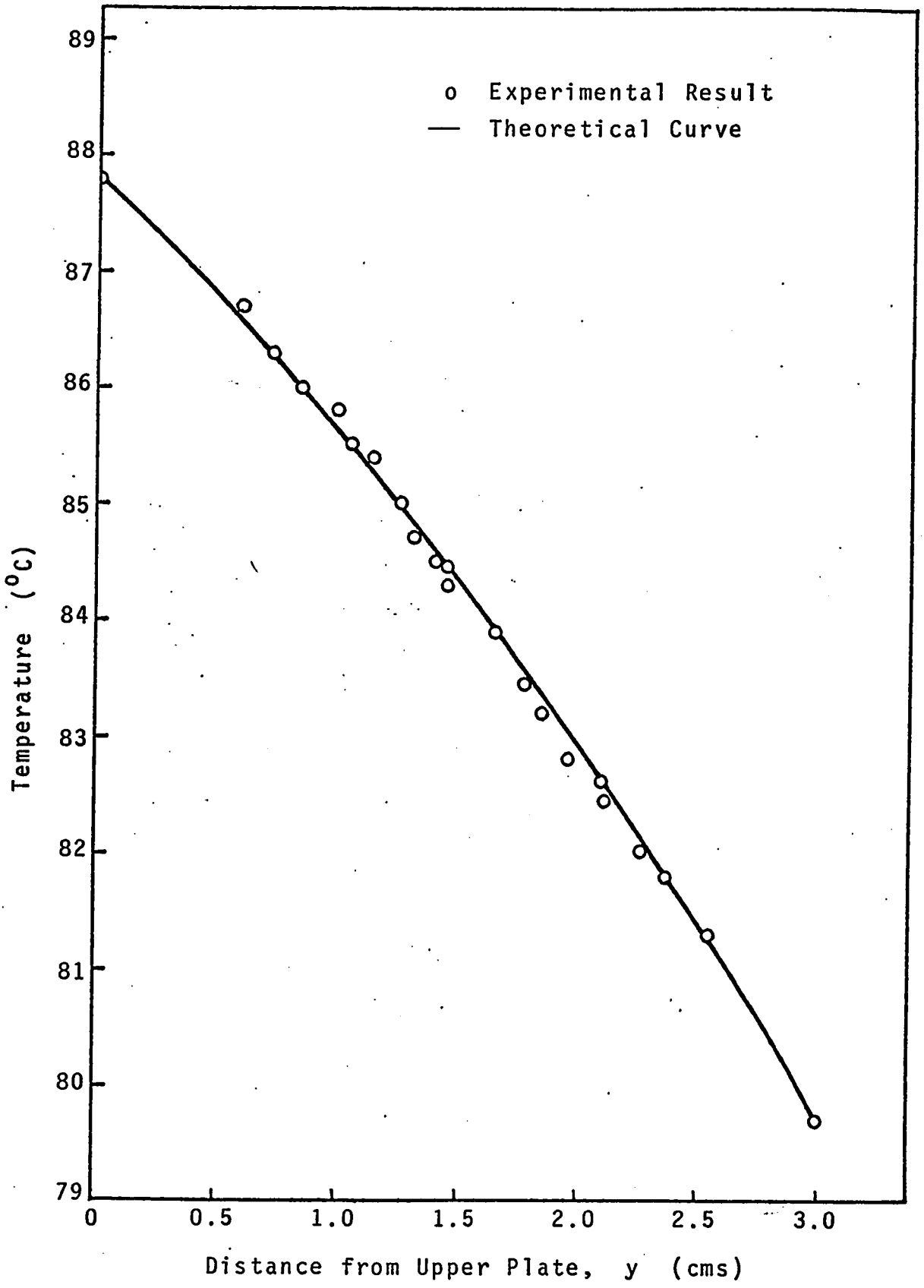

FIG. 37 TEMPERATURE PROFILE (GAP = 3 cms)

Table 21

Temperature Profile

Experimental Data for GAP = 3 cms

Cathetometer Reading for

- Upper Surface = 57.34 cms
- Lower Surface = 54.34 cms

Cathetometer Reading, (cms)	Distance from Upper Plate, y (cms)	Temperature D* (High Scale)	Temperature ^{o}C
57.34	0.00	2.72	87.6
56.74	0.60	2.93	86.7
56.49	0.81	3.10	86.0
56.34	1.00	3.15	85.8
56.20	1.14	3.23	85.4
56.08	1.26	3.33	85.0
55.93	1.41	3.45	84.5
55.88	1.46	3.50	84.3
55.50	1.84	3.76	83.2
55.25	2.09	3.91	82.6
54.97	2.37	4.10	81.8
54.91	2.43	4.11	81.8
54.78	2.56	4.22	81.3
54.34	3.00	4.64	79.7
54.78	2.56	4.24	81.3
54.91	2.43	4.13	81.7
55.08	2.26	4.05	82.0
55.22	2.12	3.95	82.4
55.38	1.96	3.85	82.8
55.57	1.77	3.72	83.4
55.70	1.64	3.60	83.9
55.90	1.44	3.47	84.4
56.03	1.31	3.41	84.7
56.28	1.06	3.22	85.5
56.47	0.87	3.08	86.1
56.61	0.73	3.02	86.3
56.77	0.57	2.94	86.7
57.34	0.00	2.75	87.5
54.34	3.00	4.64	79.7

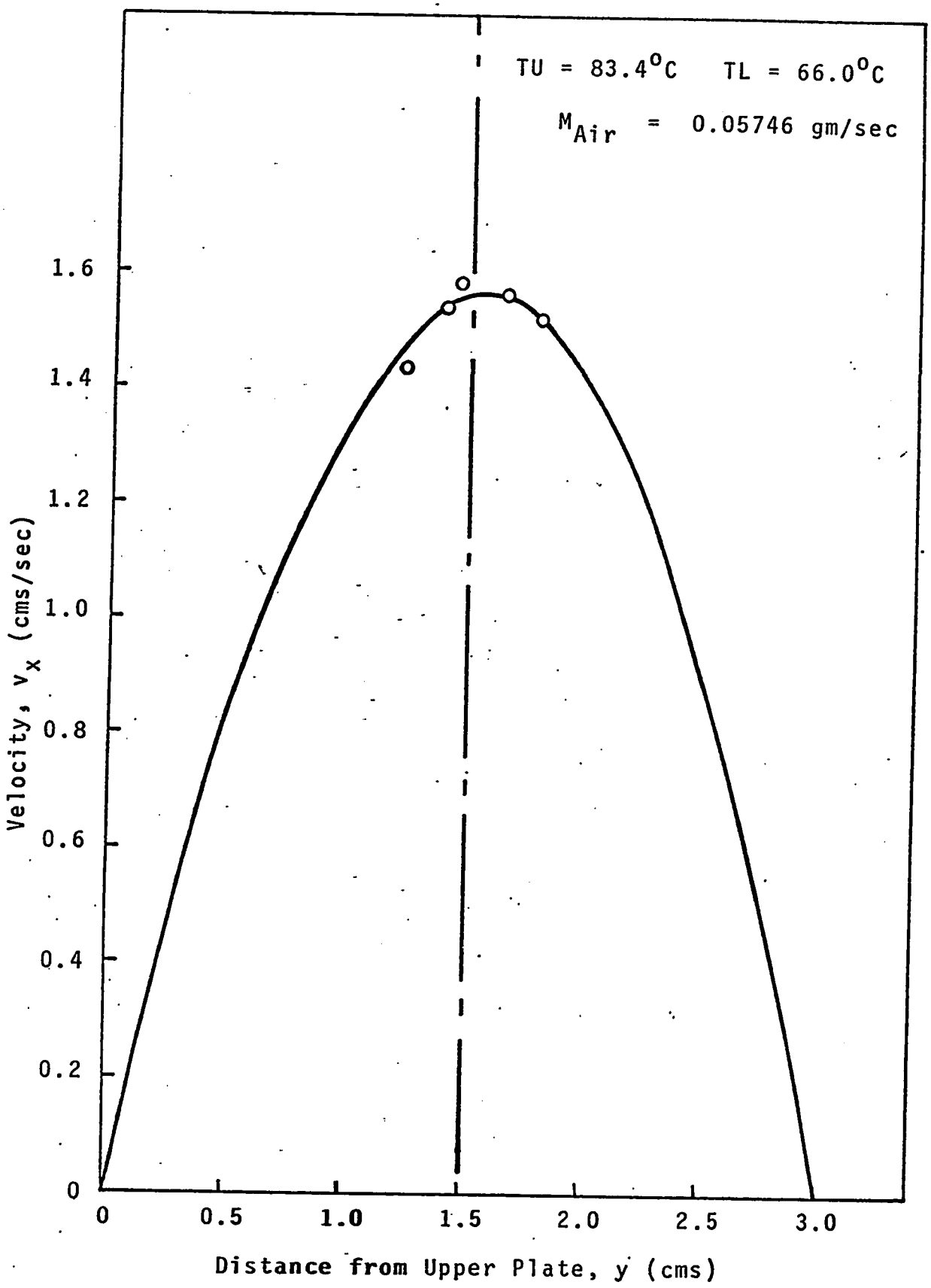

FIG.38 VELOCITY PROFILE (GAP = 3 cms)

Table 22

Velocity Profile (Theoretical Results)

TU = 83.4°C

TL = 66.0°C

GAP = 3 cms

DELPX = $-2.4342*10^{-4}$ gm/(cm sec)^2

M_{Air} = 0.057460 gm/sec

Distance from Upper Plate, y (cms)	Linear Velocity, v_x (cms/sec)
0.0	0.0
0.3	0.536
0.6	0.967
0.9	1.285
1.2	1.488
1.5	1.571
1.8	1.528
2.1	1.354
2.4	1.045
2.7	0.595
3.0	0.0

Table 23

Velocity Profile (Experimental Data)

TU = 83.4°C TL = 66.0°C

GAP = 3 cms Rotameter Float Height = 5.44

Cathetometer Reading for

- Upper Plate = 57.24 cms
- Lower Plate = 54.24 cms

Cathetometer Reading for Anemometer, (cms)	Anemometer Distance from Upper Plate, y (cms)	Anemometer Recorder, mV	Linear Velocity, v_x (cms/sec)
56.04	1.20	0.68	1.43
55.98	1.36	0.73	1.54
55.88	1.46	0.75	1.58
55.70	1.64	0.74	1.56
55.55	1.79	0.72	1.52

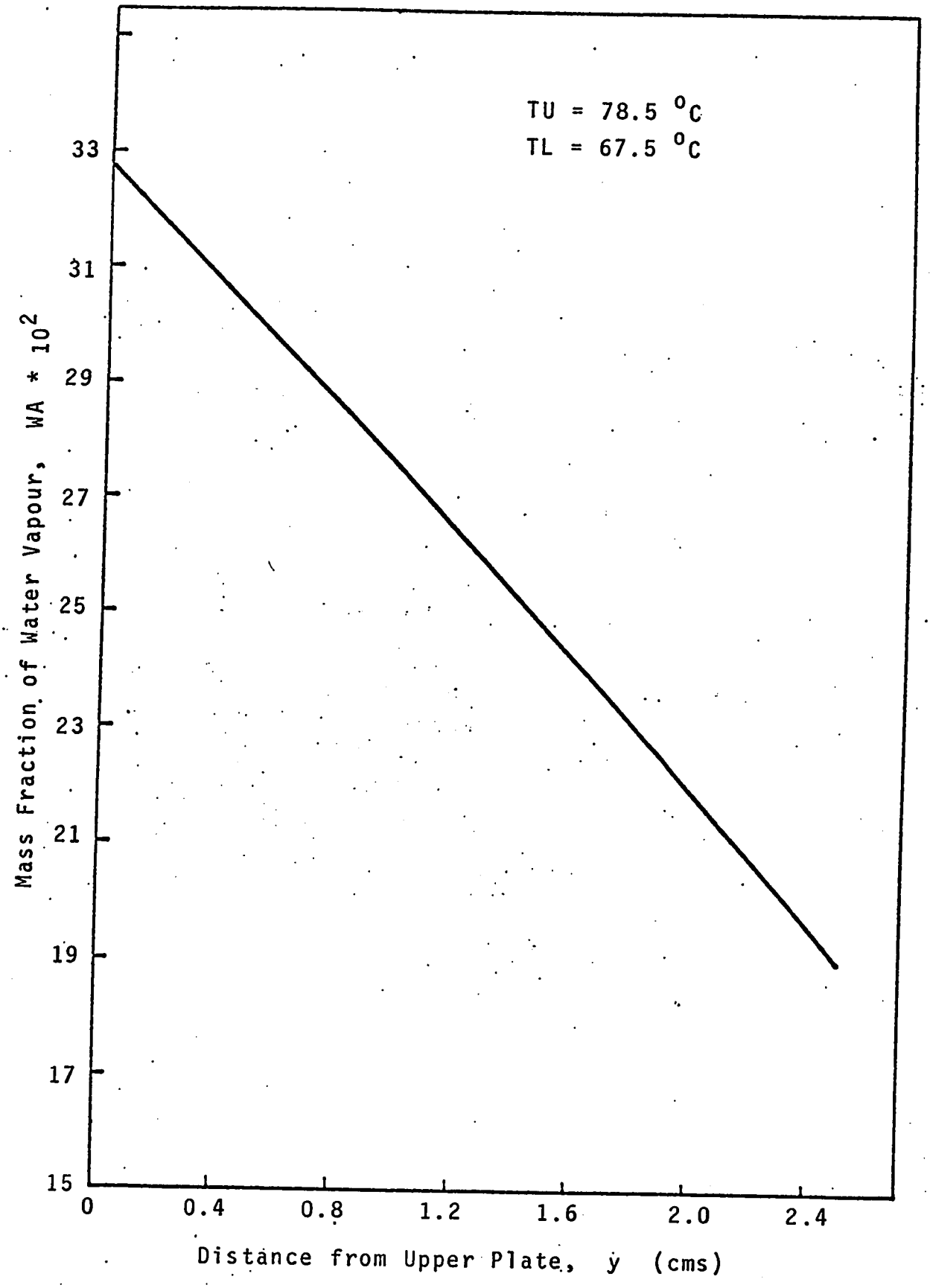

FIG. 39 THEORETICAL MASS FRACTION PROFILE (GAP = 2.5 cms)

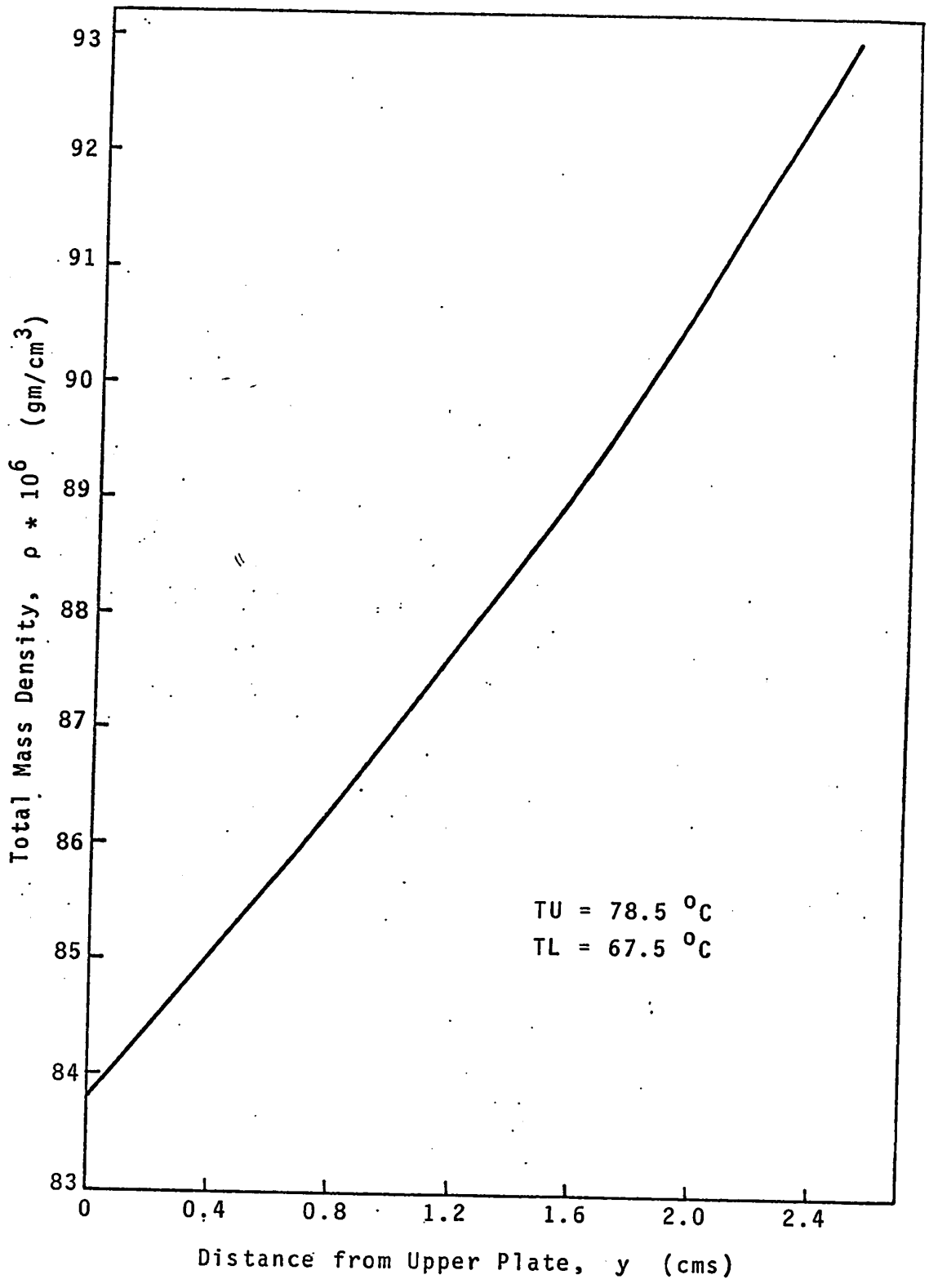

FIG. 40 THEORETICAL TOTAL MASS DENSITY PROFILE
(GAP = 2.5 cms)

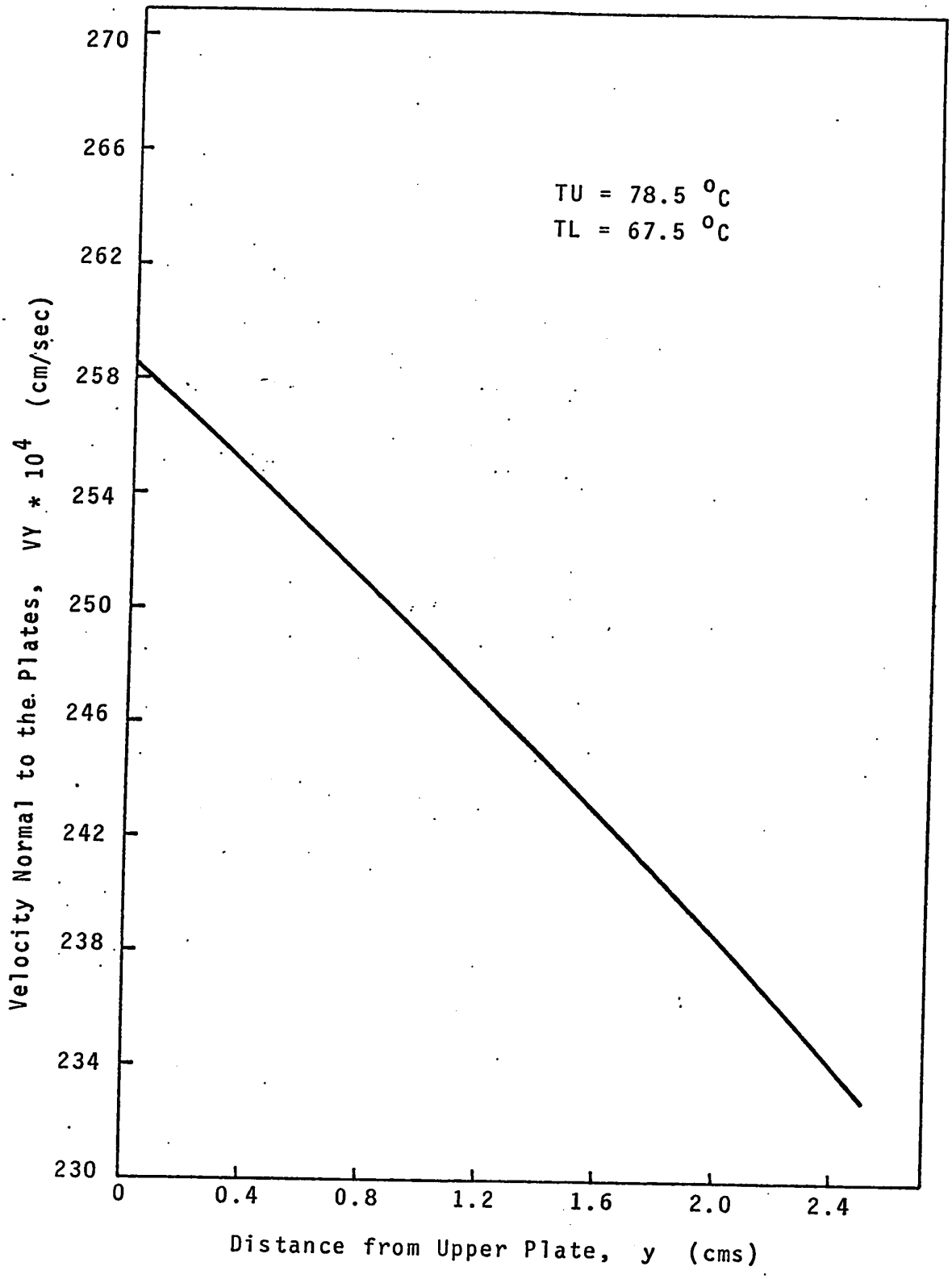

FIG.41 THEORETICAL PROFILE OF VELOCITY NORMAL TO THE PLATES (GAP = 2.5 cms)

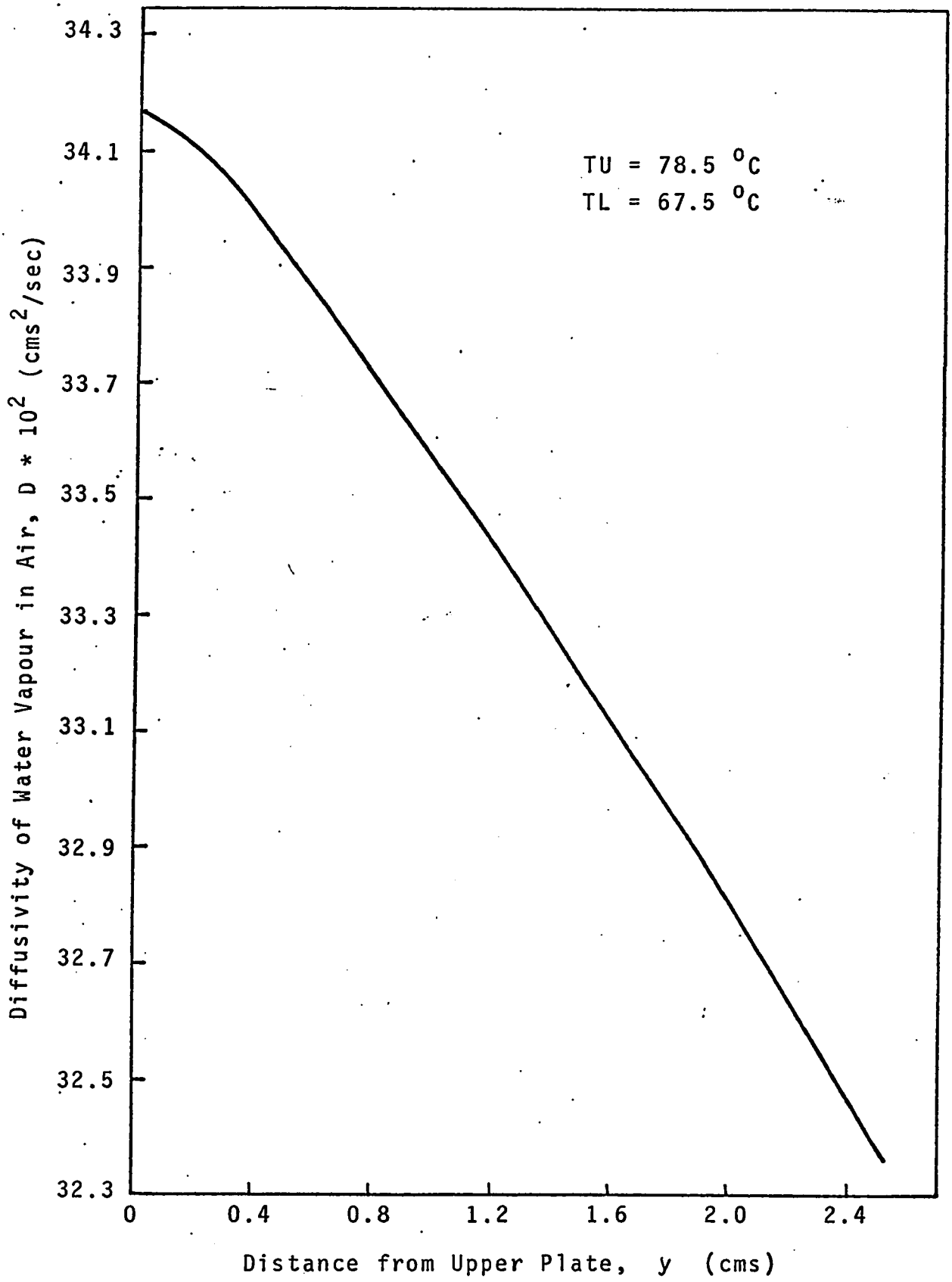

FIG.42 THEORETICAL DIFFUSIVITY PROFILE (GAP = 2.5 cms)

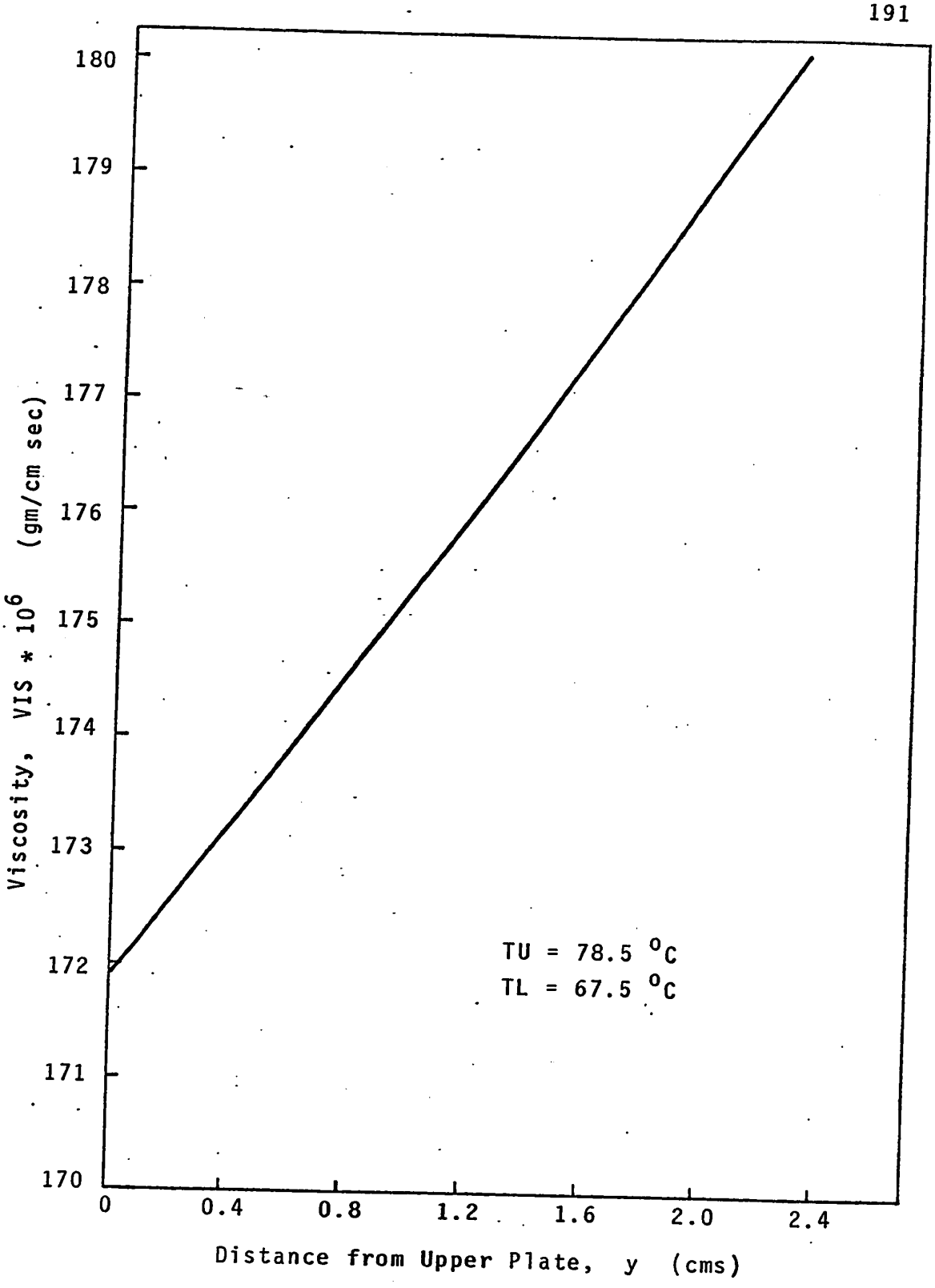

FIG.43 THEORETICAL VISCOSITY PROFILE (GAP = 2.5 cms)

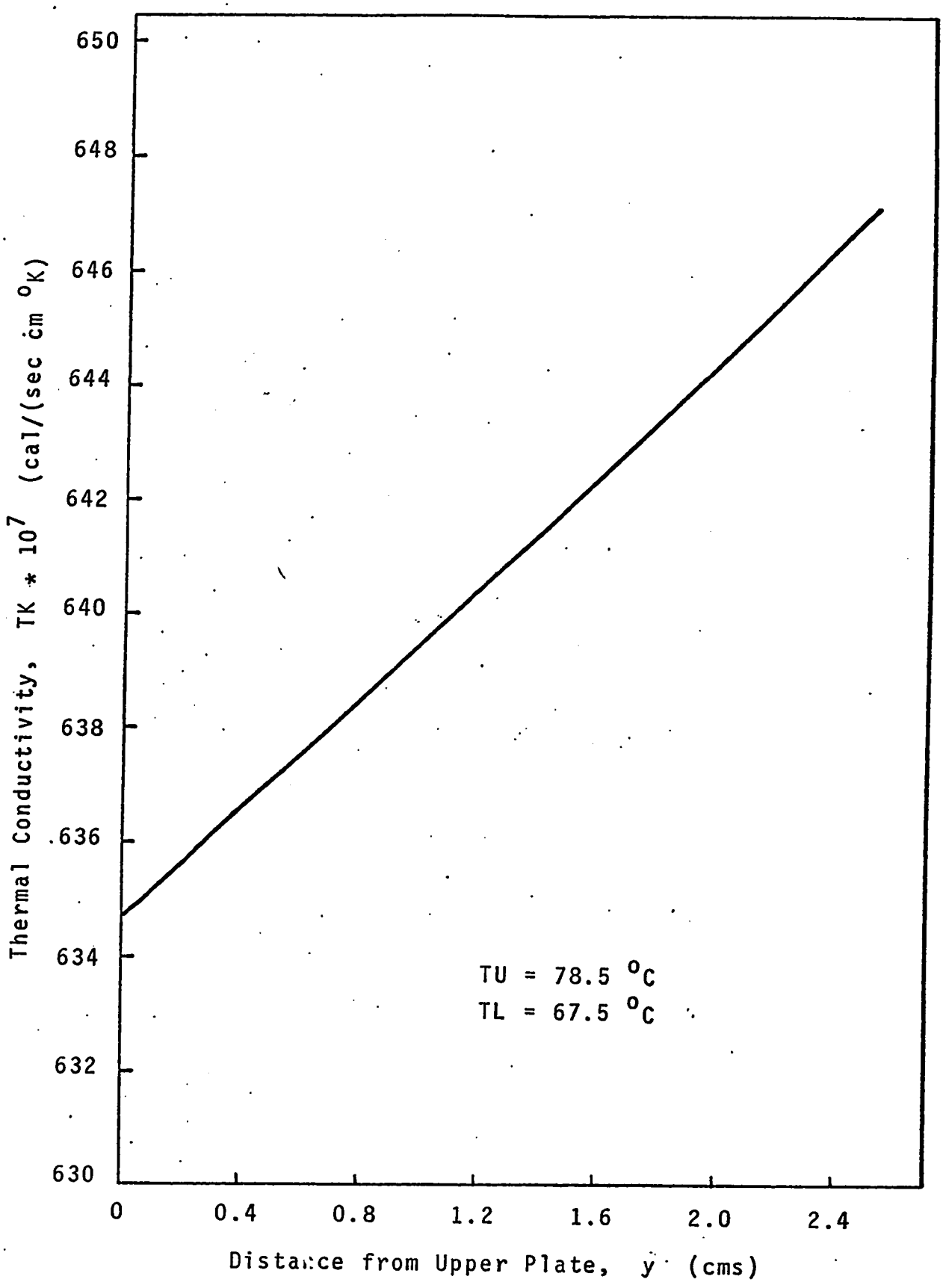

FIG.44 THEORETICAL THERMAL CONDUCTIVITY PROFILE
(GAP = 2.5 cms)

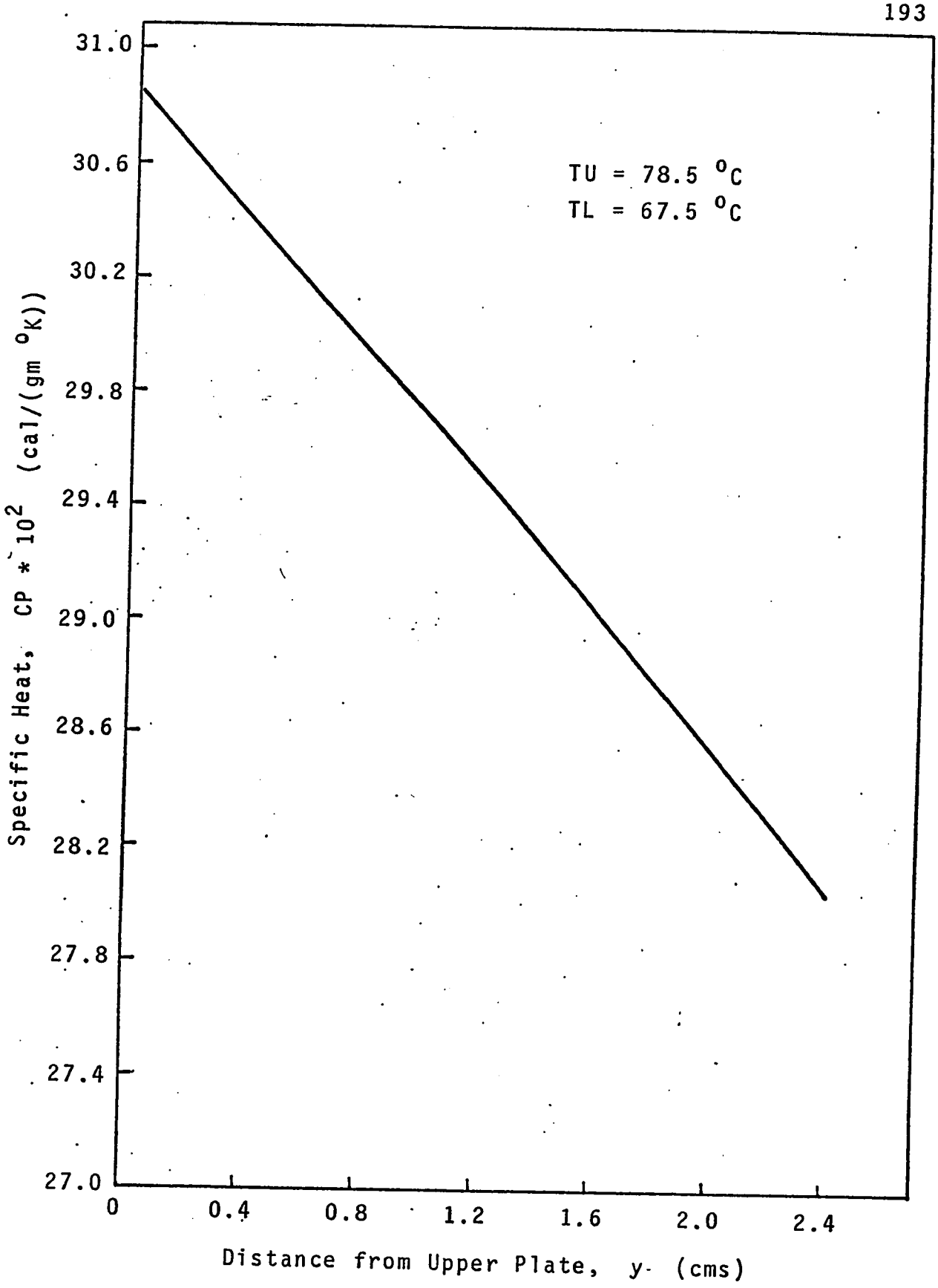

FIG.45 THEORETICAL SPECIFIC HEAT PROFILE (GAP = 2.5 cms)

Table 24

FLUID PROPERTIES

GAP= 2.50 TU= 351.50 TL= 340.50 DELPX= -0.20266E-02
DP = 0.80000E-04 RP = 1.0000
H= 0.10000E-01 EMAX= 0.10000E-05 TOL= 0.10000E-03

Y	= 0.0				
WA	= 0.32725D 00	RA	= 0.27422E-03	XA	= 0.43937E 00
T	= 0.78500E 02	R	= 0.83795E-03	VY	= 0.25858E-01
VIS	= 0.17190E-03	TK	= 0.63472E-04	D	= 0.34238E 00
CP	= 0.30845E 00				

Y	= 0.25000D 00				
WA	= 0.31446D 00	RA	= 0.26593E-03	XA	= 0.42496E 00
T	= 0.77570E 02	R	= 0.84568E-03	VY	= 0.25621E-01
VIS	= 0.17272E-03	TK	= 0.63587E-04	D	= 0.34080E 00
CP	= 0.30571E 00				

Y	= 0.50000D 00				
WA	= 0.30148D 00	RA	= 0.25737E-03	XA	= 0.41016E 00
T	= 0.76605E 02	R	= 0.85369E-03	VY	= 0.25381E-01
VIS	= 0.17356E-03	TK	= 0.63704E-04	D	= 0.33916E 00
CP	= 0.30294E 00				

Y	= 0.75000D 00				
WA	= 0.28832D 00	RA	= 0.24853E-03	XA	= 0.39493E 00
T	= 0.75605E 02	R	= 0.86200E-03	VY	= 0.25136E-01
VIS	= 0.17442E-03	TK	= 0.63822E-04	D	= 0.33746E 00
CP	= 0.30012E 00				

Y	= 0.10000D 01				
WA	= 0.27498D 00	RA	= 0.23940E-03	XA	= 0.37928E 00
T	= 0.74568E 02	R	= 0.87061E-03	VY	= 0.24888E-01
VIS	= 0.17529E-03	TK	= 0.63942E-04	D	= 0.33570E 00
CP	= 0.29727E 00				

Y	= 0.12500D 01				
WA	= 0.26145D 00	RA	= 0.22995E-03	XA	= 0.36319E 00
T	= 0.73493E 02	R	= 0.87953E-03	VY	= 0.24635E-01
VIS	= 0.17618E-03	TK	= 0.64064E-04	D	= 0.33389E 00
CP	= 0.29438E 00				

Y	= 0.15000D 01				
WA	= 0.24773D 00	RA	= 0.22018E-03	XA	= 0.34664E 00
T	= 0.72378E 02	R	= 0.88880E-03	VY	= 0.24378E-01
VIS	= 0.17709E-03	TK	= 0.64187E-04	D	= 0.33201E 00
CP	= 0.29144E 00				

Y	= 0.17500D 01				
WA	= 0.23383D 00	RA	= 0.21007E-03	XA	= 0.32962E 00
T	= 0.71223E 02	R	= 0.89841E-03	VY	= 0.24118E-01
VIS	= 0.17802E-03	TK	= 0.64312E-04	D	= 0.33007E 00
CP	= 0.28847E 00				

Table 24 contd

Y	= 0.20000D 01				
WA	= 0.21974D 00	RA	= 0.19961E-03	XA	= 0.31211E 00
T	= 0.70026E 02	R	= 0.90839E-03	VY	= 0.23853E-01
VIS	= 0.17897E-03	TK	= 0.64439E-04	D	= 0.32906E 00
CP	= 0.28547E 00				

Y	= 0.22500D 01				
WA	= 0.20546D 00	RA	= 0.18877E-03	XA	= 0.29410E 00
T	= 0.68735E 02	R	= 0.91875E-03	VY	= 0.23584E-01
VIS	= 0.17994E-03	TK	= 0.64569E-04	D	= 0.32599E 00
CP	= 0.28242E 00				

Y	= 0.25000D 01				
WA	= 0.19100D 00	RA	= 0.17754E-03	XA	= 0.27556E 00
T	= 0.67500E 02	R	= 0.92952E-03	VY	= 0.23310E-01
VIS	= 0.18092E-03	TK	= 0.64700E-04	D	= 0.32385E 00
CP	= 0.27933E 00				

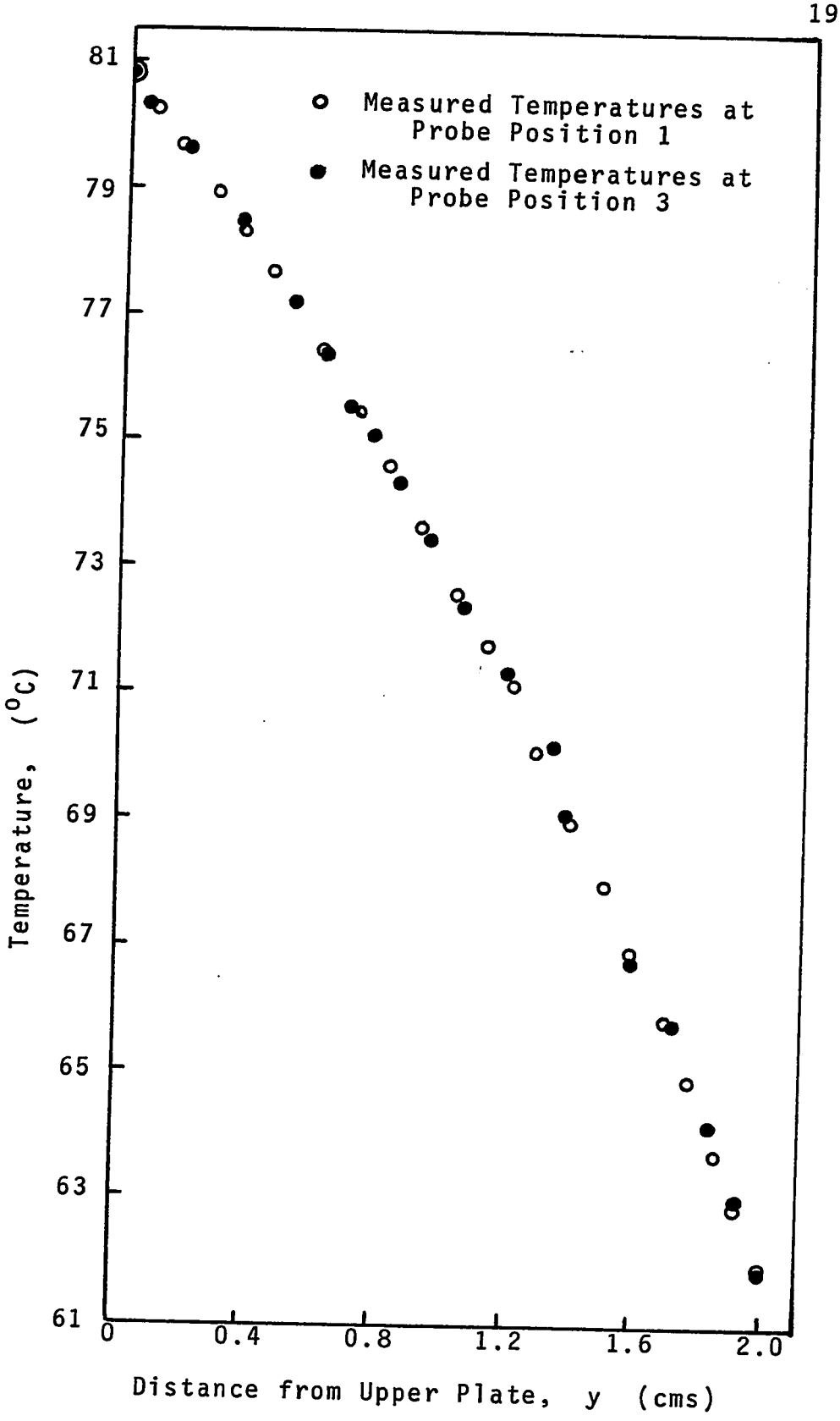

FIG. 46 TEMPERATURE PROFILES AT POSITION 1 AND POSITION 3 (GAP = 2 cms)

Table 25

Temperature Measurements at Probe Position 1

GAP = 2 cms, Cathetometer Reading for

- Upper Plate = 57.24 cms
- Lower Plate = 55.24 cms

Cathetometer Reading, (cms)	Distance from Upper Plate, y (cms)	Temperature D* (High Scale)	Temperature ^{o}C
57.24	0.00	4.35	80.82
57.16	0.08	4.50	80.23
57.08	0.16	4.65	79.66
56.97	0.27	4.85	78.89
56.86	0.38	5.01	78.29
56.79	0.45	5.18	77.66
56.63	0.61	5.51	76.45
56.51	0.73	5.79	75.45
56.42	0.82	6.03	74.60
56.32	0.92	6.31	73.63
56.21	1.03	6.62	72.58
56.11	1.13	6.87	71.74
56.03	1.21	7.05	71.15
55.95	1.29	7.37	70.11
55.84	1.40	7.71	69.02
55.74	1.50	8.03	68.02
55.66	1.58	8.38	66.94
55.55	1.69	8.73	65.88
55.47	1.77	9.05	64.93
55.39	1.85	9.45	63.76
55.32	1.92	9.75	62.90
55.24	2.00	0.04†	61.94

† Low Scale

26

Table 26

Temperature Measurements at Probe Position 3

GAP = 2 cms, Cathetometer Reading for

- Upper Plate = 57.24 cms
- Lower Plate = 55.24 cms

Cathetometer Reading, (cms)	Distance from Upper Plate, y (cms)	Temperature D* (High Scale)	Temperature ^{o}C
57.24	0.00	4.35	80.82
57.19	0.05	4.46	80.39
57.05	0.19	4.65	79.66
56.89	0.35	4.95	78.52
56.73	0.51	5.29	77.25
56.62	0.62	5.52	76.41
56.55	0.69	5.74	75.63
56.48	0.76	5.87	75.16
56.39	0.85	6.11	74.32
56.29	0.95	6.35	73.50
56.19	1.05	6.68	72.38
56.05	1.19	6.98	71.38
55.91	1.33	7.35	70.17
55.85	1.39	7.70	69.05
55.65	1.59	8.46	66.70
55.53	1.71	8.76	65.79
55.41	1.83	9.30	64.20
55.33	1.91	9.70	63.04
55.24	2.00	0.06†	61.82

† Low Scale

VI. SUMMARY AND CONCLUSIONS

A simple, parallel plate particle collector which removed micron-size particles from air by diffusiophoresis was studied experimentally and theoretically. The following major conclusions were reached:

1. The experimental particle collector removed micron-size particles from air effectively. The primary mechanism of removal was diffusiophoresis.

2. Two different mathematical models were considered for describing the particle behaviour:
   (i) Model I assumed that the particles move with the local fluid velocity and good agreement with experimental data was obtained.
   (ii) Schmitt and Waldmann's expression for the diffusiophoretic force was used in Model II. This model also took the thermophoretic and gravity effects into consideration.

   The particle velocities calculated by Models I and II differed by less than 10 percent provided diffusiophoresis was the dominant mechanism for particle removal.

3. Particle settling lengths and settling times were determined theoretically and experimentally. It was found that the particle settling lengths and times were strong functions of the vapour pressure difference between the collector plates, the average vapour concentration, and

the plate spacing.

4. The operating ratio, i.e. the mass of water vapour required to clean unit mass of air, was found to lie between 1 and 2.

5. The transport equations governing the fluid behaviour in the particle collector were solved numerically. The experimentally measured velocity and temperature profiles were in good agreement with the previously calculated results.

6. It was shown that diffusion through a stagnant gas is primarily determined by the continuity equations and that the effect of the momentum equation is negligible under most conditions.

VII. NOMENCLATURE

A	Denoting water vapour
A_0	Constant defined by Equation (III-116)
A_1	Constant defined by Equation (III-113)
A_2	Constant defined by Equation (III-114)
A_{th}	Thermistor constant
a, a_o, a_1	Constants defined in Section III-E-2
a_c	Constant defined in Section III-E-5
a'	Constant defined in Equation (IV-2)
B	Denoting air
B_{th}	Thermistor constant
b_c	Constant defined in Section III-E-5
$b_{f,e}$	Parameter defined in Equation (IV-3)
b'	Constant in Equation (IV-2)
C1	Integration constant defined by Equation (III-56)
C2	Integration constant defined by Equation (III-58)
C3	Integration constant defined by Equation (III-60)
C4	Integration constant defined by Equation (III-74)
C_m	Quantity defined in Equation (II-34)
C_p	Specific heat at constant pressure
CR	Constant defined by Equation (III-98)
C_t	Quantity defined in Equation (II-33)
c, c_o, c_1	Constants defined in Section III-E-3
c_c	Constant defined in Section III-E-5

D	Diffusivity
D'	The differential operator, d/dy
D^*	Units of recorder-pen deflection
DELPX	Pressure gradient, dP/dx
D_p	Particle diameter
$\frac{D}{Dt}$	Substantive derivative
E	Total internal energy
E_a	Average anemometer voltage defined in Equation (IV-6)
$E(I)$	Errors defined by Equation (III-184)
EC	Constant defined by Equation (III-102)
E_c	Concentration entrance length
E_t	Temperature entrance length
E_v	Velocity entrance length
e	Anemometer voltage
e_{ac}	AC component of e
$\underline{e}_i$	Unit vector pointing in direction i
F	Constant defined by Equation (III-103)
$\underline{F}_d$	Drag on a particle
$\underline{F}_g$	Force due to gravity on a particle
$\underline{F}_{dp}$	Diffusiophoretic force on a particle
$\underline{F}_{tp}$	Thermophoretic force on a particle
$F(y,Z)$	Vector defined by Equation (III-173) and (III-174)
$f(X)$	Function defined by Equation (III-185)
$f_i'(X)$	Functions defined by Equation (III-183)
G	Constant defined by Equation (III-125)
GAP	Distance between plates

$\underline{g}$ Gravitational acceleration vector

H Total Enthalpy

$\overline{H}_k$ Partial mass enthalpy of component k

HC Constant defined by Equation (III-126)

$\underline{H}_d$ Enthalpy diffusion flux vector

H1 See Fig. 9

I_1 Integration constant in Equation (III-98)

$\underline{j}_k$ Diffusive flux vector of component k

K Thermal conductivity

K1 Constant defined by Equation(III-123)

KN Parameters defined by Equations (III-176 to 180) where N = 1, 2, 3, 4, 5

K_a Parameter defined in Equation (IV-9)

K_F, K'_F Constants in Equations (II-7) and (II-8)

K_n Knudsen number, see Equation (II-1)

k_B Boltzmann constant

k_{trans} Translational part of thermal conductivity

M_A Molecular weight of water

M_B Molecular weight of air

M_{Air} Mass flow rate of air defined by Equation (III-162)

M_{H_2O} Minimum water vapour requirement for removing particles defined by Equation (III-163)

M_R Constant defined by Equation (III-95)

M_{RS} Constant defined by Equation (III-96)

m Total mass of control volume

m_k Mass of species k in control volume

N Total number of components

n Molar density

ORATIO Operating rate defined by Equation (III-164)

P Pressure

PSAT Saturated vapour pressure of water

Q Volumetric gas flow rate defined by Equation (III-166)

$\underline{q}$ Conductive heat flux vector

r Resistance

R1, R2, R3, RV Resistances in thermistor circuit

R_c Universal gas constant

Re Reynolds number

RF Resistance giving a full recorder-pen deflection

RO Resistance giving a zero recorder-pen deflection

S Entropy

S_o Surface area of control volume

dS Element of surface area

SL Particle settling length defined by Equation (III-144)

SLP Particle settling length defined by Equation (III-160)

ST Particle settling time defined by Equation (III-148)

STP Particle settling time defined by Eqaution (III-161)

T Temperature

TO Observed mercury-in-glass thermometer reading

TC Corrected mercury-in-glass thermometer reading

TC1 to TC11 Parameters defined in Section IV-12

TKTDOT Variable defined by Equation (III-83)

TR Reciprocal of the absolute temperature

TL	Temperature of the lower plate
TU	Temperature of the upper plate
t	Time
V	Volume
V_o	Volume of control-volume
$\underline{v}$	Velocity vector
v_a	Amplitude of anemometer-wire vibration velocity
$\underline{v}_p$	Particle velocity
v_{ydp}	Diffusiophoretic velocity in y direction
v_{ytp}	Thermophoretic velocity in y direction
v_{yg}	Velocity due to gravity in y direction
v_{yp}	Particle velocity in y direction given by Equation (III-157)
W	Width of plates
w_{AL}	Mass fraction of water vapour at lower plate
w_{AU}	Mass fraction of water vapour at upper plate
w_k	Mass fraction of component k
X(I)	Gradients at upper plate defined by Equation (III-182)
x	x-coordinate
x_k	Mole fraction of component k
y	y-coordinate
Z	Vector defined by Equations (III-173) and (III-174)

Greek Letters:

α	Constant defined by Equation (III-107)
α^1	Constant defined by Equation (IV-1)
α_m	Momentum accommodation coefficient in Equation (II-33)

α_t Thermal accommodation coeficient in Equation (II-34)

β Constant defined by Equation (III-108)

γ Constant defined by Equation (III-109)

$\underline{\delta}$ Unit tensor

ε Integration error defined by Equation (III-181)

κ Bulk viscosity

λ Mean free path of gas molecules

μ Viscosity

ρ Mass density

σ Projected area of an aerosol particle

σ_{AB} Diffusion-slip factor

σ_i diameter of molecule i

$\underline{\tau}$ Stress tensor

$-\phi$ Viscous dissipation

Ψ_{kj} Parameter defined by Equation (III-133)

ω Vibration frequency of anemometer wire

Miscellaneous:

$\underline{\nabla}$ Differential operator

$\hat{}$ per unit mass

VIII REFERENCES

1. J. Aitken, Roy. Soc. Edinb., 32, 239 (1883)
2. B.V. Deriagin and S.S. Dukhin, Doklady Akad. Nauk SSSR, 106, 851 (1956)
3. B.V. Deriagin and S.S. Dukhin, Doklady Akad. Nauk SSSR, 111, 613 (1956)
4. B.V. Deriagin and S.S. Dukhin, Doklady Akad. Nauk SSSR, 112, 407 (1957)
5. J.R. Brock, J. Colloid Sci., 18, 489 (1963)
6. J. Stefan, Wien. Ber., 83, 943 (1881)
7. B.V. Deriagin and S.P. Bakanov, Soviet Phys. Doklady, 2, 563 (1957)
8. L. Waldmann, Z. Naturf., 14a, 589 (1959)
9. S. Chapman and T.G. Cowling, The Mathematical Theory of Non-Uniform Gases, Cambridge University Press, Cambridge (1964)
10. K.H. Schmitt and L. Waldmann, Z. Naturf.,15a, 843 (1960)
11. K.H. Schmitt, Staub, 21, 173 (1961)
12. M.L. Facy, Compt. Rend., 246, 3161 (1958)
13. M.L. Facy, Compt. Rend., 246, 102 (1958)
14. V. Freise, J. Chem. Physique, 54, 879 (1957)
15. A. Einstein, Z. Phys., 27, 1 (1924)
16. P.S. Epstein, Phys. Rev., 23, 710 (1924)
17. K.H. Schmitt and L. Waldmann, Z. Naturf.,15a, 843 (1960)
18. K.H. Schmitt, Z. Naturf., 16a, 144 (1961)
19. R.A. Millikan, Phys. Rev., 32, 382 (1911)
20. H.A. Kramers and J. Kistemaker, Physica, 10, 699 (1943)

21. S.P. Bakanov and B.V. Derjaguin, Disc. Farad. Soc., 30, 130 (1960)

22. E.A. Mason and S. Chapman, J. Chem. Phys., 36, 627 (1962)

23. P. Goldsmith, H.J. Delafield, and L.C. Cox, Geof. Pura. Applic., 50, 278 (1963)

24. P. Goldsmith, H.J. Delafield and L.C. Cox, Q.J.R. Met. Soc., 89, 43 (1963)

25. A.L. Metnieks and L.W. Pollak, Geophys. Bull. Dublin, 16 (1959)

26. B.V. Derjaguin, Yu.I. Yalamov, and A.I. Storozhilova, J. Colloid and Interf. Sci., 22, 117 (1966)

27. B.V. Derjaguin and A.I. Storozhilova, J. Colloid and Interf. Sci., 21, 35 (1966)

28. J.R. Brock, J. Colloid and Interf. Sci., 27, 95 (1968)

29. L. Waldmann in Rarified Gas Dynamics, Edited by L. Talbot, Academic Press, New York (1961)

30. L. Waldmann and K.H. Schmitt in Aerosol Science, Edited by C.N. Davies, Academic Press, London (1966)

31. P. Goldsmith and F.G. May in Aerosol Science, Edited by C. N. Davies, Academic Press, London (1966)

32. W. Strauss, Industrial Gas Cleaning, Pergamon Press, Oxford (1966)

33. J. Tyndall, Proc. Roy. Inst., 6, 3 (1870)

34. Rayleigh, Proc. Roy. Soc., 34,414 (1882)

35. Rayleigh, Nature, 28, 139 (1882)

36. W. Cawood, Trans. Farad. Soc., 32, 1068 (1936)

37. G. Hettner, Z.Phys., 27, 12 (1924)

38. E. Einstein, Ann. d. Phys., 69, 241 (1922)

39. H.H. Watson, Trans. Farad. Soc., 32, 1073 (1936)

40. P. Rosenblatt and V.K. LaMer, Phys. Rev., 70, 385 (1946)

41. P. Epstein, Z. Phys., 54, 537 (1929)

42. H.S. Taylor, Treatise on Physical Chemistry, D. van Nostrand Co., New York (1931)

43. B.V. Deryagin and S.P. Bakanov, Koll. Zh., 21, 377 (1959)

44. K.H. Schmitt, Z. Naturf., 14a, 870 (1959)

45. C.F. Schadt and R.D. Cadle, J. Phys. Chem., 65, 1689 (1961)

46. J.R. Brock, J. Colloid Sci., 17, 768 (1962)

47. J.R. Brock, J. Phys. Chem., 66, 1763 (1962)

48. S. Jakobsen and J.R. Brock, J. Colloid Sci., 20, 544 (1965)

49. J.R. Brock, J. Colloid and Interf. Sci., 23, 448 (1967)

50. J.R. Brock, J. Colloid and Interf. Sci., 25, 392 (1967)

51. B.V. Derjaguin and Yu. Yalamov, J. Colloid Sci., 20, 555 (1965)

52. R.B. Bird, W.E. Stewart, and E.N. Lightfoot, Transport Phenomena, John Wiley & Sons Inc., New York (1960)

53. J.O. Hirschfelder, C.F. Curtiss, and R.B. Bird, Molecular Theory of Gases and Liquids, John Wiley & Sons Inc., New York (1954)

54. W. Jost, Diffusion in Solids, Liquids, Gases, Academic Press Inc., New York (1952)

55. J. Crank, The Mathematics of Diffusion, Oxford University Press, Oxford (1956)

56. T.K. Sherwood and R.L. Pigford, Absorption and Extraction, McGraw-Hill Book Company Inc., New York (1952)

57. H.S. Carslaw and J.C. Jaeger, Conduction of Heat in Solids, Oxford University Press, London (1959)

58. M. Jakob, Heat Transfer, John Wiley & Sons Inc., New York (1949)

59. E.R.G. Eckert, Einfuehrung in den Waerme- und Stoffaustausch, Springer Verlag, Berlin (1966)

60. D.B. Spalding, Convective Mass Transfer, Edward Arnold (Publishers) Ltd., London (1963)

61. H.Schlichting, Boundary Layer Theory, McGraw-Hill Book Company Inc., New York (1955)

62. C.O. Bennett and J.E. Myers, Momentum, Heat, and Mass Transfer, McGraw-Hill Book Company Inc., New York (1962)

63. H.H. Rosenbrock and C. Storey, Computational Techniques for Chemical Engineers, Pergamon Press Ltd., Oxford (1966)

64. V.G. Jenson and G.V. Jeffreys, Mathematical Methods in Chemical Engineering, Academic Press, London (1963)

65. L. Lapidus, Digital Computation for Chemical Engineers, McGraw-Hill Book Company Inc., New York (1962)

66. H.S. Mickley, T.K. Sherwood, and C.E. Reed, Applied Mathematics in Chemical Engineering, McGraw-Hill Book Company Inc., New York (1957)

67. J. Todd (editor), A Survey of Numerical Analysis, McGraw-Hill Book Company Inc., New York (1962)

68. G.N. Lance, Numerical Methods for High Speed Computers, Iliffe & Sons Ltd., London (1960)

69. International Critical Tables, McGraw-Hill Book Company Inc., New York (1928)

70. F.G. Keyes, Trans. ASME, 73, 589 (1951)

71. O.A. Hougen and K.M. Watson, Chemical Process Principles, John Wiley and Sons Inc., London (1843)

72. C.H. Keith and J.C. Derrick, Tobacco Sci., 5, 84 (1961)

73. DISA Elektronik A/S, Instruction and Service Manual for Type 55D80/81 Low Velocity Anemometer, Herlev, Denmark

APPENDIX I

ABSTRACT

The effect of the y-momentum equation on the transport processes in diffusion through a stagnant gas is considered in this appendix.
The effect was analysed qualitatively and quantitatively and it was shown to be negligible in all situations encountered with the present particle collector.

THE PROBLEM

So far only the momentum equation in the x-direction was considered in simulating the particle collector. However, there exists also a momentum equation for the y-direction.

Incorporating the y-momentum equation in the mathematical model resulted in severe numerical problems. The effect of the y-momentum equation in a simpler system, i.e. an isothermal system in which there is no flow parallel to the plates,was therefore studied.

GEOMETRY

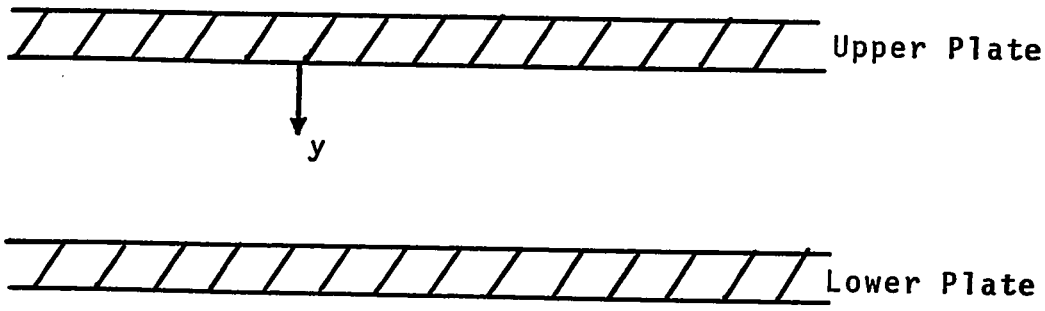

OPERATING CONDITIONS AND ASSUMPTIONS

1. The conditions are developed, i.e. all dependent variables are functions of y only.
2. The physical properties of the fluid are constant.
3. The effect of gravity is neglected.

EQUATIONS

Continuity Equations:

These are Equations (III-56) and (III-70) in Section III, i.e.

$$\rho v_y = C1 \tag{1}$$

$$\frac{dw_A}{dy} = \frac{C1\ (w_A - 1)}{\rho\ D} \tag{2}$$

with boundary conditions:

$$y = 0 \qquad w_A = w_{AU} \tag{3}$$

$$y = GAP \qquad w_A = w_{AL} \tag{4}$$

Momentum Equation:

The momentum equation in terms of the stress tensor $\underline{\tau}$ was given in Section III (Equation (III-22)):

$$\rho \frac{D\underline{v}}{Dt} = - \underline{\nabla} P + \underline{\nabla} \cdot \underline{\tau} + \rho \underline{g} \tag{5}$$

and the simplified stress tensor $\underline{\tau}$ is:

$$\underline{\tau} = - \mu \left(\underline{\nabla} \cdot \underline{v} + (\underline{\nabla} \cdot \underline{v})^{+} - \frac{2}{3} (\underline{\nabla} \cdot \underline{v}) \, \underline{\delta} \right) \tag{6}$$

(see Equation (III-23))

The Stress Tensor, $\underline{\tau}$:

The components of $\underline{\tau}$ are found as follows:

$$\underline{\nabla} \cdot \underline{v} = \frac{\partial v_x}{\partial x} + \frac{\partial v_y}{\partial y} + \frac{\partial v_z}{\partial z} = \frac{dv_y}{dy} \tag{7}$$

since v_x and v_z are zero.

$$\tau_{xx} = + \frac{2}{3} \mu \frac{dv_y}{dy} \tag{8}$$

$$\tau_{yy} = - 2 \mu \frac{dv_y}{dy} + \frac{2}{3} \mu \frac{dv_y}{dy} = - \frac{4}{3} \mu \frac{dv_y}{dy} \tag{9}$$

$$\tau_{zz} = + \frac{2}{3} \mu \frac{dv_y}{dy} \tag{10}$$

$$\tau_{xy} = \tau_{yx} = 0 \qquad \text{since } v_y = v_y(y) \tag{11}$$

$$\tau_{yz} = \tau_{zy} = 0 \tag{12}$$

$$\tau_{zx} = \tau_{xz} = 0 \tag{13}$$

These components of the tensor $\underline{\tau}$ are now substituted into Equation (6). The momentum equation for the x-direction vanishes identically. The y-momentum equation is given by:

$$\rho v_y \frac{dv_y}{dy} = - \frac{dP}{dy} - \left[\underline{\nabla} \cdot \underline{\tau}\right]_y \tag{14}$$

$$\rho v_y \frac{dv_y}{dy} = - \frac{dP}{dy} - \frac{d}{dy}\{\tau_{yy}\} \tag{15}$$

or

$$\rho v_y \frac{dv_y}{dy} = - \frac{dP}{dy} + \frac{4}{3} \frac{d}{dy} \mu \frac{dv_y}{dy} \tag{16}$$

The boundary conditions will be considered later.

Equation of State:

For an ideal gas-mixture

$$\rho = \left(\frac{P\ M_A}{R_c\ T}\right) \frac{1}{M_R - w_A\ M_{RS}} \tag{17}$$

(see Equation (III-94))

Let $$M_R / M_{RS} = M \tag{18}$$

and $$R_c\ T\ M_{RS} / M_A = S1 \tag{19}$$

Thus:

$$\rho = \frac{P}{S1\ (M - w_A)} \tag{20}$$

SIMPLIFIED NOTATION

Let $$v_y = v \qquad w_A = w \tag{21}$$

$$w_{AU} = w_U \qquad w_{AL} = w_L \tag{22}$$

Hence the equations to be solved are:

$$\rho v = C1 \tag{1}$$

$$\frac{dw}{dy} = \frac{v\,(w - 1)}{D} \tag{23}$$

$$\rho v \frac{dv}{dy} = - \frac{dP}{dy} + \frac{4}{3} \frac{d}{dy} \mu \frac{dv}{dy} \tag{24}$$

$$\rho = \frac{P}{S1\,(M - w)} \tag{25}$$

The problem is thus defined except for the boundary conditions of the y-momentum equation.

BOUNDARY CONDITIONS FOR Y - MOMENTUM EQUATION

Integration of Equation (24) and recalling that $\rho v = C1$ gives:

$$C1 \cdot v = - P + \frac{4}{3} \mu \frac{dv}{dy} + C4 \tag{26}$$

where C4 is the integration constant. Consider a control volume lying partially in the upper plate and partially in the gas mixture below it.

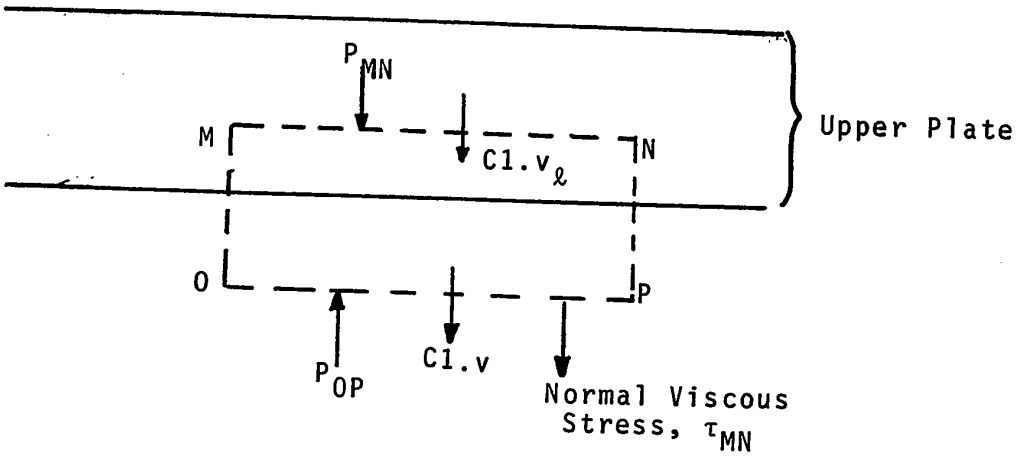

The momentum fluxes and forces (pressures) are as shown in the above figure. It is noted that there is no normal stress in the liquid since it is considered to be incompressible. When the system is at steady state, the momentum theorem states:

> The net flow of momentum through the surfaces of the control volume equals the sum of the forces acting on the control volume.

Since the forces and momentum are vector quantities, the theorem may be written for the y-direction only, giving for the present system:

$$- C1 \cdot v_\ell + C1 \cdot v = P_{MN} - \left\{P - \frac{4}{3}\mu \frac{dv}{dy}\right\} \qquad (27)$$

or

$$C1 \cdot v = - \left\{P - \frac{4}{3}\mu \frac{dv}{dy}\right\} + P_{MN} + C1 \cdot v_\ell \qquad (28)$$

where v_ℓ denotes the velocity of the liquid.

Comparing Equations (26) and (28) gives:

$$C4 = P_{MN} + C1 \cdot v_\ell \qquad (29)$$

If the line MN is drawn just inside the upper plate, $P_{MN} = PU$ and hence Equation (29) becomes:

$$C4 = PU + C1 \cdot v_\ell \qquad (30)$$

where PU is the pressure at the upper plate (= 1 atm).

SUMMARY OF EQUATIONS

$$\rho v = C1 \qquad (1)$$

$$\frac{dw}{dy} = \frac{C1\ (w - 1)}{\rho\ D} \qquad (23)$$

$$\frac{dv}{dy} = \left(\frac{3}{4\mu}\right)\left[C1 \cdot v + P - C4\right] \qquad (26)$$

$$C4 = PU + C1 \cdot v_{\ell} \qquad (30)$$

$$= \frac{P}{S1\ (M - w)} \qquad (25)$$

Boundary conditions:

$$y = 0 \qquad w = w_u \qquad P = PU \qquad (21)$$

$$y = GAP \qquad w = w_L \qquad (22)$$

The problem is now completely defined since:

1. Unknown variables are ρ, v, P, and w, i.e. 4
2. Equations are (1), (23), (26), and (25), i.e. 4
3. Unknown constants are C1, C4 plus 2 integration constants, i.e. 4
4. Boundary conditions: 3 plus Equation (30)

STRATEGY OF SOLUTION

It is obvious that the set of simultaneous differential equations cannot be solved analytically. Hence there are two different strategies which may be adopted for the solution:

1. Make an order of magnitude analysis and thereby show that the equations reduce to a simpler and soluble set

2. Solve the equations numerically.

Both approaches will be described subsequently. However, before proceeding with this, the set of equations is reduced to just one equation. This equation is of course more complicated than the former ones making up the set.

REDUCTION OF EQUATIONS TO ONE

Substituting Equation (30) into (26) and rearranging gives:

$$\frac{4\mu}{3}\frac{dv}{dy} = (P-PU) + C1\ (v - v_\ell) \qquad (31)$$

Substituting Equation (1) into (25) and solving for P:

$$P = S1 \cdot C1 \cdot \left(\frac{M - w}{v}\right) \qquad (32)$$

But at $y = 0$, $v = v_u$, $w = w_u$, $P = PU$ and hence Equation (31) becomes:

$$\frac{4\mu}{3}\frac{dv}{dy} = S1 \cdot C1 \left[\frac{M - w}{v} - \frac{M - w_u}{v_u}\right] + C1\ (v - v_\ell) \qquad (33)$$

Since

$$\frac{dw}{dy} = \frac{v(w - 1)}{D} \qquad (23)$$

dividing Equation (33) by (23) eliminates y and makes w the new independent variable. This change of variables is only successful because the original set of equations is autonomous.

$$\frac{4\mu}{3D}\frac{dv}{dw} = \frac{S1 \cdot C1 \left[\frac{M - w}{v} - \frac{M - w_u}{v_u}\right] + C1\ (v - v_\ell)}{v\ (w - 1)} \qquad (34)$$

No known analytical solution exists for the non-linear Equation (34). A numerical solution by the standard techniques is also precluded because the constant S1 is very large ($\simeq -10^9$) and

$$\frac{M - w}{v} - \frac{M - w_u}{v_u} \simeq 0 \qquad (35)$$

The latter follows from the fact that

$$P \simeq PU \qquad (36)$$

Substituting Equation (32) into (36) gives Equation (35) upon rearrangement.

Hence a very small term, Equation (35), is multiplied by a very large constant, S1, in Equation (34). It follows that even a slight error in estimating v causes the right hand side of Equation (34) to be very large. A special iterative technique was therefore developed to solve Equation (34) numerically.

Before proceeding with this, Equation (34) is solved approximately by making an order of magnitude analysis.

APPROXIMATE SOLUTION OF EQUATION (34) - Strategy 1

The solution consists of two parts:

1. Estimating the maximum value of the velocity v
2. Solving Equation (34) by using the result of part 1 and the Mean Value Theorem.

1. The Maximum Velocity:

Let the maximum velocity be denoted by v_m. At the maximum (or minimum) $dv/dw = 0$. Hence Equation (34) becomes:

$$0 = \frac{S1 \cdot C1 \left[\frac{M - w}{v} - \frac{M - w_u}{v_u}\right] + C1 (v_m - v_\ell)}{v_m (w_m - 1)} \qquad (37)$$

where w_m is the mass fraction at which the velocity is a maximum (or minimum). Equation (37) implies:

$$S1 \left[\frac{M - w_m}{v_m} - \frac{M - w_u}{v_u}\right] + (v_m - v_\ell) = 0 \qquad (38)$$

Since S1 is very large, Equation (38) reduces to

$$\frac{M - w_m}{v_m} - \frac{M - w_u}{v_u} \simeq 0 \qquad (39)$$

or

$$w_m \simeq w_u \qquad (40)$$

$$v_m \simeq v_u \qquad (41)$$

Hence the maximum (or minimum) velocity occurs at $w = w_u$, i.e. at the upper plate.

It remains to be shown that v_m as given by Equation (41) is a maximum and not a minimum. Differentiating Equation (34) once again gives:

$$\frac{4\mu}{3D}\frac{d^2v}{dw^2} = \frac{C1}{v^2(w - 1)}\left[v (w - 1)\left[\frac{S1}{v^2}(- v - (M - w)\frac{dv}{dw}) + \frac{dv}{dw}\right] - \left[S1\left(\frac{M - w}{v} - \frac{M - w_u}{v_u}\right) + (v - v_\ell)\right]\left[(w - 1)\frac{dv}{dw} + v\right]\right] \qquad (42)$$

At a maximum or minimum dv/dw = 0 and Equation (38) is valid. Hence Equation (42) becomes:

$$\frac{d^2v}{dw^2} = -\left(\frac{3\ C1\ .\ D}{4\ \mu}\right) \frac{S1}{v_m^2\ (w_m - 1)} \qquad (43)$$

Since

$$\frac{3\ C1\ .\ D}{4\ \mu} > 0$$

$$v^2 > 0$$

$$(w - 1) < 0 \qquad (0 < w < 1)$$

$$S1 < 0$$

it follows that

$$\frac{d^2v}{dw^2} < 0 \qquad (44)$$

and hence v_m given by Equation (38) or (39) is a true maximum.

As already indicated, Equation (39) implies that $P \simeq PU$. If it is assumed that the pressure is constant, the velocity v is just given by the Continuity Equation (23) and the Equation of State (25). Solving these equations simultaneously shows that v is of the order of unity.

2. Use of the Mean Value Theorem:

The mean value theorem states that for any interval $[0, x]$

$$\int_0^x f(s)\ ds = f(\xi)\ x \qquad (45)$$

where $0 \leq \xi \leq x$ (46)

The meaning of $f(\xi)$ is that it is the "average value" of $f(s)$ in the interval $[0, x]$ since the average is defined as

$$\langle f \rangle = \frac{1}{x} \int_0^x f(s)\, ds \tag{47}$$

Integrating Equation (33) gives:

$$\frac{4\mu}{3}(v - v_u) = S1 \cdot C1 \int_0 \frac{M - w}{v}\, dy - S1 \cdot C1 \left(\frac{M - w_u}{v_u}\right) y + C1 \int_0 v\, dy - C1\, v_\ell\, y \tag{48}$$

Denoting average values by $\langle\ \rangle$, one gets:

$$\frac{4\mu}{3}(v - v_u) = S1 \cdot C1 \left\langle \frac{M - w}{v} \right\rangle y - S1 \cdot C1 \left(\frac{M - w_u}{v_u}\right) y + C1 \langle v \rangle\, y - C1\, v_\ell\, y \tag{49}$$

Dividing by $S1 \cdot C1$:

$$\frac{4\mu}{3\ S1 \cdot C1}(v - v_u) = \left\langle \frac{M - w}{v} \right\rangle y - \left(\frac{M - w_u}{v_u}\right) + \frac{\langle v \rangle\, y}{S1} - \frac{v_\ell\, y}{S1} \tag{50}$$

But it was already shown that the maximum value of v is v_u. Hence,

$$v - v_u < v_u \tag{51}$$

and

$$\langle v \rangle \leq v_u \tag{52}$$

All terms in Equation (50) are therefore bounded. Since $S1 \simeq -10^9$, $\mu / C1 \simeq 1$, $v_u \simeq 1$, it follows from Equation (50) that:

$$\left\langle \frac{M - w}{v} \right\rangle y \simeq \left(\frac{M - w_u}{v_u} \right) y \tag{53}$$

or

$$\left\langle \frac{M - w}{v} \right\rangle \simeq \left(\frac{M - w_u}{v_u} \right) \tag{54}$$

Hence the average value of $\frac{M - w}{v}$ is independent of y and approximately constant. It therefore follows that:

$$\frac{M - w}{v} \simeq \frac{M - w_u}{v_u}$$

or

$$P \simeq PU$$

Conclusions for Order of Magnitude Analysis:

It has been shown that the maximum velocity occurs at the upper plate and that the velocity profile may be obtained to a high degree of accuracy by assuming that the pressure is the same at any point between the plates.

The y-momentum equation, therefore, exerts only a small influence on the velocity profile. The velocity can hence be calculated to a high degree of accuracy just from the continuity equation and the equation of state.

NUMERICAL SOLUTION - Strategy 2

Standard integration techniques (eg. Runge-Kutta, Milne) fail to solve Equation (34) since they depend on predicting and then correcting the value of v at mesh point n+1, on the basis of information calculated at mesh points n, n-1, n-2,.. etc. The reason for this is that any error made in estimating v_{n+1} makes the term,

$$S1\left[\frac{M - w}{v} - \frac{M - w_u}{v_u}\right]$$

and hence dv/dw very large (recalling that $S1 \simeq -10^9$).

It is therefore proposed to solve Equation (34) by an iterative technique.

Let

$$S2 = \frac{3\ C1\ .\ D}{4\ \mu} \tag{55}$$

$$S3 = \frac{v_u}{M - w_u} \tag{56}$$

$$\frac{dv}{dw} = DC = \frac{v_{n+1} - v_n}{\Delta w} \tag{57}$$

$$\bar{v} = (v_{n+1} + v_n) / 2 \tag{58}$$

or

$$v_{n+1} = 2\bar{v} - v_n \tag{59}$$

$$\bar{w} = w_n + \Delta w / 2 \tag{60}$$

and

$$w_{n+1} = w_n + \Delta w \tag{61}$$

Hence Equation (34) can be replaced approximately by the finite difference expression:

$$DC = \frac{S1 \cdot S2\left[\frac{M - \bar{w}}{\bar{v}} - \frac{M - w_u}{v_u}\right] + S2\,(\bar{v} - v_\ell)}{\bar{v}\,(\bar{w} - 1)} \qquad (62)$$

Let

$$S4 = S2\left[-S1\left(\frac{M - w_u}{v_u}\right) - v_\ell\right] \qquad (63)$$

$$= -S2\left[S1 / S3 + v_\ell\right] \qquad (64)$$

Hence:

$$DC = \frac{S1 \cdot S2\left(\frac{M - \bar{w}}{\bar{v}}\right) + S2\,\bar{v} + S4}{\bar{v}\,(\bar{w} - 1)} \qquad (65)$$

Since $\bar{w}$ is known (because that w_n and Δw are given) one can define:

$$S5 = S1 \cdot S2\,(M - \bar{w}) / (\bar{w} - 1) \qquad (66)$$

$$S6 = S2 / (\bar{w} - 1) \qquad (67)$$

$$S7 = S4 / (\bar{w} - 1) \qquad (68)$$

Hence Equation (65) becomes:

$$DC = S5 / \bar{v}^2 + S6 + S7 / \bar{v} \qquad (69)$$

Equation (57) may be written as:

$$DC = 2\,(\bar{v} - v_n) / \Delta w \qquad (70)$$

and Equations (69) and (70) must be solved iteratively. There are two methods by which this can be accomplished:

Method I:

1. Guess $\bar{v}$ and calculate DC from Equation (70).
2. Solve the quadratic equation (69) for $\bar{v}$, i.e.:

$$\bar{v} = \frac{S7 - \sqrt{(S7)^2 + 4\ S5\ (DC - S6)}}{2\ (DC - S6)} \qquad (71)$$

3. Compare this value of $\bar{v}$ with the one guessed in Step 1. If no agreement is achieved, substitute $\bar{v}$ from Equation (71) into Step 1 and repeat.

Method II:

1. Guess $\bar{v}$ and determine DC from Equation(69).
2. Solve Equation (70) for $\bar{v}$.
3. Compare the guessed and calculated values of $\bar{v}$. If no agreement is obtained, use the value of $\bar{v}$ from Equation (70) in Step 1 and repeat the procedure.

Only Method I converges. The reason for this is seen by equating Equations (69) and (70), i.e.:

$$\frac{2\ (\bar{v} - v_n)}{\Delta w} = S5\ /\ \bar{v}^2 + S6 + S7\ /\ \bar{v} \qquad (72)$$

Since S6 is small in comparison with S5 and S7, this equation may be written as:

$$f(\bar{v}) = K\ g(\bar{v}) \qquad (73)$$

where K is a large constant involving S5 and S7 and $g(\bar{v})$ is very close to 0.

Writing Equation (73) as:

$$\bar{v} = g^{-1}\left[K^{-1}\ f(\bar{v})\right] \qquad (74)$$

and denoting the t^{th} try of $\bar{v}$ by $\bar{v}^{(t)}$, Equation (74) then becomes:

$$\bar{v}^{(t+1)} = g^{-1}\left[K^{-1} f(\bar{v}^{(t)})\right] \qquad (75)$$

This iterative scheme converges rapidly because any error in $\bar{v}^{(t)}$ results only in a small error of $K^{-1} f(\bar{v}^{(t)})$ since K^{-1} is very small (in the present case $\simeq -10^{-9}$).

If Equation (73) is however solved by putting:

$$\bar{v}^{(t+1)} = f^{-1}\left[K\, g(\bar{v}^{(t)})\right] \qquad (76)$$

then the iteration does not converge, since an error in $\bar{v}^{(t)}$ is magnified by the large constant K.

Method I and Method II correspond to Equation (75) and (76), respectively. Hence only Method I is successful.

The first guess required by Step 1 of Method I is of course obtained by assuming that P is constant and putting:

$$\frac{M - \bar{w}}{\bar{v}} \simeq \frac{1}{S3} \qquad (77)$$

ERROR

In order to have confidence in the numerical results, the error in v_{n+1} (or $\bar{v}$) is estimated. Comparing $\bar{v}^{(t+1)}$ and $\bar{v}^{(t)}$ is not sufficient since

$$\left|\bar{v}^{(t+1)} - \bar{v}^{(t)}\right| = \text{small}$$

may imply either that the correct value of $\bar{v}$ has been found

or that the convergence is slow. Instead it is preferable to calculate DC both from Equations (69) and (70) and compare the values. Let

$$DC = 2\,(\bar{v} - v_n) \,/\, \Delta w \tag{78}$$

$$RHS = S5 \,/\, \bar{v}^2 + S6 + S7 \,/\, \bar{v} \tag{79}$$

and define the error as:

$$ER = DC - RHS \tag{80}$$

Hence, given a particular value for ER, what is the corresponding error in v_{n+1}? Differentiating Equation (80) partially with respect to v_{n+1} one obtains:

$$\frac{\partial ER}{\partial v_{n+1}} = \frac{\partial DC}{\partial v_{n+1}} - \frac{\partial RHS}{\partial v_{n+1}} = DEV \tag{81}$$

But:

$$\frac{\partial ER}{\partial v_{n+1}} \simeq \frac{ER - 0}{v_{n+1}^{(t)} - v_{n+1}} \tag{82}$$

where v_{n+1} is the accurate value of v at mesh point n+1. (This corresponds to ER = 0.)

$v_{n+1}^{(t)}$ is the estimated value of v corresponding to the error ER.

Hence:

$$v_{n+1}^{(t)} - v_{n+1} = EV = ER \,/\, DEV \tag{83}$$

where EV is the error in the estimated value of the velocity. From the definitions of DC and RHS, i.e. Equations (52) and

(69), it follows that:

$$DEV = 1 / \Delta w + S5 / \bar{v}^3 + 0.5 * S7 / \bar{v}^2 \quad (84)$$

The percentage error in v_{n+1} is then approximately given by:

$$PER = 100. * ER / v_{n+1}^{(t)} \quad (85)$$

RESULTS AND DISCUSSION

In this section the results of the numerical solution of Equation (34) are presented and discussed.

All results were calculated for a temperature of $360^{o}K$, 1 atmosphere pressure (= $1.0133 * 10^{6}$ $g/cm.sec^2$) and constant physical properties. The dependence of the velocity, v, on the following variables was investigated: the mass fractions of water vapour at the upper and lower plates (i.e. w_u and w_L), the plate spacing (GAP), the step-size in the iteration (DLW = Δw) and the tolerable error in the velocity,v (i.e. TOL).

The output from the computer program is given in Tables I to X and is self-explanatory with the help of the table of symbols.

From Tables I, II, and III it is seen that the difference between the velocities calculated with and without the y-momentum equation, i.e. PERPC, is of the order of 10^{-5}%, or that no difference can be detected in the velocities up to about 6 significant figures.

Tables III to VI show the dependence on plate-spacing for fixed w_u and w_L. As expected, the total water vapour flux, C1, and hence the velocity is a strong function of the plate spacing because C1 is approximately proportional to the total concentration gradient between the plates. Thus when GAP = 1 cm., VN ≃ 0.5 cm /sec. whereas for GAP = 0.001 cm, VN ≃ 500 cm /sec. When the velocities are small (VN < 50 cm/sec), the y- momentum equation has virtually no influence on VN. However, for larger velocities the y-momentum equation becomes more important, but even for VN ≃ 500 cm/sec. the error incurred by neglecting the extra momentum equation is only about 0.03%.

It should be pointed out that the particle collector was not suitable for plate spacings less than 0.5 cms and hence the y-momentum equation could be disregarded.

Tables III, VII, VIII, and IX show that the results are independent of the iteration step-size, DLW.

Comparing Table III and Table X indicates that VN is also independent of error as defined by Equation (85).

It may be noticed that for the GAP = 1 cm runs (i.e. where VN ≃ 0.5 cm/sec) the errors PER and PERPC are of the same order of magnitude. Hence it is possible that PERPC is even less than indicated by the results. It was not possible to reduce PER substantially without increasing the running time of the program significantly.

CONCLUSION

It was found that in isothermal diffusion through a stagnant gas the effect of the y-momentum equation on the velocity normal to the plates is very small and hence the total pressure in the gas mixture may be regarded as constant under moist conditions. In view of this the y-momentum equation was also neglected in the main mathematical model which described a non-isothermal system

NOTATION IN COMPUTER PROGRAM

WN	=	mass fraction of water vapour at mesh point n
VN	=	velocity normal to the plates calculated from Equation (34)
VNPC	=	velocity normal to the plates assuming the pressure is constant
PERPC	=	percentage error in VNPC
PER	=	percentage error in VN occurring at mesh point n
C1	=	flux of water vapour between the plates.

Computer Program for Solving the Simplified y-momentum Equation

```
C       EFFECT OF THE Y-MOMENTUM EQUATION ON THE
C       VY-VELOCITY IN ISOTHERMAL DIFFUSION
C       THROUGH A STAGNANT GAS
        REAL*8 M,MR,MRS
        DOUBLE PRECISION T,ROLIQ,D,VIS,RC,WU,WL,DLW
        DOUBLE PRECISION C1,PU,S(10),ROU,VU,VLIQ,W,V
        DOUBLE PRECISION WN,WB,VN,DC,VB,VN1
        DOUBLE PRECISION ER,PER,VNPC,PERPC,WDOTU,E,F,GAP,TOL
        DOUBLE PRECISION RHS,DEV,EV
C       DATA
        T=360.
        ROLIQ=1.
        D=0.37
        VIS=1.4D-4
        RC=8.3140+07
        WU=0.900000001
        WL=0.1
        DLW=-0.001
        GAP=1.
        PU=1.0133D+06
        NPPINT=50
        TOL=1.D-06
C       CONSTANTS
        N=0
        NTRY=1000
        MR=18./29.
        MRS=MR-1.
        M=MR/MRS
        S(1)=RC*T*MRS/18.
        ROU=PU/(S(1)*(M-WU))
        E=(MR-WU*MRS)/(WU-1.)
        F=(WL-1.)/(MR-WL*MRS)
        WDOTU=(MR-WU*MRS)**2*DLOG(E*F)/(GAP*F)
        C1=ROU*D*WDOTU/(WU-1.)
        VU=C1/ROU
        VLIQ=C1/ROLIQ
        S(2)=0.75*C1*D/VIS
        S(3)=VU/(M-WU)
        S(4)=-S(2)*(S(1)/S(3)+VLIQ)
        PRINT 1003
1003    FORMAT('  '/9X,'EFFECT OF THE Y-MOMENTUM EQUATION '
       1'ON THE VY-VELOCITY'/9X,'IN ISOTHERMAL DIFFUSION'
       2' THROUGH A STAGNANT GAS.'/9X,'PROGRAM NAME: PRES9'//)
        PRINT 10100,T,PU
10100   FORMAT(9X,'T  =',F11.6,' DEGR. K',9X,
       1'PU =',1PD11.4,'  G/(CM*SEC**2)')
        PRINT 10101,D,VIS
10101   FORMAT(9X,'D  =',F11.6,' CM**2/SEC',7X,'VIS=',
       1 1PD11.4,'  G/(CM*SEC)')
        PRINT 10102,WU,WL
10102   FORMAT(9X,'WU =',F11.6,17X,'WL =',F11.6)
```

```
      PRINT 10103,C1,GAP
10103 FORMAT(9X,'C1 =',1P1D11.4,' G/(CM**2 SEC)',3X,
     1'GAP=',0P1F11.6,'  CM')
      PRINT 10106,S(2)
10106 FORMAT(9X,'S2 =',1P1D11.4,' CM/SEC')
      PRINT 10104,DLW,TOL
10104 FORMAT(9X,'DLW=',1P1D11.4,17X,'TOL=',D11.4///)
C     STARTING VALUE FOR V(N+1)=NV
      W=WU
      V=VU
      KPRINT=0
      ISTART=0
20    WN=W+DLW
      NWN=WN*10000.
      WN=NWN
      WN=WN*1.D-04
      WB=W+DLW/2.
      VN=S(3)*(M-WN)
      VNPC=VN
      DC=(VN-V)/DLW
      IF(ISTART.EQ.0)PRINT 1010,W,V,V
      ISTART=1
      KPRINT=KPRINT+1
1010  FORMAT('      WN',12X,'VN',11X,'VNPC',10X,'PERPC',11X,
     1'PER'//F11.8,1P2D15.6)
      DO 100 J=1,NTRY
      S(5)=S(1)*S(2)*(M-WB)/(WB-1.)
      S(6)=S(2)/(WB-1.)
      S(7)=S(4)/(WB-1.)
      S(9)=(DC-S(6))/S(7)
      S(10)=S(5)/S(7)
      S(8)=1.+4.*S(9)*S(10)
      VB=0.5*(1.-DSQRT(S(8)))/S(9)
      VN1=2.*VB-V
      RHS=S(5)/VB**2 + S(6) +S(7)/VB
      DC=2.*(VB-V)/DLW
      ER=DC-RHS
      DEV=1./DLW + S(5)/VB**3 +0.5*S(7)/VB**2
      EV=ER/DEV
      PER=100.*EV/VN1
      PERPC=100.*(VN1-VNPC)/VNPC
      IF(DABS(PER).GT.TOL)GO TO 150
C     CONVERGENCE
      IF(KPRINT.LT.NPRINT)GO TO 200
      KPRINT=0
      PRINT 1011,WN,VN,VNPC,PERPC,PER
1011  FORMAT(F11.8,1P4D15.6)
      GO TO 200
150   IF(J.EQ.NTRY)GO TO 999
100   VN=VN1
200   IF(WN.LE.WL)GO TO 998
      W=WN
      V=VN
      GO TO 20
999   PRINT 1020
1020  FORMAT(' J.EQ.NTRY')
      GO TO 1000
998   PRINT 1021
1021  FORMAT(' WL IS REACHED')
1000  STOP
```

TABLE I

EFFECT OF THE Y-MOMENTUM EQUATION ON THE VY-VELOCITY
IN ISOTHERMAL DIFFUSION THROUGH A STAGNANT GAS.
PROGRAM NAME: PRES8

T = 360.000000 DEGR. K
D = 0.370000 CM**2/SEC
WU = 0.900000
C1 = 5.8086D-04 G/(CM**2*SEC)
S2 = 1.1514D 00 CM/SEC
DLW=-1.0000D-03

PU = 1.0133D 06 G/(CM*SEC**2)
VIS= 1.4000D-04 G/(CM*SEC)
WL = 0.100000
GAP= 1.000000 CM

TOL= 1.0000D-06

WN	VN	VNPC	PERPC	PER
0.90000000	9.170251D-01	9.170251D-01		
0.85000000	8.989475D-01	8.989475D-01	4.703775D-07	3.597283D-07
0.80000000	8.808700D-01	8.808700D-01	6.220986D-07	5.119761D-07
0.75000000	8.627924D-01	8.627924D-01	5.957370D-07	4.862038D-07
0.70000000	8.447148D-01	8.447148D-01	7.978829D-07	6.135946D-07
0.65000000	8.266373D-01	8.266373D-01	1.272660D-07	1.909905D-08
0.60000000	8.085597D-01	8.085597D-01	1.637622D-07	5.637165D-08
0.55000000	7.904822D-01	7.904822D-01	-1.507034D-06	3.125885D-07
0.50000000	7.724046D-01	7.724046D-01	9.024151D-07	7.967633D-07
0.45000000	7.543271D-01	7.543271D-01	8.066325D-07	4.674457D-07
0.40000000	7.362495D-01	7.362495D-01	-1.396863D-06	7.549855D-07
0.35000000	7.181719D-01	7.181719D-01	-1.631292D-06	-8.357085D-08
0.30000000	7.000944D-01	7.000944D-01	-1.253300D-06	9.371162D-07
0.25000000	6.820168D-01	6.820168D-01	-4.650899D-06	2.779544D-07
0.20000000	6.639393D-01	6.639393D-01	2.413758D-06	8.775726D-07
0.15000000	6.458617D-01	6.458617D-01	-2.425195D-06	1.828386D-07
0.10000000	6.277842D-01	6.277842D-01	-7.336988D-07	9.932694D-07

WL IS REACHED

TABLE II

EFFECT OF THE Y-MOMENTUM EQUATION ON THE VY-VELOCITY
IN ISOTHERMAL DIFFUSION THROUGH A STAGNANT GAS.
PROGRAM NAME: PRES8

T = 360.000000 DEGR. K		PU = 1.0133D 06	G/(CM*SEC**2)
D = 0.370000 CM**2/SEC		VIS= 1.4000D-04	G/(CM*SEC)
WU = 0.800000		WL = 0.400000	
C1 = 2.8815D-04 G/(CM**2*SEC)		GAP= 1.000000	CM
S2 = 5.7115D-01 CM/SEC			
DLW=-1.0000D-03		TOL= 1.0000D-06	

WN	VN	VNPC	PERPC	PER
0.80000000	4.369718D-01	4.369718D-01		
0.75000000	4.280042D-01	4.280041D-01	5.201117D-06	3.283280D-07
0.70000000	4.190364D-01	4.190364D-01	-7.397407D-06	4.698950D-08
0.65000000	4.100686D-01	4.100687D-01	-1.940455D-05	1.341234D-07
0.60000000	4.011011D-01	4.011010D-01	2.286737D-05	9.237563D-07
0.55000000	3.921333D-01	3.921333D-01	-2.248899D-06	6.262298D-07
0.50000000	3.831655D-01	3.831656D-01	-1.628262D-05	6.182763D-07
0.45000000	3.741979D-01	3.741979D-01	7.180508D-07	1.573965D-07
0.40000000	3.652302D-01	3.652302D-01	1.608959D-06	3.884010D-07

WL IS REACHED

TABLE III

EFFECT OF THE Y-MOMENTUM EQUATION ON THE VY-VELOCITY
IN ISOTHERMAL DIFFUSION THROUGH A STAGNANT GAS.
PROGRAM NAME: PRES8

T = 360.000000 DEGR. K		PU = 1.0133D 06	G/(CM*SEC**2)
D = 0.370000 CM**2/SEC		VIS= 1.4000D-04	G/(CM*SEC)
WU = 0.800000		WL = 0.0	
C1 = 4.5264D-04 G/(CM**2*SEC)		GAP= 1.000000	CM
S2 = 8.9719D-01 CM/SEC			
DLW=-1.0000D-03		TOL= 1.0000D-06	

WN	VN	VNPC	PERPC	PER
0.80000000	6.864155D-01	6.864155D-01		
0.75000000	6.723286D-01	6.723286D-01	-1.121442D-06	5.447384D-07
0.70000000	6.582417D-01	6.582418D-01	-2.020734D-06	9.525968D-07
0.65000000	6.441549D-01	6.441549D-01	8.123998D-07	1.896349D-07
0.60000000	6.300680D-01	6.300680D-01	-1.487395D-06	4.068717D-07
0.55000000	6.159811D-01	6.159811D-01	-3.288600D-06	5.634522D-07
0.50000000	6.018942D-01	6.018942D-01	-2.496862D-06	3.589085D-07
0.45000000	5.878073D-01	5.878073D-01	8.457964D-07	7.809286D-07
0.40000000	5.737205D-01	5.737204D-01	3.097113D-06	3.990817D-07
0.35000000	5.596336D-01	5.596335D-01	8.209301D-07	7.572764D-07
0.30000000	5.455467D-01	5.455467D-01	-2.219210D-06	8.919925D-07
0.25000000	5.314598D-01	5.314598D-01	-4.385770D-07	8.587361D-07
0.20000000	5.173729D-01	5.173729D-01	-3.508745D-06	3.737430D-07
0.15000000	5.032860D-01	5.032860D-01	-1.843835D-06	6.516028D-07
0.10000000	4.891991D-01	4.891991D-01	6.397839D-07	5.797736D-07
0.05000000	4.751122D-01	4.751122D-01	-8.070796D-06	2.220812D-07
0.0	4.610253D-01	4.610253D-01	-2.832922D-06	5.577742D-07

WL IS REACHED

TABLE IV

EFFECT OF THE Y-MOMENTUM EQUATION ON THE VY-VELOCITY
IN ISOTHERMAL DIFFUSION THROUGH A STAGNANT GAS.
PROGRAM NAME: PRES8

T = 360.000000 DEGR. K
D = 0.370000 CM**2/SEC
WU = 0.800000
C1 = 4.5264D-03 G/(CM**2*SEC)
S2 = 8.9719D 00 CM/SEC
DLW=-1.0000D-03

PU = 1.0133D 06 G/(CM*SEC**2)
VIS= 1.4000D-04 G/(CM*SEC)
WL = 0.0
GAP= 0.100000 CM

TOL= 1.0000D-06

WN	VN	VNPC	PERPC	PER
0.80000000	6.864158D 00	6.864158D 00		
0.75000000	6.723289D 00	6.723289D 00	6.511147D-06	3.254833D-08
0.70000000	6.582420D 00	6.582420D 00	6.438612D-06	3.300119D-09
0.65000000	6.441551D 00	6.441551D 00	6.391991D-06	3.914332D-09
0.60000000	6.300682D 00	6.300682D 00	6.371773D-06	3.487838D-08
0.55000000	6.159813D 00	6.159813D 00	6.290181D-06	8.417341D-09
0.50000000	6.018944D 00	6.018944D 00	6.234658D-06	1.197209D-08
0.45000000	5.878075D 00	5.878075D 00	6.160779D-06	1.118434D-09
0.40000000	5.737206D 00	5.737206D 00	6.113388D-06	2.070001D-08
0.35000000	5.596337D 00	5.596337D 00	6.047166D-06	2.539767D-08
0.30000000	5.455469D 00	5.455469D 00	5.961322D-06	1.441972D-08
0.25000000	5.314600D 00	5.314600D 00	5.902242D-06	3.415202D-08
0.20000000	5.173731D 00	5.173731D 00	5.822909D-06	3.757719D-08
0.15000000	5.032862D 00	5.032862D 00	5.722264D-06	2.363601D-08
0.10000000	4.891993D 00	4.891993D 00	5.599092D-06	-8.836253D-09
0.05000000	4.751124D 00	4.751124D 00	5.502411D-06	-1.097318D-08
0.0	4.610255D 00	4.610255D 00	5.433398D-06	1.855154D-08

WL IS REACHED

TABLE V

EFFECT OF THE Y-MOMENTUM EQUATION ON THE VY-VELOCITY
IN ISOTHERMAL DIFFUSION THROUGH A STAGNANT GAS.
PROGRAM NAME: PRES8

T = 360.000000 DEGR. K
D = 0.370000 CM**2/SEC
WU = 0.800000
C1 = 4.5264D-02 G/(CM**2*SEC)
S2 = 8.9719D 01 CM/SEC
DLW=-1.0000D-03

PU = 1.0133D 06 G/(CM*SEC**2)
VIS= 1.4000D-04 G/(CM*SEC)
WL = 0.0
GAP= -0.010000 CM
TOL= 1.0000D-06

WN	VN	VNPC	PERPC	PER
0.80000000	6.864157D 01	6.864157D 01		
0.75000000	6.723288D 01	6.723288D 01	6.475852D-04	7.267628D-07
0.70000000	6.582419D 01	6.582419D 01	6.432515D-04	8.306290D-07
0.65000000	6.441550D 01	6.441550D 01	6.385226D-04	9.214056D-07
0.60000000	6.300681D 01	6.300681D 01	6.333983D-04	9.993640D-07
0.55000000	6.159812D 01	6.159812D 01	6.658987D-07	1.297831D-09
0.50000000	6.018943D 01	6.018943D 01	7.088165D-07	1.463321D-09
0.45000000	5.878074D 01	5.878074D 01	7.402469D-07	1.767802D-09
0.40000000	5.737206D 01	5.737206D 01	7.611275D-07	1.794473D-09
0.35000000	5.596337D 01	5.596337D 01	7.717578D-07	1.635337D-09
0.30000000	5.455468D 01	5.455468D 01	7.729780D-07	1.723911D-09
0.25000000	5.314599D 01	5.314599D 01	7.651736D-07	1.868040D-09
0.20000000	5.173730D 01	5.173730D 01	7.489218D-07	1.414878D-09
0.15000000	5.032861D 01	5.032861D 01	7.257064D-07	1.841346D-09
0.10000000	4.891992D 01	4.891992D 01	6.945858D-07	1.545670D-09
0.05000000	4.751123D 01	4.751123D 01	6.575147D-07	1.621403D-09
0.0	4.610254D 01	4.610254D 01	6.141917D-07	1.198625D-09

WL IS REACHED

TABLE VI

EFFECT OF THE Y-MOMENTUM EQUATION ON THE VY-VELOCITY
IN ISOTHERMAL DIFFUSION THROUGH A STAGNANT GAS.
PROGRAM NAME: PRES8

T = 360.000000 DEGR. K PU = 1.0133D 06 G/(CM*SEC**2)
D = 0.370000 CM**2/SEC VIS= 1.4000D-04 G/(CM*SEC)
WU = 0.800000 WL = 0.0
C1 = 4.5264D-01 G/(CM**2*SEC) GAP= 0.001000 CM
S2 = 8.9719D 02 CM/SEC
DLW=-1.0000D-03 TOL= 1.0000D-06

WN	VN	VNPC	PERPC	PER
0.80000000	6.864156D 02	6.864156D 02		
0.75000000	6.725464D 02	6.723287D 02	3.239387D-02	5.834558D-07
0.70000000	6.584536D 02	6.582418D 02	3.217447D-02	-1.512892D-07
0.65000000	6.443607D 02	6.441549D 02	3.193692D-02	-2.925188D-07
0.60000000	6.302677D 02	6.300680D 02	3.167960D-02	-4.963955D-07
0.55000000	6.161746D 02	6.159811D 02	3.140235D-02	-7.611140D-07
0.50000000	6.020815D 02	6.018943D 02	3.110941D-02	1.941381D-07
0.45000000	5.879884D 02	5.878074D 02	3.079354D-02	2.689765D-07
0.40000000	5.738952D 02	5.737205D 02	3.045793D-02	3.485096D-07
0.35000000	5.598020D 02	5.596336D 02	3.010252D-02	4.260760D-07
0.30000000	5.457089D 02	5.455467D 02	2.972730D-02	4.948654D-07
0.25000000	5.316157D 02	5.314598D 02	2.933224D-02	5.489044D-07
0.20000000	5.175225D 02	5.173729D 02	2.891735D-02	5.838452D-07
0.15000000	5.034294D 02	5.032860D 02	2.848261D-02	5.974287D-07
0.10000000	4.893362D 02	4.891991D 02	2.802803D-02	5.895906D-07
0.05000000	4.752432D 02	4.751123D 02	2.755362D-02	5.622617D-07
0.0	4.611501D 02	4.610254D 02	2.705938D-02	5.189066D-07

WL IS REACHED

TABLE VII

EFFECT OF THE Y-MOMENTUM EQUATION ON THE VY-VELOCITY
IN ISOTHERMAL DIFFUSION THROUGH A STAGNANT GAS.
PROGRAM NAME: PRES8

T = 360.000000 DEGR. K
D = 0.370000 CM**2/SEC
WU = 0.800000
C1 = 4.5264D-04 G/(CM**2*SEC)
S2 = 8.9719D-01 CM/SEC
DLW=-2.0000D-03

PU = 1.0133D 06 G/(CM*SEC**2)
VIS= 1.4000D-04 G/(CM*SEC)
WL = 0.0
GAP= 1.000000 CM
TOL= 1.0000D-06

WN	VN	VNPC	PERPC	PER
0.80000000	6.864155D-01	6.864155D-01		
0.72000000	6.638765D-01	6.638765D-01	-1.083405D-06	1.619934D-07
0.64000000	6.413375D-01	6.413375D-01	5.840960D-07	3.220015D-07
0.56000000	6.187985D-01	6.187985D-01	-2.432638D-06	3.766255D-08
0.48000000	5.962595D-01	5.962595D-01	-3.368271D-06	4.292863D-07
0.40000000	5.737204D-01	5.737204D-01	-2.819858D-06	-6.878504D-09
0.32000000	5.511814D-01	5.511814D-01	-2.169991D-06	9.104213D-07
0.24000000	5.286424D-01	5.286424D-01	1.919044D-06	3.219722D-07
0.16000000	5.061034D-01	5.061034D-01	3.948387D-06	3.194129D-07
0.08000000	4.835644D-01	4.835644D-01	-1.007061D-06	8.411272D-07
0.0	4.610253D-01	4.610253D-01	-5.274610D-06	3.823191D-07

WL IS REACHED

TABLE VIII

EFFECT OF THE Y-MOMENTUM EQUATION ON THE VY-VELOCITY IN ISOTHERMAL DIFFUSION THROUGH A STAGNANT GAS.
PROGRAM NAME: PRES8

T = 360.000000	DEGR. K	PU = 1.0133D 06	G/(CM*SEC**2)
D = 0.370000	CM**2/SEC	VIS= 1.4000D-04	G/(CM*SEC)
WU = 0.800000		WL = 0.0	
C1 = 4.5264D-04	G/(CM**2*SEC)	GAP= 1.000000	CM
S2 = 8.9719D-01	CM/SEC		
DLW=-2.0000D-04		TOL= 1.0000D-06	

WN	VN	VNPC	PERPC	PER
0.80000000	6.864155D-01	6.864155D-01		
0.72000000	6.638765D-01	6.638765D-01	-1.846356D-06	6.193820D-07
0.64000000	6.413375D-01	6.413375D-01	9.079433D-07	4.270548D-07
0.56000000	6.187985D-01	6.187985D-01	1.807110D-06	4.336182D-07
0.48000000	5.962595D-01	5.962595D-01	-4.414008D-07	5.934083D-07
0.40000000	5.737204D-01	5.737204D-01	1.044473D-06	9.833484D-07
0.32000000	5.511814D-01	5.511814D-01	-2.149205D-06	1.493211D-07
0.24000000	5.286424D-01	5.286424D-01	5.208612D-07	4.621280D-07
0.16000000	5.061034D-01	5.061034D-01	3.639545D-06	5.724896D-07
0.08000000	4.835644D-01	4.835644D-01	2.100214D-06	5.873014D-07
0.0	4.610254D-01	4.610253D-01	2.032350D-07	1.488401D-07

WL IS REACHED

TABLE IX

```
T  = 360.000000 DEGR. K                PU = 1.0133D 06  G/(CM*SEC**2)
D  =   0.370000 CM**2/SEC              VIS= 1.4000D-04  G/(CM*SEC)
WU =   0.800000                        WL =   0.0
C1 = 4.5264D-04 G/(CM**2*SEC)          GAP=   1.000000  CM
S2 = 8.9719D-01 CM/SEC
DLW=-1.0000D-04                        TOL= 1.0000D-06
```

WN	VN	VNPC	PERPC	PER
0.80000000	6.864155D-01	6.864155D-01		
0.72000000	6.638765D-01	6.638765D-01	4.902164D-07	8.699019D-07
0.64000000	6.413375D-01	6.413375D-01	8.705105D-07	8.063449D-07
0.56000000	6.187985D-01	6.187985D-01	8.373226D-07	7.739937D-07
0.48000000	5.962595D-01	5.962595D-01	-2.072123D-06	-5.664445D-08
0.40000000	5.737204D-01	5.737204D-01	8.464384D-07	5.856086D-08
0.32000000	5.511814D-01	5.511814D-01	2.242824D-07	1.640629D-07
0.24000000	5.286424D-01	5.286424D-01	-1.421097D-06	8.035328D-07
0.16000000	5.061034D-01	5.061034D-01	-1.444783D-06	3.210548D-07
0.08000000	4.835644D-01	4.835644D-01	4.016318D-07	3.454168D-07
0.0	4.610254D-01	4.610253D-01	1.695741D-06	4.699077D-07

WL IS REACHED

TABLE X

EFFECT OF THE Y-MOMENTUM EQUATION ON THE VY-VELOCITY
IN ISOTHERMAL DIFFUSION THROUGH A STANANT GAS.
PROGRAM NAME: PRES8

T = 360.000000 DEGR. K
D = 0.370000 CM**2/SEC
WU = 0.800000
C1 = 4.5264D-04 G/(CM**2*SEC)
S2 = 8.9719D-01 CM/SEC
DLW=-1.0000D-03

PU = 1.0133D 06 G/(CM*SEC**2)
VIS= 1.4000D-04 G/(CM*SEC)
WL = 0.0
GAP= 1.000000 CM

TOL= 1.0000D-07

WN	VN	VNPC	PERPC	PER
0.80000000	6.864155D-01	6.864155D-01		
0.72000000	6.638765D-01	6.638765D-01	-2.587228D-07	8.899471D-08
0.64000000	6.413374D-01	6.413375D-01	-1.494164D-05	6.567436D-08
0.56000000	6.187984D-01	6.187985D-01	-5.814798D-06	-5.413768D-08
0.48000000	5.962594D-01	5.962595D-01	-3.322899D-06	2.000965D-08
0.40000000	5.737204D-01	5.737204D-01	1.386930D-07	7.441481D-08
0.32000000	5.511814D-01	5.511814D-01	-6.625787D-06	3.667290D-08
0.24000000	5.286424D-01	5.286424D-01	-2.254253D-07	5.112332D-08
0.16000000	5.061034D-01	5.061034D-01	9.357451D-06	-5.086217D-08
0.08000000	4.835643D-01	4.835644D-01	-9.364002D-06	-4.980406D-08
0.0	4.610253D-01	4.610253D-01	-1.600752D-06	-1.813081D-08

WL IS REACHED.

APPENDIX II

PLATE MATERIALS CONSIDERED

Material:	Porous Metal	Porous Metal	Porous Metal
Manufacturer/ Distributor:	Pall Corp.	Pall Corp.	Huyak Metals Corp., Conn.
Trade Name:		Rigimesh	Feltmetal
Description:	Sintered stainless steel or bronze spherical particles	Sintered and rolled stainless steel and bronze wire mesh	Sintered stainless steel or bronze fibres
Size:	12" x 60"	12" x 60"	12" x 60"
Delivery Time:	8 weeks	8 weeks	7 weeks
Cost:	$400	$500	$500
Wettability:	None	None	None
Strength:	Good	Good	Good
Pore Size:	As desired	As desired	As desired

Material:	Porous Carbon	Fibreglass	Fibreglass
Manufacturer/ Distributor:	Union Carbide, Speer Carbon, Montreal	Fibreglass Canada Ltd.	Williams and Wilson Ltd., Montreal
Trade Name:			Fibrefax
Description:		Glass fibre joined by organic resin	Silica, Alumina wool strengthened by cement
Size:	12" x 60"	12" x 60"	12" x 60"
Delivery Time:	2 weeks	1 week	2 weeks
Cost:	$100	$50	$30
Wettability:	None	Poor	Good
Strength:	Good	Poor	Adequate
Pore Size:	As desired	High unless compressed	Unknown

Material:	Cement	Asbestos	Felt
Manufacturer/ Distributor:	Williams and Wilson Ltd., Montreal	Pascals	
Trade Name:	Coating Cement		
Description:	Inorganic cement	Asbestos fibres joined by soluble, inorganic filler	Compressed wool
Size:	12" x 60"	12" x 60"	12" x 60"
Delivery Time:	2 weeks	1 week	1 week
Cost:	$40	$10	$30
Wettability:	Good	Good	Good
Strength:	Good	Poor	Poor
Pore Size:	Unknown	As desired	Too great

Material:	Plaster of Paris	Porous Ceramic*	Porous Ceramic
Manufacturer/ Distributor:	Pascals	Johns-Manville	Norton
Trade Name:		Celite	Alundum
Description:	$CaSO_4$	Silicate	Aluminium silicate
Size:			12" x 12"
Delivery Time:	Immediate	3 weeks	5 weeks
Cost:	$20	$40	$60
Wettability:	Good	Good	Good
Strength:	Good	Good	Good
Pore Size:	Too low	As desired	Unknown

* Sold as powder which needs firing at $\simeq 1000^{o}C$ and compressed to make flat plates.

Material:	Porous Ceramic	Porous Glass	Porous Glass
Manufacturer/ Distributor:	Selas Flot-ronics, Penn.	Corning, Kimbal	Corning
Trade Name:	Microporous Plates	Fritted Glass	Vycor Porous Glass
Description:	Silicate	Sintered Pyrex	Pyrex
Size:	5" x 5"	3" x 3"	at least 5" x 5"
Delivery Time:	7 weeks	2 weeks	6 weeks
Cost:	?	$5	$25
Wettability:	Good	Good	Good
Strength:	Good	Good	Good
Pore Size:	As desired	Good	Good

Material:	Blotting Paper
Manufacturer/ Distributor:	Domtar Ltd. Montreal
Trade Name:	
Description:	Paper
Size:	27" x 100'
Delivery Time:	4 weeks
Cost:	Gratis
Wettability:	Good
Strength:	Poor
Pore Size:	Correct

APPENDIX III

Computer Program for Solving the Transport, Particle, and Operating-Cost Equations.

```
      COMMON /RUN/YFIN,EMAX,H,TOL,NCASE,KPRINT,MX
      COMMON /OUT/PRDEL
      COMMON /FUN/Y,Z(15),F(15)
      COMMON /PARAM/TU,MA,MB,P,RC,GAP,PAU,DELPX,TL,VXU
      COMMON /PARPRO/DP,RP
      COMMON /OUTPUT/C1,TK,D,CP,VIS, VY,RA,R,XA,PA,PSAT,
     1 REP,RE,CDS
      DOUBLE PRECISION Y,Z,F,TU,C1
      REAL MA,MB
      PRINT 10
10    FORMAT('1')
C     PHYSICAL DATA
      DELPX=-0.20266E-02
      P=1.
      RC=82.05
      MA=18.
      MB=29.
      VXU=0.
C     RUN CONTROL
      TOL=0.0001
      EMAX=0.000001
C     PARTICLE PROPERTIES
      DP=0.8E-04
      RP=1.
4     READ(5,2)GAP,TU,TL,DTL,PRDEL,IADJ
2     FORMAT(5F10.4,I1)
      IF(GAP.EQ.0.)GO TO 3
      NCDS=0
      ICDS=0
      TLO=TU
      NCASE=1
      MX=50
      H=0.01
      YFIN=GAP
200   PRINT 1000,GAP,TU,TL,DELPX
1000  FORMAT('  GAP=',F7.2,'   TU=',F7.2,'   TL=',F7.2,
     1'   DELPX=',E15.5)
      PRINT 300,DP,RP
300   FORMAT('  DP =',E12.5,'   RP =',F9.4)
      PRINT 2000,H,EMAX,TOL
2000  FORMAT(' H=',F13.5,'   EMAX=',E13.5,'   TOL=',E13.5,/)
C     INITIAL CONDITIONS
      CALL MODEL
      IF(IADJ.EQ.1)GO TO 4
      NCDS=NCDS+1
      IF(NCDS-10)100,100,4
100   CALL TLADJ(TL,TLO,CDS,ICDS,DTL,IADJ)
      GO TO 200
3     STOP
      END
      SUBROUTINE TLADJ(TL,TLO,CDS,ICDS,DTL,IADJ)
```

```
C       FINDS TL MINIMUM BY 'DICHOTOMOUS' SEARCH
        INTEGER CDS
        IF(CDS)10,10,40
10      IF(ICDS)20,20,30
20      TL0=TL
        TL=TL-DTL
        GO TO 999
30      TL0=TL
        GO TO 50
40      ICDS=1
        TL1=TL
50      TL=(TL1+TL0)/2.
999     PRINT 1000,TL,TL0,TL1,DTL,CDS,ICDS
1000    FORMAT(4E15.5,2I6)
        IF(ABS(TL0-TL1).LE.0.2)IADJ=1
        RETURN
        END
        SUBROUTINE MODEL
C       SUBROUTINE CONTAINS MODEL EQUATIONS
        COMMON /START/N,IPRINT,JPRINT
        COMMON/PARTIC/VYP,VYDP,VYTP,VYG,SAB
        COMMON /PARPRO/DP,RP
        COMMON /OUT/PRDEL
        INTEGER CDS
        COMMON /OUTPUT/C1,TK,D,CP,VIS, VY,RA,R,XA,PA,PSAT,
       1 REP,RE,CDS
        COMMON /FUN/Y,Z(15),F(15)
        COMMON /CONVRG/X(3),YL(3),NOPRNT
        COMMON /PARAM/TU,MA,MB,P,RC,GAP,PAU,DELPX,TL,VXU
        DOUBLE PRECISION Y,Z,F,X,WA,VX,T,TKTDOT,C1,C4,C5,TU,YL,WAU
        EQUIVALENCE (Z(1),WA), (Z(2),VX), (Z(3),T), (Z(4),TKTDOT)
        REAL MA,MB
        NOPRNT=0
C       INITIAL CONDITIONS AND GUESSES OF DERIVATIVES
        CALL IDERIV(MA,MB,P,PAU,DELPX,GAP,RC,TU,TL,WAL,RU,DU,WAU,VISU,TKU,
       1X(1),X(2),X(3))
C       CONVERGE TO
        YL(1)=WAL
        YL(2)=0.
        YL(3)=TL
        N=4
2       CONTINUE
        CALL INITLZ
        CALL INTCON(RU,DU,X(1),TKU,X(3),VISU,X(2),WAU,C1,C4,C5)
        TKTDU=X(3)*TKU
C       INITIAL CONDITIONS OF DEPENDENT VARIABLES
        CDS=0
        WA=WAU
        T=TU
        VX=VXU
        TKTDOT=TKTDU
        Z(5)=0.
        Z(6)=0.
        Z(7)=0.
        Z(8)=0.
        Z(9)=0.
        Z(10)=0.
```

```
C       DENSITY
1        RA=(MB*P/(RC*T))/(1./WA-(1.-MB/MA))
         R=RA/WA
C       MOLE FRACTION
         XA=(MB*WA)/((MB-MA)*WA+MA)
         XB=1.-XA
C       TRANSPORT COEFFICIENTS
C        VISCOSITY
        CALL VISC(T,XA,XB,VISA,VISB,VIS)
C        THERMAL CONDUCTIVITY
         TK=TCOND(T,XA,XB,VISA,VISB)
C        DIFFUSIVITY
         D=DIFF(T,P)
C        SPECIFIC HEAT
        CALL SPHEAT(T,WA,CP,CPA,CPB)
C       PARTIAL PRESSURES
C        SATURATED STEAM
         PSAT=PSA(T)
C        AS CALCULATED BY PROGRAMME
         PA=XA*P
        IF(Y-0.99*GAP)10,10,20
10      IF(PA*0.999.GT.PSAT)CDS=1
C       LOCAL REYNOLDS NUMBER BASED ON TOTAL GAP WIDTH
20      RE=(R*VX*GAP)/VIS
C       TRANSPORT EQUATIONS
C        CONTINUITY
        F(1)= C1*(WA-1.)/(R*D)
C        MOMENTUM
        F(2)=(C1*VX + DELPX*Y -C4)/VIS
         VY=C1/R
C        ENERGY
        F(4)=C1*CPA*TKTDOT/TK-VX*DELPX*2.3901E-08
        F(3)=TKTDOT/TK
C       PARTICLE EQUATIONS - MODEL I
        F(5)=VX/VY
        F(6)=1./VY
C       PARTICLE EQUATIONS - MODEL II
        SAB=-0.26
        DRAG=(1.+(0.364+0.29*EXP(-6.25))/5.)
        VYDP=-(1.+XB*SAB)*(D/XB)*(1./(MA*MB*(XA/MA+XB/MB)**2))*F(1)/DRAG
        VYTP=-0.75*(VIS/(R*T))*(2.*TK/(2.*TK+0.001))*F(3)/DRAG
        VYG=DP*DP*981.*(PP-R)/(18.*VIS)/DRAG
        VYP=VYDP+VYTP+VYG
        F(7)=VX/VYP
        F(8)=1./VYP
C       MASS FLOW RATE OF AIR, MAIR
        F(9)=30.48*(R-RA)*VX
C       VOLUMETRIC GAS FLOW RATE, Q
        F(10)=30.48*VX
        CALL MERS2(&1)
        IF(NOPRNT.EQ.1)GO TO 999
        CALL NEWTON(&2)
        NOPRNT=1
        N=10
        GO TO 2
999     RETURN
        END
        SUBROUTINE VISC(T,XA,XB,VISA,VISB,VIS)
C       VISCOSITY SUBROUTINE
C       A=STEAM       B=AIR
```

```
      DOUBLE PRECISION T
      VISA=(1.501*DSQRT(T)*1.E-5)/(1.+446.8/T)
      VISB=(1.488*DSQRT(T)*1.E-5)/(1.+122.1/(T*10.**(5./T)))
      CALL COMB(XA,XB,VISA,VISB,VISA,VISB,R)
      VIS=R
      RETURN
      END
      FUNCTION TCOND(T,XA,XB,VISA,VISB)
C     THERMAL CONDUCTIVITY SUBROUTINE
C     A=STEAM       B=AIR
      DOUBLE PRECISION T
      TKA=(1.546*DSQRT(T)*1.E-5)/(1.+1737.3/(T*10.**(12./T)))
      TKB=(0.632*DSQRT(T)*1.E-5)/(1.+245./(T*10.**(12./T)))
      CALL COMB(XA,XB,VISA,VISB,TKA,TKB,R)
      TCOND=R
      RETURN
      END
      SUBROUTINE COMB(XA,XB,VISA,VISB,DA,DB,R)
C     COMB. SUBR. FOR VISC. AND THERM. COND. OF STEAM/AIR MIXTURE
C     DA,DB ARE DUMMIES
      PHIAB=0.27804*(1.+((VISA/VISB)**0.5)*1.12857)**2
      PHIBA=0.2183*(1.+((VISB/VISA)**0.5)*0.88608)**2
      R=(XA*DA)/(XA+PHIAB*XB)+(XB*DB)/(XA*PHIBA+XB)
      RETURN
      END
      FUNCTION DIFF(T,P)
C     DIFFUSIVITY FOR STEAM/AIR MIXTURE
      DOUBLE PRECISION T
      DIFF=0.22*((T/273.)**1.75)*(1./P)
      RETURN
      END
      SUBROUTINE SPHEAT(T,WA,CP,CPA,CPB)
      DOUBLE PRECISION T,WA
C     SPECIFIC HEAT OF AIR/STEAM MIXTURE
C     UNITS       T= DEGR. K       CP= CALS/(GRAM*DEGR. K)
C     AIR
      CPB=0.2202+(6.077E-05)*T-(9.158E-09)*T**2
C     STEAM
      CPA=0.3964+(1.467E-04)*T+(2.55E-09)*T**2
C     MIXTURE
      CP=WA*CPA+(1.-WA)*CPB
      RETURN
      END
      FUNCTION PSA(T)
C     VAPOUR PRESSSURE CURVE FOR WATER
      DOUBLE PRECISION T,TR
      TR=1./T
      PSA =DEXP(0.11628596D02-(0.36936937D04)*TR-(0.23825879D06)*TR*TR)
      RETURN
      END
      SUBROUTINE IDERIV(MA,MB,P,PAU,DELPX,GAP,RC,TU,TL,WAL,R,D,WAU,VIS,
     1TK,WADOT,VXDOT,TDOT)
C     SUBROUTINE CALCULATES FIRST GUESSES OF MASS
C     FRACTION,TEMPERATURE AND VELOCITY AT THE UPPER PLATE.
C     ANALYTICAL SOLUTIONS OF DECOUPLED TRANSPORT EQUATIONS WITH
C     CONSTANT COEFFICIENTS ARE TAKEN AS BASES OF GUESSES.
      DOUBLE PRECISION WADOT,VXDOT,TDOT,TU,DDTL,WAU
      REAL MA,MB,MR,MRS,GAP
      MR=MA/MB
      MRS=MR-1.
```

```
C       CONCENTRATION GRADIENT
        PAU=PSA(TU)
        XAU=PAU/P
        DDTL=TL
        PAL=PSA(DDTL)
        XAL=PAL/P
        WAU=(MR*XAU)/(XAU*MRS+1.)
        WAL=(MR*XAL)/(XAL*MRS+1.)
        E=(MR-WAU*MRS)/(WAU-1.)
        F=(WAL-1.)/(MR-WAL*MRS)
        WADOT=((MR-WAU*MRS)**2)*(ALOG(E*F))/(GAP*E)
        R=(P*MA/(RC*TU))/(MR-WAU*MRS)
        D=DIFF(TU,P)
        C1=(D*R*WADOT)/(WAU-1.)
C       VELOCITY GRADIENT
        XBU=1.-XAU
        CALL VISC(TU,XAU,XBU,VISA,VISB,VIS)
        CV=C1/VIS
        VXDOT= DELPX*((CV*GAP/(EXP(CV*GAP)-1.))-1.)/C1
C       TEMPERATURE GRADIENT
        TK=TCOND(TU,XAU,XBU,VISA,VISB)
        CALL SPHEAT(TU,WAU,CP,CPA,CPB)
        CS=C1*CP
        TDOO=((TU-TL)*CS)/(TK*(1.-EXP(CS*GAP/TK)))
        CK1=C1*CPA/TK
        TDOT=CK1*(TU-TL)/(1.-EXP(CK1*GAP))
        RETURN
        END
        SUBROUTINE INTCON(R,D,WADOT,TK,TDOT,VIS,VXDOT,WA ,C1,C4,C5)
C       INTEGR. CONS. SUBROUTINE
        DOUBLE PRECISION WADOT,TDOT,VXDOT,C1,C4,C5,WA
        C1= R*D*WADOT/(WA-1.)
        C5=TK*TDOT
        C4=-VIS*VXDOT
        RETURN
        END
        SUBROUTINE SPRINT(H,KPRINT)
        COMMON /PARAM/TU,MA,MB,P,RC,GAP,PAU,DELPX,TL,VXU
        COMMON/PARTIC/VYP,VYDP,VYTP,VYG,SAB
        DIMENSION E(3)
        COMMON /CONVRG/X(3),YL(3),NOPRNT
        COMMON /FUN/Y,Z(15),F(15)
        COMMON /START/N,IPRINT,JPRINT
        COMMON /OUTPUT/C1,TK,D,CP,VIS, VY,RA,R,XA,PA,PSAT,
       1 REP,RE,CDS
        INTEGER CDS
        DOUBLE PRECISION X,Y,Z,F,C1,YL,TU
        PRINT 1000,Y
1000    FORMAT('0',' Y   =',E12.5)
        PRINT 1100,Z(1),RA,XA
1100    FORMAT(' WA  =',E12.5,'  RA  =',E12.5,'  XA  =',E12.5)
        S=Z(3)-273.
        PRINT 1110,S,R,PSAT
1110    FORMAT(' T   =',E12.5,'  R   =',E12.5,'  PSAT=',E12.5)
        PRINT 1120, Z(2),RE,CDS
1120    FORMAT(' VX  =',E12.5,'  RE  =',E12.5,'  CDS =',I2)
        PRINT 1130, C1,Z(9),Z(10)
1130    FORMAT(' C1  =',E12.5,'  MAIR=',E12.5,'  Q   =',E12.5)
        PRINT 1140, VY,Z(5),Z(6)
1140    FORMAT(' VY  =',E12.5,'  SL  =',E12.5,'  ST  =',E12.5)
```

```
      PRINT 1150, VYP,Z(7),Z(8)
1150  FORMAT('  VYP =',E12.5,'  SLP =',E12.5,'  STP =',F12.5)
      PRINT 1155,VYDP,VYTP,VYG
1155  FORMAT('  VYDP=',E12.5,'  VYTP=',E12.5,'  VYG =',E12.5)
      PRINT 1160,VIS,TK,D
1160  FORMAT('  VIS =',E12.5,'  TK  =',E12.5,'  D   =',E12.5)
      PRINT 1170,CP,SAB
1170  FORMAT('  CP  =',F12.5,'  SAB =',E12.5)
      IF(KPRINT-1)10,10,20
10    DO 30 I=1,3
30    E(I)=Z(I)-YL(I)
      PRINT 3000,(E(I),I=1,3)
3000  FORMAT(' ERROR IN',/,' WA  =',E12.5/,' VX  =',E12.5/,
     1' T   =',E12.5)
C     MASS OF WATER VAPOUR / MASS OF AIR, ORATIO
      ORATIO=30.48*C1*Z(5)/Z(9)
C     WORK REQUIRED TO PUMP 1 GRAM OF AIR THROUGH COLLECTOR, WORK
      WORK=-DELPX*Z(5)*Z(10)/Z(9)
      PRINT 4000,ORATIO,WORK
4000  FORMAT('0  ORATIO =',E12.5/,'    WORK =',E12.5)
      PRINT 3500
3500  FORMAT('1')
20    RETURN
      END
      SUBROUTINE NEWTON(*)
C     NEWTON RAPHSON CONVERGENCE PROGRAMME FOR 3 INDEP. VARIABLES
      COMMON /CONVRG/X(3),YL(3),NOPRNT
      COMMON /FUN/Y,Z(15),F(15)
      COMMON /RUN/YFIN,EMAX,H,TOL,NCASE,KPRINT,MX
      DIMENSION XO(3), YO(3), E(3), EO(3), PE(3), DE(3,3), CF(3,3),
     1 TCF(3,3),XS(3)
      DOUBLE PRECISION Y,Z,F,X,YL,XO,YO,E,EO,PE,DE,CF,TCF,XS
C     COMMENTS
C     I=1 FOR MOLE FRAC.,    I=2 FOR VEL. VX,    I=3 FOR TEMP.
C     X(I)=INDEP. VARI.,      Z(I)=DEP. VARI.
C     YL(I)=DESIRED VALUE OF DEP. VARI.
C     E(I)=ERROR IN DEP. VARI.,      PE(I)= FRACTIONAL ERROR
C     DE(I,J)=DERIVATIVES,    CF(I,J)=COFACTORS OF DERIV. MATRIX
C     TCF(I,J)=TRANSPOSE OF COFACTOR MATRIX
C     CONSTANTS FOR  ---     CONTINUITY EQUA.     C1
C                            ENERGY EQUA.         C5
C                            MOMENTUM EQUA.       C4
C     MX=MAX. NUMBER OF ITERATIONS,     TOL=ERROR TOLERANCE
C     IGES=1 IF X(I) ARE READ IN (ZERO OTHERWISE)
C     NEW CASE INITIALIZATION
      IF (NCASE.EQ.0)GO TO 10
      CONV=1.
      NN=0
      DO 1 I=1,3
      XO(I)=0.
1     EO(I)=0.
      NBASE=1
      NCASE=0
C     ERROR CALCS
10    IF(NBASE.EQ.0)GO TO 172
      NOLD=NN
      DO 5 J=1,3
      E(J)=Z(J)-YL(J)
      IF(YL(J).EQ.0.) GO TO 6
      DUMY1=E(J)/YL(J)
```

```
      GO TO 5
 6    DUMY1=-1.+10.**E(J)
 5    PE(J)=ABS(DUMY1)
      EMAX=DMAX1(PE(1),PE(2),PE(3))
      NN=NN+1
      IF(EMAX.LT.TOL) GO TO 990
      CONV=1.
      IF (NN.LT.MX) GO TO 170
      PRINT 1700
1700  FORMAT(41H****MAX. NUMBER OF ITERATIONS EXCEEDED***)
      GO TO 1000
C     INITIATE CONVERGENCE ROUTINE
C     DERIVATIVE MATRIX
170   J=0
171   J=J+1
      XS(J)=X(J)
      CHANGE=0.02
      DELTA=(CHANGE/(CHANGE + 1.))*X(J)
      X(J)=(CHANGE + 1.)*X(J)
      NBASE=0
      RETURN 1
172   DO 100 I=1,3
100   DE(I,J)=(Z(I)-YL(I)-E(I))/DELTA
      X(J)=XS(J)
      IF(J.LT.3)GO TO 171
      DE(1,2)=0.
C     DETERMINANT
      DET=0.
      DO 300 J=1,3
      L=4/(J+1)
      N=3-(J/3)
300   DET=DET+((-1.)**(J+1))*(DE(2,L)*DE(3,N)-DE(3,L)*DE(2,N))*DE(1,J)
C     COFACTOR MATRIX
      IS=1
      DO 400 I=1,3
      K=4/(I+1)
      M=3-(I/3)
      DO 400 J=1,3
      L=4/(J+1)
      N=3-(J/3)
      IS=IS+1
400   CF(I,J)=((-1.)**IS)*(DE(K,L)*DE(M,N)-DE(M,L)*DE(K,N))
C     TRANSPOSE OF COFACTORS
      DO 500 I=1,3
      DO 500 J=1,3
500   TCF(I,J)=CF(J,I)
C     CONSERVING OLD VALUES
777   DO 600 I=1,3
      XO(I)=X(I)
600   FO(I)=E(I)
C     NEW INDEP. VARIABLES
      DO 800 I=1,3
      S=0.
      DO 700 J=1,3
700   S=S+TCF(I,J)*E(J)
800   X(I)=X(I)-(S/DET)
      NBASE=1
      RETURN 1
990   CONTINUE
C     CONVERGENCE
```

```
1000  RETURN
      END
      SUBROUTINE INITLZ
C     SUBROUTINE SETS INITIAL VALUES FOR BOOK-KEEPING
      COMMON /START/N,IPRINT,JPRINT
      COMMON /FUN/Y,Z(15),F(15)
      COMMON /RUN/YFIN,EMAX,H,TOL,NCASE,KPRINT,MX
      COMMON /OUT/PRDEL
      DOUBLE PRECISION Y,Z,F
      Y=0.
      JPRINT=1
      KPRINT=YFIN/PRDEL + 1.5
      IPRINT=0
      RETURN
      END
      SUBROUTINE MERS2(*)
C     KUTTA - MERSON INTEGRATION RCUTINE
C     REFERENCE :   G.N. LANCE, NUMERICAL METHODS FOR HIGH SPEED
C                   COMPUTERS, ILIFFE & SONS LTD, LONDON 1960, P. 56
      COMMON /START/N,IPRINT,JPRINT
      COMMON /FUN/Y,Z(15),F(15)
      COMMON /RUN/YFIN,EMAX,H,TOL,NCASE,KPRINT,MX
      COMMON /OUT/PRDEL
      COMMON /OUTPUT/C1,TK,D,CP,VIS, VY,RA,R,XA,PA,PSAT,
     1 REP,RE,CDS
      INTEGER CDS
      COMMON /CONVRG/X(3),YL(3),NOPRNT
      DOUBLE PRECISION Y,Z,F,X,ZOLD,YOLD,C1,YL
      REAL*8 K(5,10)
      DIMENSION ZOLD(10)
10    IF(IPRINT.NE.0)GO TO 100
      IF(NOPRNT.EQ.1)CALL SPRINT(H,KPRINT)
      KPRINT=KPRINT-1
      IF(KPRINT.LE.0)GO TO 999
C     MODIFIED STEP SIZE AND NUMBER
      IF(IPRINT.EQ.0)IPRINT=1
      IPRINT=PRDEL/H + 0.5
      APRINT=IPRINT
      H=PRDEL/APRINT
C     INITIAL VALUES FOR EACH INTEGRATION STEP
90    I=0
      RETURN 1
100   H3=H/3.
      EMX=0.
      KY=0
      I=I+1
      DO 200 J=1,N
      K(I,J)=H3*F(J)
      KY=KY+1
       GO TO (1,2,3,4,5),I
1     ZOLD(J)=Z(J)
      Z(J)=Z(J) + K(I,J)
      IF(KY.NE.1)GO TO 200
      YOLD=Y
      Y=Y+H3
      GO TO 200
2     Z(J)=Z(J) + (K(I,J)-K(I-1,J))/2.
      GO TO 200
3     Z(J)=Z(J) +(9.*K(I,J) - K(I-2,J) - 4.*K(I-1,J))/8.
      IF (KY.EQ.1) Y=Y+H/6.
```